In vitro and *in vivo* investigations on the interaction of bacterial RNase P with tRNA 3’-CCA

Dissertation
zur
Erlangung des Doktorgrades
der Naturwissenschaften
(Dr. rer. nat.)

dem Fachbereich
Pharmazeutische Chemie
der Philipps-Universität Marburg
vorgelegt von

Barbara Wegscheid
aus Werneck

Marburg/Lahn 2006

Vom Fachbereich Pharmazeutische Chemie
der Philipps-Universität Marburg als Dissertation am________________angenommen.

Erstgutachter: Prof. Dr. Roland K. Hartmann
Zweitgutachter: PD Dr. Klaus Reuter

Tag der mündlichen Prüfung am: 30.11.2006

Table of Contents

Table of Contents **I-IV**

1 Introduction **1**

1.1 RNase P 1

1.2 Bacterial RNA subunit 2

1.3 General substrate recognition 4
1.3.1 CCA interaction 6

1.4 Role of the protein subunit 6

1.5 Tertiary structure of bacterial RNase P 8

1.6 Holoenzyme Model 12

1.7 References 14

2 Goal of the Project **21**

3 Methods **23**

3.1 Bacterial cell cuture 23
3.1.1 Bacterial cell culture in liquid medium 23
3.1.2 Growth curves - Determination of cell doubling time 24
3.1.3 Cell growth on agar plates 25
3.1.4 Preparation of competent cells 25
3.1.4.1 Preparation of chemically competent *E. coli* cells, RbCl method 25
3.1.4.2 Preparation of electrocompetent *E. coli* cells 25
3.1.4.3 Preparation of electrocompetent *B. subtilis* cells 26
3.1.4.4 Natural competence - *B. subtilis* 26
3.1.4.4.1 HS/LS medium method 26
3.1.4.4.2 SpC/SpII medium method 28
3.1.5 Transformation 29
3.1.5.1 Transformation of chemically competent *E. coli* cells 29
3.1.5.2 Transformation of electrocompetent *E. coli* cells 29
3.1.5.3 Transformation of electrocompetent *B. subtilis* cells 30
3.1.6 *In vivo* complementation tests 30

3.2 General nucleic acids techniques 31
3.2.1 Nucleic acid gel electrophoresis 31
3.2.1.1 Agarose gel electrophoresis 31
3.2.1.1.1 Crystal violet gels 32
3.2.1.2 Polyacrylamide gel electrophoresis (PAGE) 32
3.2.1.2.1 Denaturing PAGE 32
3.2.1.2.2 Native polyacrylamide gels 34
3.2.1.2.3 Non-denaturing polyacrylamide gel electrophoresis for RNA folding analysis 34
3.2.1.3 Detection of nucleic acids from gels 35
3.2.1.3.1 Ethidium bromide staining 35
3.2.1.3.2 UV-shadowing 36
3.2.1.3.3 Visualization using crystal violet 36
3.2.1.3.4 Radioluminography 36

3.2.2 Photometric concentration determination of nucleic acids 37
3.2.3 Isolation of DNA from agarose gels 38
3.2.4 Isolation of DNA/RNA from PAA gels 39
3.2.5 Alcohol precipitations 39
3.2.5.1 Ethanol precipitation 39
3.2.5.2 Isopropanol precipitation 40
3.2.6 Phenol/chloroform extraction 40
3.2.7 NAP gel filtration 40

3.3 DNA techniques 41
3.3.1 Preparation of genomic DNA 41
3.3.1.1 Rapid isolation of DNA from bacteria 41
3.3.2 Preparation of plasmid DNA 41
3.3.2.1 Preparative plasmid DNA isolation from *E. coli* cells 41
3.3.2.2 Analytical scale preparation of plasmid DNA 42
3.3.3 Restriction digest of DNA 43
3.3.4 Dephosphorylation of DNA 44
3.3.5 5’- Phosphorylation of DNA 44
3.3.6 Fill-in reaction using Klenow fragment 45
3.3.7 Ligation 46
3.3.8 Polymerase chain reaction (PCR) 46
3.3.9 Site-directed *Dpn* I mutagenesis 48

3.4 RNA Techniques 49
3.4.1 Preparation of total RNA 49
3.4.1.1 Growth of DW2 bacteria for total RNA isolation 49
3.4.1.2 Growth of BW bacteria for total RNA isolation 49
3.4.1.3 Growth of SSB318/SSB320 bacteria for total RNA isolation 50
3.4.1.4 Trizol RNA preparation 50
3.4.2 T7 Transcription 51
3.4.2.1 Homogeneous 3’-ends of RNA transcripts 53
3.4.3 5’- end labelling of RNA 54
3.4.4 3’- end labelling of RNA 54
3.4.5 Primer extension 55
3.4.6 RT-PCR 56
3.4.7 5’- RACE 58
3.4.8 Folding analysis on non-denaturing gels 60

3.5 Protein methods 62
3.5.1 TCA-Precipitation 62
3.5.2 SDS-PAGE 62
3.5.2.1 Schägger/Jagow SDS-PAGE 63
3.5.2.2 Laemmli SDS-PAGE 64
3.5.3 Coomassie Staining 65
3.5.4 Western Blot 65
3.5.5 Immunodetection 66
3.5.6 Preparation of recombinant RNase P proteins 67
3.5.7 Partial purification of RNase P from *E. coli* cells 68

3.6 Kinetic Analysis 69
3.6.1 Kinetic analysis of RNase P holoenzymes 69
3.6.1.1 Kinetic analysis of *in vivo* assembled holoenyzmes 70
3.6.1.2 Kinetic analysis of i*n vitro* reconstituted RNase P holoenzymes 70
3.6.2 Evaluation of kinetic anaylses 71

3.7 Cloning experiments 71
3.7.1 One Step inactivation of chromosomal genes in *E. coli* 71
3.7.1.1 Construction and verification of *rnpB* mutant strain BW 72
3.7.2 Plasmids for complementation studies in *E. coli rnpB* mutant strains 73
3.7.2.1 pSP64 *E. coli rnpB* EP 73
3.7.2.2 Construction of the low copy plasmid pACYC177 *Ecoli rnpB* 74
3.7.2.3 Construction of pBR322 derivatives for expression of *E. coli rnpA* 74
3.7.2.4 Construction of pBR322 encoding mutated 4.5S RNAs 75
3.7.2.5 Construction of pSP64 *B. subtilis rnpB* BPT (*B. subtilis rnpB* promoter and terminator) 76
3.7.2.6 Construction of pSP64 *B. subtilis rnpB* EP/BT *(E. coli rnpB* promoter and *B. subtilis rnpB* terminator) 77
3.7.2.7 Construction of pACYC177 *B. subtilis rnpB* EP/BT (*E. coli rnpB* promoter, *B. subtilis rnpB* terminator) 77
3.7.3 Chromosomal integration in *B. subtilis* 78
3.7.3.1 Construction of the *B. subtilis* conditional RNase P mutant strain SSB318 (done by Ciaran Condon) 78
3.7.3.2 Construction of a strain containing *E. coli rnpB* BPT integrated into the chromosome of *B. subtilis* SSB318 79
3.7.4 Plasmids for complementation studies in *B. subtilis* mutant strain SSB318 79
3.7.4.1 Construction of pHY300 *B. subtilis rnpB* BPT 79
3.7.4.2 Construction of pHY300 xylRP *B. subtilis rnpB* (xylose promoter) 80
3.7.4.3 Construction of pHY300 xylRP *B. subtilis rnpB* + xyl *rnpA* (*B. subtilis*) 81
3.7.4.4 Construction of pHY300 *S. aureus rnpB* BPT 81
3.7.4.5 Construction of pHY300 *S. aureus rnpB* BPT + xyl *B. subtilis rnpA* 82
3.7.4.6 Construction of pHY300 *E. coli rnpB* BPT 83
3.7.4.7 Construction of pHY300 *E. coli rnpB* EP 83
3.7.4.8 Construction of pHY300 *E. coli rnpB* EP + xyl *B. subtilis rnpA* 84
3.7.4.9 Construction of pHY300 + xyl *B. subtilis rnpA* 84

3.8 References 85

4 Results and Discussion 89

4.1 Type A and B RNase P RNAs are interchangeable *in vivo* despite substantial biophysical differences 91

4.2 The precursor tRNA 3'-CCA interaction with *Escherichia coli* RNase P RNA is essential for catalysis by RNase P *in vivo* 107

4.3 *In vivo* role of bacterial type B RNase P interaction with tRNA 3'-CCA 123

5 Summary 159

6 Zusammenfassung 161

7 Outlook 163

8 Appendix 165

8.1 Chemicals 165

8.2 Radioisotopes 165

8.3 Size markers 166

8.4 Enzymes 166
8.5 Equipment 166
8.6 Antibodies 167
8.7 Synthetic DNA Oligonucleotides 167
8.8 DNA/RNA-Oligonucleotides 173
8.9 Bacterial strains 173
8.10 Plasmid vectors 174
8.11 Plasmid vectors for T7 transcriptions 174
8.12 PCR Mutagenesis performed within this study 174
8.13 Abbreviations and Units 175
8.14 Index of Buffers and Solutions 177
8.15 Sequence of the *E. coli rnpB* context in strain BW 178
8.16 References 179

Acknowledgements 181

Publications arising from this work 182

Lebenslauf 183

Selbstständigkeitserklärung 184

1 Introduction

1.1 RNase P

Ribonuclease P (RNase P) is a ribonucleoprotein that is responsible for the 5'-maturation of precursor RNAs (ptRNAs), one of several post-transcriptional modifications necessary for the functional synthesis of tRNA. RNase P cleaves the 5'-leader of ptRNAs by hydrolysing the phosphodiester bond immediately 5' of the first nucleotide of mature tRNA; it produces 5'-OH and 3'-phosphate groups. tRNA processing is the most widely studied activity of RNase P, but RNase P also cleaves other substrates, such as some viral RNAs (Mans *et al.*, 1990; Hartmann *et al.*, 1995), p4.5S RNA (Peck-Miller and Altman, 1991), ptmRNA (Komine *et al.*, 1994), a few mRNAs (Li and Altman, 2003; Alifano *et al.*, 1994) and some riboswitches (Altman *et al.*, 2005).

RNase P is present in all domains of life (bacteria, archaea and eukarya). So far, all known RNase P enzymes consist of one RNA subunit and at least one protein subunit (Fig. 1.1). Some chloroplast RNase P enzymes (Wang *et al.*, 1988, Thomas *et al.*, 1995) and mitochondrial RNase of *Trypanosoma brucei* (Salavati *et al.*, 2001) are proposed to be exceptions, being putative protein enzymes.

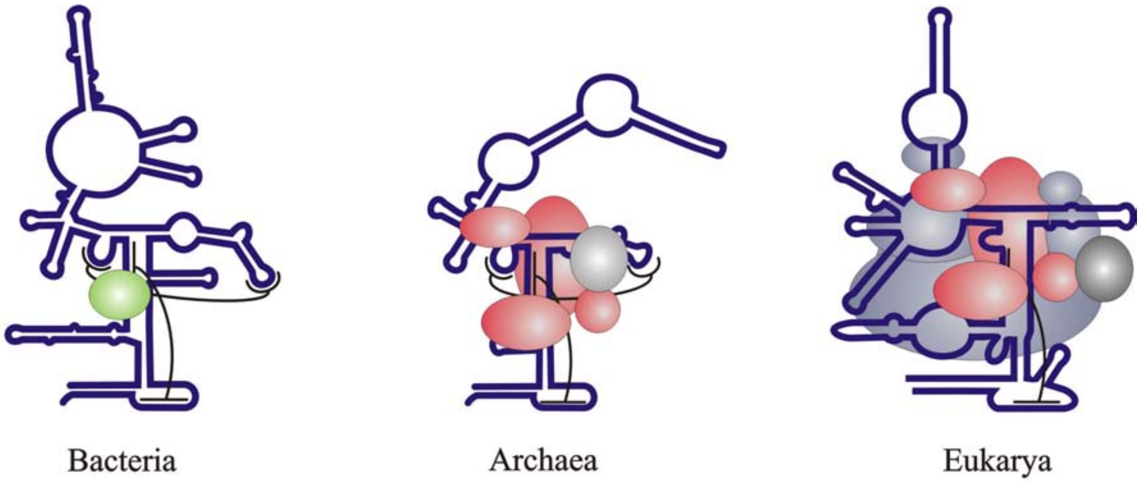

Fig. 1.1: Schematic representation of bacterial, archaeal and eukaryotic RNase P. Secondary structure of the respective exemplary RNA subunits are shown in dark blue. The green oval indicates the bacterial RNase P protein subunit. Homologous protein subunits in archaea and eukarya are drawn in red, while blue ovals represent proteins only associated with eukaryotic RNase P. Grey ovals indicate an additional protein in archaea or eukarya, which cannot be found in all representatives of the respective domain of life.

The first RNase P to be characterised was isolated from *Escherichia coli* (Altman and Smith, 1971). In general, bacterial RNase P enzymes consist of one RNA (~400 nt; ~130 kDa) and one protein subunit (~120 aa; 13-14 kDa), encoded by the *rnpB* and *rnpA* genes, respectively.

The RNA subunit is responsible for the catalytic activity (Guerrier-Takada *et al.*, 1983). Composition of RNase P from archaea and eukarya reveals increased complexity (reviewed in Walker and Engelke, 2006):

Beside one RNA subunit, archaeal RNase P enzymes have been described to consist of at least four protein subunits (Andrews *et al.*, 2001; Hartmann and Hartmann, 2003; Fukuhara *et al.*, 2006). Whereas the RNA subunit is structurally similar to bacterial RNase P RNA, the archaeal protein subunits have been identified as homologues of yeast and human RNase P proteins (Frank *et al.*, 2000; Hall und Brown, 2002).

Nuclear RNase P from yeast or human consists of one RNA subunit and nine (Chamberlain *et al.*, 1998) or ten (Jarrous und Altman, 2001; Van Eenennaam *et al.*, 1999 & 2001) associated proteins, respectively. Eukaryal RNase P proteins were shown to be essential under all conditions tested.

In bacteria (Schedl and Primakoff, 1973; Gößringer *et al.*, 2006), yeast nuclei (Lee *et al.*, 1991), human (Jarrous and Altman, 2001) and mitochondria (Morales *et al.*, 1992; 1989) RNase P has been shown to be essential.

1.2 Bacterial RNA subunit

The RNase P RNA subunit in bacteria consists of about 350-450 nucleotides. The RNA subunit has been shown to be catalytically active in the absence of the protein subunit under high salt conditions *in vitro* (Guerrier-Takada *et al.*, 1983), thus being a typical ribozyme. RNase P RNA is basically composed of two domains which can fold independent of each other (Pan, 1995; Loria and Pan, 1996): The specificity domain (S-domain) comprises helices P7-P17 and is involved in substrate binding by contacting the T-arm of ptRNA as demonstrated by biochemical experiments (Pan *et al.*, 1995; Loria and Pan, 1998) and photocrosslinking studies (Nolan *et al.*, 1993; Chen *et al.*, 1998; for details see Chapter 1.3). The catalytic domain (C-domain) is composed of helices P1–6 and P15–18. This domain contains universally conserved residues, recognizes the acceptor-stem of tRNAs and the tRNA 3’-CCA. It includes all structural elements required for catalysis, including catalytically important metal ion binding sites. RNA subunits of different bacteria share a common core; these conserved core sequences and structures, when combined in a synthetic minimal RNase P RNA, were shown to be sufficient for catalytic activity (Siegel *et al.*, 1996; Waugh *et al.*, 1989; see also bacterial minimal consensus Fig. 1.2). Only about 40 nts in bacterial RNase P RNAs are absolutely conserved based on the sequences known until now. These conserved residues are concentrated in the vicinity of the ptRNA binding interface (Haas and Brown 1998).

Most RNase P RNAs belong to the structural type A (A for ancestral) represented e.g. by *E. coli* RNase P RNA. Furthermore, in low G+C Gram-positive bacteria, such as *B. subtilis,* type B RNAs are found (Haas *et al.*, 1996). An intermediate structure (type C) is found in green non-sulfur bacteria (Haas and Brown, 1998).

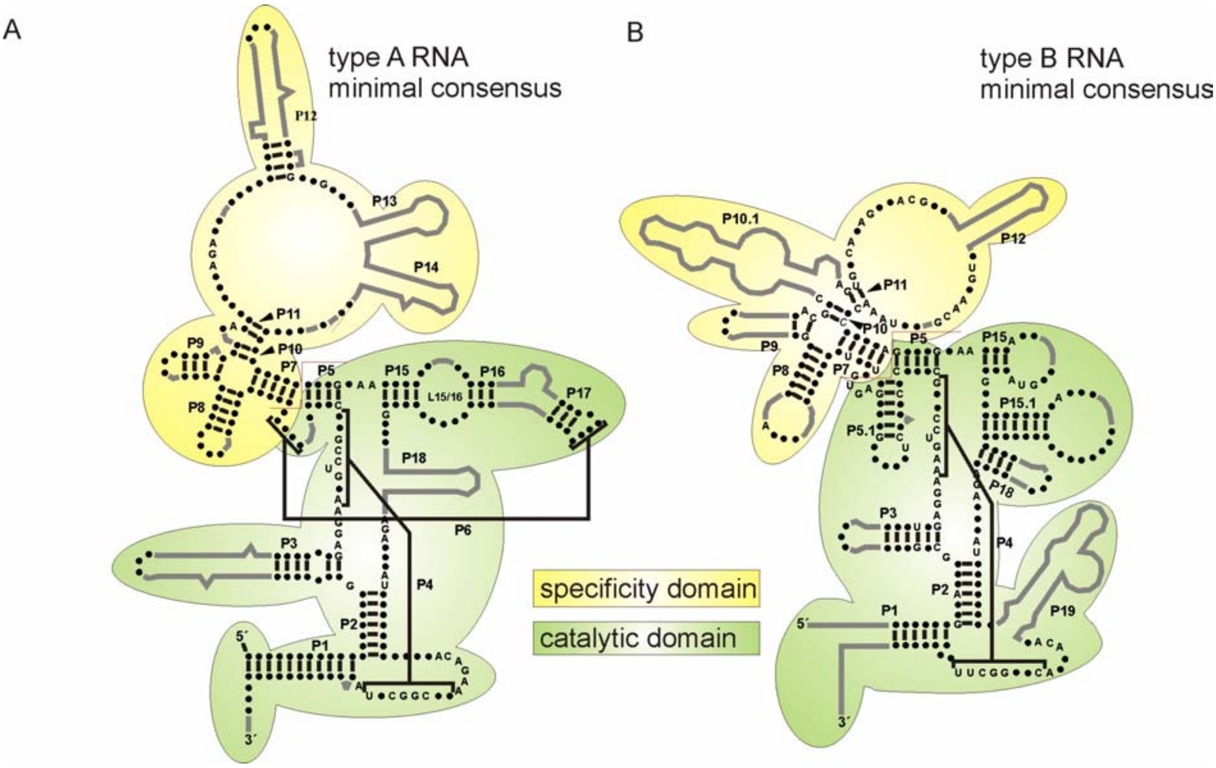
A
type A RNA
minimal consensus
P12
P13
P14
P11
P10
P9
P7
P8
P5
P15
L15/16
P16
P17
P18
P6
P3
P4
P2
P1
5´
3´
B
type B RNA
minimal consensus
P10.1
P12
P11
P10
P9
P8
P7
P5
P15
P15.1
P5.1
P18
P3
P4
P2
P1
P19
5´
3´
specificity domain
catalytic domain

Fig. 1.2: Consensus type A and type B RNase P RNAs. Invariant nucleotides are indicated by capital letters (A, G, C or U), variable nucleotides are marked as dots (●). Only nucleotide positions that are present in all members of each type of RNA are shown. Grey lines indicate elements of the *E. coli* (type A) or *B. subtilis* (type B) RNAs that are absent in some of the RNAs of each type (adapted from Haas *et al.*, 1996). The catalytic domain is highlighted in green, the specificity domain in yellow.

The structural differences between type A and type B RNAs are mainly caused by the absence and presence of helical elements. In addition, there is variation in the form of small differences in the lengths of helices, loops and joining regions (Fig. 1.2; Haas and Brown, 1998).

The main differences in secondary structure between type A and B RNAs concern helical regions which are only present in one or the other, respectively. P6, J15/16 and helix P18 are e. g. only part of *E. coli* RNase P RNA. Helix P6 of *E. coli* RNase P RNA, a pseudoknot formed by peripheral distal nucleotides, and helix P17 are thought to be replaced with helix

P5.1 in *B. subtilis* (Haas *et al.*, 1991). Helix P15 is reduced from 4 to 3 bp in type B RNA, and P16/17 are missing. Helix P18 is shortened in length in *B. subtilis*. However the helices P15.1 and P19 as additional elements in *B. subtilis* are possible to take over structural functionality.

Despite the differences in secondary structure, the overall structural arrangement of the different RNAs is very similar. This could be shown in the X-ray crystal structures of type A and type B RNase P RNA, originally only solved for the specificity domains of *Bacillus subtilis* (Krasilnikov *et al.*, 2003) and *Thermus thermophilus* (Krasilnikov *et al.*, 2004) and more recently for entire RNA subunits of *Bacillus stearothermophilus* (Kazantsev *et al.*, 2005) and *Thermotoga maritima* (Torres-Larios *et al.*, 2005). A more detailed insight into the structural features of RNase P will be given in Chapter 1.5.

1.3 General substrate recognition

RNase P cleaves various substrates (see Chapter 1.1) for which no obvious sequence similarity exists between their 5'-flanks. Therefore it is of special interest, how correct recognition and positioning of substrates is obtained.

In early studies it has been shown that introduction of mutations within the ptRNA which caused structural perturbations affected cleavage efficiency by RNase P (Altman *et al.*, 1974). This finding indicated that in general three dimensional structural features of tRNAs are recognised by RNase P (Altman *et al.*, 1993).

T-stem and T-loop (conferred to as T-arm in Fig. 1.3) form non-Watson-Crick contacts with the S-domain of the RNA subunit, which was shown by modification-interference and crosslinking studies (Kirsebom and Vioque, 1996; and references therein). Most native tRNA molecules have a 7 base pair long acceptor-stem (while $tRNA^{His}$ and $tRNA^{SeCys}$ are exceptions having an 8-bp stem). Biochemical experiments showed that the acceptor-stem is in close contact with the RNase P RNA (Harris *et al.*, 1994; Kahle *et al.*, 1990; Thurlow *et al.*, 1991) and that the length and its primary structure is a major determinant for cleavage site selection (Holm and Krupp, 1992; Kirsebom and Svärd, 1992). The coaxially stacked T-arm and acceptor-stem normally defines a distance of 12 base pairs from the T-loop to the cleavage site. This distance-ruler has been suggested to be involved in localization of the cleavage site (Kahle *et al.*, 1990; Thurlow *et al.*, 1991). The variable loop and the D-arm only play an indirect role in substrate recognition, as they are responsible for fixing the T-arm in its genuine conformation and position (Hardt *et al.*, 1993; Gaur *et al.*, 1996). The contacts with the acceptor-stem are mainly mediated by the C-domain of the RNA subunit.

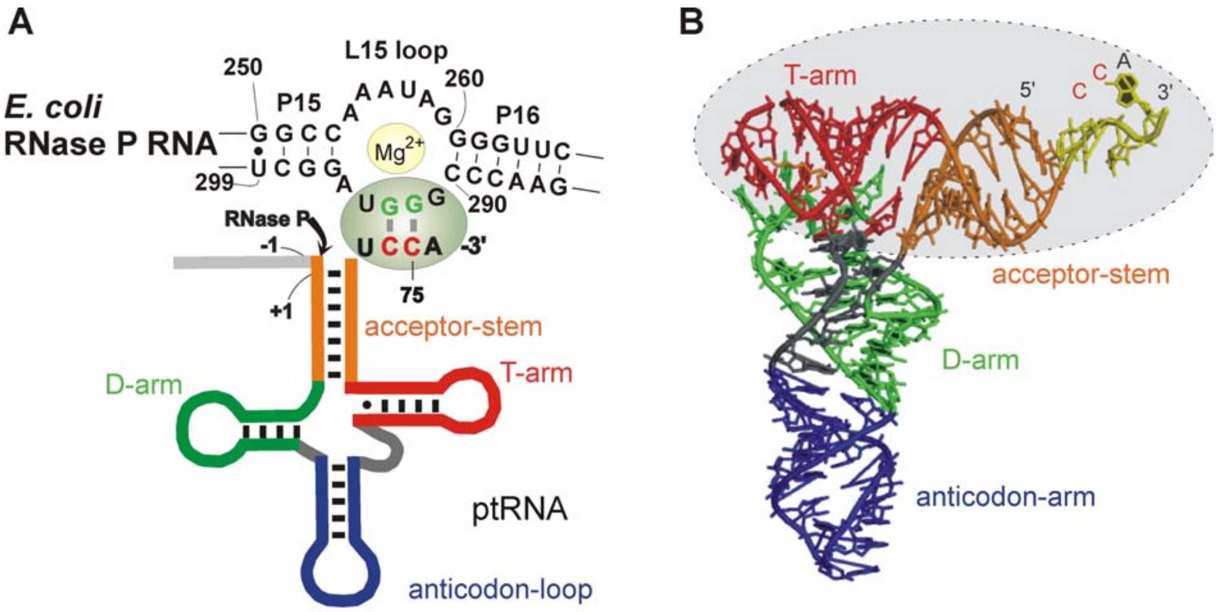
A
L15 loop
250
260
E. coli
RNase P RNA
P15
P16
A A U A
A
G
G G C C
U C G G
A
Mg2+
G G G U U C
C C C A A G
299
290
RNase P
-1
+1
U G G G
U C C A
-3'
75
acceptor-stem
T-arm
D-arm
ptRNA
anticodon-loop
B
T-arm
5'
C
C
A
3'
acceptor-stem
D-arm
anticodon-arm

Fig. 1.3: Scheme of the secondary structure of a ptRNA. The black arrow indicates the site of cleavage by RNase P. The green oval highlights the Watson-Crick base pairs formed between tRNA 3'-CCA and nucleotides G292 and G293 in loop 15 of RNase P RNA from *E. coli* (A). In panel B the tertiary structure of tRNA^{Phe} from yeast is shown; the structural domains are coloured according to the scheme in panel A. The region recognised and directly interacting with RNase P RNA is marked by the grey oval.

In 4.5S RNA, a non-tRNA substrate of *E. coli* RNase P, the terminal stem structure seems to mimic the coaxially stacked acceptor-stem and T-stem (Forster and Altman 1990; Peck-Miller and Altman, 1991).

Aside from the secondary structural features, also the base identity of positions close to the RNase P cleavage site seems to be of importance (Kirsebom and Vioque 1996 and references therein). In more than 80% of all characterised tRNAs the nucleotide at position +1 is a guanosine (Sprinzl *et al.*, 1998). Especially the identity of the G_1-C_{72} base pair was shown to be important in the RNA-alone reaction (without the protein subunit), and the +1 nucleotide was suggested to serve as guiding nucleotide (Svärd and Kirsebom 1992). However, the presence of the protein subunit seems to reduce the importance of the G_1-C_{72} base pair, as the holoenzyme, in contrast to the RNA alone, was shown to cleave substrates with other canonical and non-canonical base pairs at position 1-72 with the same efficiency as substrates containing the G_1-C_{72} base pair (Harris *et al.*, unpublished data).

1.3.1 CCA interaction

The interaction of tRNA 3'-CCA with RNase P RNA is of special interest in this study. A first hint to the involvement of the 3'-terminus in RNase P catalysis was provided in an early study demonstrating that puromycin, an analogue of the 3'-termini of aminoacyl-tRNAs, inhibits the RNase P reaction (Vioque 1989). Further experiments showed that in *E. coli* the two cytosines (position C74 and C75) of 3'-CCA of tRNAs interact with the two conserved G residues G292 and G293 in loop 15 (*E. coli* numbering), by Watson-Crick base pairing (Fig. 1.3; Kirsebom and Svärd, 1994). The importance is underlined by the fact that in *E. coli* all tRNA genes already encode 3'-CCA. This interaction provides a substantial contribution of the free energy of (p)tRNA binding *in vitro* (Hardt *et al.*, 1995; Oh *et al.*, 1998; Busch *et al.*, 2000), supports selection of the correct cleavage site (Kirsebom and Svärd, 1994) and is suggested to play a role in the binding of catalytic Mg^{2+} (Oh *et al.*, 1998; Busch *et al.*, 2000). Also non-tRNA substrates encode 3'-CCA, or in the case of 4.5S RNA 3'-CCC, and therefore allow base-pairing with the mentioned residues in loop 15.

The interactions with the T-arm, acceptor-stem and the CCA-terminus occur to the RNA subunit of RNase P. An additional contact occurs to the 5'-leader of ptRNAs, however, a function of the protein subunit of bacterial RNase P.

1.4 Role of the protein subunit

In bacteria the protein component contributes only one-tenth to the mass of the holoenzyme. However, the protein component facilitates cleavage by RNase P under physiological salt concentrations and is required for efficient tRNA processing *in vivo* (Guerrier-Takada *et al.*, 1983; Reich *et al.*, 1988; Kurz *et al.*, 1998; Kole *et al.*, 1980).

The three-dimensional structures of RNase P proteins from three different bacteria have been determined by X-ray crystallography (*Bacillus subtilis*: Stams *et al.*, 1998; *Thermotoga maritima*: Kazantsev *et al.*, 2003) or NMR (*Staphylococcus aureus*: Spitzfaden *et al.*, 2000). Based on these structures and phylogenetic conservation, three potential RNA binding motifs have been identified: an RNR-motif which consists of an ~11 aa conserved consensus sequence (Altman, 1989; Pace and Brown, 1995), a metal ion binding loop and a conserved cleft formed by an alpha helix and a four-stranded β-sheet as depicted in Fig. 1.4. The first two RNA binding motifs are thought to interact with RNase P RNA and the third with ptRNA (Niranjanakumari *et al.*, 1998; Sharkady and Nolan, 2001; Biswas *et al.*, 2000).

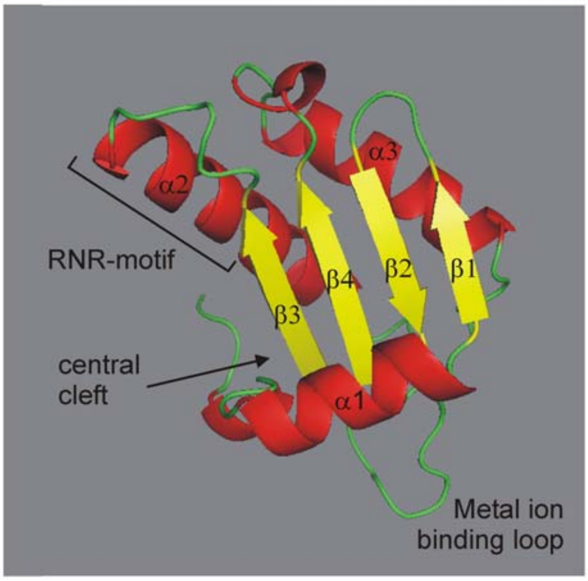
α3
α2
RNR-motif
β4
β2
β1
β3
central
cleft
α1
Metal ion
binding loop

Fig. 1.4: Three-dimensional structure of the *B. subtilis* RNase P protein. α-helices (red) and the β-sheet (yellow) are numbered sequentially from the N- to the C-terminus. The RNR-motif, the metal ion binding loop and the central cleft formed by α1 and the β-sheet are potential RNA-binding sites.

For the *B. subtilis* and *E. coli* RNase P proteins, both of which play a central role in this study, a similar fold is suggested (Fig. 1.5).

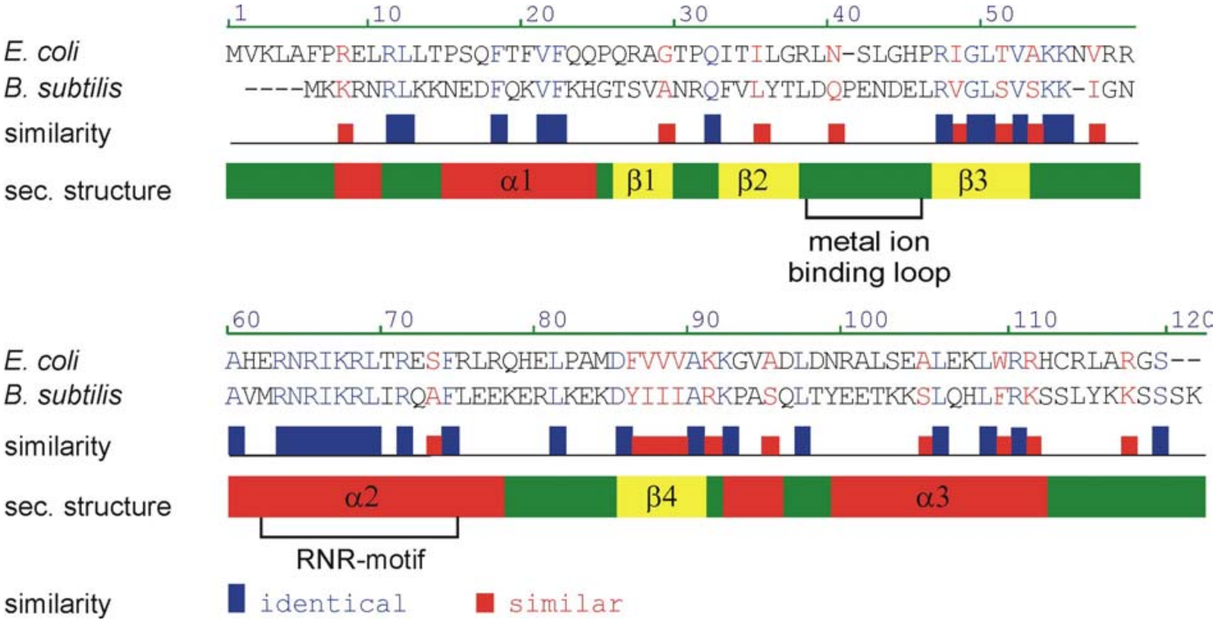
1
10
20
30
40
50
E. coli
MVKLAFPRELRLLTPSQFTFVFQQPQRAGTPQITILGRLN-SLGHPRIGLTVAKKNVRR
B. subtilis
----MKKRNRLKKNEDFQKVFKHGTSVANRQFVLYTLDQPENDELRVGLSVSKK-IGN
similarity
sec. structure
α1
β1
β2
β3
metal ion
binding loop
60
70
80
90
100
110
120
E. coli
AHERNRIKRLTRESFRLRQHELPAMDFVVVAKKGVADLDNRALSEALEKLWRRHCRLARGS--
B. subtilis
AVMRNRIKRLIRQAFLEEKERLKEKDYIIIARKPASQLTYEETKKSLQHLFRKSSLYKKSSSK
similarity
sec. structure
α2
β4
α3
RNR-motif
similarity
identical
similar

Fig. 1.5: Sequence alignment of *E. coli* and *B. subtilis* RNase P proteins done with AlignX (Invitrogen). Below the secondary structural elements found in *B. subtilis* RNase P protein are aligned. Similarity describes the degree of conservation between the two proteins (identical or similar based on physico-chemical properties).

By phosphorothioate-iodine protection assays it has been shown that the protein protects residues located in helices P2, P3 and at the periphery of P4 (Buck *et al.*, 2005b; see also Fig.

1.10). Several residues within these structural elements of the C-domain are known to be important for catalytic function, but the protein itself does not play a direct role in catalysis (Christian *et al.*, 2002 and references therein). Furthermore, binding of the protein appears to induce local conformational changes in both type A (P5-P8,L15/16) and type B (P15.1-P5.1, L15) RNA (Buck *et al.*, 2005b). Recent data also suggest a stabilization of the RNase P protein upon binding to the RNA subunit (Guo *et al.*, 2006).

The precise role of the protein subunit is still not fully clear. In some studies with the *E. coli* holoenzyme, the protein has been shown to stabilize the active tertiary structure of the RNA subunit (Guerrier-Takada *et al.*, 1983; Kim *et al.*, 1997, Westhof *et al.*, 1996). Additional experiments pointed out a role in dimer formation of the *B. subtilis* holoenzyme (Fang *et al.*, 2001) and in broadening of substrate specificity (Gopalan *et al.*, 1997; Liu and Altman, 1994). *In vitro* studies showed that the protein has profound effects on reactivity of the RNA subunit by increasing the affinity for substrate over product (Reich *et al.*, 1988; Kurz *et al.*, 1998). This effect is mainly caused by a direct protein contact to the 5'-leader (Niranjanakumari *et al.*, 1998) and may prevent inhibition of the *B. subtilis* holoenzyme by mature tRNA which *in vivo* is present in excess over ptRNA.

More recent data suggest that the protein contributes to all these effects, including enhanced specificity for ptRNA versus mature tRNA. Inconsistencies derived from various observations may be explained by structural and functional differences between type A and type B RNase P; such differences seem to reside mainly in the respective RNA subunits. For example, the P protein was shown to stabilize its RNA subunit in the *E. coli* system, while such an effect was not evident for *B. subtilis* RNase P (Buck *et al.*, 2005a).

1.5 Tertiary structure of bacterial RNase P

The recently solved crystal structures of two RNase P S-domains gave first insights into the details of RNase P RNA architecture. These S-domains of RNase P RNA from *T. thermophilus* (type A) and *B. subtilis* (type B), despite their different composition of structural elements, share a common arrangement of regions involved in ptRNA recognition, namely stems P9, P10 and P11 and the joining regions J11/12-J12/11. This creates a similar ptRNA binding interface in type A and B RNase P RNA (Fig. 1.6; Krasilnikov et, al. 2004), although the stabilisation of the similar core is achieved by different overall folds.

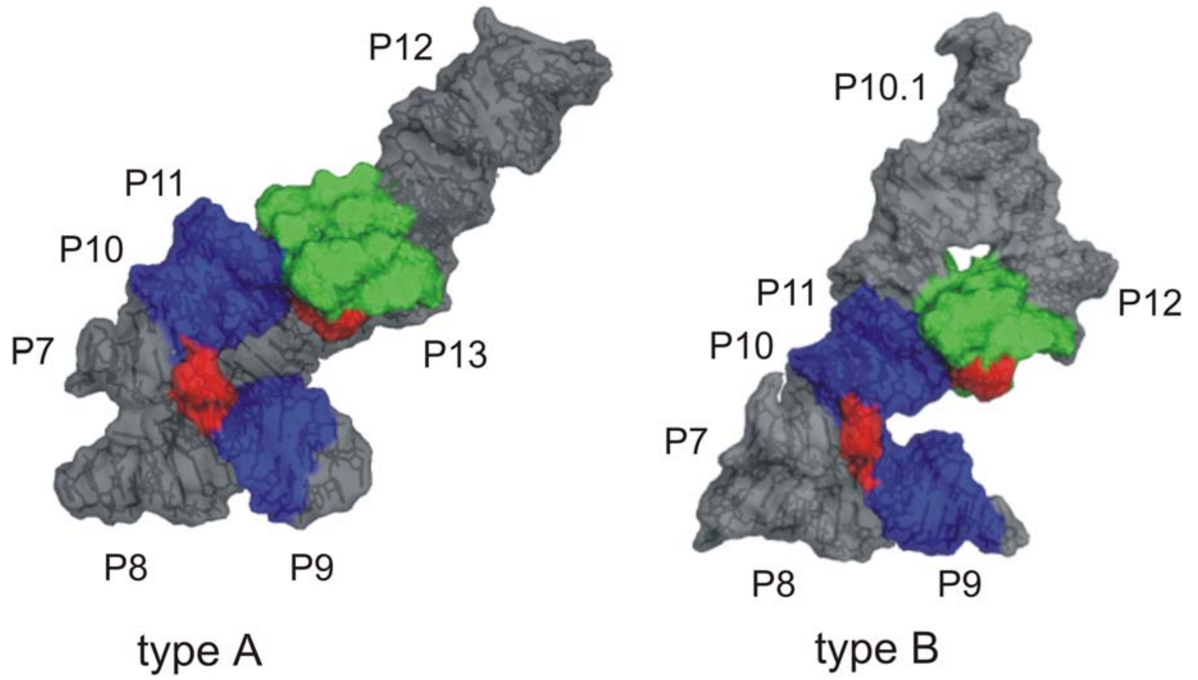

Fig. 1.6: Structural conservation of the putative ptRNA recognition interface in the S-domains of *T. thermophilus* (type A) and *B. subtilis* (type B) RNase P RNA. Region J11/12-J12/11 (green) and stems P9, P10 and P11 (blue) contain nucleotides involved in ptRNA recognition (red). ptRNA recognition regions adopt a very similar geometry but are stabilized differently (Krasilnikov *et al.*, 2004).

X-ray structures of the complete RNA subunits of *T. maritima* RNase P (Torres-Larios *et al.*, 2005) and *B. stearothermophilus* (Kazantsev *et al.*, 2005) have provided further insights into RNase P RNA architecture. Here, the structure of *T. maritima* P RNA (a representative of type A RNase P RNA) will be discussed in more detail.

The molecule is generally very flat and is built up of two layers. The larger layer consists of P1-P12 and P15-P17, including the junctions J5/15, J11/12-J12/11 and the loop L15 region. The second layer comprises P13, P14 and P18 (Fig. 1.7). S- and C-domains interact via three main tertiary interactions, P8/L18, P4/L8 and P1/L9. Most of the universally conserved regions, including the putative ptRNA binding interface, are positioned within the larger layer. The S-domain structure is essentially identical to the one from *T. thermophilus* and underscores the structural stability of the domain. The C-domain comprises several coaxially arranged helices; one helical stack is formed by P1/P4/P5 another one by P2/P3. P18 protrudes almost perpendicularly from the two afore mentioned two helical stacks, linking P2/P3 to P15/P17 stems and folding back onto the large layer by means of the L18/P8 interaction. A pseudoknot is performed between P15/P17 and P6, however, this part is not defined in the electron density map of this structure. No canonical tertiary interactions are seen between the helices forming the C-domain; however the major structural elements

(P1/P4/P5, P2/P3, P15/P16 and P18) are held together by short single-stranded joining segments, which include several highly conserved residues involved in complex interactions not resolved in this X-ray structure. P1 seems to be essential for folding, since it interacts with P9. The central organizer of the structure is the P8/P9 helical stack, while the overall structure is mainly stabilised by tetraloop-helix and A-minor interactions. The region P15/P16/P17 seems to be very dynamic in structure, because electron density could not be detected for these residues. It is suggested that this region is able to undergo slight conformational changes e.g. during holoenzyme assembly or substrate binding. The fact that the molecule crystallised as a dimer by formation of an intermolecular pseudoknot P6 raises the question about the functional significance of the structure. Packing effects can influence the arrangement of biomolecules within a crystal and may therefore distort the biologically active conformation of the observed biopolymer (Eyal *et al.*, 2005). However, the observed overall structure agrees well with the predictions based on various biochemical approaches.

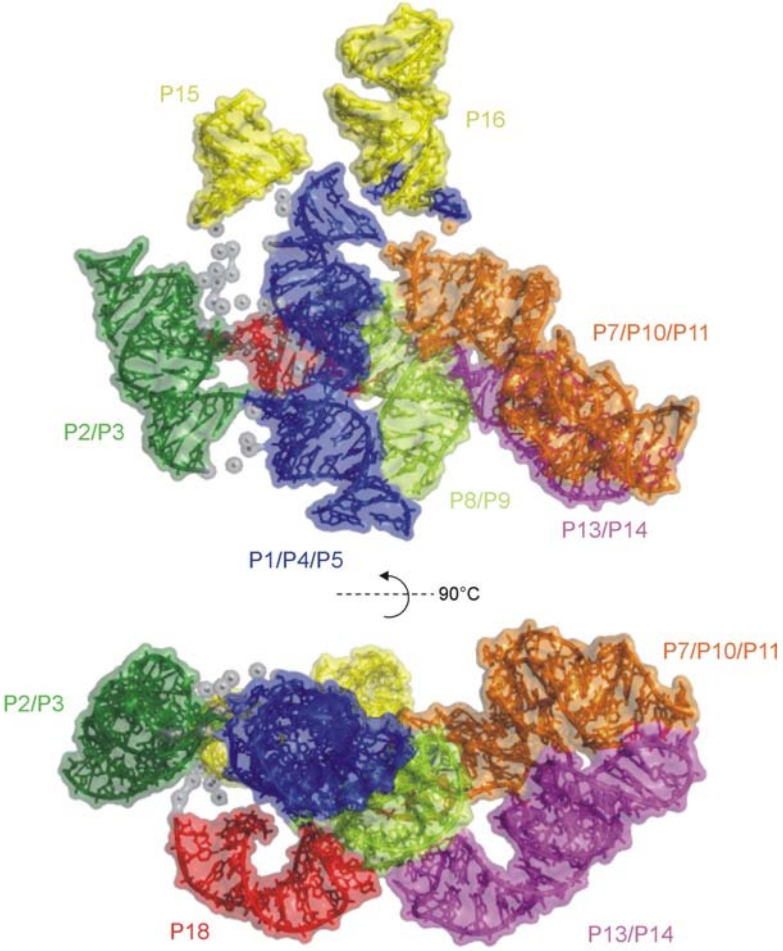

Fig. 1.7: Three-dimensional structure of *T. maritima* RNase P RNA (PDB code 2a2e) in two orthogonal views. Unconnected grey spheres indicate nucleotides, for which electron density map was insufficient to map their exact positions, likely due to increased flexibility of these residues.

The structure of *B. stearothermophilus* type B RNase P RNA has a very similar flat structure as well, consisting of mainly coaxially stacked helices held together by three long-range interactions (Kazantsev *et al.*, 2005), including a characteristic interaction between L5.1 and L15.1, a hallmark of type B RNase P RNAs. There are several structural features unique to type A or type B RNase P, as it was expected from the basic differences proposed in the secondary structure models and the already existing crystal structures of the S-domain of each type. However, particularly interesting are the similarities between the two types of RNase P. Comparison of the type A and B full-length RNA structures revealed that different structural scaffolds support similar substrate recognition surfaces in the C-domain. The highly conserved structural core element of the S- and C-domain, consisting of coaxially stacks P1/P4/P5, P2/P3, P8/P9 and P15, the J11/12-J12/11 module and a connector module between stem P3 and P4, are similar in structure and in relative orientation (Fig. 1.8 ;Torres-Larios *et al.*, 2006). According to what has been observed already in the crystal structure of the separate S-domains, a similar core seems to be stabilised by different structural features. The function of stabilization is taken over by different helical and structural elements typical either for type A or type B RNase P.

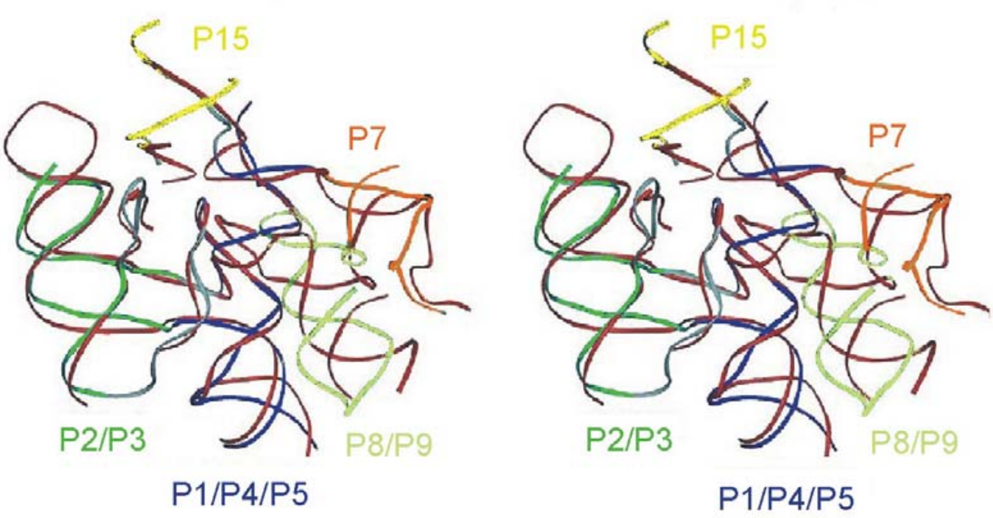

Fig. 1.8: Stereo image of the superimposition of the structural cores. The type A structure is shown using the same colours as in Fig. 1.7, whereas the type B structure is shown in red (adapted from Torres-Larios *et al.*, 2006).

Therefore, the modelling of the substrate into the RNA structure of the two types of RNase P gave very similar results. The tRNA could be positioned in such a way that the acceptor-stem lies roughly parallel to the P4 helix, while the T-arm interacts with conserved nucleotides in the S-domain as depicted in Fig. 1.9. The 5'-end of the tRNA, which corresponds to the cleavage site, lies near the universally conserved region within the C-domain, while the 3'-

end is in proximity to the L15 region which remained unresolved in both X-ray structures of RNase P RNA. The proposed models fully agree with the biochemical observations that have focussed on the RNase P RNA-substrate interaction (Christian *et al.*, 2002).

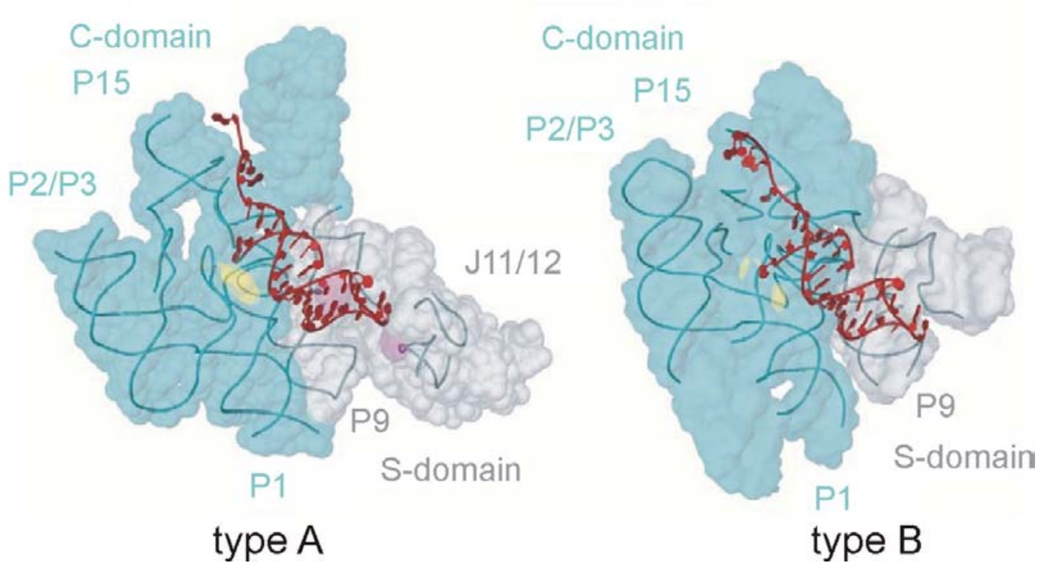

Fig. 1.9: Models of type A and B RNase P RNA-tRNA complexes. The phosphate backbone of the core of the molecules is according to those represented in Fig. 1.8. The solvent-accessible surface of the C-domain is shown in cyan and of the S-domain in grey, respectively. The acceptor-stem of the tRNA is shown in red, while the nucleotides in vicinity of the cleavage site are marked in yellow. The nucleotides marked in magenta in the type A model indicate nucleotides proposed to interact with the T-arm of the tRNA. (from Torres-Larios *et al.*, 2006)

1.6 Holoenzyme Model

Finally, the structures in combination with new protein-RNA protection data allowed to derive an updated model of the holoenyzme in complex with tRNA (Buck *et al.*, 2005b). The model is based on the *B. subtilis* RNase P protein crystal structure and the structure of *B. stearothermophilus* RNase P RNA. Residues protected by the protein occupy a region approximately the size of the protein (Fig. 1.10 A). The model places the conserved RNR-motif near helix P2 and P4 of RNase P RNA according to previous hydroxyl-radical mapping data and previous low-resolution models of the *E. coli* holoenzyme (Biswas *et al.*, 2000; Tsai *et al.*, 2003). According to a previously reported model (Kazantsev *et al.*, 2005) the tRNA has been positioned as depicted in Fig. 1.10 B. Here, the T-stem lies in the S-domain ptRNA binding interface and the 5'-end of the tRNA lies near region P4/P5. The acceptor-stem sits on the flat groove formed by the concave C-domain.

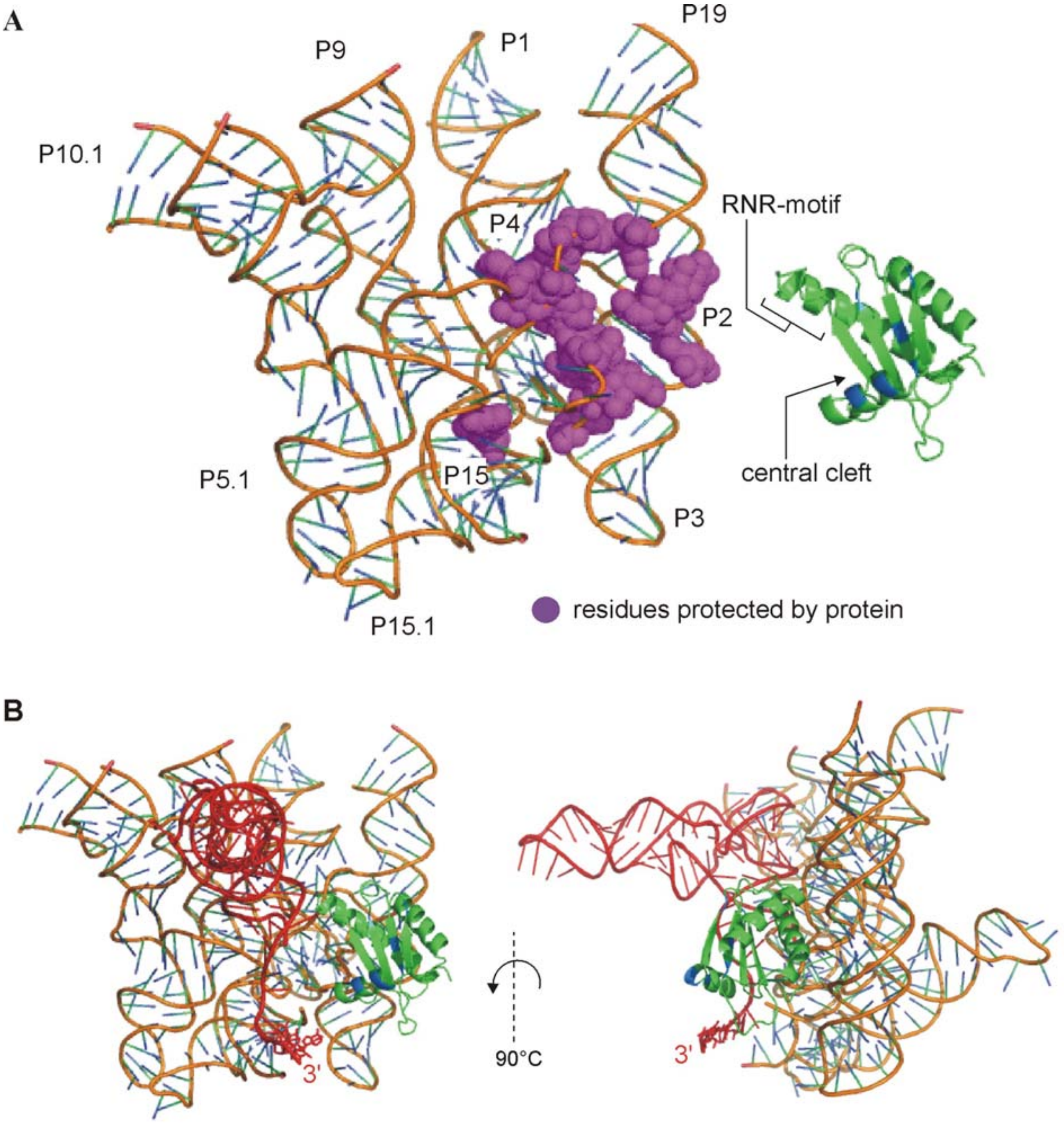

Fig. 1.10: Structure of RNase P RNA from *B. stearothermophilus* (A). Residues protected by the protein are marked in magenta. The *B. subtilis* P protein is shown in green with important features indicated; blue patches indicate amino acids that were crosslinked to the 5'-leader of ptRNA. (B) A ternary complex model in the same orientation as in panel A (left) or in orthogonal orientation (right). tRNA is shown in red. (Model from Buck *et al.*, 2005b).

According to this model, the protein recognises the 5'-leader directly, as suggested earlier, or indirectly by influencing the conformation near the cleavage site. However, further structural and biochemical analyses are necessary to get more detailed information about interactions occurring in the ternary complex of RNA-protein-ptRNA, including the mapping of catalytically important magnesium ion binding sites in order to understand the cleavage mechanism of this ribozyme.

1.7 References

Alifano, P., Rivellini, F., Piscitelli, C., Arraiano, C.M., Bruni, C.B. and Carlomagno, M.S. 1994. Ribonuclease E provides substrates for ribonuclease P-dependent processing of a polycistronic mRNA. *Genes Dev*. **8:** 3021-3031.

Altman, S. and Smith, J.D. 1971. Tyrosine tRNA precursor molecule polynucleotide sequence. *Nat. New Biol*. **62:** 1-36.

Altman, S., Bothwell, A.L.M. and Stark, B.C. 1974. Processing of *E. coli* tRNA Tyr precursor RNA *in vitro*. *Brookhaven Symp. Biol*. **26:** 12-25.

Altman, S. 1989. Ribonuclease P: an enzyme with a catalytic RNA subunit. *Adv. Enzymol. Relat. Areas. Mol. Biol.* **62:** 1-36.

Altman, S., Kirsebom, L. and Talbot, S. 1993. Recent studies of ribonuclease P. *FASEB J.* **7:** 7-14.

Altman, S., Wesolowski, D., Guerrier-Takada, C. and Li, Y. 2005. RNase P cleaves transient structures in some riboswitches. *Proc. Natl. Acad. Sci. USA* **102:** 11284-11289.

Andrews, A.J., Hall, T.A. and Brown, J.W. 2001. Characterization of RNase P holoenzymes from *Methanococcus jannaschii* and *Methanothermobacter thermoautotrophicus*. *Biol Chem.* **382**:1171-7.

Biswas, R., Ledman, D.W., Fox, R.O., Altman, S. and Gopalan, V. 2000. Mapping RNA-protein interactions in ribonuclease P from *Escherichia coli* using disulfide-linked EDTA-Fe. *J. Mol. Biol.* **296(1):**19-31.

Buck, A.H., Dalby, A.B., Poole, A.W., Kazantsev, A.V. and Pace, N.R. 2005a. Protein activation of a ribozyme: the role of bacterial RNase P protein. *EMBO J.* **24(19):** 3360-8.

Buck, A.H., Kazantsev, A.V., Dalby, A.B. and Pace, N.R. 2005b. Structural perspective on the activation of RNAse P RNA by protein. *Nat. Struct. Mol. Biol.* **12(11):** 958-64.

Busch, S., Kirsebom, L.A., Notbohm, H. and Hartmann, R.K. 2000. Differential role of the intermolecular base-pairs G292-C(75) and G293-C(74) in the reaction catalyzed by *Escherichia coli* RNase P RNA. *J. Mol. Biol.* **299:** 941-951.

Chamberlain, J.R., Lee, Y., Lane, W.S. and Engelke, D.R. 1998. Purification and characterization of the nuclear RNase P holoenzyme complex reveals extensive subunit overlap with RNase MRP. *Genes Dev*. **12(11):** 1678-1690.

Chen, J., Nolan, J.M., Harris, M.E. and Pace, N. 1998. Comparative photo-cross-linking analysis of the tertiary structures of *Escherichia coli* and *Bacillus subtilis* RNase P RNAs. *EMBO J.* **17(5):** 1515-1525.

Christian, E.L., Zahler, N.H., Kaye, N.M. and Harris, M.E. 2002. Analysis of substrate recognition by the ribonucleoprotein endonuclease RNase P. *Methods* **28:** 307-322.

Eyal, E., Gerzon, S., Potapov, V., Edelman, M. and Sobolev, V. 2005. The limit of accuracy of protein modeling: influence of crystal packing on protein structure. *J. Mol. Biol.* **351:** 431–442.

Fang, X.W., Yang, X.J., Littrell, K., Niranjanakumari, S., Thiyagarajan, P., Fierke, C.A., Sosnick, T.R. and Pan, T. 2001. The *Bacillus subtilis* RNase P holoenzyme contains two RNase P RNA and two RNase P protein subunits. *RNA* **7(2):** 233-41.

Forster, A.C. and Altman, S. 1990. External guide sequences for an RNA enzyme. *Science* **249(4970):** 783-786.

Frank, D.N., Adamidi, C., Ehringer, M.A., Pitulle, C. and Pace, N.R. 2000. Phylogenetic-comparative analysis of the eukaryal ribonuclease P RNA. *RNA* **6(12):** 1895-1904.

Fukuhara, H., Kifusa, M., Watanabe, M., Terada, A., Honda, T., Numata, T., Kakuta, Y. and Kimura M. 2006. A fifth protein subunit Ph1496p elevates the optimum temperature for the ribonuclease P activity from *Pyrococcus horikoshii* OT3. *Biochem. Biophys. Res. Commun.* **343(3):** 956-64.

Gaur, R.K., Hanne, A., Conrad, F., Kahle, D. and Krupp, G. 1996. Differences in the interaction of *Escherichia coli* RNase P RNA with tRNAs containing a short or a long extra arm. *RNA* **2(7):** 674-681.

Gopalan, V., Baxevanis, A.D., Landsman, D. and Altman, S. 1997. Analysis of the functional role of conserved residues in the protein subunit of ribonuclease P from *Escherichia coli. J. Mol. Biol.* **267(4):** 818-29.

Gößringer, M., Kretschmar-Kazemir Far, R. and Hartmann, R.K. 2006. Analysis of RNase P protein (*rnpA*) expression in *Bacillus subtilis* utilizing strains with suppressible *rnpA* expression. *J. Bacteriol.* **188(19):** 6816-23.

Guerrier-Takada, C., Gardiner, K., Marsh, T., Pace, N. and Altman, S. 1983. The RNA moiety of ribonuclease P is the catalytic subunit of the enzyme. *Cell* **35(3 Pt 2):** 849-57.

Guo, X., Campbell, F.E., Sun, L., Christian, E.L., Anderson, V.E. and Harris, M.E. 2006. RNA-dependent Folding and Stabilization of C5 Protein During Assembly of the *E. coli* RNase P Holoenzyme. *J. Mol. Biol.* **360(1):** 190-203.

Haas, E.S., Banta, A.B., Harris, J.K., Pace, N.R. and Brown, J.W. 1996. Structure and evolution of ribonuclease P RNA in Gram-positive bacteria. *Nucleic Acids Res*. **24**, 4775–4782.

Haas, E.S. and Brown, J.W. 1998. Evolutionary variation in bacterial RNase P RNAs. *Nucleic Acids Res.* **26(18):** 4093-4099

Haas, E.S., Morse, D.P., Brown, J.W., Schmidt, F.J. and Pace, N.R. 1991. Long-range structure in ribonuclease P RNA. *Science*, **254:** 853–856.

Hall, T.A. and Brown, J.W. 2002. Archaeal RNase P has multiple protein subunits homologous to eukaryotic nuclear RNase P proteins. *RNA* **8(3):** 296-306.

Hardt, W.D., Schlegl, J., Erdmann, V.A. and Hartmann, R.K. 1993. Role of the D arm and the anticodon arm in tRNA recognition by eubacterial and eukaryotic RNase P enzymes. *Biochemistry* **32(48):** 13046-13053.

Hardt, W.D., Schlegl, J., Erdmann, V.A. and Hartmann, R.K. 1995. Kinetics and thermodynamics of the RNase P RNA cleavage reaction: analysis of tRNA 3'-end variants. *J. Mol. Biol.* **247:**161-72.

Harris, M.E., Nolan, J.M., Malhotra, A., Brown, J.W., Harvey, S.C. and Pace, N.R. 1994. Use of photoaffinity crosslinking and molecular modeling to analyze the global architecture of ribonuclease P RNA. *EMBO J.* **13:** 3953-63.

Hartmann, E. and Hartmann, R.K. 2003. The enigma of ribonuclease P evolution. *Trends Genet.* **19(10):** 561-9.

Hartmann, R.K., Heinrich, J., Schlegl, J., Schuster, H. 1995. Precursor of C4 antisense RNA of bacteriophages P1 and P7 is a substrate for RNase P of *Escherichia coli*. *Proc. Natl. Acad. Sci. USA* **92:** 5822-5826.

Holm, P.S. and Krupp, G. 1992. The acceptor stem in pre-tRNAs determines the cleavage specificity of RNase P. *Nucleic Acids Res*. **20:** 421-423.

Jarrous, N. and Altman, S. 2001. Human ribonuclease P. *Methods Enzymol.* **342:** 93-100.

Kahle, D., Wehmeyer, U. and Krupp, G. 1990. Substrate recognition by RNase P and by the catalytic M1 RNA: identification of possible contact points in ptRNAs. *EMBO J.* **9:** 1929-1937.

Kazantsev, A.V., Krivenko, A.A., Harrington, D.J., Carter, R.J., Holbrook, S.R., Adams, P.D. and Pace, N.R. 2003. High-resolution structure of RNase P protein from *Thermotoga maritima*. *Proc. Natl. Acad. Sci. U S A.* **100(13):** 7497-502.

Kazantsev, A.V., Krivenko, A.A., Harrington, D.J., Holbrook, S.R., Adams, P.D. and Pace, N. R. 2005. Crystal structure of a bacterial ribonuclease P RNA. *Proc. Natl. Acad. Sci. U S A*, **102(38):** 13392-13397

Kim, J.J., Kilani, A.F., Zhan,X., Altman, S. and Liu, F. 1997. The protein cofactor allows the sequence of an RNase P ribozyme to diversify by maintaining the catalytically active structure of the enzyme. *RNA* **3(6):** 613–623.

Kirsebom, L.A. and Svärd, S.G. 1992 The kinetics and specificity of cleavage by RNase P is mainly dependent on the structure of the amino acid acceptor stem. *Nucleic Acids Res.* **20:** 425-32.

Kirsebom, L.A. and Svärd, S.G. 1994. Base pairing between *Escherichia coli* RNase P and its substrate. *EMBO J.* **13(20):** 4870-4876.

Kirsebom, L.A. and Vioque, A. 1996. RNase P from bacteria. Substrate recognition and function of the protein subunit. *Mol. Biol. Rep.* **22:** 99-109.

Kole, R., Baer, M.F., Stark, B.C. and Altman, S. 1980. *E. coli* RNase P has a required RNA component. *Cell* **19(4):** 881-887.

Komine, Y., Kitabatake, M., Yokogawa, T., Nishikawa, K. and Inokuchi, H. 1994. A tRNA-like structure is present in 10Sa RNA, a small stable RNA from *Escherichia coli*. *Proc. Natl. Acad. Sci. USA* **91:** 9223-9227.

Krasilnikov, A.S., Yang, X., Pan, T. and Mondragon, A. 2003. Crystal structure of the specificity domain of ribonuclease P. *Nature* **421(6924):** 760-764.

Krasilnikov, A.S., Xiao, Y., Pan, T. and Mondragon A. 2004. Basis for structural diversity in homologous RNAs. *Science* **306(5693):**104-7.

Kurz, J.C., Niranjanakumari, S. and Kierke, C.A. 1998. Protein component of *Bacillus subtilis* RNase P specifically enhances the affinity for precursor-tRNAAsp. *Biochemistry* **37(8):** 2393-400.

Lee, J.Y., Rohlman, C.E., Molony, L.A. and Engelke, D.R. 1991. Characterization of RPR1, an essential gene encoding the RNA component of *Saccharomyces cerevisiae* nuclear RNase P. *Mol. Cell Biol.* **11(2):** 721-730.

Li, Y. and Altman, S. 2003. A specific endoribonuclease, RNase P, affects gene expression of polycistronic operon mRNAs. *Proc. Natl. Acad. Sci. USA* **100:** 13213-13218.

Liu, F. and Altman, S. 1994. Differential evolution of substrates for an RNA enzyme in the presence and absence of its protein cofactor. *Cell* **77(7):** 1093-100.

Loria, A. and Pan, T. 1996. Domain structure of the ribozyme from eubacterial ribonuclease P. *RNA* **2(6):** 551-563.

Loria, A. and Pan, T. 1998. Recognition of the 5'-leader and the acceptor-stem of a pre-tRNA substrate by the ribozyme from *Bacillus subtilis* RNase P. *Biochemistry* **37(6):** 10126-10133.

Mans, R.M., Guerrier-Takada, C., Altman, S. and Pleij, C.W. 1990. Interaction of RNase P from *Escherichia coli* with pseudoknotted structures in viral RNAs. *Nucleic Acids Res.* **18:** 3479-3487.

Morales, M.J., Wise, C.A., Hollingsworth, M.J. and Martin, N.C. 1989. Characterization of yeast mitochondrial RNase P: an intact RNA subunit is not essential for activity *in vitro*. *Nucleic Acids Res.* **17(17):** 6865-6881.

Morales, M.J., Dang, Y.L., Lou, Y.C., Sulo, P. and Martin, N.C. 1992. A 105-kDa protein is required for yeast mitochondrial RNase P activity. *Proc. Natl. Acad. Sci. U S A* **89(20):** 9875-9879.

Niranjanakumari, S., Stams, T., Crary, S.M., Christianson, D.W., and Fierke, C.A. 1998. Protein component of the ribozyme ribonuclease P alters substrate recognition by directly contacting precursor tRNA. *Proc. Natl. Acad. Sci. U S A* **95(26):** 15212–15217.

Nolan, J.M., Burke, D.H. and Pace, N.R. 1993. Circularly permuted tRNAs as specific photoaffinity probes of ribonuclease P RNA structure. *Science* **261(5122):** 762-765.

Oh, B.K., Frank, D.N. and Pace, N.R. 1998. Participation of the 3'- CCA of tRNA in the binding of catalytic Mg^{2+} ions by ribonuclease P. *Biochemistry* **37:** 7277–7283.

Pace, N.R. and Brown, J.W. 1995. Evolutionary perspective on the structure and function of ribonuclease P, a ribozyme. *J. Bacteriol.* **177(8):** 1919-28.

Pan, T. 1995. Higher order folding and domain analysis of the ribozyme from *Bacillus subtilis* ribonuclease P. *Biochemistry* **34(3):** 902-909.

Pan, T., Loria, A. and Zhong, K. 1995. Probing of tertiary interactions in RNA: 2'-hydroxyl-base contacts between the RNase P RNA and pre-tRNA. *Proc. Natl. Acad. Sci. U S A* **92:** 12510-12514.

Peck-Miller, K.A. and Altman, S. 1991. Kinetics of the processing of the precursor to 4.5S RNA, a naturally occurring substrate for RNase P from *Escherichia coli*. *J. Mol. Biol.* **221:** 1-5.

Reich, C., Olsen, G.J., Pace, B. and Pace, N.R. 1988. Role of the protein moiety of ribonuclease P, a ribonucleoprotein enzyme. *Science* **239(4836):** 178-81.

Salavati, R., Panigrahi, A. K. and Stuart, K.D. 2001. Mitochondrial ribonuclease P activity of *Trypanosoma brucei*. *Mol. Biochem. Parasitol.* **115(1):** 109-117.

Schedl, P. and Primakoff, P. 1973. Mutants of *Escherichia coli* thermosensitive for the synthesis of transfer RNA. *Proc. Natl. Acad. Sci. U S A* **70(7):** 2091-2095.

Sharkady, S.M. and Nolan, J.M. 2001. Bacterial ribonuclease P holoenzyme crosslinking analysis reveals protein interaction sites on the RNA subunit. *Nucleic Acids Res.* **29(18):** 3848–3856.

Siegel, R.W., Banta, A.B., Haas, E.S., Brown, J.W. and Pace, N.R. 1996. *Mycoplasma fermentans* simplifies our view of the catalytic core of ribonuclease P RNA. *RNA* **2(5):** 452–462.

Spitzfaden, C., Nicholson, N., Jones, J.J., Guth, S., Lehr, R., Prescott, C.D., Hegg, L.A. and Eggleston, D.S. 2000. The structure of ribonuclease P protein from *Staphylococcus aureus* reveals a unique binding site for single-stranded RNA. *J. Mol. Biol.* **295(1):**105-15.

Sprinzl, M., Horn, C., Brown, M., Ioudovitch, A. and Steinberg, S. 1998. Compilation of tRNA sequences and sequences of tRNA genes. *Nucleic Acids Res.* **26(1):** 148–153.

Stams, T., Niranjanakumari, S., Fierke, C.A. and Christianson, D.W. 1998. Ribonuclease P protein structure: evolutionary origins in the translational apparatus. *Science* **280(5364):** 752-5.

Svärd, S.G. and Kirsebom, L.A. 1992. Several regions of a tRNA precursor determine the *Escherichia coli* RNase P cleavage site. *J. Mol. Biol.* **227(4):** 1019-31.

Svärd, S.G. and Kirsebom, L.A. 1993. Determinants of *Escherichia coli* RNase P cleavage site selection: a detailed *in vitro* and *in vivo* analysis. *Nucleic Acids Res.* **21(3):** 427-434.

Thomas, B.C., Gao, L., Stomp, D., Li, X. and Gegenheimer, P.A. 1995. Spinach chloroplast RNase P: a putative protein enzyme. *Nucleic Acids Symp. Ser.* **33:** 95-98.

Thurlow, D.L., Shilowski, D. and Marsh, T.L. 1991. Nucleotides in precursor tRNAs that are required intact for catalysis by RNase P RNAs. *Nucleic Acids Res.* **19(4):** 885-891.

Torres-Larios, A., Swinger, K.K., Krasilnikov, A.S., Pan, T. and Mondragon, A. 2005. Crystal structure of the RNA component of bacterial ribonuclease P. *Nature*, **437(7058)**: 584-587.

Torres-Larios, A., Swinger, K.K., Pan, T. and Mondrago, A. 2006. Structure of ribonuclease P - a universal ribozymes. *Curr. Opin. Struct. Biol.* **16:** 327–335

Tsai, H.Y., Masuida, B., Biswas, R., Westhof, E. and Gopalan, V. 2003. Molecular modeling of the three-dimensional structure of the bacterial RNase P holoenzyme. *J. Mol. Biol.* **325(4):** 661-75.

Van Eenenaam, H., Pruijn, G.J. and van Venrooij, W.J. 1999. hPop4: A new protein subunit of the human RNase MRP and RNase P ribonucleoprotein complexes. *Nucleic Acids Res*. **27:** 2465-2472.

Van Eenenaam, H., Jarrous, N., van Venrooij, W.J. and Pruijn, G.J. 2000. Architecture and function of the human endonucleases RNase P and RNase MRP. *IUBMB Life* **49:** 265-272.

Vioque, A. 1989. Protein synthesis inhibitors and catalytic RNA. Effect of puromycin on tRNA precursor processing by the RNA component of *Escherichia coli* RNase P. *FEBS Lett.* **246:** 137-139.

Walker, S.C. and Engelke, D.R. 2006. Ribonuclease P: the evolution of an ancient RNA enzyme. *Crit. Rev. Biochem. Mol. Biol.* **41(2):** 77-102.

Wang, M.Y., Chien, L.F. and Pan, R. L. 1988. Radiation inactivation analysis of chloroplast CF0-CF1 ATPase. *J Biol Chem*, **263(18):** 8838-8843.

Waugh, D.S., Green, C.J. and Pace, N.R. 1989. The design and catalytic properties of a simplified ribonuclease P RNA. *Science* **244:** 1569–1570.

Westhof, E., Wesolowski, D. and Altman, S. 1996. Mapping in three dimensions of regions in a catalytic RNA protected from attack by an Fe(II)-EDTA reagent. *J. Mol. Biol.* **258(4):** 600-13.

2 Goal of the Project

The Ribonuclease P (RNase P) is a ribonucleoprotein enzyme, which catalyses the 5'-maturation of precursor tRNAs (ptRNAs). Bacterial RNase P consists of one RNA subunit (P RNA; encoded by *rnpB*; ~400 nt), and a protein subunit (P protein, encoded by *rnpA*; ~120 aa). *In vitro*, under elevated salt concentrations, the RNA subunit is catalytically active. However, under physiological conditions the protein subunit is essential for activity.

Type A and B RNase P RNAs are interchangeable *in vivo* despite substantial biophysical differences

Regarding the RNA subunits of bacterial RNase P, two major structural types are known, type A (a̲ncestral; present in *E. coli*) and type B (*B̲acillus*; represented in *B. subtilis*).

One focus of this study was to examine to which extent type A and type B RNase P RNAs can take over each others function *in vivo*. For *in vivo* investigations in *B.subtilis*, the *B. subtilis rnpB* mutant strain SSB318 was characterized and employed for *in vivo* complementation analyses. *In vivo* studies in *E. coli* were initially performed in the *E. coli rnpB* mutant strain DW2, later in the newly constructed strain BW. These *in vivo* analyses are of special interest, as for *E. coli* and *B. subtilis* RNase P many differences in their biogenesis, in biochemical/biophysical properties and enzyme function *in vitro* have been reported.

The precursor tRNA 3'-CCA interaction with *Escherichia coli* RNase P RNA is essential for catalysis by RNase P *in vivo*

One well characterised P RNA-substrate contact is the Watson-Crick base pairing interaction formed between the two cytosines (position C74 and C75) of 3'-C̲C̲A of tRNAs with the G residues G292 and G293 in loop 15 (*E. coli* numbering), two residues well-conserved among bacterial P RNAs. This interaction had been mainly characterized for the RNA-alone reaction in *E. coli*, but less for the RNase P holoenzymes and not at all *in vivo*.

The *in vivo* role of the CCA interaction ought to be examined in the *E. coli rnpB* mutant strain DW2. Toward this goal, complementation efficiencies of various P RNAs carrying point mutations that interrupt the interaction with tRNA 3'-CCA had to be analysed. However, strain DW2 has the drawback, that complementation studies are performed under conditions, activating the cellular heat shock response mechanism. In addition, temperature-sensitive regulation is not reliably tight under certain circumstances. It was therefore desirable to construct a new tightly regulated *E. coli rnpB* mutant strain for our *in vivo* analyses. To be able to interpret the *in vivo* phenotypes of the mutant P RNAs, kinetic experiments with *in vitro* reconstituted holoenzymes were performed in parallel.

In vivo role of bacterial type B RNase P interaction with tRNA 3'-CCA

For type B RNase P holoenzymes it was unclear if a similar CCA contact occurs and is relevant to the catalytic cycle. This is of special interest, as in comparison to *E. coli*, an organism which encodes all tRNAs with the 3'-CCA motif, *B. subtilis* only encodes two-third of its tRNAs with 3'-CCA, while for the other tRNAs 3'-CCA is attached posttranscriptionally after 3'-end processing. The importance of the CCA interaction in *B. subtilis* was therefore central part on the experimental agenda.

For *in vivo* complementation analyses the *B. subtilis rnpB* mutant strain SSB318 was used. The *in vivo* growth phenotype associated with the expression of *B. subtilis, S. aureus* (type B P RNAs) and *E. coli* (type A P RNA) *rnpB* genes carrying point mutations that interrupt the interaction with tRNA 3'-CCA ought to be analysed. For better understanding of the *in vivo* results, the activity of *in vitro* reconstituted holoenzymes was characterised in parallel by kinetic experiments.

In the context of the importance of the CCA-interaction in *B. subtilis*, the question arose whether there is an obligatory order of processing events for precursor tRNAs in *B. subtilis*. The central issue was to find out, if ptRNAs not encoding 3'-CCA have first to undergo 3'-end processing by RNase Z in order to be efficiently cleaved by RNase P.

3 Methods

3.1 Bacterial cell cuture

All media, buffers, glass pipettes and flasks used for bacterial cell culture were autoclaved for 20 min at 121°C and 1 bar. Alternatively, heat labile solutions were sterile filtrated and glassware was sterilised by heating for at least 3 hours at 180°C.

3.1.1 Bacterial cell culture in liquid medium

LB (Luria Bertani) Medium	
Peptone	10 g/l
Yeast extract	5 g/l
NaCl	10 g/l
adjust pH to 7.5 (with NaOH)	

E. coli and *B. subtilis* cells were grown in LB medium at 37°C if not stated otherwise. For inducible promoter systems the media were supplemented for effective expression or repression with IPTG (1 mM), L(+)-arabinose (10 mM), xylose (2 % (w/v)) or glucose (2 or 0.5 % (w/v)), respectively. To select for the presence of antibiotic resistance genes, growth media were adjusted to the appropriate antibiotic concentration (see Table 3.1).

Table 3.1: Antibiotic concentrations applied for selection within this study.

Antibiotic	Bacteria	Concentration [µg/ml]	used for strain/plasmid
ampicillin	*E. coli*	100	pACYC177, pSP64, pTrc99a, pSBpt3’HH, pBR322, pHY300
tetracycline	*E. coli*	10	pBR322
	B. subtilis	30	pHY300
chloramphenicol	*E. coli*	25	BW
	E. coli	30	DW2
	B. subtilis	10	pDG364
kanamycin	*E. coli*	50	pDW160
	B. subtilis	5	pMAP65
erythromycin	*B. subtilis*	0.5	SSB318, SSB320
lincomycin	*B. subtilis*	12.5	SSB318, SSB320

For overnight cultures 3 ml LB medium were inoculated either directly from a glycerol stock or with a single colony from an agar plate, and incubated while shaking (180-220 rpm, GFL 3033 shaking incubator) at 37°C. Strains carrying plasmids temperature-sensitive for replication or temperature-sensitive mutant strains were grown at 30°C (DW2/pDW160;

pKD46) or under non-permissive conditions at 43°C (DW2/pDW160). These overnight cultures were either used directly for plasmid preparation (Mini-preps, 3.3.2.2) or transferred to a larger volume (100 ml for Midi-prep and 500 ml for Maxi-prep, 3.3.2.1) of LB medium. For long-term storage glycerol stocks were prepared by mixing 500 µl Glycerol (99 %) and 500 µl fresh bacterial culture. Glycerol stocks were frozen in liquid nitrogen and then stored at –80°C.

3.1.2 Growth curves - Determination of cell doubling time

***E. coli* DW2** cells harbouring complementation plasmids encoding *B. subtilis rnpB*wt or *E. coli rnpB*wt were tested for the loss of kanamycin resistance (loss of pDW160). Kanamycin-sensitive and ampicillin- chloramphenicol-resistant clones were grown overnight at 37°C and then diluted to a starting OD_{578} of 0.05-0.1 and grown at 37°C under aeration (180 rpm in a GFL 3033 shaking incubator). In the case of complementation with *B. subtilis rnpB*, kanamycin-sensitive clones were analysed by PCR for lack of pDW160-encoded *E. coli rnpB*.

***B. subtilis* SSB318** cells were grown overnight at 37°C in the presence of the appropriate antibiotics (Table 3.1) and 1 mM IPTG. IPTG was then removed by centrifugation (90 s, 9000 rpm, Eppendorf Minispin) and resuspension of the cell pellet in 1 ml LB without IPTG; after a second washing step the final cell pellet was then resuspended in 2 ml LB, adjusted to a starting OD_{578} of 0.05 - 0.1 in 50 ml LB and grown in the presence or absence of IPTG, without antibiotics at 37°C and 180 rpm as above. After growth curve monitoring, samples were withdrawn from the cultures, diluted and plated in parallel on plates with and without antibiotics to exclude the loss of plasmids/resistance gene markers, both types of plates containing 1 mM IPTG. Cell doubling times were derived from early exponential phases by fitting the data points to an exponential equation ($y=c\cdot e^{b\cdot x}$; c and b are constants, e is the base of the natural logarithm; function "Add a trendline" in Excel, Microsoft office). Cell doubling times were reproduced in at least 3 independent experiments.

***E. coli* BW** cells were grown overnight at 37°C in the presence of the appropriate antibiotics and 10 mM arabinose. Arabinose was washed out as described for *B. subtilis* SSB318 in the case of IPTG removal. 50 ml of prewarmed LB medium supplemented with the appropriate antibiotics and arabinose or glucose was adjusted to OD_{578} of 0.05 - 0.1 and grown at 37°C at 180 rpm as above. Cell density was measured at intervals of 0.5-1 h.

3.1.3 Cell growth on agar plates

To grow bacteria on agar plates, the LB medium was supplemented with 12 g/l Agar-Agar before autoclaving. Antibiotics were added after the medium was cooled down to 50°C to prevent inactivation of thermolabile antibiotics.

3.1.4 Preparation of competent cells

To transform foreign DNA into bacterial cells, we applied different methods:
For preparation of competent *E. coli* cells we used either treatment with special buffers or electroporation. *B. subtilis* cells were transformed either by utilising their natural competence or by electroporation.

3.1.4.1 Preparation of chemically competent *E. coli* cells, RbCl method

TFB1-Solution	
MOPS	10 mM
RbCl	10 mM
pH 7.0 with NaOH	
sterile filter, as MOPS precipitates during autoclaving	

TFB3-Solution	
MOPS	100 mM
$CaCl_2$	50 mM
KCl	10 mM
Glycerol	15 % (w/v)
pH 6.5 with NaOH	
sterile filter, as MOPS precipitates during autoclaving	

100 ml LB medium were inoculated with 3 ml overnight culture and incubated at 37°C and 180 rpm until OD_{578} reached 0.5-0.6. Cells were kept on ice for 5-10 min and then centrifuged for 5 min at 4°C and 6000 rpm (Eppendorf 5810R). Cell pellets were resuspended in 30 ml TFB1 solution, incubated for 5 min on ice and centrifuged again. The supernatant was discarded and the cell pellet was resuspended in 4 ml TFB3 solution. Aliquots of 200 µl cell suspension were frozen in liquid nitrogen and stored at –80°C.

3.1.4.2 Preparation of electrocompetent *E. coli* cells

Preparation was done according to the protocol provided in the manual of the electroporator GenePulser, Fa. Biorad.
500 ml LB medium were inoculated with 3 ml overnight culture and incubated at 37°C and 180 rpm. For temperature-sensitive strains temperature was adjusted to the permissive temperature of the respective strain. Cells were grown to an OD_{578} of 0.5-0.7, incubated on

ice for 20 min and then centrifuged for 15 min at 4°C, 4000 rpm (Eppendorf 5810R). The supernatant was discarded and the cell pellet was resuspended in 500 ml ice-cold 10 % (v/v) glycerol. After centrifugation cells were washed a second time with 250 ml and a third time with 50 ml 10 % (v/v) glycerol. Finally the cell pellet was resuspended in 2 ml 10 % (v/v) glycerol, and 200 µl aliquots were frozen in liquid nitrogen and stored at –80°C.

3.1.4.3 Preparation of electrocompetent *B. subtilis* cells

Growth Medium (electrocompetent cells *B. subtilis*)	
LB Medium with	
Sorbitol	0.5 M

Washing solution (electrocompetent cells *B. subtilis*)	
Glycerol	10 % (w/v)
Sorbitol	0.5 M
Mannitol	0.5 M
Use double-distilled water!	

Preparation was done according to the protocol provided in the manual of the Multiporator®, Fa. Eppendorf.

500 ml LB medium (containing 0.5 M sorbitol) were inoculated with 30 ml preculture and grown at 37°C and 180 rpm until OD_{578} reached 0.85-0.95. Cells were cooled for 10 min on ice and then centrifuged for 10 min at 4°C and 4000 rpm. Cells were washed four times with washing solution and finally resuspended in 8 ml washing solution. Aliquots of 200 µl were frozen in liquid nitrogen and stored at –80°C.

3.1.4.4 Natural competence - *B. subtilis*

3.1.4.4.1 HS/LS medium method

HS Medium	
ddH_2O	59.6 ml
10 x S-base	8 ml
Arg/His-Mix	8 ml
10 % Yeast extract (w/v)	800 µl
1 % L-Tryptophane (w/v)	400 µl
1 % L-Phenylalanine (w/v)	400 µl
20 % Peptone (w/v)	80 µl

LS Medium	
ddH_2O	17.2 ml
10 x S-base	2 ml
50 % Glucose (w/v)	200 µl
10 % Yeast extract (w/v)	200 µl
50 mM Spermine	200 µl
1 M $MgCl_2$	50 µl
1 % L-Tryptophane (w/v)	10 µl
1 % L-Phenylalanine (w/v)	10 µl
20 % Peptone (w/v)	10 µl

Arg/His-Mix	
L-Arginine	8 g
L-Histidine	0.4 g
adjust pH to 7.0 with H_3PO_4	
ddH_2O	ad 100 ml

10 x S-Base	
$(NH_4)_2SO_4$	2 g
K_2HPO_4	14 g
KH_2PO_4	6 g
$Na_3Citrat \cdot 2H_2O$	1 g
ddH_2O	ad 100 ml, then autoclave
add 100 µl 1M $MgSO_4$ and readjust the total volume to 100 ml	

An extremely efficient method, although more time consuming as cells cannot be stored and have to be freshly grown each time, is growing *B. subtilis* cells in HS and LS medium to make them competent.

B. subtilis cells were grown overnight at 37°C in HS medium (according to Spizizen, 1958; modified) in the presence of appropriate antibiotics if required (0.5 µg/ml erythromycin, 12.5 µg/ml lincomycin and 1 mM IPTG for SSB318, see also Table 3.1). The cell culture was then diluted into 20 ml of LS medium (modified Spizizen minimal salts; Spizizen, 1958) to a starting OD_{578} of 0.05 - 0.1. Cells were then grown to an OD_{578} of 0.5 - 0.7 at 30°C while shaking at 100 rpm (GFL 3033 shaking incubator). For transformation approximately 0.5- 1 µg DNA was added to 1 ml of this culture which was grown for another 1 to 2 h at 37°C under shaking at 900 rpm (Eppendorf Thermoshaker). Cells were plated on agar plates with antibiotics and inductor if required.

For direct complementation tests after transformation, cells were washed once by centrifugation (1 min, 6000 rpm, Eppendorf Minispin) and resuspension in 1 ml LB medium to remove the inductor IPTG.

To monitor complementation efficiency in SSB318, cells were plated in parallel on LB agar plates with or without 1 mM IPTG and supplemented with the respective antibiotics (Table 3.1). In cases of low transformation efficiency, cells were first plated only in the presence of IPTG and afterwards single colonies were resuspended in 600 µl LB medium and plated in appropriate (e.g. 1:50) dilution in parallel on LB agar plates with or without 1 mM IPTG as described above.

For transformation of pDG364 derivatives, cells were plated on media containing 0.5 µg/ml erythromycin, 12.5 µg/ml lincomycin, 10 µg/ml chloramphenicol (resistance encoded by pDG364) and 1 mM IPTG.

3.1.4.4.2 SpC/SpII medium method

SpC Medium	
T-Base	20 ml
50 % Glucose (w/v)	0.2 ml
1.2 % $MgSO_4 \cdot 7\,H_2O$ (w/v)	0.3 ml
1 % Peptone (w/v)	0.5 ml
10 % Yeast extract (w/v)	0.4 ml

SpII Medium	
T-Base	200 ml
50 % Glucose (w/v)	2 ml
1.2 % $MgSO_4 \cdot 7\,H_2O$ (w/v)	14 ml
1 % Peptone (w/v)	2 ml
10 % Yeast extract (w/v)	2 ml
0.1 M $CaCl_2$	1 ml

T-Base	
$(NH_4)_2SO_4$	2 g
$K_2HPO_4 \cdot H_2O$	18.3 g
KH_2PO_4	6 g
$Na_3Citrat \cdot 2H_2O$	1 g
ddH_2O	ad 1000 ml
autoclave and readjust volume	

This protocol is suited for the preparation of competent *B. subtilis* cells for long-term storage (up to several months).

A single colony was inoculated in 3 ml SpC medium supplemented with the respective antibiotics and inductors and grown overnight at 37°C and 180 rpm (GFL 3033 shaking incubator). In the morning the preculture was transferred into 20 ml prewarmed SpC medium and grown at 37°C and 180 rpm until an OD_{578} of 1.0 was reached. 5 ml of this culture were then transferred into 45 ml of SpII medium and incubated for 90 min at 37°C under shaking at 180 rpm. Cells were centrifuged for 5 min at 20°C and 6000 rpm, and finally resuspended in 4.5 ml of their supernatant (this is extremely important, as the supernatant contains the competence factors required for efficient transformation) and 0.5 ml 99 % glycerol. Aliquots of 100 µl were frozen in liquid nitrogen and stored at –80°C.

For transformation, 0.5-1.0 µg DNA were added to 100 µl cells and the cell suspension was shaken at 900 rpm for 2 h at 37°C. Cells were plated on plates containing the appropriate supplements.

3.1.5 Transformation

SOC Medium	
Peptone	20 g
Yeast extract	5 g
NaCl	0.6 g
KCl	0.17 g
adjust to pH 7.5 with NaOH and autoclave	
Glucose (autoclave separately)	20 mM
$MgCl_2$	10 mM
$MgSO_4$	10 mM
Magnesium salts (sterile filtered stock solutions) are added prior to use	

3.1.5.1 Transformation of chemically competent *E. coli* cells

10 ng DNA or 5 µl of a ligation or *Dpn* I mutagenesis reaction were added to 50 µl competent cells (chapter 3.1.4.1). Cells were incubated on ice for 30 min. A heat shock was performed for 45 s at 42°C. After another 2 min incubation on ice, 800 µl SOC medium were added and cells were incubated for 1 h at 37°C while shaking. In cases of low transformation efficiency all cells were plated. For this purpose, cells were centrifuged for 30 s, 9000 rpm (Eppendorf Minispin), resuspended in 50-100 µl of their supernatant and plated.

3.1.5.2 Transformation of electrocompetent *E. coli* cells

Recombinant DNA (10 ng) was introduced into electrocompetent cells by electroporation, using a Biorad GenePulser. For this purpose, 10 ng DNA were mixed with 30 µl cells (chapter 3.1.4.2), transferred into a cuvette (1 mm gap) and incubated on ice for ~1 min. After the pulse (1.8 kV; 5 ms, 50 µF, 100 Ω), 1 ml SOC medium (supplemented with 10 mM arabinose for strain BW) was added and cells were shaken at 37°C (or 30°C for the temperature-sensitive strain DW2) for 1 h. Cell suspensions were plated directly at appropriate dilutions on LB agar plates containing the appropriate antibiotics.

3.1.5.3 Transformation of electrocompetent *B. subtilis* cells

Outgrowth Medium (electrocompetent cells *B. subtilis*)	
LB Medium with	
Sorbitol	0.5 M
Mannit	0.38 M

60 µl competent cells (chapter 3.1.4.3) were thawed on ice and mixed with 1-2 µg plasmid DNA, transferred into a electroporation cuvette (2 mm gap) and incubated for 3-5 min on ice. The electric pulse was performed at 2.1 kV (or varied from 1.8-2.5 if required), 25 µF and 100 Ω for 5 ms. Directly after the pulse 3 ml outgrowth medium (supplemented with IPTG for strain SSB318) was added and incubated for 1 h at 37°C, 900 rpm (Eppendorf Thermoshaker). To plate the entire transformation sample, cells were centrifuged and resuspended in a smaller volume.

3.1.6 *In vivo* complementation tests

For complementation studies the inductor which was added after transformation was removed by washing the cells 1-2 times by successive centrifugation (1 min, 6000 rpm, Eppendorf Minispin) and resuspension in 1 ml LB medium. Those cells were plated on agar plates with inductor (arabinose, xylose or IPTG) or 0.5 % (v/v) (*E. coli*)/ 2 % (v/v) (*B. subtilis*) glucose for catabolite repression in strains with IPTG/arabinose inducible promoter systems, followed by incubation at 37°C for 20 to 60 h.

In the case of temperature-sensitive strains like DW2 a set of plates was incubated in parallel at 30 and 43°C. For elimination of pDW160, DW2/pDW160 cells harbouring a second complementation plasmid (pACYC177 or pSP64 derivatives carrying a functional *rnpB* gene) were grown at 43°C and then tested for loss of pDW160-encoded kanamycin resistance (50 µg/ml).

For complementation analysis it was important that comparable numbers of colonies grew under permissive and non-permissive conditions. Retarded growth was regarded as a defective phenotype.

In some cases of low transformation efficiency, single colonies were resuspended in 0.6-1 ml LB medium and replated in appropriate dilution.

3.2 General nucleic acids techniques

3.2.1 Nucleic acid gel electrophoresis

Electrophoresis is the separation of charged particles within an electric field. Separation efficiency of macromolecules correlates with differences in size and charge. Electrophoretic mobility is proportional to the field strength and the net charge of the molecule.

3.2.1.1 Agarose gel electrophoresis

5 x TBE buffer	c_{End}	5 liters
Tris	445 mM	269.54 g
Boric acid	445 mM	137.57 g
EDTA	10 mM	18.61 g

5 x DNA sample buffer	
Bromophenol blue (BPB)	0.25 % (w/v)
Xylene cyanol blue (XCB)	0.25 % (w/v)
Glycerol	25 % (w/v)
In 5 x TBE buffer; pH 8.0	

Agarose gels were mainly used for separation of DNA fragments. Agarose is a polysaccharide (composed of galactose and galactose derivatives). For gel preparation agarose is dissolved in 1 x TBE buffer by heating (e.g. in a microwave). When the gel solution has cooled down to about 50-60°C, ethidium bromide is added to a final concentration of 40 µg/100 ml, and the solution is poured into a prepared gel tray with comb. Agarose concentrations are chosen according to the size of the expected fragments (see Table 3.2). Electrophoresis chambers are also filled with 1 x TBE buffer. Before loading, 1 volume DNA loading buffer is mixed with 4 volumes of the sample. Gels are run at 7.5 mA/cm.

Table 3.2. Separation range of DNA fragments in agarose gels of different concentration

% agarose (w/v)	DNA fragment size (kbp)
0.5	1.0-30
0.7	0.8 - 12
1.0	0.5 - 7
1.2	0.4 – 6.0
1.5	0.2 – 3.0
2.0	0.1 – 2.0

3.2.1.1.1 Crystal violet gels

In some cases it is necessary to avoid ethidium bromide for preparative gels, as ethidium bromide is mutagenic. Moreover, DNA fragments stained with ethidium bromide are only visible under UV light, which may induce mutations. To circumvent this problem, crystal violet at a final concentration of 10 µg/ml (stock solution 10 mg/ml) is added to the agarose gel solution as well as to the running buffer. Migrating DNA is visible as a dark violet band. Staining with crystal violet is less sensitive compared to ethidium bromide staining, which has to be taken into account when chosing the pocket size in relation to the amount of DNA.

3.2.1.2 Polyacrylamide gel electrophoresis (PAGE)

Polyacrylamide (PAA) is a cross-linked polymer of acrylamide; the crosslinks are introduced by bisacrylamide. Unpolymerized polyacrylamide is a neurotoxin, therefore it has to be handled extremely carefully. Polymerisation of polyacrylamide is initiated by addition of APS (Ammonium persulfate, $(NH_4)_2S_2O_8$) and TEMED (N,N,N,N,-Tetramethylethylendiamin). In aqueous solution APS forms radicals, which react with PAA. TEMED also serves as a catalyst, as it alleviates radical formation of APS while self being more stable as a radical.

The length of the polymer chains and therefore the pore size is dictated by the concentration of acrylamide used, which is typically between 3.5 and 20 %, and by the ratio of acrylamide – bisacrylamide (48:2 in our lab).

3.2.1.2.1 Denaturing PAGE

5 x TBE, see Agarose gel electrophoresis, 3.2.1.1

denaturing sample buffer	
3 x Stock solution sample buffer	
Urea (f. c. = 8 M)	0.48 g
5 x TBE	200µl
Bromophenol blue (BPB)	0.001 % (w/v)
Xylene cyanol blue (XCB)	0.001 % (w/v)
H_2O	ad 1 ml
Before use mix **1 ml of 3 x Stock solution sample buffer** with **2 ml formamide → 1 x buffer**	
For kinetic analyses **504 µl 1 x buffer** was supplemented with **156 µl EDTA (0.5 M, pH 8)**, in order to complex magnesium, which is required for RNase P catalysis.	

PAA gel solution	c_{End}	20 %	10 %
5 x TBE	1 x TBE	200 ml	200 ml
Acrylamide (48 %)/ Bisacrylamide (2 %)	in appropriate concentration	400 ml	200 ml
Urea	8 M	480 g	480 g
H_2O		ad 1000 ml	ad 1000 ml

In denaturing gels the native structure of macromolecules that run within the gel is disrupted. PAA gels are usually supplemented with 8 M urea or another denaturing substance (e.g. formamide) before polymerisation.

Table 3.3 indicates the fragment sizes of single-stranded DNA that comigrate with the BPB and XCB dyes of the sample buffer in denaturing polyacrylamide gels of different percentage; According to this, tRNAs used in this study (~95 nt) where usually analysed on 8-10 % gels and RNase P RNAs (~400 nt) on 5-8 % gels.

Table 3.3. The size of single-stranded DNA fragments (given in nucleotides) comigrating with the dyes of the sample buffer in denaturing polyacrylamide gels.

% Polyacrylamide	Bromophenol blue	Xylene cyanol
5	35	130
6	26	106
8	19	70-80
10	12	55
20	8	25

For preparation of a PAA gel solution (usually 20 %), urea was dissolved in the appropriate volume of 5 x TBE and the required volume of Acrylamide/Bisacrylamide stock solution was added. The final volume was adjusted with distilled water if necessary. For gel preparation glass plates were cleaned with 70 % ethanol and assembled with spacers. For PAA gel solutions of < 20 %, the 20 % PAA gel solution (see above) was diluted by addition of the appropriate volume of 8 M urea in 1 x TBE. Polymerisation was initiated by mixing with 1/100 volume 10 % (w/v) APS and 1/1000 volume TEMED. The gel solution was poured between the clamped glass plates, and a comb was inserted between the glass plates at the top, to create pockets for later sample loading. After polymerisation (approximately 1 h), the comb was removed, and pockets were immediately rinsed using a syringe filled with 1 x TBE buffer to remove urea that diffuses from the gel matrix and tends to accumulate in the pockets, and to avoid later polymerisation of unpolymerised acrylamide within the pockets. The glass plates containing the gel were fixed in the electrophoresis equipment to bridge the buffer reservoirs filled with 1 x TBE buffer and electrophoresis was performed at 5–30 mA (depending on gel size and PAA concentration).

3.2.1.2.2 Native polyacrylamide gels

Native gels are non-denaturating as they do not contain any denaturing agent. They are commonly used for the separation of double-stranded DNA or folded RNAs. The migration mobility thus depends not only on the size but also the secondary/tertiary structure of the nucleic acid. This can result in substantial migration differences between fragments of the same size, but different structure. In Table 3.4 the approximate sizes of DNA fragments (in base pairs) that comigrate with the two dyes of the sample buffer in non-denaturing polyacrylamide gels of different concentration are listed:

Table 3.4. The size of DNA fragments (given in base pairs) comigrating with the dyes of the sample buffer in non-denaturing polyacrylamide gels.

% polyacrylamide	Bromophenol blue	Xylene cyanol
3.5	100	460
5	65	260
8	45	160
12	20	70
20	12	45

The PAA gel solution for native gels was the same as for denaturing PAA gels except for the omission of urea. The preparation of the gels was identical to the procedure described for denaturing gels. As sample buffer 5 x DNA sample buffer (see chapter 3.2.1.1) was used.

3.2.1.2.3 Non-denaturing polyacrylamide gel electrophoresis for RNA folding analysis

2 x native loading buffer	
Glycerol	10 % (v/v)
$MgCl_2$	2 or 10 mM
Bromophenol blue	0.025 % (w/v)
Xylene cyanol	0.025 % (w/v)

10 x THE buffer	c_{End}	1 liter
Tris	660 mM	38.98 g
Hepes	330 mM	157.28 g
EDTA	1 mM	0.37 g
For folding experiments 1 x THE buffer was supplemented with 100 mM NH_4OAc and 0.3-10 mM $MgCl_2$.		

PAA gel solution	c_{End}	11.25 %
10 x THE buffer	1 x THE	10 ml
2 M NH_4OAc	100 mM	5 ml
2 M $MgCl_2$	0.3 - 10 mM	x µl
Acrylamide (48 %)/ bisacrylamide (2 %)	4.5-20 %	22.5 ml
H_2O		ad 100 ml

For RNA folding assays a special buffer system for native gels was used (adapted from Buck *et al.*, 2005a). Mg^{2+}-ions and monovalent cations as NH_4^+ are involved in stabilisation of RNA tertiary structures. As bound ions they may dissociate irreversibly during electrophoresis, resulting in changes in the tertiary structure of RNA. To prevent this effect, the running buffer and gel solution were supplemented with 100 mM NH_4OAc and varying amounts (0.3 – 10 mM) of $MgCl_2$. Samples were diluted with an equal amount of 2 x native loading buffer and loaded on thin (< 1 mm) polyarylamide gels. Gels were run in a 4°C cold room. Internal gel temperature did not exceed 15°C during electrophoresis. Usually 180-240 V were applied.

3.2.1.3 Detection of nucleic acids from gels

To visualize DNA/RNA within gels, different methods were used depending on the experimental context and downstream application.

3.2.1.3.1 Ethidium bromide staining

Ethidium bromide intercalates between the stacked bases of DNA and RNA. When excited by UV light between 254 nm (short wave) and 366 nm (long wave) it emits fluorescent light at 590 nm (orange).

For staining DNA in agarose gels, the agarose gel solution was supplemented with 40 mg/100 ml ethidium bromide as described in chapter 3.2.1.1. Therefore, DNA fragments could be visualized directly after or even during electrophoresis using an UV transilluminator.

For visualisation of DNA/RNA in PAA gels, glass plates were removed after electrophoresis. Gels were carefully inserted into plastic bags, ethidium bromide staining solution (0.5 µg/ml in 1 x TBE) was added, bags were sealed and incubated while shaking for 10 min at room temperature. Staining solution was carefully removed and gels were analysed using an UV transilluminator.

3.2.1.3.2 UV-shadowing

Especially for preparative purposes, DNA and RNA in PAA gels was visualized by UV-shadowing (254 nm). After electrophoresis glass plates were removed and the gel was wrapped in clingfilm. The wrapped gel was then placed on a thinlayer chromatography plate with fluorescence indicator (254 nm). Nucleic acid bands were visualized by focussing a hand-held UV light source (254 nm) on the surface of the gel; DNA/RNA appears as dark band, since the nucleic acids absorb the UV light and fluorescence is extinguished. Time of UV exposure was kept as short as possible, as UV light might induce damages to DNA/RNA. Bands were marked with an overhead marker, carefully cut out and eluted by diffusion as described in chapter 3.2.4.

3.2.1.3.3 Visualization using crystal violet

To avoid the use of UV radiation and the fluorescent dye ethidium bromide for visualisation and subsequent extraction of DNA from agarose gels, crystal violet was used. Crystal violet binds to DNA via electrostatic interactions. In some cases cloning efficiency could be improved by this procedure.

As described for crystal violet agarose gels (3.2.1.1.1), gel solution and electrophoresis buffer were supplemented with 1/1000 of a 10 mg/ml aqueous crystal violet solution. Bands could be detected under normal light and appeared as dark violet bands. The detection limit of crystal violet staining (~50 ng/1 cm band) is below that of ethidium bromide staining (10 ng/1 cm band), therefore the pocket width had to be reduced with decreasing amounts of DNA.

3.2.1.3.4 Radioluminography

^{32}P- labelled RNA or DNA was detected using a phosphoimager. For this purpose, the gel was wrapped in clingfilm, and then an image plate was exposed to it. Depending on the amount of radioactivity, exposition times varied (e.g. a 1-min exposure for labelling reactions and overnight exposure for kinetic analyses with radiolabelled substrate). For preparative radioactive gels, stickers with radioactive signs serving as alignment marks are attached to the wrapped gel beside the expected bands to define their location. The imaging plate was scanned using a BIO-imaging analyser BAS 1000 (Raytest, Fujifilm) and the PC-BAS software. Further evaluation was done with the software AIDA.

3.2.2 Photometric concentration determination of nucleic acids

The concentration of nucleic acids was determined by measuring the absorption at 260 nm. Concentration could be calculated according to the Lambert Beer law:

$A = \varepsilon \cdot c \cdot d$

(A: Absorbance; c: molar concentration of DNA/RNA [mol/l]; ε: molar extinction coefficient [1/(M·cm)]; d: path length of the cuvette [cm])

Samples were diluted 1:70 –1:600 in water (depending on the expected concentration) and the absorbance at 260 nm was measured against water using a UV spectrophotometer. The concentration was calculated using the known values c(1 A_{260}) that represent the concentration corresponding to one absorbance unit at 260 nm (1 A_{260}):

1 A_{260} **double-stranded DNA**	corresponds to a c(1 A_{260}) of ~ 50 µg / ml
1 A_{260} **single-stranded DNA**	corresponds to a c(1 A_{260}) of ~ 33 µg / ml
1 A_{260} **RNA**	corresponds to a c(1 A_{260}) of ~ 40 µg / ml

This results in a general formula for RNA/DNA concentration calculation:

$$c\left[\mu g/\mu l\right] = \frac{A_{260} \cdot c\left(1\,A_{260}\right) \cdot D_f}{1000}$$

(c is concentration in µg/µl, D_f is the dilution factor)

As stable RNAs like RNase P RNA or tRNAs tend to form extensive secondary structures, a special method to determine RNA concentrations was used for applications that require highly precise quantifications as e. g. kinetic analysis. The classical approach is alkaline or ribonuclease hydrolysis of the RNA to mononucleotides and subsequent calculation of RNA concentration on the basis of ε_{260} values for the individual mononucleotides. To obtain ε_{260} of the intact RNA, the sum of mononucleotide ε_{260} values is then corrected by a factor corresponding to the ratio of A_{260} values of the RNA sample before and after hydrolysis.

As RNA structure may also depend on ion concentration, measurements were performed in 50 mM NH_4OAc (pH 7.0). RNA was diluted in 50 mM NH_4OAc and A_{260} ($A_{260,\text{ intact RNA}}$) was measured against 50 mM NH_4OAc. Then a mixture of RNases (0.5 µg RNase A, 0.01 U RNase T1, 0.01 U RNase T2) was added to this dilution and incubated for at least 3 hours at room temperature or 37°C to ensure that the RNA was quantitatively degraded to single nucleotides. A_{260} of this hydrolysed RNA ($A_{260,\text{ hydrolysed RNA}}$) was measured. To ensure complete hydrolysis, the measurement was repeated after another 30 min of incubation. No significant change in A_{260} was expected for the two subsequent measurements in the case of complete hydrolysis. For the RNA concentration calculation, a specific extinction coefficient of the measured RNA had to be calculated as follows:

$$\varepsilon_{RNA} = \sum_{1}^{n_A} \varepsilon_A + \sum_{1}^{n_C} \varepsilon_C + \sum_{1}^{n_G} \varepsilon_G + \sum_{1}^{n_U} \varepsilon_U$$

where ε_A, ε_C, ε_G, ε_U, are the extinction coefficients for the individual ribonucleotides after hydrolysis; n_A, n_C, n_G and n_U are the numbers of each nucleotide contained in the RNA sequence.

The ε_{260} values for mononucleotides at neutral pH:

ε_{ATP}: 15.02 [1 / (M·cm)]

ε_{GTP}: 12.08 [1 / (M·cm)]

ε_{UTP}: 9.66 [1 / (M·cm)]

ε_{CTP}: 7.07 [1/ (M·cm)] (Cavaluzzi and Borer, 2004)

Based on the ratio of intact and hydrolysed RNA a new extinction coefficient was calculated:

$$\varepsilon'_{RNA} = \frac{A_{260,\ \text{intact RNA}}}{A_{260,\ \text{hydrolysed RNA}}} \cdot \varepsilon_{RNA}$$

The molecular weight of the respective RNA (M_R) was calculated and then the c(1 A_{260}) for this particular RNA was determined using the following equation:

$$c\ (1\ A_{260})[\mu g / \mu l] = \frac{1}{\varepsilon'_{RNA}} \cdot M_R \qquad \text{for } d = 1 \text{ cm}$$

3.2.3 Isolation of DNA from agarose gels

To isolate double-stranded DNA from agarose gels, bands containing the DNA fragment of interest were cut out using a scalpel. Commercially available spin columns from Qiagen (QIAquick Gel Extraction Kit) were used for further purification. The principle of these spin columns is DNA binding to a silica membrane in the presence of chaotropic salts. Contaminations like salts and soluble macromolecular components are removed by a simple washing step. Pure DNA is finally eluted under low ionic strength conditions. The procedure was carried out exactly according to the protocol provided by the manufacturer. In the case of crystal violet gels, no attention was paid to the colour code of the binding buffer, as crystal violet dominated the colour of the buffer.

3.2.4 Isolation of DNA/RNA from PAA gels

Isolation of DNA oligonucleotides and RNA transcripts from PAA gels was mainly done by diffusion elution. The band of interest was detected by UV shadowing or using a phosphoimager (for radiolabelled RNA/DNA), cut out and transferred into a 1.5 ml reaction tube (or 50 ml falcon e.g. for preparative scale T7 transcriptions) containing elution buffer. The volume of buffer depended on the size of the excised gel slice; a standard 15 µl labelling reaction was e. g. eluted in 500 µl buffer or in a buffer volume which efficiently covered the gel piece. Samples were shaken overnight at 4°C.

Different elution buffers were used:

Elution buffer 1	
Tris / HCl, pH 7.0	200 mM
EDTA	1 mM

Elution buffer 2	
NaOAc pH 5.0	1 M

3.2.5 Alcohol precipitations

3.2.5.1 Ethanol precipitation

Ethanol precipitation is a very common method to concentrate nucleic acids from aqueous solutions and to remove salts. The precipitate of DNA/RNA, which is formed at low temperature (-20°C or less) in the presence of moderate concentrations of monovalent cations, is recovered by centrifugation and redissolved in an appropriate buffer. Salts remain predominantly in the ethanol supernatant. For short DNA or RNA (< 30 nucleotides) or very small amounts of DNA/RNA, 20-40 µg glycogen were added as carrier for better recovery.

For precipitation, 1/10 volume of 3 M NaOAc pH 5.0 was added to one volume of DNA/RNA solution, followed by mixing with 2.5 volumes of absolute ethanol. Samples were kept at least for 30 min at –20°C and were then centrifuged for at least 30 min at 4°C, 13,000 rpm (Biofuge fresco). For more efficient removal of salts, the pellet was eventually washed with 70 % (v/v) ethanol and centrifuged for another 15 min at 13,000 rpm. The supernatant was discarded, the pellet was dried at room temperature or at 37°C for ~2-5 min and finally dissolved in an appropriate volume of double-distilled water or buffer for downstream application.

3.2.5.2 Isopropanol precipitation

Larger volumes of DNA/RNA solution were in some cases precipitated by adding 0.8 volumes of isopropanol at room temperature. Samples were centrifuged as described for ethanol precipitation and if necessary washed with 70 % ethanol.

3.2.6 Phenol/chloroform extraction

Phenol/chloroform extraction is a common technique used to purify DNA or RNA samples. Such extractions are used whenever it is necessary to inactivate or remove enzymes. The procedure takes advantage of the fact that deproteinisation is more efficient when two different organic solvents are used instead of one. The final extraction with chloroform also removes residual phenol.

An equal volume of TE-saturated (10 mM Tris-HCl, 1 mM EDTA, pH 7.5-8.0) phenol is added to an aqueous DNA/RNA sample, vigorously vortexed (30 s) and then centrifuged (5 min, 13,000 rpm at room temperature) to achieve phase separation. The upper aqueous layer is removed carefully, avoiding the protein-containing interface, and transferred into a new tube. The lower organic layer and interface are discarded. The aqueous phase is extracted a second time using phenol and then once using chloroform. The aqueous layer is also the upper one in chloroform extractions. Afterwards DNA/RNA is concentrated by ethanol precipitation or purified using NAP gel filtration columns.

3.2.7 NAP gel filtration

The NAP 5 and NAP 10 columns used in this study were purchased from GE Healthcare, and are filled with Sephadex 25. They are commonly used to remove salts and single nucleotides from reaction mixtures. The columns were equilibrated with double-distilled water according to the manufacturer’s protocol. The sample was loaded onto the column (500 µl for NAP 5 columns; the volume had to be adjusted to 500 µl total volume if smaller) and entered the gel matrix by gravity flow. Elution was accomplished by adding an exact volume of double-distilled water (see manufacturer’s protocol). If necessary the sample was concentrated by ethanol precipitation.

3.3 DNA techniques

3.3.1 Preparation of genomic DNA

For isolation of genomic DNA, the DNeasy Tissue Kit (Qiagen) was used. Bacterial cells were grown overnight and DNA isolation was done exactly as described in the protocol provided by the manufacturer.

3.3.1.1 Rapid isolation of DNA from bacteria

In special cases PCR analysis of genomic DNA was not influenced by the presence of proteins. For rapid isolation of DNA, bacterial cells were grown overnight under standard conditions. 500 µl of this bacterial culture were pelleted by centrifugation (2 min, 13,000 rpm, Eppendorf Minispin), and the pellet was resuspended in 300 µl double-distilled water and heated for 3 min at 95°C. The suspension was centrifuged for 10 min at 4°C, 13,000 rpm (Biofuge fresco) to remove cell debris and the supernatant was used for subsequent PCR analysis.

3.3.2 Preparation of plasmid DNA

The method used for plasmid DNA isolation is based on a modified alkaline lysis procedure (Birnboim and Doly, 1979; Birnboim, 1983).

3.3.2.1 Preparative plasmid DNA isolation from *E. coli* cells

Midi-preps were usually done starting from 50-100 ml bacterial culture, Maxi-preps using 500 ml bacterial cell culture. Cells were resuspended in a buffer containing RNase A. After an SDS/alkaline lysis step, the solution was neutralised and then applied onto an anion exchange resin (preparative scale, Midi-/Maxi-prep). Using a buffer of intermediate ionic strength, contaminations like proteins, RNA, dyes and soluble macromolecular components were removed. Pure plasmid DNA was finally eluted in a high salt buffer. Eluted DNA was concentrated by isopropanol precipitation followed by a washing step using 70 % ethanol. Commercially available kits from different companies were used (Macherey-Nagel, Qiagen).

Procedure using the Qiagen Plasmid Midi Kit

- 50-100 ml bacterial culture are harvested by centrifugation for 15 min at 4°C, 8,000 rpm.
- the cell pellet is resuspended in 4 ml resuspension buffer.

- 4 ml of lysis buffer are added, followed by gentle mixing and incubation for 5 min at room temperature.
- The solution is mixed with 4 ml of neutralization buffer and incubated for 15 min on ice.
- clear the solution by centrifugation for 30 min at 10,000 rpm.
- apply clear supernatant to a QIAGEN-tip 100 column, which has been equilibrated with 4 ml of equilibration buffer, and allow supernatant to enter resin by gravity flow.
- Column is washed twice with 10 ml washing solution.
- Plasmid DNA is eluted with 5 ml elution buffer.
- DNA is concentrated by isopropanol precipitation and resuspended in water or TE buffer.

Buffers used for preparative plasmid preparation

Cell resuspension buffer	50 mM Tris / HCl, pH 8.0 10 mM EDTA 100 µg/ml RNase A
Lysis buffer	200 mM NaOH 1 % (w/v) SDS
Neutralisation buffer	3 M KOAc, pH 5.5
Column equilibration buffer	750 mM NaCl 50 mM MOPS pH 7.0 15 % (v/v) Isopropanol 0.15 % (v/v) Triton X-100
Washing buffer	1 M NaCl 50 mM MOPS pH 7.0 15 % (v/v) Isopropanol
Elution buffer	1.25 M NaCl 50 mM Tris / HCl pH 8.5 15 % (v/v) Isopropanol

3.3.2.2 Analytical scale preparation of plasmid DNA

For isolation of plasmid DNA for analytical purposes the commercially available Nucleospin Plasmid Kit (Macherey-Nagel) and the supplied protocol were used. 3 ml (for cells containing high-copy plasmids like pSP64 derivatives) or 5-10 ml (for cells containing low-copy plasmids such as pACYC177 or pBR322 derivatives) of an overnight culture were lysed under alkaline conditions.

DNA yields could be improved for low-copy-number plasmids containing the pMB1 (e.g. pBR322) or ColE1 origin of replication by adding chloramphenicol. Therefore, the overnight culture was grown as usually, supplemented with chloramphenicol (to a final concentration of 170 µg/ml) in the morning and incubated at least for another 6 hours under shaking. Plasmid pBR322 does not use the short lifetime host proteins used in host chromosome replication. By adding chloramphenicol, chromosomal replication and cell division is stopped without stopping plasmid replication, thus increasing plasmid yields.

For the isolation of plasmid DNA from *B. subtilis* cells, the cell suspension was incubated with 2 mg/ml lysozyme for 5 min at room temperature before addition of lysis buffer to improve the effectiveness of lysis.

After the lysis step, the cell suspension was neutralised and adjusted to high-salt binding conditions in one step. After lysate clearing, the sample was ready for purification on a spin column with a silica membrane. Elution was performed under low ionic strength conditions, and the eluted DNA could be directly used for e. g. digestion by restriction enzymes or sequencing.

For plasmids isolated from *end*A+ strains (e.g. *E. coli* wild-type strains), an additional washing step with prewarmed buffer AW was performed to completely remove high levels of endonucleases. In some cases this procedure was not efficient and residual endonucleases had to be removed by phenol/chloroform extraction prior to downstream applications.

In some cases the cleared supernatant after neutralisation and centrifugation was not loaded onto a column, but the plasmid DNA was concentrated by isopropanol precipitation.

3.3.3 Restriction digest of DNA

A very common method to analyse DNA is cleavage by restriction endonucleases. Type II restriction endonucleases cleave double-stranded DNA at defined positions close to or within their (mostly palindromic) recognition sequences. Restriction enzymes generate DNA fragments with either 5'- or 3'-overhangs (sticky ends) or blunt ends and 3'-hydroxyl and 5'-phosphate termini.

Restriction digest	
DNA (0.1–20 µg)	x µl
10 x buffer	2 µl
Restriction enzyme	0.2 - 2 µl
H_2O	ad 20 µl
	Σ 20 µl

Buffer conditions and incubation temperature depend on the specific restriction enzyme. Incubation time varies from 1-3 h for analytical digestion to 4 h or overnight for the preparative scale. Although the amount of enzyme is varied, the added volume of enzyme stock solution (usually provided as a 50 % glycerol solution) should not exceed, as a rule of thumb, 1/10 of the total reaction volume to avoid relaxed cleavage specificities (star activities).

After digestion DNA was analysed on agarose gels (chapter 3.2.1.1). If the DNA was subjected to additional reactions, restriction enzymes were heat-inactivated or removed by phenol/chloroform extraction. If the DNA was used in cloning experiments, usually gel purification was performed to remove primers, small cleavage fragments or, in the case of plasmids, to get also rid of uncut plasmid.

3.3.4 Dephosphorylation of DNA

Calf intestinal alkaline phosphatase (CIAP) catalyses the removal of terminal 5'-phosphates from DNA, RNA and ribo- and deoxyribonucleotide triphosphates. Dephosphorylation was required to prevent religation of linearized plasmid vectors in cloning experiments.

Dephosphorylation reaction		
DNA	x µl	1-10 µg
10 x CIAP buffer	3 µl	
CIAP 1 U/µl	3 µl	
H_2O	ad 30 µl	
	Σ 30 µl	30 min 37°C
10 x CIAP buffer	+ 2 µl	
H_2O	+ 16 µl	
CIAP 1 U/µl	+ 2 µl	
	Σ 50 µl	30 min 50°C, 30 min 37°C

Linearised plasmid DNA was mixed with the appropriate buffer and CIAP as specified above and then incubated for 1 h at 37°C. Especially for blunt end vectors a slightly expanded protocol was used, as removal of 5'-phosphates from DNA with blunt ends is less efficient. After 30 min incubation at 37°C, the reaction volume was increased by adding 10 x buffer, water and additional enzyme; the sample was incubated for another 30 min at 50°C and finally 30 min at 37°C. Dephosphorylation was usually performed before gel purification of the linearised plasmid. Alternatively, the phosphatase was removed by phenol/chloroform extraction and the DNA was concentrated by ethanol precipitation.

3.3.5 5'- Phosphorylation of DNA

T4 Polynucleotide Kinase (T4 PNK) is a polynucleotide 5'-hydroxyl kinase that catalyses the transfer of the γ-phosphate from ATP to the 5'-OH group of single- and double-stranded DNA and RNA (forward reaction) or transfers the 5'-phosphate of DNA/RNA to ADP and rephosphorylates the 5'-OH of DNA/RNA generated in the first step (exchange reaction).

For subsequent blunt end ligation of PCR products, primers were 5'-phosphorylated prior to the PCR reaction or the DNA fragment was phosphorylated directly following PCR. The

DNA oligonucleotide (primer) or double-stranded DNA fragment was phosphorylated as specified below.

Phosphorylation reaction		
DNA	x µl	10-1000 pmol
100 mM ATP	0.5 µl	
10 x T4 PNK buffer (forward)	2 µl	or buffer from previous reaction if appropriate
T4 PNK	1 µl	
H_2O	ad 20 µl	
	Σ 20 µl	1 h 37°C

The phosphorylated primers could be used directly in the PCR reaction. If necessary the enzyme was removed by phenol/chloroform extraction and the DNA was concentrated by ethanol precipitation.

Radioactive labelling of DNA oligonucleotides was done using γ-^{32}P ATP according to the protocol for 5'-labelling of RNA (3.4.3).

3.3.6 Fill-in reaction using Klenow fragment

The Klenow Fragment DNA polymerase is the large fragment of DNA Polymerase I from *E.coli*. It exhibits 5'→ 3' polymerase activity and 3'→ 5' exonuclease (proofreading) activity, but lacks the 5'→ 3' exonuclease activity of DNA polymerase I.

Klenow treatment		
DNA (digested)	x µl	0.1 - 4 µg
10 x buffer	2 µl	e.g. Y+, Fermentas
Klenow fragment 10 U/µl	0.5 µl	
H_2O	ad 19.5 µl	5 min 37°C
2 mM dNTPs	+ 0.5 µl	10 min 37°C, 10 min 70°C

To convert the sticky ends of digested plasmid DNA to blunt ends, either by removing the overhanging nucleotides or by the fill-in reaction, DNA was treated with Klenow fragment. DNA, buffer and Klenow fragment were incubated for 5 min 37°C in the absence of dNTP substrates, conditions under which the Klenow fragment exhibits primarily exonuclease activity. After addition of dNTPs the reaction was incubated for 10 min at 37°C (5'→ 3' fill-in activity) and the enzyme finally inactivated at 70°C for 10 min. Klenow-treated DNA was 5'-phosphorylated (see 3.3.5), concentrated by ethanol precipitation and directly used for ligation reactions.

3.3.7 Ligation

Ligation was used to clone DNA fragments (‘inserts’) into linearized vectors. T4 DNA Ligase, which catalyses the formation of a phosphodiester bond between juxtaposed 5'-phosphate and 3'-hydroxyl termini in duplex DNA with blunt or cohesive termini, was incubated with insert DNA (5’- phosphorylated) and plasmid vector (dephosphorylated). DNA fragments and plasmid vectors were gel purified prior to ligation (chapter 3.2.3). Concentration was estimated based on an ethidium bromide agarose gel.

A typical ligation reaction is shown below. A control reaction with plasmid vector only permitted to monitor for the presence of uncut/inefficiently dephosphorylated vector. Molar ratios of vector : insert were usually 1:3 or 1:9. For difficult ligation reactions a broader range of ratios, including excess of vector DNA, was applied.

Ligation reaction	control	1:3	1:9	
Vector	2 µl	2 µl	2 µl	30-100 ng
Insert	-	1 µl	3 µl	
5 x T4 DNA ligase buffer	2 µl	2 µl	2 µl	
H_2O	5 µl	4 µl	2 µl	
T4 DNA ligase	1 µl	1 µl	1 µl	
	Σ 10 µl	Σ 10 µl	Σ 10 µl	1 h 37°C or overnight 16°C or 4°C

Ligation of DNA with ‘sticky ends’ was incubated for 1 h at 37°C. Problematic ligations or blunt end ligations were incubated overnight at 16°C or even at 4°C. T4 DNA ligase was heat inactivated for 10 min at 65°C and then the ligation reaction was directly used for transformation of *E. coli* cells (chapter 3.1.5.1).

3.3.8 Polymerase chain reaction (PCR)

The polymerase chain reaction (PCR) is a method for the amplification of very small amounts of DNA. The following components are required:

A thermostable DNA polymerase; for cloning experiments, usually *Pfu* polymerase (originally isolated from *Pyrococcus furiosus*) was used, as *Pfu* polymerase exhibits a proofreading activity (3'→ 5' exonuclease activity) and does not produce 3’-overhangs. For templates that could not be amplified by *Pfu* polymerase or for analytical PCR, *Taq* polymerase (originally isolated from *Thermus aquaticus*) was used. *Taq* polymerase has an error rate of 1/10,000 and produces adenine overhangs, which permit to use the PCR product directly for TA-cloning. As template, single- or double-stranded DNA is required. A forward and a reverse DNA primer, a buffer containing Mg^{2+} and dNTPs complete the reaction mix.

The reaction is basically performed in three steps:

Denaturation of the double-stranded DNA at 95°C.

Annealing of primers to the DNA template at a temperature specific for the primers used.

Elongation at 68-72°C for 5’→ 3’ elongation of the annealed primer; elongation velocity is 1 min/1 kb using *Taq* polymerase and 2 min/1 kb using *Pfu* polymerase.

The components listed below were mixed in a PCR reaction tube. Polymerase was added during the initial denaturation step at 95°C to prevent unspecific elongation (hot start PCR).

PCR program

Initial denaturation	95 °C	2 min	
denaturation	95 °C	30 s	
annealing	45- 65°C	30 s	
elongation	68 –72°C	30 s – 5 min	25-30 cycles
Final elongation	68 –72°C	5 min	

PCR reaction

template	x µl	single bacterial colony, 10 ng plasmid or 500 ng genomic DNA
10 x PCR buffer MBI ($-MgCl_2$, + KCl)	5 µl	
25 mM $MgCl_2$	3 µl	or c_{End} = 1.5 – 4.5 mM
10 mM dNTPs	0.5 µl	
Primer forward 100 pmol/µl	0.5 µl	
Primer reverse 100 pmol/µl	0.5 µl	
H_2O	ad 49.5 µl	
Pfu/*Taq* (5 U/µl)	+ 0.5 µl	added at 95°C during initial denaturation step
	Σ 50 µl	

An 5-10 µl aliquot of each reaction was checked on an agarose gel. If the PCR fragment was used for cloning, the PCR reaction was concentrated by ethanol precipitation, digested if required and gel purified prior to ligation.

For PCR of overlapping DNA fragments, 5-10 cycles were performed in the absence of primers for overlap extension. Thereafter, the primers were added and the PCR reaction was continued as usually.

TA-cloning

For cloning of PCR fragments amplified with *Taq* polymerase and carrying single 3’-adenine overhangs, the TOPO-TA cloning Kit from Invitrogen was used. The reaction was carried out exactly according to the protocol provided by the manufacturer. 0.5-2 µl of the PCR reaction (depending on PCR efficiency) were incubated with 0.5 µl salt solution (provided) and 0.5 µl of vector pCR2.1-TOPO for 5-25 min at room temperature. 2 µl of this reaction were used for transformation of chemically competent *E. coli* cells.

3.3.9 Site-directed *Dpn* I mutagenesis

PCR mutagenesis was performed according to the protocol provided with the QuikChange Site-Directed Mutagenesis Kit (Stratagene). This method can be used to introduce point mutations or single base deletions. Melting temperature T_m of primers introducing point mutations was calculated using the following equation:

$$T_m = 81.5 + 0.41\cdot (\%\ GC) - 675/N - \%\ mismatch$$

N is the length of the primer, and % GC (GC content) and % mismatch are whole numbers.

Calculation example for a 38 nt primer, 45 % GC, 1 mismatch:

$$T_m = 81.5 + 0.41\cdot 45 - 675/38 - (1/38 \cdot 100) = 79.6$$

Primers were designed to have a T_m of > 78°C and a length of 25-55 nucleotides. The desired mutation should be approximately in the middle of the primer sequence.

As template, 50 ng plasmid DNA (isolated from *dam*$^+$ strains) was used. Reaction components were mixed in a PCR tube and the PCR program was run as described below. As a control, one reaction was run in parallel in the absence of *Pfu* polymerase.

PCR mutagenesis	control	mutagenesis
template (10 ng/µl)	5 µl	5 µl
10 x *Pfu* buffer (Promega)	5 µl	5 µl
10 mM dNTPs	2 µl	2 µl
Primer forward (100 pmol/µl)	0.25 µl	0.25 µl
Primer reverse (100 pmol/µl)	0.25 µl	0.25 µl
H_2O	39.5 µl	39 µl
Pfu (2 U/µl)	-	0.5 µl
	Σ 50 µl	Σ 50 µl

PCR program mutagenesis		
95°C	1 min	
95°C	1 min	
50 – 60°C	90 s	
70°C	2 min/ kb	16 cycles
70°C	10 min	
10°C	pause	

6-8 µl of the PCR mutagenesis reaction were checked on an agarose gel. Usually an additional band compared to the control reaction could be seen in the case of successful PCR mutagenesis.

20 µl of the PCR reaction were directly digested with 1 µl *Dpn* I for 1-4 h at 37°C. As *Dpn* I is a *dam*$^-$ sensitive restriction enzyme, only methylated DNA (plasmid DNA isolated from *dam*$^+$ strains) containing the recognition sequence GATC is digested, whereas the newly synthesised unmethylated DNA is not affected. The control reaction was digested in parallel to test for efficient digestion. 4 µl of *Dpn* I digested DNA were used to transform chemically competent cells (3.1.5.1). Plasmid DNA from single colonies was isolated, checked by restriction digestion and finally the region of interest was confirmed by sequencing.

3.4 RNA Techniques

For all experiments with RNA double distilled-water was used.

3.4.1 Preparation of total RNA

3.4.1.1 Growth of DW2 bacteria for total RNA isolation

DW2 bacteria harbouring derivatives of plasmid pSP64 were grown at 30°C overnight in LB medium containing 100 µg/ml ampicillin and 30 µg/ml chloramphenicol. On the next morning, the same culture was incubated for 2 h at 43°C, followed by inoculation of fresh prewarmed LB medium (100 or 250 ml) to a starting OD_{578} of 0.05 to 0.1, and further cultivation at 43°C until cell density reached an OD_{578} of about 0.6. Cultivation at 43°C was necessary to repress expression of *E. coli rnpB* wt encoded on the temperature-sensitive plasmid pDW160. In the case of kanamycin-sensitive clones (loss of pDW160 encoding *E. coli rnpB* wt) cells could be grown at 37°C.

3.4.1.2 Growth of BW bacteria for total RNA isolation

BW cells harbouring pACYC177 and pBR322 derivatives were grown at 37°C overnight in 3 ml LB medium supplemented with 100 µg/ml ampicillin, 25 µg/ml chloramphenicol, 10 mM arabinose and 10 µg/ml tetracycline if cells contained pBR322 derivatives. Cells were then used to inoculate 50 ml of the same medium to a starting OD_{578} of 0.05 to 0.1, followed by incubation at 37°C. At an OD_{578} of about 0.5, cells were centrifuged for 5 min at 5,000 rpm (Eppendorf 5810R) at room temperature and washed once with 20 ml LB medium to remove residual arabinose. Cells were resuspended in 100 ml LB supplemented with antibiotics and 0.5 % (v/v) Glucose and incubated for another 3 h at 37°C and 180 rpm. Under these conditions, the chromosomally encoded *rnpB* gene was not transcribed.

3.4.1.3 Growth of SSB318/SSB320 bacteria for total RNA isolation

SSB318/SSB320 cells were grown at 37°C overnight in 3 ml LB medium supplemented with 12.5 µg/ml lincomycin, 0.5 µg/ml erythromycin, 1 mM IPTG and in the case of cells harbouring pHY300 derivatives 30 µg/ml tetracycline. Cells with pDG364 derivatives integrated into the *amyE* locus were additionally grown in the presence of 5 µg/µl chloramphenicol. Cells were washed twice by centrifugation (6000 rpm Eppendorf Minispin, 1 min) and resuspension in 1 ml LB medium to remove residual IPTG and were used to inoculate 50 ml LB medium supplemented with the respective antibiotics to a starting OD_{578} of 0.05-0.1, followed by incubation at 37°C at 180 rpm. Depending on the purpose of the following experiments, cells were grown in the presence or absence of IPTG, and, for xylose-inducible genes provided on pHY300 derivatives, in the presence of 2 % xylose or 2 % glucose until OD_{578} reached 0.6-0.8.

3.4.1.4 Trizol RNA preparation

Total cellular RNA from strains DW2, BW, SSB318 and SSB320 was isolated by the TRIzol method (Invitrogen) according to the protocol provided by the manufacturer:
2.2 ml TRIzol were used to resuspend 1 g cell pellet. The cell suspension was incubated for 5 min at room temperature. 0.2 ml chloroform were added per 1 ml TRIzol and shaken for 15 s. After another 2 min incubation at room temperature, the suspension was centrifuged for 15 min at 4°C and 13,000 rpm (Biofuge fresco, Heraeus). The aqueous phase (approximately 60 % of the starting TRIzol volume) was transferred into a new reaction tube and RNA was precipitated by adding 0.5 ml isopropanol per ml TRIzol, and, after incubation for 10 min at room temperature, centrifugation for at least 15 min at 4°C and 13,000 rpm. The pellet was washed once with 70 % ethanol (at least 1 ml 70 % ethanol per ml TRIzol) and centrifuged as described above.

RNA was dissolved in double-distilled water and further digested with DNase I (Turbo DNase, Ambion) in order to remove residual DNA, which interferes with subsequent experiments. As DNA digestion often turned out to be incomplete, 3 digestion steps were performed in a row (see reaction scheme below). In the presence of high copy plasmids eventually up to 6 DNase I digestion steps were performed. To remove proteins a phenol/chloroform extraction was performed followed by an ethanol precipitation in the presence of 0.12 M NaOAc, pH 5.0. RNA was dissolved in double-distilled water and concentrations were measured in H_2O at 260 nm (1 A_{260} unit = 40 µg).

DNase I digestion	1. digestion	2. digestion, additionally added	3. digestion, additionally added
RNA	40 µl		
H_2O		+ 16 µl	+ 16 µl
10x Turbo DNase buffer	5 µl	+ 2 µl	+ 2 µl
Turbo DNase (2 U/µl)	5 µl	+ 2 µl	+ 2 µl
	Σ 50µl	Σ 70 µl	Σ 90 µl
	1 h 37°C	1 h 37°C	1 h 37°C

3.4.2 T7 Transcription

RNA can be transcribed *in vitro* using DNA-dependent phage RNA polymerases (e. g. T7 RNA polymerase). T7 RNA polymerase recognises the specific T7 phage promoter sequence (5'-TAA TAC GAC TCA CTA TA -3'; sense strand) and starts polymerisation immediately downstream in 5'→ 3' direction. To synthesize RNA run-off transcription was used (i.e. polymerisation is terminated when the polymerase reaches the end of the template). Therefore either linearized plasmids or PCR products were used as templates. If the RNA synthesized should be used for 5'-end labelling with γ-^{32}P ATP, guanosine was added in excess over 5'-GTP to the transcription reaction to compete with 5'-GTP for incorporation at the 5'-end (provided that the template encodes a G residue a position +1). The majority of transcripts start with guanosine providing the 5'-terminal hydroxyl group for 5'-end labelling purposes.

T7 transcription reaction

	c_{Stock}	c_{End}	small scale reaction	preparative reaction
HEPES pH 8.0	1 M	80 mM	4 µl	80 µl
DTT	100 mM	15 mM	2.5 µl	50 µl
$MgCl_2$	3 M	33 mM	0.55 µl	11 µl
Spermidine	100mM	1 mM	0.5 µl	10 µl
NTP mix	25 mM each	3.75 mM each	7.5 µl	150 µl
BSA	20 mg/ml	0.12 mg/ml	0.3 µl	6 µl
Template (linearised plasmid)	1 µg/µl	40 µg/ml	4 µl	80 µl
guanosine	**30 mM**	**9 mM**	**15 µl**	**300 µl**
pyrophosphatase	200 U/ml	2 U/ml	0.25 µl	5 µl
T7 RNA Polymerase	200 U/µl	4000 U/ml	1 µl	20 µl
RNase-free water			ad 50µl	ad 1000 µl
			Σ 50 µl	Σ 1000 µl

The guanosine stock solution is only soluble at 72°C and was only added if the RNA transcribed should be 5'-end labelled afterwards.

If a PCR product was used as template the final concentration was adjusted to 5 µg/ml DNA. All components (see above) were mixed in a 1.5 ml reaction tube, T7 RNA polymerase was added at the end, followed by incubation at 37°C for 2-4 h. To check the efficiency of transcription, aliquots of 2 to 10 µl were analysed by denaturing PAGE. For analysing transcription efficiency, a small scale (50 µl) reaction was performed and optimised if necessary (this was necessary especially for new templates), before preparative scale reactions were performed in larger volumes (see 1000 µl reaction). Preparative scale 1000 µl reactions were divided into 2 aliquots of 500 µl each (for better thermal equilibration) and T7 RNA polymerase was added in two steps: at the beginning only 5 µl (1000 U) T7 RNA polymerase were added individually to each aliquot and incubated at 37°C. After two hours 5 µl (1000 U) T7 RNA polymerase were added to each aliquot and incubated for two additional hours at 37°C. Transcription efficiency was analysed by denaturing PAGE. For concentration estimation a defined amount of RNA (of the same or similar size) was loaded in parallel. After successful transcription, RNA was purified by the following steps:

- If the DNA template roughly comigrated with the RNA transcript on denaturing PAA gels (e.g. for PCR templates), 1 µl DNase I (20 U/µl) was added to each 500 µl aliquot and incubated for 1 h at 37°C.
- Proteins were removed by phenol/chloroform extraction (3.2.6.).
- For desalting and removal of mononucleotides samples were loaded on NAP 5 or NAP 10 columns (depending on the reaction volume for T7 transcription) (3.2.7.).
- The eluate was concentrated by ethanol precipitation (3.2.5.). The pellet was dissolved in double-distilled water and RNA sample buffer was added at a ratio of 1:1.
- The sample was purified by denaturing PAGE. If not stated otherwise, 1 mm thick gels were used. The pocket size was chosen according to the efficiency of T7 transcription (for example, if the transcription efficiency check revealed RNA amounts of ~1.5 µg/5 µl, then the RNA transcribed in a 1 ml reaction sample was loaded into a 12.5 cm wide pocket). If available, an RNA sample of comparable size was loaded in parallel as control. Gel percentage was adapted to the size of the RNA transcript (Table 3.3, chapter 3.2.1.2.1). For good resolution, gels were run at medium speed to avoid extreme heating of the gel; the running time should be long enough to get good band separation.
- Bands were cut out using UV shadowing and transferred into 1 M NaOAc for elution (overnight at 4°C under shaking; chapter 3.2.4). A subsequent second elution step was optional.

- RNA was concentrated by ethanol precipitation from the elution buffer and resuspended in double-distilled water.
- Concentration determination was performed as described in 3.2.2.
- The quality of purified RNA was checked by denaturing PAGE.

3.4.2.1 Homogeneous 3’-ends of RNA transcripts

In some cases (template pSBpt3’HH and variants thereof), the DNA template encoded a hammerhead cassette 3’-adjacent to the structural RNA gene. Hammerhead ribozymes are small autocatalytic RNA motifs that catalyse phosphodiester bond hydrolysis at a single defined position. Naturally the hammerhead ribozyme has been found to be involved in the replication of a plant viroid and some plant viral satellite RNAs. Immediately after synthesis the hammerhead ribozyme folds into its active conformation. Cleavage occurs already during transcription provided that Mg^{2+} ions are present at sufficiently high concentrations, thus generating homogeneous 3’-ends. A prerequisite for the application of hammerhead ribozymes at 3’-ends of RNA transcripts is the presence of a trinucleotide upstream of the cleavage site, optimally 3’-GUC (Fig. 3.1). Hammerhead cleavage leaves a 2’, 3’-cyclic phosphate at the 3’-end of the RNA.

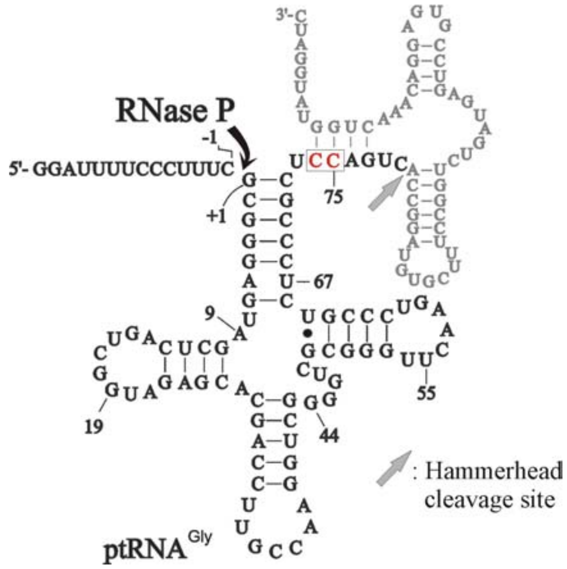

Fig. 3.1: Secondary structure of $ptRNA^{Gly}$ from *Thermus thermophilus* encoded on plasmid pSBpt3’HH. 3’-proximal nucleotides in grey indicate the hammerhead sequence; the grey and black arrows indicate the hammerhead and RNase P cleavage site, respectively. The two C residues highlighted in red within the 3’-CCA terminus of the tRNA show the nucleotides, which were changed to G residues by site-directed mutagenesis within this study.

In the case of pSBpt3’HH with introduced point mutations G74 or G75, base paring of the hammerhead ribozyme was partially affected. As a consequence, the activity of these ribozymes was decreased compared with optimal sequence hammerhead ribozyme. For better stimulation of hammerhead *cis*-cleavage activity, T7 transcription was supplemented with 10 µl 3 M $MgCl_2$ per 500 µl transcription sample after the regular reaction and incubated for another 3 h at 37°C. If these tRNAs are to be purified in large scale, one should think about introducing compensatory mutations within the hammerhead ribozyme in order to restore full ribozyme activity.

3.4.3 5'- end labelling of RNA

For 5'- end labelling of RNA the T4 polynucleotide kinase (T4 PNK) from *E. coli* phage T4 was used (see 3.3.5). As T4 PNK requires 5'-OH ends, RNA transcripts have to be started with guanosine (see chapter 3.4.2) or ApG, or have to be dephosphorylated prior to the reaction. For radioactive labelling γ-^{32}P ATP was used.

5'- end labelling reaction	
10 x T4 PNK buffer (forward reaction)	1.5 µl
25 mM DTT	1.5 µl
RNA (purified by denaturing PAGE)	x µl (10-25 pmol)
RNase-free water	ad 11 µl
γ-^{32}P ATP (3000 Ci/mmol, 10 µCi/µl, 3.3 µM)	3.0 µl
T4 PNK (10 U/µl)	1.0 µl
	Σ 15 µl

Components were mixed in a reaction tube in the order listed above and incubated for 1-2 hours at 37°C. Sample volume was adjusted to 100 µl and ethanol precipitated in the presence of 10 µg glycogen as precipitation adjuvant. The sample was mixed with RNA sample buffer and purified by denaturing PAGE using thin (< 1mm) spacers. For localization of labelled RNA bands, small stickers were fixed on the clingfilm covering the gel and marked with radioactivity and detected using imaging plates which can be scanned by a phosphoimager. The band of interest was cut out, eluted by diffusion (see 3.2.4), concentrated by ethanol precipitation and finally resuspended in 10-20 µl double-distilled water. Efficiency of the labelling reaction was determined by measuring 1 µl of labelled RNA using a scintillation counter.

3.4.4 3'- end labelling of RNA

3'- end labelling is carried out by T4 RNA ligase, which 'ligates' a single labelled nucleotide (^{32}P-pCp) to the 3'-OH end of the RNA (England and Uhlenbeck, 1978). The smallest recognized substrates are nucleoside- 3', 5'- bis-phosphates (such as cytidine 5', 3'- bis-phosphate, pCp); the resulting 3'-end is a phosphate, and no longer a substrate for the enzyme.

3'- end labelling reaction	
10 x T4 RNA ligase buffer	0.6 µl
1.5 mM ATP (use fresh dilution)	0.33 µl
RNA (purified by denaturing PAGE)	x µl (5-10 pmol)
[5'-^{32}P] pCp (3000 Ci/mmol, 10 µCi/µl,)	3.0 µl
T4 RNA Ligase (10 U/µl)	1.0 µl
	Σ 6 µl

Components were mixed in a reaction tube in the order listed above and incubated overnight at 8°C. 6 µl RNA loading buffer was added and the radiolabelled RNA was purified by denaturing PAGE (3.2.1.2.1). The band of interest was cut out, eluted and concentrated by ethanol precipitation as described for 5'- end labelling of RNA in chapter 3.4.3.

3.4.5 Primer extension

Primer extension assays were performed with total cellular RNA or *in vitro* transcribed RNA as template. The primers were either specific to *E. coli* RNase P RNA, *B. subtilis* RNase P RNA, *S. aureus* RNase P RNA, *E. coli* 4.5S RNA or mutated 4.5S RNA. This assay was either used to verify expression of mutant *rnpB* genes of *E. coli*, *B. subtilis* and *S. aureus*, or to map the 5'-end of 4.5S RNA to estimate the ratio of mature to precursor 4.5S RNA.

5 x RT Annealing Buffer	
KCl	275 mM
Tris/HCl pH 8.3	340 mM

Annealing mix		
RNA	x µl	10-30 µg of total RNA, or 20 ng of *in vitro* transcribed RNA
5 x RT Annealing Buffer	0.3 µl	
5'- end labelled primer	x µl	5000 Cerenkov cpm
H_2O	ad 3 µl	
	Σ 3 µl	

RT mix	
Annealing mix (see above)	3 µl
5 x first strand synthesis buffer	2 µl
100 mM DTT	1 µl
dNTPs, 10mM each	0.5 µl
H_2O	2.85 µl
Thermoscript (15 U/µl)	0.15 µl
	Σ 10 µl

Primer extension – PCR Program	
Annealing mix	
90°C	2 min
cool down in 1 h to 55°C	
+ RT mix	
55°C	45 min

Primer annealing was conducted in 1 x RT Annealing Buffer for about 60 min applying a linear temperature gradient from 90 to 55°C. Reverse transcription was then performed at 55°C for 45 min using Thermoscript reverse transcriptase (Invitrogen) by preparing the RT mix as described above.

For primer extension assays to verify expression of *E. coli rnpB*C292/C293 mutant alleles, primer 49 was used and 0.5 mM dGTP was replaced with ddGTP (see also Fig. 3.2). To verify expression of *B. subtilis rnpB*C258/C259 (primer 93) or *S. aureus rnpB*C238/C239 (primer 53) mutant alleles, dGTP and dTTP were replaced with ddGTP and ddTTP 0.5 mM each. To distinguish in parallel *B. subtilis rnpB* from *S. aureus rnpB* primer 92 was used and either dTTP was replaced with ddTTP or dGTP was replaced with ddGTP.

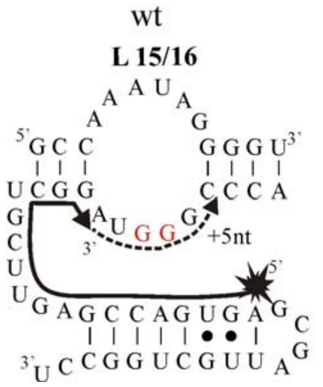

Fig. 3.2: Schematic representation of primer extension assays to verify expression of mutant *E. coli rnpB*C292/3 alleles. The arrow marked with an asterisk indicates the position of the radioactively labelled primer. Broken lines indicate primer extension in the presence of ddGTP for *E. coli* P RNA wt (left) or C292/3 mutant P RNAs (right).

For analysing *E. coli* 4.5S RNA primer 96 was used for wild-type or primer 215 for mutated 4.5S RNA. For *in vitro* transcribed precursor 4.5S RNA serving as size marker 0.5 mM each dGTP and ddGTP was used. Precursor 4.5S RNA was transcribed from a PCR template under control of the T7 promoter; the PCR template was amplified from plasmid pT7-4.5S (constructed and kindly provided by Norman R. Pace and coworkers), a derivative of plasmid pT71 (Tabor and Richardson, 1985) encoding *E. coli* 4.5S RNA with 23 nt of its natural 5'-flanking sequence and 17 additional 5'-flanking nt; the 4.5S RNA precursor transcript carried an additional AUA at the 3' end in comparison with natural mature 4.5S RNA (Peck-Miller and Altman, 1991); PCR primers to produce the PCR template for T7 transcription were primer X1 (including T7 promoter) and primer X2.

3.4.6 RT-PCR

Verification of gene expression on the RNA level can be performed by reverse transcription (synthesis of cDNA), coupled with the polymerase chain reaction.

In this study, the Quick Access RT-PCR Kit (Promega) was employed. As template either total cellular RNA or *in vitro* transcribed RNA was used. In the case of total RNA special attention had to be paid to efficient DNase I treatment. For the RT-PCR reaction components as listed below were mixed in a PCR tube except for AMV reverse transcriptase. The 2 x MM (Mastermix) contains buffer, dNTPs, Mg^{2+} and *Tfl* DNA polymerase. The first strand was synthesised by AMV reverse transcriptase (a reverse transcriptase isolated from Avian Myeloblastosis Virus) at 45°C. As this enzyme is not thermostable, it was just added when the reaction temperature had reached 45°C after the initial denaturation step. As a control, to check for DNA contamination, one reaction was performed in parallel omitting AMV reverse transcriptase. In the subsequent PCR reaction the thermostable *Tfl* DNA polymerase (from *Thermus flavus)* completed the synthesis of the second strand DNA. The annealing temperature was adjusted according to the primers used. Products were analysed (6-8 µl of total reaction) on agarose ethidium bromide gels. In some cases, for better sensitivity, one primer was radioactively labelled (*) and added in trace amounts (20,000 Cerenkov cpm per 25 µl reaction).

RT- PCR reaction

	+ AMV	negative control – AMV
RNA (200-500 ng total RNA, or ~5 pg of *in vitro* transcribed RNA)	x µl	x µl
Primer forward (100 pmol/µl)	0.25 µl	0.25 µl
Primer reverse (100 pmol/µl)	0.25 µl	0.25 µl
2 x MM Quick Access Kit	12.5 µl	12.5 µl
H_2O	ad 24.5 µl	ad 25 µl
AMV	0.5 µl	-
	Σ 25 µl	Σ 25 µl

RT-PCR program

90°C	2 min	add AMV at 45°C
45°C	45 min	
95°C	45 s	
54°C	1 min	
70°C	1 min	12-30 cycles
70°C	2 min	
10°C	pause	

For verification of *E. coli* RNase P RNA we used primers 49 (49*) and 150. For *B. subtilis* RNase P RNA we used primers 149, 93 (93*). Radioactive RT-PCRs were checked on 10 % denaturating polyacrylamide gels.

For semi-quantitative concentration estimation we performed an RT-PCR with different amounts of *in vitro* transcribed RNA, to define the range in which product yields correlated with RNA concentration.

3.4.7 5'- RACE

5'- RACE (rapid amplification of cDNA ends) experiments are used to map the 5'- ends of RNA transcripts.

Within this study, SSB320 cells were grown as described in chapter 3.4.1.3 (Growth of SSB318/SSB320 bacteria for total RNA isolation) and total RNA was isolated as described in chapter 3.4.1.4 (Trizol RNA preparation). In order to also include primary transcripts in the analysis, one half of the total RNA preparation was treated with Tobacco Acid Pyrophosphatase (TAP, Epicentre). During this procedure, the RNA 5'- triphosphates of primary transcripts are converted to monophosphates as a prerequisite for amplification by RACE. The second half of the total RNA was treated identically, except that TAP was omitted. Components as listed below were mixed, including an RNase Inhibitor to prevent RNA degradation, and incubated for 1 h at 37°C.

5'-RACE (I) **TAP treatment**

	Total RNA (from cells grown + IPTG)		Total RNA (from cells grown – IPTG)	
RNA (~25 µg)	x µl		x µl	
10 x TAP buffer	20 µl		20 µl	
RNase Inhibitor (40 U/µl)	1 µl		1 µl	
ddH$_2$O	ad 196 µl		ad 196 µl	
divide in 2 portions each	⬃	⬂	⬃	⬂
	98 µl	98 µl	98 µl	98 µl
TAP (10 U/µl)	-	1.5 µl	-	1.5 µl
	1 h 37°C	1 h 37°C	1 h 37°C	1 h 37°C

To remove proteins a phenol/chloroform extraction (chapter 3.2.6) was performed; for concentration and salt removal the samples were ethanol precipitated including a subsequent washing step using 70 % ethanol (chapter 3.2.5.1). RNA pellets were resuspended in 14.5 µl double-distilled water each. In the following step, an adapter oligonucleotide A1 (5'- GTC AGC AAT CCC TAA GGA G; the last three underlined nucleotides were ribonucleotides, all others were deoxyribonucleotides) was ligated to the RNA.

RNA was mixed with adapter oligonucleotide, heated for 5 min at 90°C, and then incubated for 5 min on ice to allow adapter annealing. Then components as listed below were added, gently mixed and incubated at 4°C overnight for ligation.

5’-RACE (II)	**Adapter ligation reaction**
RNA	14.5 µl
Adapter oligo (100 pmol/µl)	10 µl heat 5 min at 90°C, followed by 5 min incubation on ice
0.1 % (w/v) BSA	4 µl
10 x T4 RNA Ligation buffer	4 µl
10 mM ATP	4 µl
RNase Inhibitor (40 U/µl)	0.5 µl
T4 RNA Ligase	3 µl
	Σ 40 µl, 4°C overnight

The ligation reaction was treated with phenol/chloroform, concentrated by ethanol precipitation and resuspended in 36 µl H_2O.

Subsequently, RT-PCR was performed, but here using a protocol that differed from the one described in chapter 3.4.6 (RT-PCR).
For cDNA (first strand) synthesis, the RNA from the adapter ligation reaction was mixed with primers specific for trnSL-Val2 (primer 177, 178) or trnSL-Ala1 (primer 179, 180), heated for 5 min at 65°C and then kept on ice. The RNA/primer mixture was then mixed with the components listed below, and the program for reverse transcription was run as described.

5’-RACE (III)	**RT reaction**	
RNA	4.5 µl	
Primer (4 pmol/µl)	0.5 µl	
	Σ 5 µl	5 min 65°C, → on ice
+ RT-Mix:		
5 x first strand synthesis buffer	2 µl	
dNTPs, 10 mM each	1 µl	
100 mM DTT	0.5 µl	
H_2O	0.75 µl	
RNase Inhibitor (40 U/µl)	0.25 µl	
Thermoscript Reverse Transcriptase (15 U/µl)	0.5 µl	
	Σ 10 µl	

5’-RACE (III)	**RT program**
42°C	5 min
55°C	20 min
60°C	20 min
65°C	20 min
85°C	5 min

The synthesised cDNA was used as template for the subsequent PCR reaction. The reverse primer was specific for the RNA under investigation (same primer as used for the RT reaction), Primer X3 matched the sequence introduced by adapter ligation. 10 µl of PCR reaction were analysed on a native 8 % polyacrylamide gel. For size estimation, a 10 bp ladder (Invitrogen) was loaded in parallel.

5’-RACE (IV)	**PCR reaction**
cDNA	2 µl
10 x PCR buffer (−$MgCl_2$/+KCl)	5 µl
25 mM $MgCl_2$ (c_{End}= 2.5 mM)	5 µl
dNTPs, 10 mM each	1 µl
Primer reverse (specific) 100 pmol/µl	0.25 µl
Primer X3 (adapter) 100 pmol/µl	0.25 µl
H_2O	35 µl
Taq (5 U/µl, MBI)	0.5 µl
	Σ 50 µl

5’-RACE (IV)	**PCR program**	
94°C	2 min	
94°C	1 min	
52°C	65 s	
72°C	1 min	35 cycles
72°C	7 min	
8°C	pause	

Primers 177 and 178 were specific for *B. subtilis* trnSL Val2 and primers 179 and 180, specific for trnSL Ala1.

3.4.8 Folding analysis on non-denaturing gels

Buffer A (FPLC)	
NH_4Cl	100 mM
$Mg(OAc)_2$	2 or 10 mM
DTT	6 mM
Tris-HCl, pH 7.2 to 7.5	50 mM

Buffer F 2/10	
Mes, pH 6.1	50 mM
KCl	100 mM
$MgCl_2$	2 or 10 mM

Buffer KN 2/4.5 (Dinos *et al.*, 2004)	
Hepes-KOH, pH 7.4	20 mM
$Mg(OAc)_2$	2 or 4.5 mM
NH_4OAc	150 mM
Spermidine	2 mM
Spermine	0.05 mM
β-mercaptoethanol	4 mM

Folding analysis		c_{End}
M1 RNA (50 fmol)	x µl	10 nM
5 x buffer A/F/KN	1 µl	1 x
RNase P protein	x µl	37 or 50 nM
H_2O	ad 5 µl	
	Σ 5 µl	
Preincubation:	a) No preincubation (4°C) b) 55 min 37°C, +/- protein 15 min 37°C c) 5 min 55°C, 50 min 37°C, +/- protein 15 min 37°C	
	+ 5 µl 2 x native loading buffer Analysis on 11.25 % PAA (1 x THE, 100 mM NH_4OAc, x mM $MgCl_2$)	

50 fmol wt or mutant RNase P RNA, including trace amounts of 3'- or 5'-end labelled material of the same RNA, were incubated in buffer A (containing 2 or 10 mM $Mg(OAc)_2$) or buffer KN (containing 2 or 4.5 mM $Mg[OAc]_2$) or buffer F (containing 2 or 10 mM $MgCl_2$). Conditions were chosen to mimic those of the kinetic experiments (chapter 3.6.1). RNase P RNAs were either kept at 4°C (no preincubation) or preincubated for 55 min at 37°C, or 5 min at 55°C followed by 50 min at 37°C. We also tested a protocol starting with 2 min at 85°C, followed by 5 min at 55°C and 50 min at 37°C. The results were, however, identical to those obtained with 5 min at 55°C plus 50 min at 37°C.

For samples including the protein subunit, the *E. coli* or *B. subtilis* P proteins were added to final concentration of 50 and 37 nM, respectively, after the preincubation step. All samples, except those kept at 4°C, were incubated for another 15 min at 37°C and finally adjusted to room temperature. Immediately before gel loading, 1 volume of loading buffer (3.2.1.2.3) was added. The non-denaturing 11.25 % (v/v) polyacrylamide gels (thickness < 1 mm) contained 66 mM Hepes, 33 mM Tris, pH 7.4 and 0.1 mM EDTA (1 x THE), supplemented with 100 mM NH_4OAc and 0.3-10 mM $MgCl_2$ (3.2.1.2.3). Gels were run at 180-250 V until xylene cyanol had migrated 11.5 cm from the top. The gel temperature was controlled to not exceed 15°C.

RNA bands were visualized with a Bio-Imaging Analyzer (FLA 3000-2R, FUJIFILM). Results were the same for 5'- and 3'-end labelled P RNAs. End homogeneity of P RNAs was checked on denaturing gels. Results for RNase P RNAs incubated in buffer KN containing 4.5 mM $MgCl_2$ were the same if gels were run in the presence of 4.5 or 10 mM $MgCl_2$.

3.5 Protein methods

3.5.1 TCA-Precipitation

PUV Buffer	
Tris/HCl pH 7.4	50 mM
NaCl	100 mM
Urea	8 M

To isolate and, particulary, concentrate proteins from bacteria a TCA precipitation was performed. Cells were grown at 37°C in the presence of 25 µg/ml chloramphenicol, 100 µg/ml ampicillin (for BW cells harbouring pACYC177), 10 µg/ml tetracycline (for cells containing pBR322 derivatives), 10 mM arabinose and 1 mM IPTG or in the presence of 12.5 µg/ml lincomycin, 0.5 µg/ml erythromycin, 30 µg/ml tetracycline, 1 mM IPTG and 2 % xylose (for SSB318 bacteria harbouring pHY300 derivatives) to an OD_{578} of ~ 0.7. If not stated otherwise cultures were grown in 50 ml LB. Cells were cooled on ice for 10 min. 45 ml of this bacterial suspension were transferred to a 50 ml falcon tube containing 5 ml ice-cold 50 % (w/v) TCA (Trichloro acetic acid). This suspension was incubated for another 15 min on ice and then centrifuged for 10 min at 6000 rpm at 4°C (centrifuge Eppendorf 5810R). The supernatant was discarded and the protein pellet was washed 3 times with 2 ml ice-cold acetone by resuspension of the pellet and centrifugation (5 min, 4°C, 13000 rpm, Biofuge fresco). For easier handling, the protein pellet was transferred into a 2 ml reaction tube for this procedure. The protein pellet was dried at room temperature and resuspended in ~200-400 µl PUV-Buffer.

3.5.2 SDS-PAGE

Sodium dodecylsulphate-polyacrylamide gel electrophoresis (SDS-PAGE) is used to separate proteins in polyacrylamide gel systems according to their molecular weight. Based on the protocol by Laemmli (1970), SDS, an anionic detergent, denatures proteins by binding to hydrophobic amino acid side chains. Thereby, SDS attaches negative charge to the polypeptide roughly in proportion to its length. Another modified protocol was established by Schägger and Jagow (1987). In this gel system the resolution for small proteins (5-20 kDa) was improved by increasing the molarity of the buffer and replacing glycine with tricine. This system is also more resistant to samples with high salt concentrations (up to 2.2 M NaCl are tolerated). For Schägger/Jagow gels, different buffers are used in the cathode and anode reservoirs. The pH of stacking and separation gel is identical, because the mobility of tricine is largely independent of pH.

3.5.2.1 Schägger/Jagow SDS-PAGE

3 x Gel buffer (Schägger)	
Tris/HCl pH 8.45	3 M
SDS	0.4 % (w/v)

5 x Anode buffer (Schägger)	
Tris/HCl pH 8.9	1 M

5 x Cathode buffer (Schägger)	
Tris/HCl pH 8.25	0.5 M
Tricine	0.5 M
→ 1 x concentrated buffer has to be supplemented with 0.1 % (w/v) SDS!	

4 x SDS-PAGE sample buffer (Schägger)	
Tris/HCl pH 6.8	100 mM
SDS	8 % (w/v)
Glycerol	24 % (v/v)
β-mercaptoethanol	4 % (v/v)
→ after adjustment of pH, 0.04 % (w/v) bromophenol blue is added	

For the analysis of the RNase P protein (~13 kDa), stacking gels of 4 % and separation gels of 13 % were used (the composition below is calculated for 2 mini gels). Gels for the Mini Protean® 3 cell chamber system (Biorad) were prepared with 0.75 mm combs (approximate total volume for 2 gels: 5 ml).

SDS-PAGE (Schägger)	Stacking gel (4 %)	Separation gel (13 %)
Acrylamide (48 %)/ bisacrylamide (2 %)	400 µl	2.6 ml
3 x Gel buffer (Schägger)	1.25 ml	3.35 ml
H_2O	3.3 ml	4.05 ml
TEMED	5 µl	10 µl
APS (10 %)	50 µl	100 µl

After addition of the starting reagents (TEMED and APS) to the acrylamide solution, the separation gel solution was poured between the glass plate assembly and overlaid with isopropanol to ensure a smooth surface and to exclude air. Isopropanol was washed away with water after gel polymerization (~15 min). The stacking gel was then poured onto the separation gel and the comb was inserted.

The glass plates with the gel were inserted into the electrophoresis apparatus, and the electrode tanks were filled with the appropriate electrophoresis buffer. Protein samples were mixed with 3 volumes of 4 x SDS-PAGE sample buffer and heated for 2 min at 95°C before gel loading. A commercially available protein marker (e.g. prestained protein marker broad range, Fermentas) was loaded in parallel for size estimation. If not stated otherwise, two gels with identical samples were run in parallel; one was stained with Coomassie Brilliant Blue and the second was used for Western blotting.

The gel was run at 35 V until BPB had traversed the stacking gel, after which the voltage was increased to 90 V.

3.5.2.2 Laemmli SDS-PAGE

4 x Separation gel buffer (Laemmli)

Tris/HCl pH 8.8	1.5 M

8 x Stacking gel buffer (Laemmli)

Tris/HCl pH 6.8	1 M

5 x Gel running buffer (Laemmli)

Tris/HCl pH 8.3	20 mM
Glycine	0.25 M
SDS	0.1 % (w/v)
minigels are run in 1 x running buffer (25 mA/180 V)	

4 x Loading buffer (Laemmli)

SDS	4 % (w/v)
Glycerol	20 % (w/v)
β-mercaptoethanol	5 % (w/v)
Tris/HCl pH 6.8	250 mM
Bromophenol blue	0.001 %

SDS-PAGE gels (Laemmli)

Separation gel (5 ml)	10 %	13 %	15 %	17 %
Acrylamide (48 %)/ bisacrylamide (2 %)	1 ml	1.3 ml	1.5 ml	1.7 ml
4 x Separation gel buffer (Laemmli)	1.25 ml	1.25 ml	1.25 ml	1.25 ml
20 % (w/v) SDS	25 µl	25 µl	25 µl	25 µl
H_2O	2.73 ml	2.45 ml	2.23 ml	2.03 ml
10 % (w/v) APS	50 µl	50 µl	50 µl	50 µl
TEMED	5 µl	5 µl	5 µl	5 µl

Stacking gel (5 ml)	4 %
Acrylamide (48 %)/ bisacrylamide (2 %)	400 µl
8 x Stacking gel buffer (Laemmli)	625 µl
20 % (w/v) SDS	25 µl
H_2O	3.95 ml
10 % (w/v) APS	50 µl
TEMED	5 µl

Gels were prepared as described for SDS-PAGE according to Schägger/Jagow, but using the Laemmli buffer solutions (see above). Note that cathode and anode buffers are identical for Laemmli SDS-PAGE.

3.5.3 Coomassie Staining

Gel staining solution	
Methanol	40 % (v/v)
Acetic acid	10 % (v/v)
Coomassie Brilliant Blue R250	0.5 % (w/v)

Destaining solution
same composition, but without Coomassie

The gel was covered with gel staining solution and left for 30 min at room temperature with agitation. The gel was then transferred to the destaining solution and destained overnight under shaking. The destaining solution was exchanged in between for more efficient destaining. For conservation, the gel was dried on a gel dryer. For this purpose, the gel was put on filter paper (GB002, Schleicher and Schuell), moistened with destaining solution, covered with clingfilm and dried for 1 h at 60°C under vacuum, followed by 2 h of drying at room temperature (Biorad Slab dryer model 483).

3.5.4 Western Blot

Western Blotting is the procedure to transfer proteins to a membrane for immobilization. Usually Polyvinylidene fluoride- (PVDF-) or Nitrocellulose- (NC-) Membranes are used. The semi dry blotting method was used.

Transfer buffer	
Tris base pH ~ 9.2 (pH was not adjusted!)	48 mM
Glycine	39 mM
Methanol	20 % (v/v)
SDS	0.04 % (v/v)

After SDS-PAGE, gels were equilibrated for 10 min in transfer buffer. The PVDF membrane (Immobilon P, Millipore; cut to have same size as the gel) was briefly wetted with methanol, rinsed by dipping into water and then also equilibrated for 5 min in transfer buffer. 5 filter papers (GB004, Schleicher & Schuell) were also moistened with transfer buffer and arranged in the following order on the blotting device:

- Graphite cathode
- 2 layers of filter paper
- Gel
- PVDF membrane
- 3 layers of filter paper
- Graphite anode

Graphite plates were wetted with water. Special attention was paid to the absence of air bubbles, to allow effective transfer. Proteins were blotted applying 1 mA/mm^2 for 75 min. (As a rule of thumb, the voltage was 6 mV in the beginning and increased to 30 mV at the end of the transfer).

3.5.5 Immunodetection

The proteins immobilized on the PVDF membrane by Western blotting can be detected with specific antibodies. In this study, specific antigen-antibody complexes were detected by secondary antibodies, which were conjugated with an alkaline phosphatase (AP). By adding Bromo-4-Chloro-3-Indolylphosphate (BCIP) and Nitroblue Tetrazolium (NBT), alkaline phosphatase activity on the PVDF membrane could be made visible. BCIP is an AP substrate, which reacts further after the dephosphorylation to give a dark blue indigo dye as oxidation product. NBT serves herein as the oxidant and gives also a dark blue dye. It thereby intensifies the colour and makes the detection more sensitive.

5 x TBS Buffer	
Tris/HCl pH 7.6	100 mM
NaCl	2.5 M

Washing Buffer	
TBS	1 x final concentration
Skim milk powder	0.5 % (w/v)
Tween 20	0.1 % (v/v)

Blocking Buffer	
TBS	1 x final concentration
Skim milk powder	5 % (w/v)

Substrate Buffer	
Tris/HCl pH 9.5	100 mM
NaCl	100 mM
$MgCl_2$	50 mM

Colour reagents for AP	
NBT in 70 % DMF (Promega)	25 mg/ml
BCIP in 70 % DMF (Promega)	25 mg/ml

After blotting the PVDF membrane was moistened with methanol. Unspecific protein binding sites on the membrane were saturated by incubation in blocking buffer for 30 min at room temperature while gently shaking. The membrane was washed twice (5 min each) with 1 x TBS buffer. The primary antibody was diluted in 1 x TBS buffer supplemented with 0.5 % skim milk powder and incubated with the membrane for 1.5 h under gentle shaking at room temperature. *E. coli* RNase P protein-specific antibodies were diluted 1:900; those specific for the *B. subtilis* RNase P protein were diluted 1:2500. For *B. subtilis* RNase P protein immunodetection, unspecific background bands could be reduced by incubating the primary antibody with 3 ml *E. coli* cell lysate (11 mg protein/ml) in 27 ml TBS/0.5 % skim milk powder for 30 min at room temperature prior to incubation with the PDVF membrane. The membrane was then washed 3 times (5 min each) with washing buffer before the secondary antibody (goat-anti-rabbit-AP, 1:4000 diluted) was added in 1 x TBS/0.5 % skim milk powder, followed by incubation for 1 hour at room temperature. The membrane was again washed twice (5 min each) with washing buffer. Afterwards, the membrane was equilibrated for 10 min in substrate buffer. Colour reagents were diluted (BCIP 1:750 and NBT 1:1500) in substrate buffer and the colour reaction was started by adding this solution to the membrane. When the band intensities reached a satisfactory extent, the reaction was stopped by transferring the membrane into distilled water. The membrane was dried and scanned for documentation purposes.

3.5.6 Preparation of recombinant RNase P proteins

E. coli and *B. subtilis* RNase P proteins carrying an N-terminal His-tag (His-tagged peptide leader: MRGSHHHHHHGS, encoded in plasmid pQE-30 in *E. coli* JM109) were expressed essentially as described (Rivera-León *et al.*, 1995). Cell cultures (LB broth containing 100 µg/ml ampicillin) were grown to an OD_{578} of 0.6 and IPTG was added to a final concentration of 1 mM. Cells were harvested after 3 h (OD_{578} ~ 2.5) by centrifugation for 10 min at 5,000 rpm at 4°C. The following steps were performed at 4°C or on ice, and all buffers contained 40 µg/ml of the protease inhibitor phenylmethylsulfonyl fluoride (PMSF). Cells were then resuspended in 10 to 15 ml sonication buffer SB (50 mM Tris-HCl, pH 8.0, 0. 3 M NaCl, 0.1 % triton X-100, 1 M NH_4Cl). After sonication (Branson Sonifier 250, output 20, duty cycle 50 %, 15 min on ice), the sample was centrifuged for 30 min (4°C, 14,500 g), and the supernatant was mixed with Ni-NTA agarose (400 µl for 2 liters of cell culture) which had been prewashed twice with 10 ml SB buffer. The sample was incubated for 1 to 2 h at 4°C under gentle mixing or rotating. The Ni-NTA agarose slurry was washed threetimes (centrifugation-resuspension cycles; centrifugation at 4°C and 8,500 rpm in a desktop centrifuge) with ice-cold washing buffer (30 mM imidazol, 50 mM Tris-HCl, pH 8.0, 8 M urea, 0.1 % triton X-100); the RNase P protein started to precipitate during this procedure; therefore, the supernatant after each washing step was removed carefully to avoid release of protein aggregates from the matrix. The protein was then eluted with 500 µl elution buffer (50 mM Tris-HCl, pH 7.0, 10 % glycerol, 7 M urea, 20 mM EDTA, 0.3 M imidazol) for 45 min at 4°C under gentle shaking. Eluates were dialyzed twice for 1 h and subsequently overnight against volumes of 500 ml dialysis buffer (50 mM Tris-HCl, pH 7.0, 0.1 M NaCl, 10 % glycerol; dialysis bags: Roth, molecular weight cut off 12-14 kDa); during dialysis, a white precipitate formed. The content of dialysis bags was transferred to a 2- ml Eppendorf tube and centrifuged for 20 min at 4°C and 12,000 rpm in a desktop centrifuge. The supernatant contained RNase P protein devoid of any RNase P RNA contamination, whereas the pellet included traces of RNase P RNA and was therefore discarded. All purification steps were monitored by 17 % SDS-PAGE to assess the purity and concentration of RNase P proteins.

3.5.7 Partial purification of RNase P from *E. coli* cells

Buffer A (FPLC)	
NH_4Cl	60 mM/550 mM
$Mg(OAc)_2$	10 mM
DTT	6 mM
Tris-HCl, pH 7.2 to 7.5	50 mM

DW2 cells were grown at 43°C as described (chapter 3.4.1.1), and SSB318 cell were grown in the absence of IPTG as described (chapter 3.4.1.3). Cell pellet (~600 mg) was resuspended in about 4 ml of buffer A (FPLC), containing 60 mM NH_4Cl, and lysed by sonication (Branson Sonifier 250, output 20, duty cycle 30-40 %, 10 min on ice), followed by centrifugation for 45 min at 4°C and 10,000 g. For the preparation of DEAE fractions, the supernatant was loaded onto a DEAE fast flow sepharose column (column XK16, Pharmacia). Flow rate was adjusted to 2 ml/min. After the first peak, indicating unbound flow through, had been detected and absorbance again reached the basal level, a NH_4Cl gradient from 60 to 550 mM NH_4Cl was applied. Active fractions eluted at about 300 to 400 mM NH_4Cl. The fractions were collected in 2 ml reaction tubes on ice; a small aliquot was taken from each fraction to check for RNase P processing activity, whereas the rest was frozen in liquid nitrogen. For washing, the column was eluted with 1 M NaCl and then rinsed with double-distilled water followed by washing with 70 % ethanol. The activity was checked as described in 3.6.1.1.

The most active fraction was divided into 2-10 µl aliquots and stored at –80°C after freezing in liquid nitrogen.

For verification of wt and mutant *rnpB* alleles, DEAE fractions were phenol/chloroform extracted, concentrated by ethanol precipitation and used as template for primer extension analyses (3.4.5).

3.6 Kinetic Analysis

3.6.1 Kinetic analysis of RNase P holoenzymes

Buffer F 2/10

Mes, pH 6.1	50 mM
KCl	100 mM
$MgCl_2$	2 or 10 mM

Buffer KN 2/4.5 (Dinos *et al.*, 2004)

Hepes-KOH, pH 7.4	20 mM
$Mg(OAc)_2$	2 or 4.5 mM
NH_4OAc	150 mM
Spermidine	2 mM
Spermine	0.05 mM
β-mercaptoethanol	4 mM

Kinetic analyses of RNase P holoenzymes were all performed under multiple turnover conditions. In multiple turnover kinetics substrate is present in excess over enzyme; thus, one enzyme can cleave more than one substrate during reaction. Rates were calculated as k_{obs} (turnover µmol substrate per min and µmol enzyme). The rate-determining step can be either substrate association (k_1), cleavage (k_2) or product release (k_3) or a conformational rearrangement of the substrate/enzyme or product/enzyme complex (the later is not considered in the scheme below).

$$E \quad + \quad S \quad \underset{k_{-1}}{\overset{k_1}{\leftrightarrows}} \quad ES \quad \xrightarrow{k_2} \quad EP \quad \underset{k_{-3}}{\overset{k_3}{\leftrightarrows}} \quad E \quad + \quad P$$

Reaction scheme for RNase P processing under multiple turnover conditions; E: enzyme; S: substrate; k_n: rate constants.

For all processing assays *Thermus thermophilus* ptRNA^{Gly} (ptRNAwt) or G74 or G75 variants thereof were used. This tRNA contains a 14-mer 5'-flank. The sequence of ptRNAwt is shown in Fig. 3.1.

3.6.1.1 Kinetic analysis of *in vivo* assembled holoenyzmes

For analysing RNase P-catalysed processing by *in vivo* assembled RNase P holoenzymes, active DEAE fractions (0.25 to 1.0 µl; equal amounts based on A_{260} measurements; chapter 3.5.7) were incubated in buffer A (see chapter 3.5.7; 2 or 10 mM $Mg(OAc)_2$, 6 mM DTT, 50 mM Tris-HCl, pH 7.5) containing 100 mM NH_4Cl for 10 min at 37°C (reaction volume 16 µl). Trace amounts (< 1 nM) of the 5'-end labelled ptRNA^{Gly} substrate were preincubated under the same conditions for 5 min at 55°C and 25 min at 37°C. Processing reactions were started by combining enzyme and substrate solutions and assayed at 37°C (final volume 20 µl). As the negative control, the substrate mix was incubated in parallel under same conditions. For each time point, a 4 µl aliquot was withdrawn from the reaction mix and mixed immediately with 4 µl denaturing sample buffer/EDTA solution and kept on ice.

denaturing sample buffer/EDTA	
denaturing sample buffer (3.2.1.2.1)	504 µl
0.5 M EDTA pH 8.0	156 µl

3.6.1.2 Kinetic analysis of i*n vitro* reconstituted RNase P holoenzymes

Processing assays of *in vitro* reconstituted RNase P holoenzymes were performed either in buffer F (containing 2 or 10 mM Mg^{2+}) or in buffer KN (containing 2 or 4.5 mM Mg^{2+}), originally optimised for functional analyses of *E. coli* ribosomes. The magnesium concentration was decreased to 2 mM to closely mimic physiological conditions. *In vitro* reconstitution of RNase P holoenzymes was performed as follows: If not stated otherwise, 10 nM RNase P RNAs were incubated in buffer KN or buffer F for 5 min at 55°C and 50 min at 37°C, after which RNase P protein (concentration varied) was added, followed by another 5 min at 37°C before addition of substrate (the volume was 8 or 16 µl). 100 nM ptRNA^{Gly} supplemented with trace amounts (< 1 nM) of 5'-end labelled ptRNA^{Gly}, were preincubated under the same conditions for 5 min at 55°C and 25 min at 37°C (substrate mix). Processing reactions were started by combining enzyme and substrate mixes, and assayed at 37°C (final volume 10 or 20 µl).

The $Mg(OAc)_2$ concentration was raised to 100 mM in control reactions with *E. coli* RNase P RNA alone.

3.6.2 Evaluation of kinetic anaylses

Samples were analysed on 20 % denaturing PAA gels and imaging plates were exposed to the gel overnight. This permitted to detect the bands corresponding to (uncleaved) ptRNA or released 5'-flank (equals mature tRNA). Bands were quantified using a Bio-Imaging System (Raytest) and the software AIDA. The processed portion of tRNA could be calculated as follows:

$$tRNA_{processed} = \frac{[5'-flank]}{[5'-flank] + ptRNA}$$

Further evaluation was done using the software Grafit to calculate the k_{obs} values by fitting the data to a single order rate equation as follows:

$$A_t = A \cdot \left(1/e^{-kobs} \cdot t \right)$$

with A_t: amount of tRNA cleaved at timepoint t, A: maximum amount of tRNA that could be cleaved, k_{obs}: observed rate constant.

3.7 Cloning experiments

3.7.1 One Step inactivation of chromosomal genes in *E. coli*

One strategy for efficient recombination between short linear DNA fragments and the bacterial chromosome involves phage recombination systems (reviewed in Court *et al.* 2002). The phage λ Red locus, which encodes a system that promotes homologous recombination, includes three genes: *bet* (β), *exo*, and *gam* (γ) (Datsenko and Wanner, 2000; Murphy, 1998; Yu *et al.*, 2000; Poteete and Fenton, 2000; Kuzminov, 1999). *Exo* is a 5'→ 3' exonuclease that degrades the 5'-ends of linear DNA molecules. *Bet* is a single-stranded DNA binding protein that binds to the single-stranded 3'-ends generated by Exo and promotes annealing to complementary DNA. Gam binds to the host RecBCD complex and inhibits its exonuclease activity (Murphy 1991; Murphy 1998; Karu 1975).

In our lab we used pKD46, a low copy plasmid which encodes γ, β and exo under the IPTG-inducible pBAD promoter (Datsenko and Wanner, 2000). As the plasmid has the temperature-sensitive origin of replication repA101ts it is easily to eliminate from the cells afterwards. The pBAD promoter system can be tighly repressed and therefore prevents unwanted recombination under uninduced conditions. In the literature homologous flanking regions as short as 36 nt were described to be sufficient for successful recombination (Datsenko and

Wanner, 2000). However, in our case the cloning was only successful after increasing the homologous regions to 370-630 nt.

3.7.1.1 Construction and verification of *rnpB* mutant strain BW

To inactivate essential genes, it is necessary to put the gene of interest under an inducible, tight regulatable promoter system. Construction of *rnpB* mutant strain BW followed the strategy described by Roux *et al.* (2005), which applies the IPTG-inducible pBAD promoter system for this purpose. The so-called catRExBAD cassette, carrying the chloramphenicol resistance gene (*cat*), a gene coding for an arabinose operon regulatory protein (*araC*), and the arabinose-inducible pBAD promoter (see chapter 4.2 and Fig. 3.3), was amplified from strain TG1 cat-AraC (Roux *et al*., 2005) using primers 135 (containing sequences identical to the region upstream of the *E. coli rnpB* promoter) and 134 (partially overlapping with nt 1-50 of *rnpB*). Initially, we could isolate a recombinant strain, which had the 5'-end of the described catRExBAD cassette successfully recombined within the 5' *rnpB* promoter upstream region, but the 3'-boundary was altered. This strain was used to amplify a 326-bp fragment, containing the 5'-boundary, with primers 137 and 138. The *E. coli rnpB* gene was amplified from *E. coli* K12 with primers 163 and 150. This *rnpB* fragment and the 326-bp fragment with *E. coli rnpB* upstream sequence were combined with the catRExBAD cassette by overlap extension PCR. The resulting PCR product was purified by agarose gel electrophoresis and transformed into *E. coli* MG1655 bacteria carrying pKD46 (the Red helper plasmid, encoding the λ Red recombinase system, temperature-sensitive for replication, Datsenko and Wanner, 2000). For this purpose, MG1655/pKD46 cells were grown to an OD_{578} of 0.15 at 28°C and then induced with 10 mM arabinose. Induced cultures were grown to an OD_{578} of 0.6 at 28°C and made electrocompetent by 100-fold concentration and three washing steps with ice-cold 10 % glycerol. Electroporation was performed with a Biorad Gene Pulser in 1 mm cuvettes (1.8 kV, 200 µF, 25 Ω) using 40 µl competent cells and 100-200 ng purified PCR fragment. Shocked cells were added to 1 ml SOC medium supplemented with 10 mM arabinose, shaken for 1 h at 37°C and 900 rpm (Eppendorf Thermomixer comfort), and then plated and incubated at 37°C on LB agar plates containing 25 µg/ml chloramphenicol and 10 mM arabinose. Clones were analysed by PCR for correct 5'- and 3'-boundaries of the integrated catRExBAD cassette and screened for ampicillin sensitivity to test for the loss of the temperature-sensitive helper plasmid pKD46. The primers 195, 194, 193, 158, 157, 136, 138, 49, 186, and 183 were used to scrutinize correct insertion and sequence of the integrated cassette (primer locations within the recombined region are shown in Fig. 3.3):

Integrity of the 5’-boundary was checked by primer combinations 157/138 and 138/186, and that of the 3’-boundary by the combinations 136/158 and 136/183; the absence of the native *rnpB* promoter region was verified with the primer pair 193/49, which produced a PCR fragment with genomic DNA from strain MG1655 (the original strain), but not with DNA from correct recombinants. Primer pairs 194/49 and 195/157 were used to amplify the inserted cassette in roughly two halves (upstream and downstream of *araC*, see Fig. 3.3) for verification by sequencing. Verified recombinant bacteria were named strain BW.

Detailed sequence information on the *rnpB* environment in strain BW can be found in the appendix (8.15).

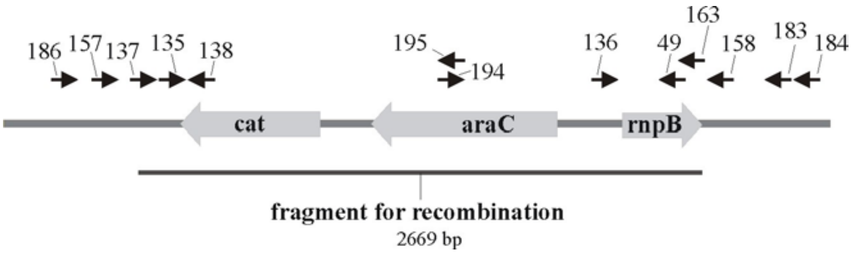
186
157
137
135
138
195
194
136
49
163
158
183
184
cat
araC
rnpB
fragment for recombination
2669 bp

Fig. 3.3: *E. coli rnpB* environment after recombination with the fragment containing the catRExBAD cassette. Arrows above indicate positions of primers used for strain analysis and verification.

3.7.2 Plasmids for complementation studies in *E. coli rnpB* mutant strains

3.7.2.1 pSP64 *E. coli rnpB* EP

For complementation studies in strain DW2/pDW160, complementing *rnpB* genes were under control of the native *E. coli rnpB* promoter (termed EP or $P_{E.c\ rnpB}$) and cloned in plasmid pSP64 as described (Hardt and Hartmann, 1996). Note, that there is no terminator sequence encoded adjacent to the *rnpB* gene on the plasmid. The pSP64 derivative carrying *E. coli rnpB* (pSP64 *E. coli rnpB*) served as template to introduce the point mutations C292 or C293 by site-directed *Dpn* I mutagenesis (3.3.9).

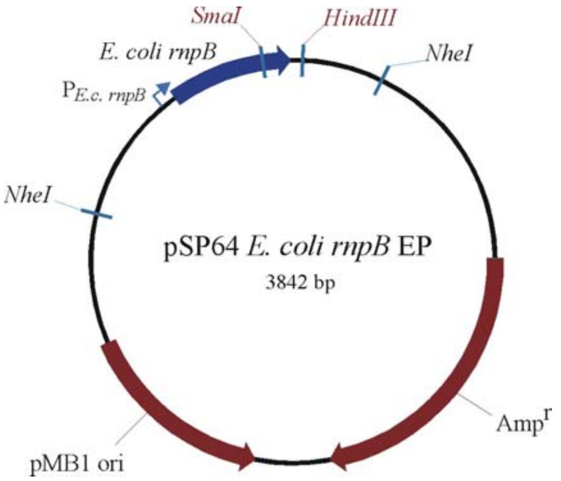
SmaI
HindIII
E. coli rnpB
NheI
PE.c. rnpB
NheI
pSP64 E. coli rnpB EP
3842 bp
Ampr
pMB1 ori

3.7.2.2 Construction of the low copy plasmid pACYC177 *Ecoli rnpB*

To construct derivatives of low copy plasmid pACYC177 encoding *E. coli rnpB*wt, *rnpB*C292 and *rnpB*C293, plasmids pSP64 *E. coli rnpB*wt, *rnpB*C292 or *rnpB*C293 were digested with *Nhe* I and *Hind* III and the fragments carrying the *E. coli rnpB* variants were inserted into pACYC177 also cut with *Hind* III and *Nhe* I.

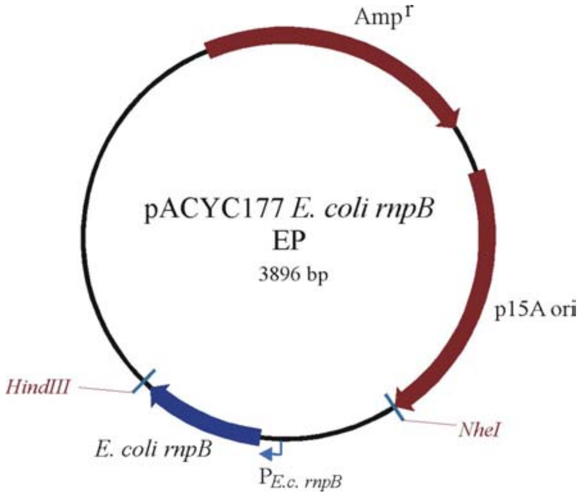

3.7.2.3 Construction of pBR322 derivatives for expression of *E. coli rnpA*

To put *E. coli rnpA* under the control of the IPTG-inducible pTrc promoter (Amann *et al.*, 1988), the *rnpA* gene was amplified with primer 196 (introducing an *Nco* I site at the 5'-end of *rnpA*) and primer 197 (introducing an *Xba* I site at the 3'-end of *rnpA*). The *E. coli rnpA* fragment was digested with *Nco* I and *Xba* I, and ligated into pTrc99a (Amann *et al.*, 1988) also linearized with *Nco* I and *Xba* I, resulting in plasmid pTrc99a *E. coli rnpA*. This plasmid was unsuitable for transformation of bacteria harbouring pACYC177 derivatives, because it encodes the ampicillin resistance as plasmid pACYC177; also, the high copy number of pTrc99a *E. coli rnpA* would have potentially increased an imbalance between *rnpA* expression and that of *rnpB* genes encoded by the low copy plasmid pACYC177. Therefore, the *rnpA* gene including the pTrc promoter and the *rrnB*t1t2 terminator from pTrc99a *E. coli rnpA* was amplified, using the primers 203 (introducing an *Mph*1103 I site) and 206 (introducing a *Mun* I site) and ligated the fragment into pBR322 cut with *Pst* I and *Eco* RI (ends compatible with those of *Mph*1103 I and *Mun* I, respectively). Digestion of pBR322 with *Pst* I and *Eco* RI destroyed the ampicillin resistance, only leaving the tetracycline resistance.

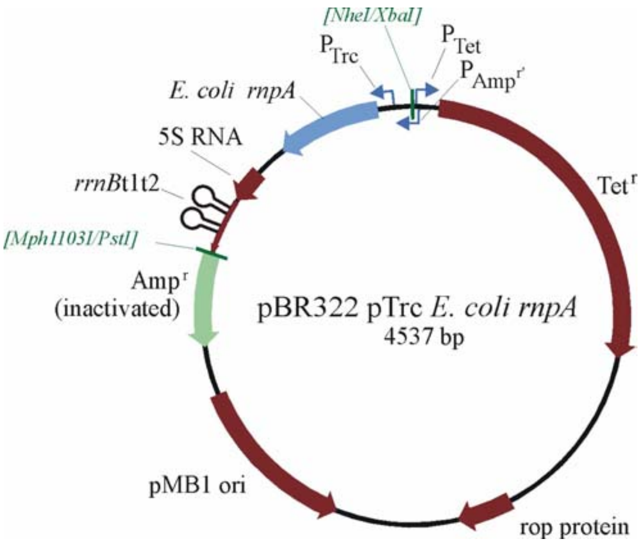

3.7.2.4 Construction of pBR322 encoding mutated 4.5S RNAs

The chromosomal region of *E. coli* K12 harbouring the bicistronic trancription unit of *ffs* (encoding 4.5S RNA) and *ybaA*, including the native promoter upstream of *ffs* as well as 100 bp downstream of *ybaA*, was amplified and cloned into pBR322. During PCR amplification, the terminal stem region was already altered by inversion of 4 base pairs within the stem structure (chapter 4.2) for specific reverse transcriptase priming in order to be able to distinguish native from plasmid-encoded 4.5S RNA. The promoter region and the 5’-end of *ffs* were amplified using primers 207 (introducing an *Eco* RI site) and 208 (including the 5’-terminal 4.5S RNA stem mutations); the 5’-portion of the *ffs* gene was amplified with the primers 209 and 216 (introducing *Mlu* I and *Pst* I sites). These two fragments were combined by overlap extension PCR, cut with *Eco* RI and *Pst* I, followed by ligation into pBR322 cut with the same enzymes. The 3’-half of *ffs* was amplified with primer 209 and 210 (3’-terminal stem with mutations). The chromosomal region spanning the 3’-portion of *ffs* and the *ybaA* cistron was amplified using forward primer 211 and reverse primer 214. To further introduce point mutations into the 3’-CCC end of 4.5S RNA, the same PCR reaction was performed, except that primer 212 (3’-GCC“76”) or primer 213 (3’-CGC“76”) were used as the forward primer. The latter amplification products were combined with the PCR fragment harbouring the 3’-half of *ffs* (see above) by overlap extension PCR. The resulting product was then cut with *Pst* I/*Mlu* I and ligated into the pBR322 derivative containing the promoter and 5’-half of *ffs* and cut with the same restriction enzymes.

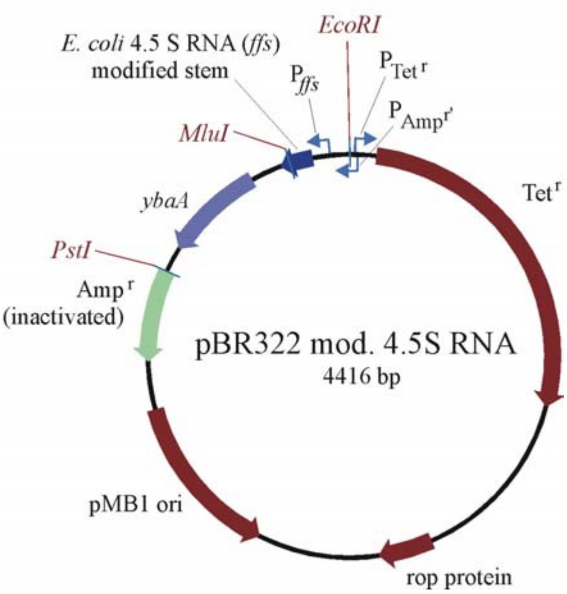
E. coli 4.5 S RNA (ffs) modified stem
EcoRI
P_{ffs}
P_{Tet^r}
$P_{Amp^{r'}}$
MluI
Tet^r
ybaA
PstI
Amp^r (inactivated)
pBR322 mod. 4.5S RNA
4416 bp
pMB1 ori
rop protein

3.7.2.5 Construction of pSP64 *B. subtilis rnpB* BPT (*B. subtilis rnpB* promoter and terminator)

For cloning of *B. subtilis rnpB* gene into pSP64, *B. subtilis rnpB* including its natural promoter ($P_{B.s.\ rnpB}$) and terminator sequence was amplified from genomic *B. subtilis* DNA (strain W168) using primer 19 (including the native *Hind* III site upstream of *rnpB*) and primer 21 (introducing a *Hind* III site at the 3'-end of *B. subtilis rnpB*). The resulting PCR fragment was cloned into the *Hind* III site of pSP64; the orientation of the *rnpB* gene was such that its 3'-portion was adjacent to the *Xba* I site in the pSP64 multi-cloning site. The plasmid is referred to as pSP64 *B. sub rnpB* BPT (BPT: native *B. subtilis rnpB* promoter and terminator)

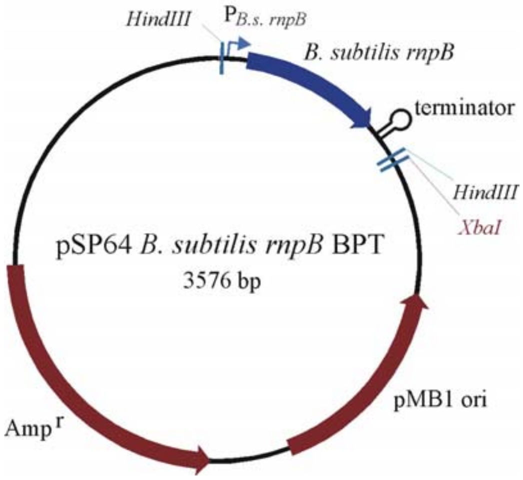
HindIII
$P_{B.s.\ rnpB}$
B. subtilis rnpB
terminator
HindIII
XbaI
pSP64 B. subtilis rnpB BPT
3576 bp
Amp^r
pMB1 ori

3.7.2.6 Construction of pSP64 *B. subtilis rnpB* EP/BT *(E. coli rnpB* promoter and *B. subtilis rnpB* terminator)

To clone the *B. subtilis rnpB* gene under control of the native *E. coli rnpB* promoter ($P_{E.c.\ rnpB}$), the *E. coli rnpB* promoter region was amplified from *E. coli* K12 genomic DNA using primers 157 and 156 (introducing an overlap with the 5'-end of *B. subtilis rnpB*). *B. subtilis rnpB* including its native terminator was amplified with primers 149 and primer 21 (including a *Hind* III site). *rnpB* promoter and terminator fragments were combined by overlap extension PCR, digested with *Kpn* I and *Hind* III and cloned in pSP64 *E. coli rnpB* EP (Busch *et al.* 2000; chapter 3.7.2.1), which was cut with the same enzymes, thereby eliminating *E. coli rnpB*.

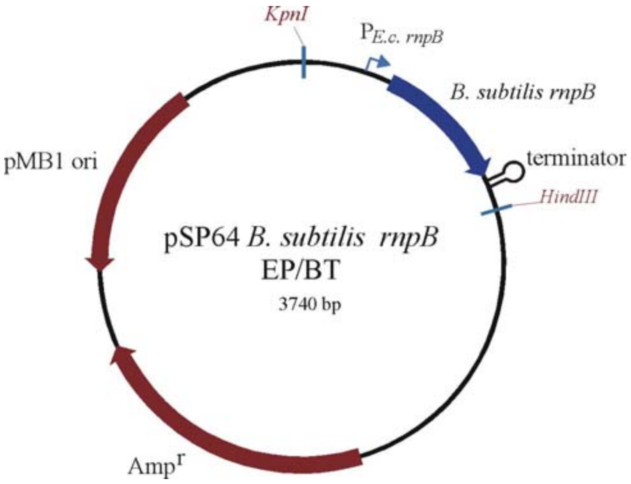

3.7.2.7 Construction of pACYC177 *B. subtilis rnpB* EP/BT (*E. coli rnpB* promoter, *B. subtilis rnpB* terminator)

To transfer the *B. subtilis rnpB* insert with *E. coli rnpB* promoter and *B. subtilis rnpB* terminator (EP/BT) into the low copy plasmid pACYC177, we amplified the corresponding fragment from pSP64 *B. sub rnpB* EP/BT with primers 12 and 223 (introducing an *Nhe* I site at the 5'-end of the *E. coli rnpB* promoter), digested the PCR product with *Nhe* I and *Hind* III and cloned it into pACYC177 cut with the same enzymes.

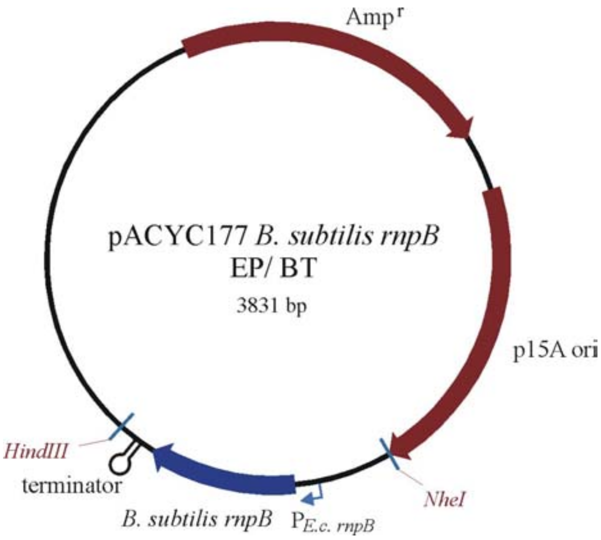

3.7.3 Chromosomal integration in *B. subtilis*

For the integration of DNA sequences into the genome of *B. subtilis* special integration vectors are used. One feature of these vectors is that they can replicate e. g. in *E. coli* (and allow therefore easy cloning in *E. coli*), but lack an origin of replication recognized in *B. subtilis*. Integration is targeted to a particular locus on the chromosome by including homologous sequences in the plasmid. If there is a single homologous region, the whole plasmid will be integrated by single crossover. In the case of two homologous regions, which are in close proximity on the chromosome, a double crossover recombination will result in integration of a cassette between the two targeted chromosomal regions.

3.7.3.1 Construction of the *B. subtilis* conditional RNase P mutant strain SSB318 (done by Ciaran Condon)

The *B. subtilis* conditional RNase P mutant (SSB318) was constructed as follows: a 251-nt PCR fragment, containing nucleotides +1 to +231 of the *rnpB* gene, was amplified using oligonucleotides HP499 (introducing a *Hind* III site) and HP500 (introducing a *Bam* HI site), digested with *Hind* III and *Bam* HI and cloned into pMUTIN-4M (Vagner *et al*., 1998) digested with the same enzymes. The resulting plasmid pMUTIN-*rnpB* was transformed into *B. subtilis* wild-type strain W168, selecting for erythromycin resistance in the presence of 1 mM IPTG. 95 out of 100 transformants tested showed IPTG-dependent growth, indicating correct insertion into the *rnpB* gene which is predicted to be essential. One of these transformants, SSB318, was retained for subsequent studies. In this strain, the chromosomal *rnpB* gene is under control of the IPTG-inducible *spac* promoter. In the absence of IPTG, cell growth becomes dependent on the expression of a complementing *rnpB* gene (Fig. 3.4).

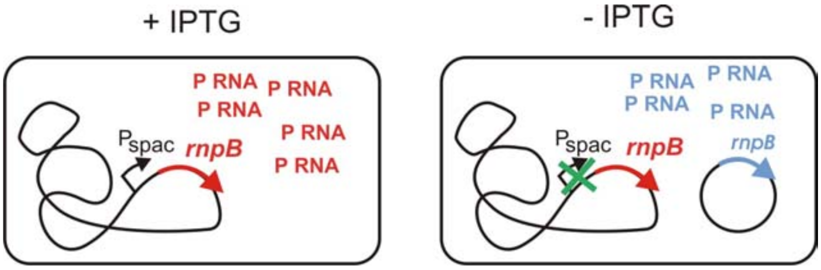

Fig. 3.4: Schematic representation of *B. subtilis rnpB* mutant strain SSB318. In SSB318 the chromosomal *rnpB* gene is put under the control of an IPTG-inducible P_{spac} promoter (left). In the absence of IPTG cell growth becomes dependent on a complementing *rnpB* gene provided on a plasmid (right).

3.7.3.2 Construction of a strain containing *E. coli rnpB* BPT integrated into the chromosome of *B. subtilis* SSB318

For construction of a strain containing *E. coli rnpB*wt with the native *B. subtilis* promoter and terminator (BPT) integrated into the chromosome of *B. subtilis* SSB318, the *E. coli rnpB*wt fragment containing *B. subtilis rnpB* promoter and terminator was cloned into the *Hind* III site of pDG364, a vector suitable for chromosomal integration into the *amy*E locus of *B. subtilis* (Cutting and Vander-Horn, 1990). Toward this goal, *E. coli rnpB* was amplified from plasmid pSP64 *E. coli rnpB*wt (Hardt and Hartmann, 1996) with primers 41 and 46 (introducing sequences that overlap with the *B. subtilis rnpB* promoter and terminator). For amplification of the *B. subtilis* promoter, primer pair 19 and 44 was used. The *B. subtilis* terminator was amplified with primer 45 and primer 21 (introducing a *Hind* III site at the 3'-end of the terminator). The *E. coli rnpB* fragment was combined with *B. subtilis* promoter and terminator fragments by overlap extension PCR, cut with *Hind* III and ligated into pDG364 cut with the same enzyme. The plasmid was linearised with *Xho* I prior to transformation in SSB318 applying the protocol that makes use of the HS/LS medium (3.1.4.4.1).

3.7.4 Plasmids for complementation studies in *B. subtilis* mutant strain SSB318

3.7.4.1 Construction of pHY300 *B. subtilis rnpB* BPT

B. subtilis rnpB was excised from pSP64 *B. sub rnpB* BPT via *Hind* III digestion and inserted into pHY300 (obtained from Takara Shuzo Co., Kyoto, Japan) cut with the same enzymes. The orientation of the *rnpB* gene was such that its 3'-portion was adjacent to the *Eco* RI site in the pHY300 multi-cloning site.

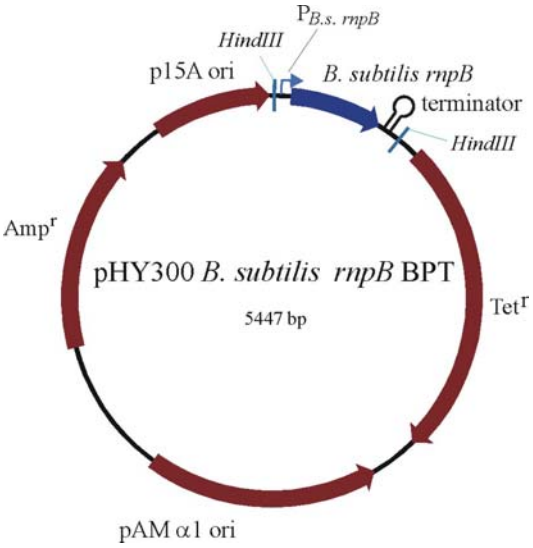

$P_{B.s.\ rnpB}$
HindIII
p15A ori
B. subtilis rnpB
terminator
HindIII
Amp^r
pHY300 B. subtilis rnpB BPT
5447 bp
Tet^r
pAM α1 ori

3.7.4.2 Construction of pHY300 xylRP *B. subtilis rnpB* (xylose promoter)

B. subtilis complementation plasmids for *B. subtilis* mutant strain SSB318 were constructed in 2 steps: first, the fragment encoding xylose repressor (xylR) and promoter (P_{xyl}) was amplified from pX2 (Mogk *et al.* 1997) with phosphorylated primer 100 (introducing a *Bam* HI site) and phosphorylated primer 105 (introducing *Psc* I/*Sma* I sites) cut with *Sma* I and *Bam* HI, and cloned into pHY300 cut with the same enzymes, resulting in plasmid pHY300 xylRP. *B. subtilis rnpB* wt was amplified from genomic DNA with primers 102 (introducing an overlap with the xylose promoter at the 5'-end of *B. subtilis rnpB*) and primer 103 (introducing a *Sma* I site downstream of *rnpB*) and cloned into *Psc* I/*Sma* I sites of pHY300 xylRP. This plasmid is referred to pHY300 xylRP *B. subtilis rnpB*. Mutations C258 and C259 were introduced by the site-directed *Dpn* I mutagenesis method (see 3.3.9).

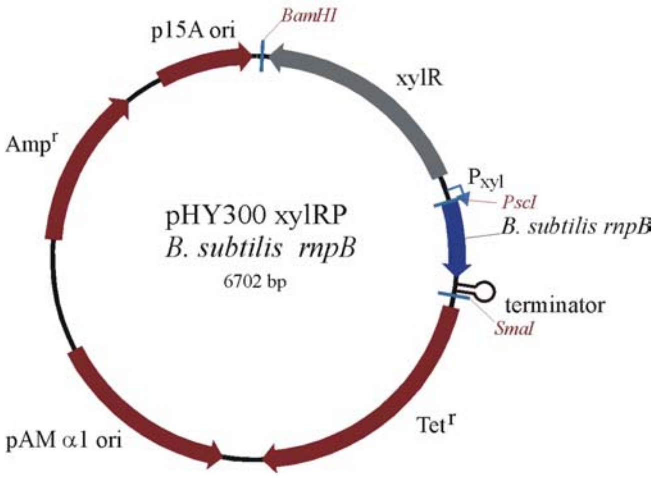

p15A ori
BamHI
xylR
Amp^r
P_{xyl}
PscI
B. subtilis rnpB
pHY300 xylRP
B. subtilis rnpB
6702 bp
terminator
SmaI
Tet^r
pAM α1 ori

3.7.4.3 Construction of pHY300 xylRP *B. subtilis rnpB* + xyl *rnpA* (*B. subtilis*)

The *B. subtilis rnpA* gene under control of the inducible xylose promoter was amplified from strain sb (Gößringer, 2004; Gößringer *et al.*, 2006) using primers 115 and 116 (both introducing a *Bam* HI site) and cloned into the *Bam* HI site of pHY300 xylRP *B. subtilis rnpB*. Constructs with insert "xyl *rnpA*-stop" carried point mutations close to the 5'- end of the xylose-inducible *rnpA* gene, resulting in two stop codons (xyl *rnpA*-stop). For construction of inserts with the xylose-inducible *rnpA*-stop gene, the xylose promoter region was first amplified from genomic DNA of strain sb (Gößringer, 2004; Gößringer *et al.*, 2006) with primers 114 and 115. The *rnpA* gene with the two stop codons was then amplified from plasmid p3dstop (Gößringer, 2004; Gößringer *et al.*, 2006) with primers 113 and 116. The two fragments were combined by overlap extension PCR using primers 115 and 116 (both introducing *Bam* HI sites) and cloned into the *Bam* HI site of pHY300 xylRP *B. subtilis rnpB.*

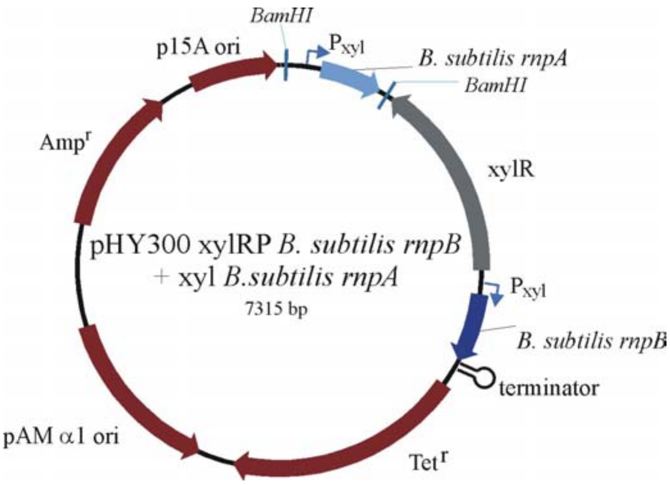

3.7.4.4 Construction of pHY300 *S. aureus rnpB* BPT

For complementation studies with *S. aureus rnpB* in *B. subtilis* strain SSB318, *S. aureus rnpB* gene was cloned under control of the natural *B. subtilis rnpB* promoter and terminator (BPT). For amplification of the *B. subtilis* promoter, primers 19 (including the naturally occurring *Hind* III site upstream of the *B. subtilis rnpB* promoter) and 44 (3' *B. sub.* promoter) were used. The *B. subtilis* terminator was amplified using primers 45 and 21 (introducing a *Hind* III site at the 3'-end of the *B. subtilis rnpB* terminator). *S. aureus rnpB* was amplified with primers 42 and 47 (containing overlapping regions with the *B. subtilis rnpB* promoter and terminator, respectively) from genomic DNA of *Staphylococcus aureus* subsp. *aureus* Rosenbach (ATCC 12600). Fragments carrying the *B. subtilis rnpB* promotor, *S. aureus rnpB* and *B. subtilis rnpB* terminator were combined by overlap extension PCR. The resulting *S.*

aureus rnpB BPT fragment was cloned into the *Hind* III site of pHY300. Point mutations at position G238 and G239 within the *S. aureus rnpB* gene were introduced by the site-directed *Dpn* I method (3.3.9).

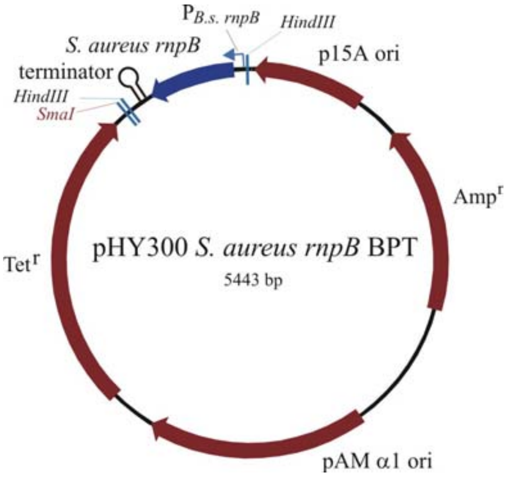
$P_{B.s.\ rnpB}$
HindIII
S. aureus rnpB
p15A ori
terminator
HindIII
SmaI
Amp^r
Tet^r
pHY300 S. aureus rnpB BPT
5443 bp
pAM α1 ori

3.7.4.5 Construction of pHY300 *S. aureus rnpB* BPT + xyl *B. subtilis rnpA*

For parallel overexpression of the *B. subtilis* RNase P protein, *B. subtilis rnpA* was amplified from strain sb including the inducible xylose promoter (Gößringer, 2004; Gößringer *et al.*, 2006) using phosphorylated primers 108 and 107, and cloned in the *Sma* I site of pHY300 *S. aureus rnpB* BPT.

As mentioned before, constructs with the insert “xyl *rnpA*-stop” carried point mutations close to the 5’-end of the xylose-inducible *rnpA* gene, resulting in two stop codons (xyl *rnpA*-stop). Here again, first the xylose promoter region was amplified from genomic DNA of strain sb (Gößringer, 2004; Gößringer *et al.*, 2006) with primers 114 and 108. The *rnpA* gene with the two stop codons close to the beginning was amplified from plasmid p3dstop (Gößringer, 2004; Gößringer *et al.*, 2006) with primers 107 and primer 113. Those two fragments were combined by overlap extension PCR using phosphorylated primers 107 and 108, and cloned into pHY300 *S. aureus rnpB* BPT cut with *Sma* I as performed for the wild-type *rnpA* gene.

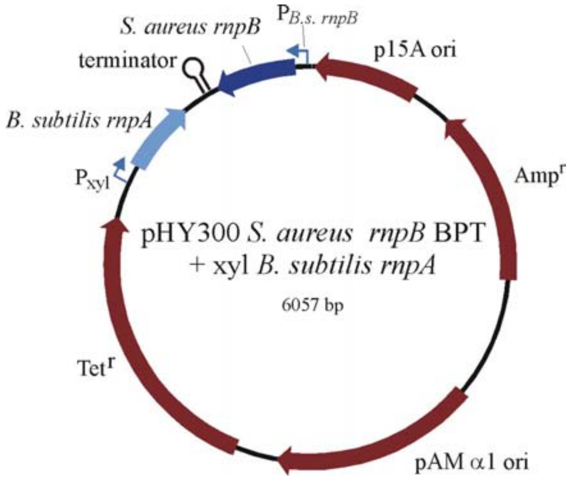
S. aureus rnpB
$P_{B.s.\ rnpB}$
terminator
p15A ori
B. subtilis rnpA
P_{xyl}
Amp^r
pHY300 S. aureus rnpB BPT
+ xyl B. subtilis rnpA
6057 bp
Tet^r
pAM α1 ori

3.7.4.6 Construction of pHY300 *E. coli rnpB* BPT

E. coli rnpB under control of the *B. subtilis rnpB* promoter and terminator (BPT) for complementation in *B. subtilis* SSB318 was constructed as follows: *B. subtilis rnpB* promoter and terminator, and *E. coli rnpB* were amplified exactly as described in 3.7.3.2. Fragments were combined by overlap extension PCR and digested with *Hind* III. This recombinant *E. coli rnpB* gene was cloned into the *Hind* III site of pHY300.

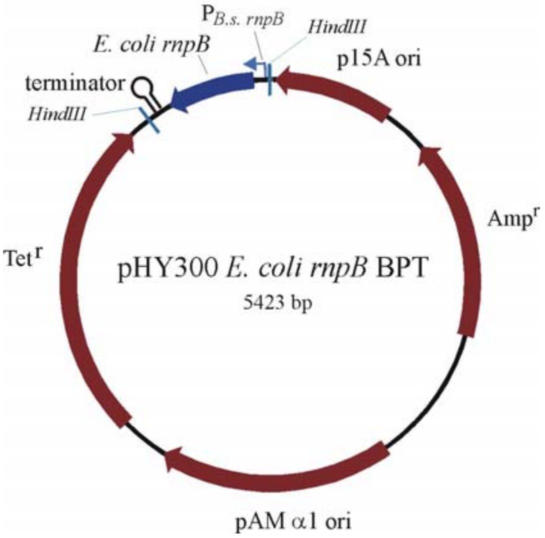
$P_{B.s.\ rnpB}$
HindIII
E. coli rnpB
p15A ori
terminator
HindIII
Amp^r
Tet^r
pHY300 E. coli rnpB BPT
5423 bp
pAM α1 ori

3.7.4.7 Construction of pHY300 *E. coli rnpB* EP

For complementation analysis of *E. coli rnpB* in *B. subtilis* mutant strain SSB318, an *Nhe* I/*Hind* III fragment from plasmid pSP64 carrying the *E. coli rnpB* gene (Hardt and Hartmann, 1996) under control of the native *E. coli rnpB* promoter was cloned into pHY300 cut with *Xba* I (compatible ends with *Nhe* I) and *Hind* III.

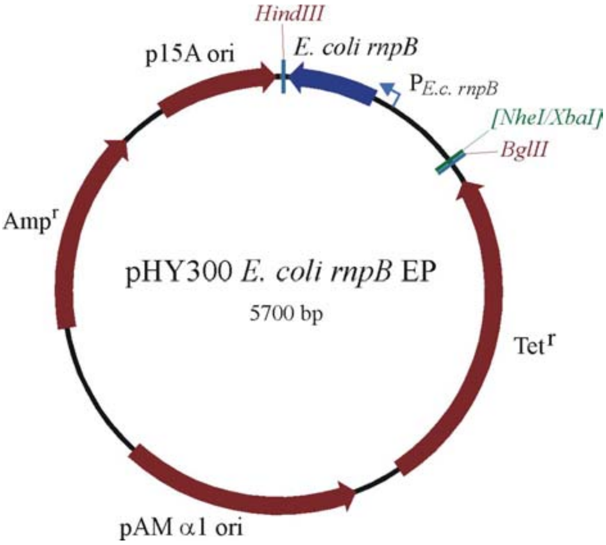
HindIII
E. coli rnpB
p15A ori
$P_{E.c.\ rnpB}$
[NheI/XbaI]
BglII
Amp^r
pHY300 E. coli rnpB EP
5700 bp
Tet^r
pAM α1 ori

3.7.4.8 Construction of pHY300 *E. coli rnpB* EP + xyl *B. subtilis rnpA*

B. subtilis rnpA under the control of the xylose-inducible promoter was amplified from strain sb (Gößringer, 2004; Gößringer *et al.*, 2006) using primers 115 and 116 (both introducing *Bam* HI sites). The PCR product was cut with *Bam* HI and cloned into the *Bgl* II site of pHY300 *E. coli rnpB* EP. Inserts containing *rnpA* encoding two stop codons close to the 5'-end were amplified from plasmid pHY300 *S. aureus rnpB* + xyl *rnpA*-stop (see 3.7.4.5) with primers 115 and 116 and cloned into the *Bgl* II site of pHY300 *E. coli rnpB* EP.

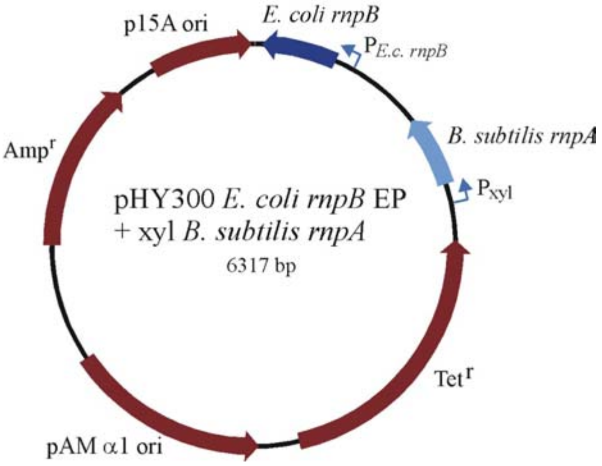
p15A ori
E. coli rnpB
P E.c. rnpB
B. subtilis rnpA
Pxyl
Amp^r
pHY300 E. coli rnpB EP
+ xyl B. subtilis rnpA
6317 bp
Tet^r
pAM α1 ori

3.7.4.9 Construction of pHY300 + xyl *B. subtilis rnpA*

B. subtilis rnpA under the control of the xylose-inducible promoter was amplified from plasmid pHY300 *S. aureus rnpB* BPT + xyl *B. subtilis rnpA* with phosphorylated primers 107 and 108. The fragment was then cloned in the *Sma* I site of pHY300. The same was done for the xylose-inducible *rnpA* gene with two stop codons close to the 5'-end of *rnpA* (xyl *rnpA*-stop).

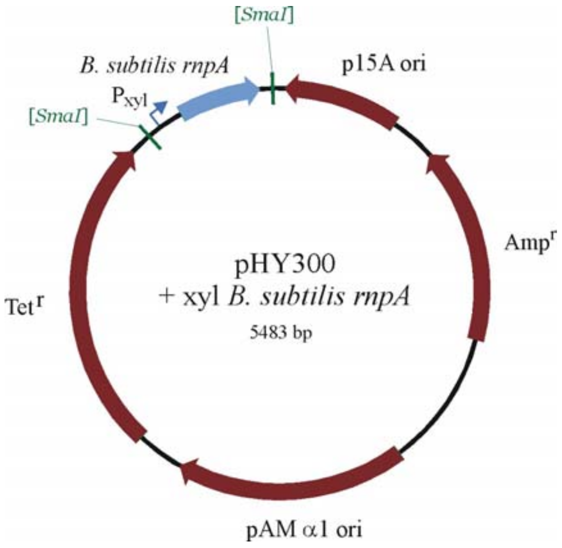
[SmaI]
B. subtilis rnpA
p15A ori
Pxyl
[SmaI]
Amp^r
pHY300
+ xyl B. subtilis rnpA
5483 bp
Tet^r
pAM α1 ori

3.8 References

Amann, E., Ochs, B. and Abel, K.J. 1988. Tightly regulated tac promoter vectors useful for the expression of unfused and fused proteins in *Escherichia coli*. *Gene* **69(2):** 301-15.

Birnboim, H.C. 1983. A rapid alkaline extraction method for the isolation of plasmid DNA. *Methods Enzymol*. **100:** 243-255.

Birnboim, H.C. and Doly, J. 1979. A rapid alkaline extraction procedure for screening recombinant plasmid DNA. *Nucleic Acids Res.* **7:** 1513-23.

Buck, A.H., Dalby, A.B., Poole, A.W., Kazantsev, A.V. and Pace, N.R. 2005. Protein activation of a ribozyme: the role of bacterial RNase P protein. *EMBO J.* **24:** 3360-3368.

Busch, S., Kirsebom, L.A., Notbohm, H. and Hartmann, R.K. 2000. Differential role of the intermolecular base-pairs G292-C(75) and G293-C(74) in the reaction catalyzed by *Escherichia coli* RNase P RNA. *J. Mol. Biol.* **299:** 941-951.

Cavaluzzi, M.J. and Borer, P.N. 2004**.** Revised UV extinction coefficients for nucleoside-5'-monophosphates and unpaired DNA and RNA. *Nucleic Acids Res.* **32(1)**:e13.

Court, D.L., Sawitzke, J.A. and Thomason, L.C. 2002. Genetic engineering using homologous recombination. *Annu. Rev. Genet.* **36:** 361-388.

Cutting, S.M., and Vander-Horn P.B. 1990. Genetic analysis, p. 27-74. *In* Molecular biological methods for *Bacillus*. eds Harwood, C.R. and Cutting S.M. , John Wiley & Sons Ltd., Chichester, United Kingdom.

Datsenko, K.A. and Wanner, B.L. 2000. One-step inactivation of chromosomal genes in Escherichia coli K-12 using PCR products. *Proc. Natl. Acad. Sci.* **97:** 6640–6645.

Dinos, G., Wilson, D.N., Teraoka, Y., Szaflarski, W., Fucini, P., Kalpaxis, D. and Nierhaus, K.H. 2004. Dissecting the ribosomal inhibition mechanisms of edeine and pactamycin: the universally conserved residues G693 and C795 regulate P-site RNA binding. *Mol. Cell.* **13:** 113-24.

England, T.E. and Uhlenbeck, O.C. 1978. 3'-terminal labelling of RNA with T4 RNA ligase. *Nature*, **275:** 560-561.

Gößringer, M. 2004. *In vivo*-Analysen zur Funktion bakterieller RNase P-Proteine in *Bacillus subtilis.* URL http://archiv.ub.uni-marburg.de/diss/z2004/0529/ Stand 07.2006

Gößringer, M., Kretschmar-Kazemir Far, R., and Hartmann, R.K. 2006. Analysis of RNase P protein (*rnpA*) expression in *Bacillus subtilis* utilizing strains with suppressible *rnpA* expression. *J. Bacteriol.* **188(19):** 6816-23.

Hardt, W.D. and Hartmann, R.K. 1996. Mutational analysis of the joining regions flanking helix P18 in E. coli RNase P RNA. *J. Mol. Biol.* **259:** 422–433.

Karu, A.E., Sakaki, Y., Echols, H. and Linn, S. 1975 The gamma protein specified by bacteriophage gamma. Structure and inhibitory activity for the recBC enzyme of *Escherichia coli*. *J. Biol. Chem.* **250:** 7377-7387.

Kuzminov, A. 1999. Recombinational repair of DNA damage in *Escherichia coli* and bacteriophage lambda. *Microbiol. Mol. Biol. Rev.* **63:** 751-813

Laemmli, U.K. 1970. Cleavage of structural proteins during the assembly of the head of bacteriophage T4. *Nature* **227(259):** 680-685.

Mogk A, Homuth G, Scholz C, Kim L, Schmid FX, Schumann W (1997) The GroE chaperonin machine is a major modulator of the CIRCE heat shock regulon of *Bacillus subtilis*. *EMBO J.* **16:** 4579–4590

Murphy, K.C. 1991. Lambda Gam protein inhibits the helicase and chi-stimulated recombination activities of *Escherichia coli* RecBCD enzyme. *J. Bacteriol.* **173:** 5808-5821.

Murphy, K.C. 1998. Use of bacteriophage lambda recombination functions to promote gene replacement in *Escherichia coli*. *J. Bacteriol.* **180:** 2063-2071.

Peck-Miller, K.A. and Altman, S. 1991. Kinetics of the processing of the precursor to 4,5 S RNA, a naturally occuring substrate for RNase P from *Escherichia coli*. *J. Mol. Biol.* **221(1):** 1-5.

Poteete, A.R., Fenton, A.C. 2000. Genetic requirements of phage lambda red-mediated gene replacement in *Escherichia coli* K-12. *J. Bacteriol.* **182:** 2336-2340.

Rivera-León, R., Green, C.J. and Vold, B.S. 1995. High-level expression of soluble recombinant RNase P protein from *Escherichia coli*. *J. Bacteriol.* **177:** 2564–2566.

Roux, A., Beloin, C. and Ghigo, J.M. 2005. Combined inactivation and expression strategy to study gene function under physiological conditions: Application to identification of new *Escherichia coli* adhesins. *J. Bacteriol.* **187:** 1001–1013.

Schägger, H. and von Jagow, G. 1987. Tricine-sodium dodecyl sulfate-polyacrylamide gel electrophoresis for the separation of proteins in the range from 1 to 100 kDa. *Anal. Biochem*. **166(2):** 368-379.

Spizizen J. 1958. Trnasformation of biochemically deficient strains of *Bacillus subtilis* by deoxyribonucleate. *Proc. Natl. Acad. Sci. U S A* **44:** 1072-8.

Tabor, S. and Richardson, C.C. 1985. A bacteriophage T7 RNA polymerase/promoter system for controlled exclusive expression of specific genes. *Proc. Natl. Acad. Sci. U S A* **82:** 1074-8.

Vagner, V., Dervyn, E. and Ehrlich, S.D. 1998. A vector for systematic gene inactivation in *Bacillus subtilis*. *Microbiology*. **144:** 3097–3104.

Yu, D., Ellis, H.M., Lee, E.C., Jenkins, N.A., Copeland, N.G. and Court, D.L. 2000. An efficient recombination system for chromosome engineering in *Escherichia coli*. *Proc. Natl. Acad. Sci. USA* **97:** 5978- 5983.

4 Results and Discussion

4.1 Type A and B RNase P RNAs are interchangeable *in vivo* despite substantial biophysical differences

Wegscheid, B., Condon, C., Hartmann, R.K.

EMBO Reports, 2006

EMBO
reports

scientific report

Type A and B RNase P RNAs are interchangeable *in vivo* despite substantial biophysical differences

Barbara Wegscheid[1], *Ciarán Condon*[2] *& Roland K. Hartmann*[1+]
[1]Institut für Pharmazeutische Chemie, Philipps-Universität Marburg, Marburg, Germany, and [2]CNRS UPR 9073, Institut de Biologie Physico-Chimique, Paris, France

We show that structural type A and B bacterial ribonuclease P (RNase P) RNAs can fully replace each other *in vivo* despite the many reported differences in their biogenesis, biochemical/biophysical properties and enzyme function *in vitro*. Our findings suggest that many of the reported idiosyncrasies of type A and B enzymes either do not reflect the *in vivo* situation or are not crucial for RNase P function *in vivo*, at least under standard growth conditions. The discrimination of mature tRNA by RNase P, so far thought to prevent product inhibition of the enzyme in the presence of a large cellular excess of mature tRNA relative to the precursor form, is apparently not crucial for RNase P function *in vivo*.

Keywords: RNase P; *in vivo* complementation studies; *Escherichia coli*; *Bacillus subtilis*

EMBO reports advance online publication 10 February 2006;
doi:10.1038/sj.embor.7400641

INTRODUCTION

Ribonuclease P (RNase P) is an essential ribonucleoprotein enzyme responsible for the 5′-end maturation of transfer RNAs (Schön, 1999). Bacterial RNase P enzymes recognize the stacked acceptor stem/T-arm module of precursor tRNA (ptRNA) substrates (Harris & Christian, 2003, and references therein), and their RNA subunits have been shown to be catalytically active in the absence of the protein subunit (Guerrier-Takada *et al*, 1983). In bacteria, the RNA subunit (about 380 nt) forms a specific complex with a small basic protein of about 13 kDa, encoded by the *rnpA* gene. RNase P RNAs (P RNAs, encoded by the *rnpB* gene) from bacteria are subdivided into two distinct structural groups, termed type A (for ‘ancestral’) and type B (for ‘*Bacillus*’; Hall & Brown, 2001). *Escherichia coli* and *Bacillus subtilis* have been the principal model systems for type A and B RNase P RNAs, respectively. Although subunits of *E. coli* and *B. subtilis* RNase P enzymes have been shown to be interchangeable *in vitro* (Guerrier-Takada *et al*, 1983), more recent studies have indicated that the differences between the type A and B RNase P RNA architectures are associated with numerous differences in their biogenesis, biochemical/biophysical properties and enzyme function *in vitro*. There is evidence for autolytic processing of *B. subtilis* P RNA 5′ and 3′ ends after association with its protein subunit (Loria & Pan, 2000), whereas the *E. coli* P RNA precursor is processed by RNase E at its 3′ end and by an as yet unidentified ribonuclease at the 5′ end (Lundberg & Altman, 1995). *B. subtilis*, but not *E. coli*, RNase P was found to form a specific dimer consisting of two RNA and two protein subunits (Fang *et al*, 2001). Dimer formation is favoured in the absence of substrate, or in the presence of a tandem tRNA substrate, but disfavoured in the presence of a monomeric ptRNA (Barrera *et al*, 2002). The dimeric form of *B. subtilis* RNase P was further observed to bind to 30S ribosomal subunits, and this association has been proposed to modulate the enzyme’s activity on potential, but as yet unidentified non-tRNA substrates (Barrera & Pan, 2004). The *B. subtilis* RNase P holoenzyme binds to ptRNA with a much higher affinity than mature tRNA (mtRNA), but this discrimination against mtRNA seems substantially attenuated in *E. coli* RNase P (Tallsjö & Kirsebom, 1993; Kurz *et al*, 1998). Indeed, a recent study reports a 1,600-fold preference of *B. subtilis* RNase P for ptRNA versus mtRNA, whereas this factor is reduced to 3 in the case of the *E. coli* holoenzyme (Buck *et al*, 2005). Finally, *E. coli* and *B. subtilis* P RNAs have distinct metal ion requirements (Warnecke *et al*, 1999).

In this report, we present the results of *in vivo* complementation experiments in RNase P mutant strains of *E. coli* and *B. subtilis*. The type B RNase P RNA of *B. subtilis* can functionally replace the type A RNA from *E. coli in vivo* and vice versa. Even a single copy of the *E. coli rnpB* gene inserted into the *B. subtilis* chromosome can fully rescue the growth defect caused by repression of endogenous *B. subtilis rnpB* gene expression.

RESULTS

In vivo complementation studies

The substantial differences between *E. coli* and *B. subtilis* RNase P outlined above raise the question as to whether the two RNAs can replace each other *in vivo*. An earlier study reported the successful

---

[1]Institut für Pharmazeutische Chemie, Philipps-Universität Marburg, Marbacher Weg 6, 35037 Marburg, Germany
[2]CNRS UPR 9073, Institut de Biologie Physico-Chimique, 13 rue Pierre et Marie Curie, 75005 Paris, France
[+]Corresponding author. Tel: +49 6421 2825827; Fax: +49 6421 2825854;
E-mail: roland.hartmann@staff.uni-marburg.de

Received 17 October 2005; revised 2 January 2006; accepted 19 January 2006; published online 10 February 2006

Table 1 | Complementation of the *Escherichia coli* RNase P mutant strain by *Bacillus subtilis rnpB*

	DW2/pDW160		DW2 doubling time (min)*
RNase P RNA source	**30 °C**	**43 °C**	**37 °C**
pSP64-*EcrnpB*	+++	+++[‡]	75 ± 7
pSP64-*BsrnpB*	+++	+++[§]	64 ± 4
pSP64	+++	—	

Growth of mutant strains transformed with *E. coli* or *B. subtilis rnpB* was analysed on LB plates at the permissive (30 °C) and non-permissive (43 °C) temperature. RNase P, ribonuclease P; +++, good complementation; —, no colonies.

*Measured after elimination of pDW160.

[‡] Colonies at 43 °C were smaller than those at 30 °C; for growth at 43 °C, the phenotype of cells transformed with *E. coli rnpB* was set as the standard.

[§] Colonies at 43 °C were larger than those for cells transformed with *E. coli rnpB*, set as the standard.

complementation of an *E. coli rnpB* mutant strain by *B. subtilis rnpB*, but not by *rnpB* genes from the related bacteria *B. brevis* and *B. megaterium* (Waugh & Pace, 1990). Here, we describe cross-species complementation analyses in both *E. coli* and *B. subtilis*. In the *E. coli* mutant strain DW2/pDW160, the chromosomal *rnpB* gene is replaced with a chloramphenicol resistance cassette and a complementing *rnpB* gene is provided on a plasmid (pDW160) with a temperature-sensitive origin of replication (Waugh & Pace, 1990). Suppression of the conditionally lethal phenotype at 43 °C is achieved by expression of functional P RNA from a second compatible plasmid. For complementation in *B. subtilis*, we constructed a conditionally lethal mutant strain (SSB318), the endogenous *rnpB* expression of which is dependent on isopropyl-β-D-thiogalactoside (IPTG).

Complementation in *E. coli*

E. coli DW2 cells were transformed with the multicopy plasmid pSP64 encoding the *E. coli* or *B. subtilis rnpB* gene (pSP64-*EcrnpB* or pSP64-*BsrnpB*; Table 1). For growth curve monitoring, corresponding transformants were cured of plasmid pDW160 (loss of kanamycin resistance), and loss of the *E. coli rnpB* gene was verified by colony PCR for DW2 cells harbouring pSP64-*BsrnpB*. Consistent with the aforementioned study (Waugh & Pace, 1990), the *B. subtilis rnpB* gene rescued growth of the DW2 mutant strain at the non-permissive temperature of 43 °C (Table 1). Remarkably and for reasons as yet unknown, bacteria expressing *B. subtilis rnpB* formed larger colonies than cells transformed with the plasmid containing the homologous *E. coli rnpB* gene at 43 °C. This was also reflected in the faster growth rate of the cured strain in liquid cultures at 37 °C (64 versus 75 min doubling time in Luria-Bertani medium for DW2 cells transformed with pSP64-*BsrnpB* and pSP64-*EcrnpB*, respectively). Thus, *B. subtilis* P RNA can provide full RNase P function in *E. coli*, despite a tenfold lower affinity of this RNA for the *E. coli* RNase P protein (Day-Storms *et al*, 2004). It is possible that higher levels of expression of *B. subtilis rnpB* from the multicopy complementation plasmid compensate for the lower protein–RNA affinity.

Activity of hybrid holoenzymes from *E. coli*

E. coli DW2 bacteria expressing *E. coli* or *B. subtilis rnpB* from the complementation plasmid were cured of pDW160 and grown at 30 °C for partial purification of RNase P holoenzymes. Holoenzymes were tested under standard assay conditions (10 mM Mg^{2+}, 100 mM NH_4^+) for processing of $ptRNA^{Gly}$, as well as $ptRNAG_{74}$ and $ptRNAG_{75}$ variants (Fig 1), to assess cleavage efficiency and processing site selection following loss of the CCA interaction. Both enzymes cleaved $ptRNA^{Gly}$ at the canonical site (+1/−1). However, whereas the *E. coli* holoenzyme promoted substantial miscleavage of the mutant substrates at −1/−2, the hybrid enzyme containing *B. subtilis* P RNA did not significantly miscleave $ptRNAG_{74}$ or $ptRNAG_{75}$ (Fig 2A,B). These findings show that hybrid RNase P holoenzymes consisting of *B. subtilis* P RNA and *E. coli* P protein form stable complexes *in vivo* that can withstand biochemical purification. The results obtained with the mutant substrates further illustrate *in vitro* differences in substrate recognition between RNase P enzymes harbouring type A versus type B RNA subunits.

Complementation in *B. subtilis*

For complementation studies in *B. subtilis*, we constructed strain SSB318. This strain expresses the chromosomal *B. subtilis rnpB* gene under control of the *spac* promoter, and cell survival depends on the presence of IPTG. The conditionally lethal phenotype cannot be rescued by overexpression of the *B. subtilis* protein subunit (*rnpA*) from a plasmid (data not shown), indicating that small quantities of P RNA that may persist owing to *spac* promoter leakiness cannot be coaxed into activity by increased amounts of the protein subunit. SSB318 grows slower in the presence of 1 mM IPTG (doubling time 67 min; Table 2) than the wild-type strain W168 (57 min), suggesting that the fully induced *spac* promoter is not as strong as the native *B. subtilis rnpB* promoter and that P RNA is limiting for cell growth under these conditions. This is supported by the observation that the SSB318-derived strain SSB318*EcrnpB* (see below) has about 3.5-fold less *B. subtilis* P RNA in the presence of IPTG than W168 (Fig 3, lane 9 versus 17).

When expressed from a multicopy plasmid, under control of either its own or the *B. subtilis rnpB* promoter, the heterologous *rnpB* gene from *E. coli* fully rescued the conditionally lethal phenotype of SSB318 (Table 2). The generation time of the strain containing the *B. subtilis rnpB*-expressing plasmid was shorter (49 min) than that containing the *E. coli rnpB* genes (60 and 63 min for the constructs driven by the *E. coli* and *B. subtilis* promoters, respectively). Although this experiment might suggest that *E. coli rnpB* is not as efficient at restoring optimal growth as its *B. subtilis* counterpart, it is also possible that this was because of unrelated effects on plasmid copy number or stability. To eliminate complications of gene dosage from the plasmid-derived *rnpB* genes and differences in expression due to varying promoter

©2006 EUROPEAN MOLECULAR BIOLOGY ORGANIZATION

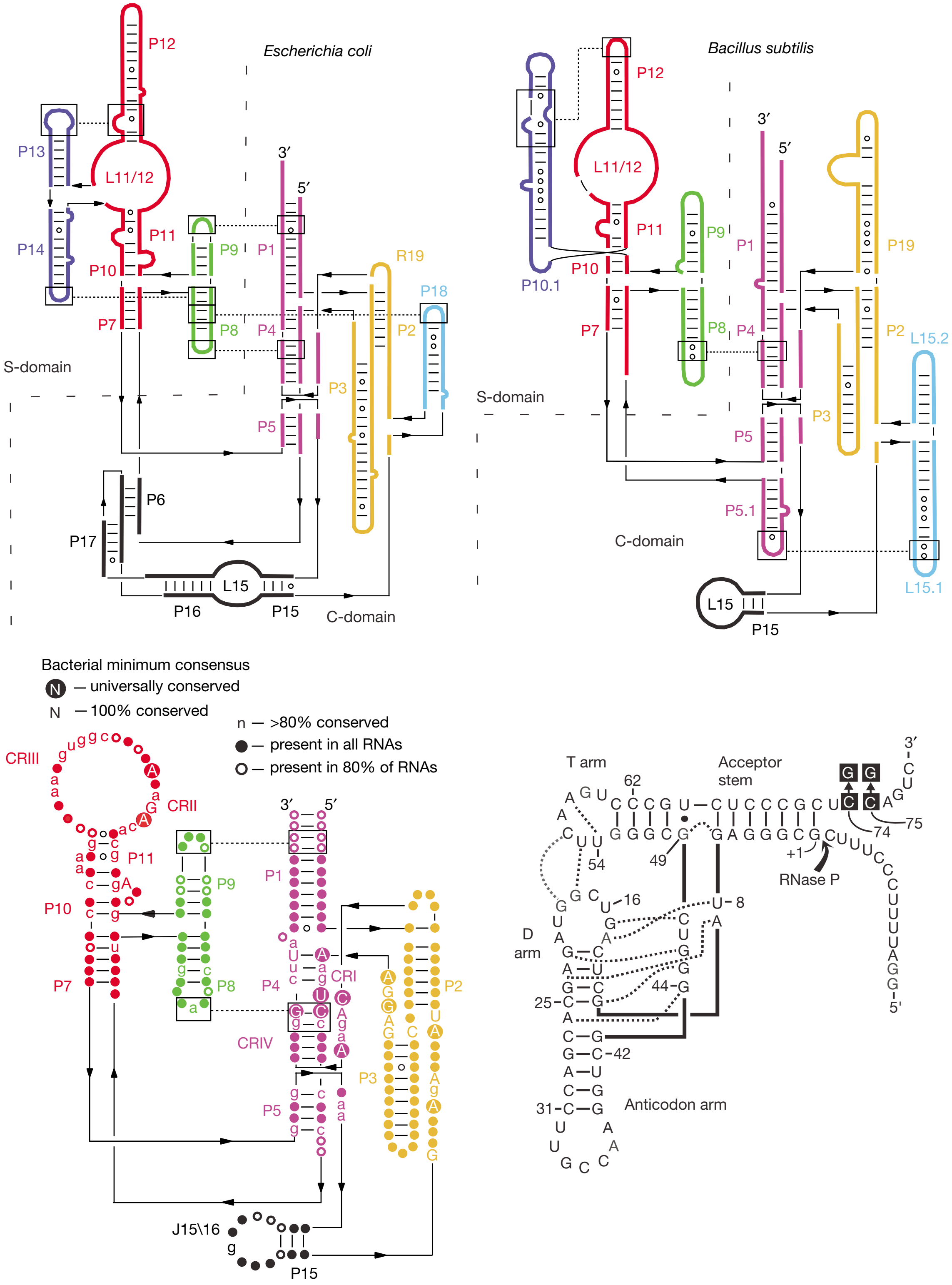
Escherichia coli
P12
P13
L11/12
P14
P11
P10
P9
P1
3′
5′
R19
P18
P7
P8
P4
P2
S-domain
P3
P5
P6
P17
L15
P16
P15
C-domain
Bacillus subtilis
P12
L11/12
P10.1
P11
P9
P1
P19
P10
P8
P4
P2
L15.2
P7
S-domain
P3
P5
P5.1
C-domain
L15
P15
L15.1
Bacterial minimum consensus
N — universally conserved
N — 100% conserved
n — >80% conserved
● — present in all RNAs
○ — present in 80% of RNAs
CRIII
CRII
P11
P10
P7
P9
P8
P1
P4
CRI
CRIV
P2
P3
P5
J15\16
P15
T arm
Acceptor stem
3′
62
54
49
75
74
+1
RNase P
16
8
D arm
25
44
42
31
Anticodon arm
5′

Fig 1 | Secondary structure illustrations (Tsai *et al*, 2003) of *Escherichia coli* (type A, top left) and *Bacillus subtilis* (type B, top right) ribonuclease P (RNase P) RNAs, and a phylogenetic minimum consensus RNase P RNA secondary structure (bottom left; Marquez *et al*, 2005); C-domain, catalytic domain; CR, conserved region; S-domain, specificity domain. Bottom right: *Thermus thermophilus* ptRNA^{Gly}; the arrow indicates the canonical RNase P cleavage site between nucleotides -1 and $+1$; the point mutations in 3′-CCA of ptRNA^{Gly} are highlighted by black squares; tertiary interactions inferred from the crystal structure of yeast tRNA^{Phe} are indicated by dotted lines (adapted from Heide *et al*, 2001).

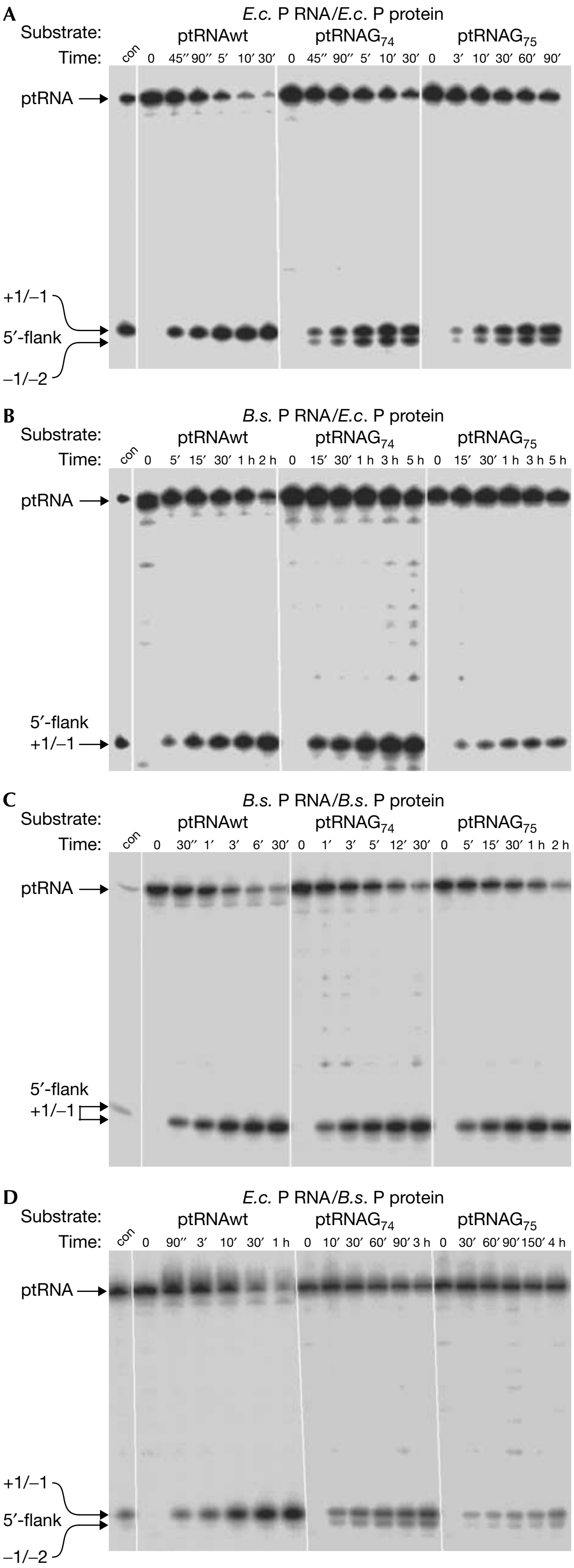
A
E.c. P RNA/*E.c.* P protein
Substrate: ptRNAwt ptRNAG$_{74}$ ptRNAG$_{75}$
Time: con 0 45″ 90″ 5′ 10′ 30′ 0 45″ 90″ 5′ 10′ 30′ 0 3′ 10′ 30′ 60′ 90′
ptRNA
+1/−1
5′-flank
−1/−2
B
B.s. P RNA/*E.c.* P protein
Substrate: ptRNAwt ptRNAG$_{74}$ ptRNAG$_{75}$
Time: con 0 5′ 15′ 30′ 1 h 2 h 0 15′ 30′ 1 h 3 h 5 h 0 15′ 30′ 1 h 3 h 5 h
ptRNA
5′-flank
+1/−1
C
B.s. P RNA/*B.s.* P protein
Substrate: ptRNAwt ptRNAG$_{74}$ ptRNAG$_{75}$
Time: con 0 30″ 1′ 3′ 6′ 30′ 0 1′ 3′ 5′ 12′ 30′ 0 5′ 15′ 30′ 1 h 2 h
ptRNA
5′-flank
+1/−1
D
E.c. P RNA/*B.s.* P protein
Substrate: ptRNAwt ptRNAG$_{74}$ ptRNAG$_{75}$
Time: con 0 90″ 3′ 10′ 30′ 1 h 0 10′ 30′ 60′ 90′ 3 h 0 30′ 60′ 90′ 150′ 4 h
ptRNA
+1/−1
5′-flank
−1/−2

◀ **Fig 2** | Processing and cleavage site selection of hybrid ribonuclease P (RNase P) holoenzymes isolated from *Escherichia coli* and *Bacillus subtilis* complementation strains. **(A,B)** RNase P partially purified from *E. coli* DW2 or **(C,D)** *B. subtilis* SSB318; holoenzymes contained *E. coli* P RNA in **(A,D)** or *B. subtilis* P RNA in **(B,C)**. con, control cleavage by *E. coli* RNase P RNA. For details, see Methods. 5′-Cleavage products are indicated on the left (canonical cleavage site at +1/−1, miscleavage at −1/−2). Although the amount of extract added to processing assays was equalized in **(A–D)**, based on absorption at 260 nm, holoenzyme concentrations are probably identical only within one panel; *E.c.*, *E. coli*; *B.s.*, *B. subtilis*.

strength, we constructed strain SSB318*EcrnpB*, which carries a single copy of the *E. coli rnpB* gene under control of the *B. subtilis rnpB* promoter in the *amyE* locus on the *B. subtilis* chromosome. Constitutive expression of *E. coli rnpB* in this strain was confirmed by radioactive reverse transcription–PCR (RT–PCR; Fig 3, lanes 7,11). The single-copy chromosomal *E. coli rnpB* gene efficiently rescued the lethal phenotype in the absence of IPTG, even when the *lac* repressor was overproduced from plasmid pMAP65 to tighten repression of the *spac* promoter (Table 2). The growth rates of SSB318*EcrnpB* and SSB318*EcrnpB* pMAP65 (57 and 64 min, respectively) were indistinguishable from those of the wild-type strains W168 and W168 pMAP65 (56 and 65 min, respectively), suggesting that *E. coli* P RNA not only carries out all the essential RNase P functions in the heterologous *B. subtilis* host, but is also highly efficient at catalysing any of its potential minor functions (see below). It is also interesting to note that expression of both P RNA types in the same cell, whether in single copy or on a plasmid, did not pose any problem for *B. subtilis* growth (Table 2).

In experiments similar to those performed with the *E. coli* DW2 strain, we partially purified holoenzymes from *B. subtilis* SSB318 transformed with *E. coli* or *B. subtilis rnpB* and grown in the absence of IPTG. In agreement with the complementary data in Fig 2A,B, the *B. subtilis* holoenzyme did not significantly miscleave ptRNAG$_{74}$ or ptRNAG$_{75}$, whereas the hybrid enzyme containing *E. coli* P RNA promoted substantial miscleavage of the mutant substrates (Fig 2C,D).

DISCUSSION

Our study shows that type A and B RNase P RNAs are interchangeable *in vivo* under standard growth conditions, indicating that the hybrid enzymes can carry out all essential cellular functions of RNase P. These findings are surprising for several reasons. First, the lower stability of hybrid holoenzyme complexes (Day-Storms *et al*, 2004) evidently does not pose a problem for holoenzyme assembly *in vivo*, as a single *E. coli rnpB* copy can provide full RNase P function in *B. subtilis* SSB318. Second, Buck *et al* (2005) determined that the native *B. subtilis* holoenzyme has a 1,600-fold preference for ptRNA compared with that for mtRNA, whereas this selectivity is reduced twofold for the hybrid enzyme containing *E. coli* P RNA. Our results show that this change in the relative affinities for ptRNA and mtRNA does not abrogate RNase P function *in vivo*. Third, the *E. coli* protein reduces the Mg^{2+} concentration requirement for tertiary structure formation of P RNA and increases the melting temperature at physiologically relevant Mg^{2+} concentrations (Buck *et al*, 2005). In contrast, the *B. subtilis* protein does not exert such stabilizing effects on its cognate or *E. coli* P RNA (Buck *et al*, 2005). As *E. coli* P RNA can

©2006 EUROPEAN MOLECULAR BIOLOGY ORGANIZATION

Table 2 | Complementation of *Bacillus subtilis* SSB318 RNase P mutant strains by *Escherichia coli rnpB* (cell doubling times given in minutes)

***rnpB* gene source**	**Promoter[*]**	**IPTG**	**No IPTG**
B. subtilis W168 (wild type)			
W168	*B.s.* native	57±2	56±2
W168+pMAP65[‡]	*B.s.* native	62±2	65±2
B. subtilis SSB318 (Pspac:rnpB)			
SSB318	*spac*	67±3	—
SSB318+pMAP65[‡]	*spac*	81±6	—
Multicopy			
pHY300 (empty plasmid)	None	69±4	—
pHY300-*BsrnpB*	*B.s.* native	49±1	49±2
pHY300-*EcrnpB*	*E.c.* native	52±2	60±2
pHY300-*EcrnpB*	*B.s.* native	58±3	63±3
Single copy			
pDG364[§]	None	63±3	—
SSB318*EcrnpB*[‖]	*B.s.* native	52±1	57±1
SSB318*EcrnpB*+pMAP65[‡]	*B.s.* native	56±2	64±4

RNase P, ribonuclease P; IPTG, isopropyl-β-D-thiogalactoside; —: no growth at all; for determination of cell doubling times, see the supplementary information online.

[*] Promoter used for the respective *rnpB* gene; *B.s.* native and *E.c.* native, native *rnpB* promoters from *B. subtilis* and *E. coli*, respectively.

[‡] Plasmid pMAP65 (pUB110 *lacI*; Petit *et al*, 1998) was used to overexpress the *lac* repressor to fully silence expression from the *spac* promoter in strain SSB318.

[§] Vector used for chromosomal integration into the *amyE* locus.

[‖] *E. coli rnpB* integrated into the *amyE* locus under control of the native *B. subtilis rnpB* promoter and terminator.

provide RNase P function in *B. subtilis* (Table 2), these differences in their biochemical and biophysical properties apparently do not have important consequences for hybrid RNase P function *in vivo*.

B. subtilis RNase P can form symmetric dimers consisting of two RNA and two protein subunits, whereas *E. coli* P RNA tends to form aggregates (Fang *et al*, 2001). Buck *et al* (2005) reinvestigated dimerization by *B. subtilis* and *E. coli* RNase P, and observed weak dimer formation by the *E. coli* holoenzyme in addition to higher order aggregation. The K_D of dimer formation was about 50–100 nM for *B. subtilis* and 500–1000 nM for *E. coli* RNase P, with the dimerization properties mainly determined by the type of P RNA subunit (Buck *et al*, 2005). Unlike the *B. subtilis* enzyme, dimers containing *E. coli* P RNA readily dissociated to monomers in the presence of mtRNA, which correlated with the high-affinity binding of mtRNA by holoenzymes containing *E. coli* P RNA. As the mtRNA concentration in an *E. coli* cell is estimated to be 500 μM in the presence of 2 μM (Hansen *et al*, 2001) or lower (Buck *et al*, 2005) concentrations of cellular RNase P, the biological relevance of dimer formation by holoenzymes containing *E. coli* P RNA is questionable. Our observation that *E. coli* P RNA functions in *B. subtilis* RNase P mutant strains also makes it unlikely that RNase P dimer formation exerts an important regulatory role in *B. subtilis*.

The maturation pathways of the primary P RNA transcripts differ in *E. coli* and *B. subtilis*. The *E. coli* pathway requires RNase E, an essential enzyme that is not found in *B. subtilis*, whereas processing of *B. subtilis* P RNA may be at least partly autocatalytic. The results presented here indicate that not only are the P RNAs interchangeable, but so too are their maturation pathways, assuming the P RNA primary transcripts have to undergo processing for proper function.

Finally, *E. coli* RNase P is known to process several non-tRNA substrates *in vivo* (Li & Altman, 2003), whereas non-tRNA substrates have not yet been identified in *B. subtilis*. As *B. subtilis* P RNA provided full RNase P function in *E. coli*, hybrid holoenzymes containing this RNA subunit are able to process at least the essential non-tRNA substrates in *E. coli*, such as 4.5S RNA (Brown & Fournier, 1984). The fact that *B. subtilis* strains expressing single-copy *E. coli* or *B. subtilis rnpB* genes have the same doubling time suggests that, should *B. subtilis* RNase P also have alternative functions, the *E. coli* hybrid enzyme is highly efficient at performing them.

In vivo analyses of the kind reported here provide a framework to test the functional relevance of the numerous biochemical, biophysical and enzymatic differences that have been observed between bacterial type A and B RNase P enzymes. Our results show that, despite these differences, the heterologous hybrid enzymes are capable of carrying out the essential functions of RNase P *in vivo*, although potential defects under particular stress conditions cannot be excluded at present. This poses the question

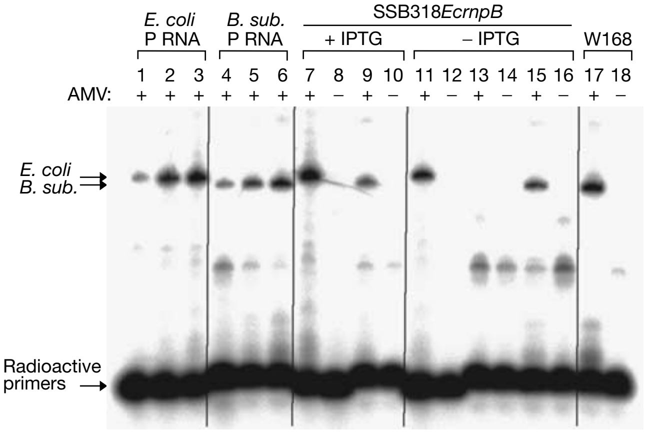

Fig 3 | Radioactive reverse transcription PCR (RT–PCR) analysis of the SSB318-derived strain, SSB318*EcrnpB*. PCR products were analysed on an 8% polyacrylamide/8 M urea gel; lanes 1–3: 0.2, 1 or 5 pg, respectively, of *in vitro*-transcribed *Escherichia coli* ribonuclease P RNA (P RNA) added to 0.5 µg *Bacillus subtilis* W168 (wild type) total cellular RNA; lanes 4–6: 0.2, 1 or 5 pg, respectively, of *in vitro*-transcribed *B. subtilis* P RNA added to 0.5 µg of total cellular RNA from *E. coli* DW2 grown at 30 °C; lanes 7–16: total RNA from SSB318*EcrnpB* grown in the presence (lanes 7–10) or absence (lanes 11–16) of 1 mM isopropyl-β-D-thiogalactoside (IPTG); lanes 7,8,11,12: RT–PCR with primers specific to *E. coli* P RNA; lanes 9,10,13–16: RT–PCR with primers specific to *B. subtilis* P RNA; lanes 15,16: the total RNA preparation was supplemented with 1 pg of *in vitro*-transcribed *B. subtilis* P RNA; lanes 17,18: total RNA from the *B. subtilis* W168 wild-type strain using primers specific for *B. subtilis* P RNA. AMV + or – indicates the presence (+) or absence (–) of reverse transcriptase. For details on RT–PCR, see the supplementary information online. Lanes 1–6 document that the amount of PCR product is sensitive to RNA template concentration (arrows on the left indicate the *E. coli* and *B. subtilis* P RNA-specific amplification products); lane 15 shows that the RNA preparation (–IPTG) does not inhibit the RT–PCR reaction with *B. subtilis* P RNA-specific primers. For all RT–PCR reactions, the total amount of RNA was 0.5 µg.

as to which conserved features of bacterial RNase P RNA and protein subunits are essential for *in vivo* function. Both the *E. coli* and *B. subtilis* P proteins increase the affinity of P RNA for ptRNA by factors of 700–1400 for hybrid and native enzymes containing *E. coli* P RNA, and 13,000–33,000 for those containing *B. subtilis* P RNA (Buck *et al*, 2005). As the *E. coli* P RNA/*B. subtilis* P protein complex permitted rescue of the mutant phenotype of *B. subtilis* strain SSB318, we can conclude that a 700-fold increase in ptRNA affinity conferred by the protein subunit is sufficient to support *in vivo* function. This increase in affinity for ptRNA is linked to an increase in the affinity for key metal ions involved in ptRNA binding and catalysis (Kurz & Fierke, 2002), probably achieved by the protein's stabilization of conserved local structure in the catalytic core of type A and B RNase P RNAs. These central functions are evidently conserved across bacterial species barriers. In the course of evolution, type A and B RNase P enzymes have developed RNA subunits with different architecture and individually tailored protein subunits, optimized for their specific cellular milieu. It is thus fascinating to observe that these RNase P enzymes still retain their biological function when their RNA subunit is exchanged with one representing a different architectural type.

METHODS

Strains. *E. coli* strain DW2/pDW160 was used for complementation studies (see text). For construction of the *B. subtilis* conditional RNase P mutant strain SSB318, its derivative harbouring a single copy of *E. coli rnpB*, as well as complementation plasmids, see the supplementary information online.

***In vitro* transcription and 5′-end labelling.** Runoff transcription with bacteriophage T7 RNA polymerase and 5′-end labelling was performed as described previously (Busch *et al*, 2000). The $ptRNA^{Gly}$ substrate, and G74 and G75 variants (Fig 1; for construction, see the supplementary information online) were transcribed from plasmid pSBpt3′HH, and *B. subtilis* and *E. coli* P RNA from plasmids pDW66 and pJA2′, respectively (Busch *et al*, 2000).

Partial purification of RNase P. Cells resuspended in about 4 ml of buffer A (60 mM NH_4Cl, 10 mM $Mg[OAc]_2$, 6 mM dithiothreitol, 50 mM Tris–HCl, pH 7.2–7.5) per 600 mg cell pellet were lysed by sonication (Branson Sonifier 250, output 20, duty cycle 30–40%, 10 min on ice), followed by centrifugation for 45 min at 4 °C and 10,000*g*. For the preparation of DEAE fractions, the supernatant was loaded onto a DEAE fast-flow Sepharose column (Aekta basic, GE Healthcare Europe, Munich, Germany). Elution was carried out by applying a continuous NH_4Cl gradient from 60 to 550 mM NH_4Cl. Active fractions eluted at about 300–400 mM NH_4Cl.

Processing assays. For RNase P-catalysed processing of *Thermus thermophilus* $ptRNA^{Gly}$ (and G_{74} or G_{75} variants; Fig 1), active DEAE fractions (0.25–1.0 µl; equal amounts based on A_{260} measurements) were incubated in buffer A (10 mM $Mg[OAc]_2$, 6 mM dithiothreitol, 50 mM Tris–HCl, pH 7.5) containing 100 mM NH_4Cl for 10 min at 37 °C. Trace amounts (<1 nM) of 5′-end-labelled substrate were preincubated under the same conditions for 5 min at 55 °C and 25 min at 37 °C. Processing reactions were started by combining enzyme and substrate solutions and assayed at 37 °C. For control cleavage by *E. coli* RNase P RNA (Fig 2), trace amounts (<1 nM) of 5′-end-labelled $ptRNA^{Gly}$ were incubated with 5 µM *E. coli* RNase P RNA for 5 s at 37 °C in 50 mM PIPES, 0.1 M $Mg[OAc]_2$ and 1 M NH_4OAc (pH 7.0 at 37 °C).

Supplementary information is available at *EMBO reports* online (http://www.emboreports.org).

ACKNOWLEDGEMENTS
This work was supported by the Deutsche Forschungsgemeinschaft and the Fonds der Chemischen Industrie. C.C. was supported by funds from the Centre National de la Recherche, Université de Paris 7 and ACI Jeunes Chercheurs from the Ministère de la Recherche Française.

REFERENCES

Barrera A, Pan T (2004) Interaction of the *Bacillus subtilis* RNase P with the 30S ribosomal subunit. *RNA* **10:** 482–492

Barrera A, Fang X, Jacob J, Casey E, Thiyagarajan P, Pan T (2002) Dimeric and monomeric *Bacillus subtilis* RNase P holoenzyme in the absence and presence of pre-tRNA substrates. *Biochemistry* **41:** 12986–12994

Brown S, Fournier MJ (1984) The 4.5S RNA gene of *Escherichia coli* is essential for cell growth. *J Mol Biol* **178:** 533–550

Buck AH, Dalby AB, Poole AW, Kazantsev AV, Pace NR (2005) Protein activation of a ribozyme: the role of bacterial RNase P protein. *EMBO J* **24:** 3360–3368

Busch S, Kirsebom LA, Notbohm H, Hartmann RK (2000) Differential role of the intermolecular base-pairs G292-C(75) and G293-C(74) in the reaction catalyzed by *Escherichia coli* RNase P RNA. *J Mol Biol* **299:** 941–951

Day-Storms JJ, Niranjanakumari S, Fierke CA (2004) Ionic interactions between PRNA and P protein in *Bacillus subtilis* RNase P characterized using a magnetocapture-based assay. *RNA* **10:** 1595–1608

Fang XW, Yang XJ, Littrell K, Niranjanakumari S, Thiyagarajan P, Fierke CA, Sosnick TR, Pan T (2001) The *Bacillus subtilis* RNase P holoenzyme contains two RNase P RNA and two RNase P protein subunits. *RNA* **7:** 233–241

Guerrier-Takada C, Gardiner K, Marsh T, Pace N, Altman S (1983) The RNA moiety of ribonuclease P is the catalytic subunit of the enzyme. *Cell* **35:** 849–857

Hall TA, Brown JW (2001) The ribonuclease P family. *Methods Enzymol* **341:** 56–77

Hansen A, Pfeiffer T, Zuleeg T, Limmer S, Ciesiolka J, Feltens R, Hartmann RK (2001) Exploring the minimal substrate requirements for *trans*-cleavage by RNase P holoenzymes from *Escherichia coli* and *Bacillus subtilis*. *Mol Microbiol* **41:** 131–143

Harris ME, Christian EL (2003) Recent insights into the structure and function of the ribonucleoprotein enzyme ribonuclease P. *Curr Opin Struct Biol* **13:** 325–333

Heide C, Busch S, Feltens R, Hartmann RK (2001) Distinct modes of mature and precursor tRNA binding to *Escherichia coli* RNase P RNA revealed by NAIM analyses. *RNA* **7:** 553–564

Kurz JC, Fierke CA (2002) The affinity of magnesium binding sites in the *Bacillus subtilis* RNase P × pre-tRNA complex is enhanced by the protein subunit. *Biochemistry* **41:** 9545–9558

Kurz JC, Niranjanakumari S, Fierke CA (1998) Protein component of *Bacillus subtilis* RNase P specifically enhances the affinity for precursor-tRNA$^{\mathrm{Asp}}$. *Biochemistry* **37:** 2393–2400

Li Y, Altman S (2003) A specific endoribonuclease, RNase P, affects gene expression of polycistronic operon mRNAs. *Proc Natl Acad Sci USA* **100:** 13213–13218

Loria A, Pan T (2000) The 3′ substrate determinants for the catalytic efficiency of the *Bacillus subtilis* RNase P holoenzyme suggestautolytic processing of the RNase P RNA *in vivo*. *RNA* **6:** 1413–1422

Lundberg U, Altman S (1995) Processing of the precursor to the catalytic RNA subunit of RNase P from *Escherichia coli*. *RNA* **1:** 327–334

Marquez SM, Harris JK, Kelley ST, Brown JW, Dawson SC, Roberts EC, Pace NR (2005) Structural implications of novel diversity in eucaryal RNase P RNA. *RNA* **11:** 739–751

Petit M-A, Dervyn E, Rose M, Entian K-D, McGovern S, Ehrlich DS, Bruand C (1998) PcrA is an essential DNA helicase of *Bacillus subtilis* fulfilling functions both in repair and rolling-circle replication. *Mol Microbiol* **29:** 261–273

Schön A (1999) Ribonuclease P: the diversity of a ubiquitous RNA processing enzyme. *FEMS Microbiol Rev* **23:** 391–406

Tallsjö A, Kirsebom LA (1993) Product release is a rate-limiting step during cleavage by the catalytic RNA subunit of *Escherichia coli* RNase P. *Nucleic Acids Res* **21:** 51–57

Tsai HY, Masquida B, Biswas R, Westhof E, Gopalan V (2003) Molecular modeling of the three-dimensional structure of the bacterial RNase P holoenzyme. *J Mol Biol* **325:** 661–675

Waugh DS, Pace NR (1990) Complementation of an RNase P RNA (*rnpB*) gene deletion in *Escherichia coli* by homologous genes from distantly related eubacteria. *J Bacteriol* **172:** 6316–6321

Warnecke JM, Held R, Busch S, Hartmann RK (1999) Role of metal ions in the hydrolysis reaction catalyzed by RNase P RNA from *Bacillus subtilis*. *J Mol Biol* **290:** 433–445

©2006 EUROPEAN MOLECULAR BIOLOGY ORGANIZATION

Supplementary information

to the paper

Type A and B RNase P RNAs are interchangeable *in vivo* despite substantial biophysical differences

Wegscheid, B., Condon, C., Hartmann, R.K

Construction of the *B. subtilis* conditional RNase P mutant strain SSB318

The *B. subtilis* conditional RNase P mutant (SSB318) was constructed as follows: a 251-nt PCR fragment, containing nucleotides +1 to +231 of the *rnpB* gene, was amplified using oligonucleotides HP499 (5'-ACC AAA GCT TGT TCT TAA CGT TCG GGT AAT CGC TG) and HP500 (5'-TCC AGG ATC CGT TTA CCG CGT TCC ACT CTC ACC ATT TC), digested with *Hind*III and *Bam*HI at the underlined sites and cloned in pMUTIN-4M (Vagner *et al*., 1998) digested with the same enzymes. The resulting plasmid pMUTIN-*rnpB* was transformed into *B. subtilis* wild-type strain W168, selecting for erythromycin resistance in the presence of 1 mM IPTG. 95 out of 100 transformants tested showed IPTG-dependent growth, indicating correct insertion into the *rnpB* gene which is predicted to be essential. One of these transformants, SSB318, was retained for subsequent studies. In this strain, the chromosomal *rnpB* gene is under control of the IPTG-inducible *spac* promoter. In the absence of IPTG, cell growth becomes dependent on the expression of a complementing *rnpB* gene.

Plasmid cloning of *rnpB* genes for complementation analyses

For analyses in *E. coli* mutant strains, the complementing *E. coli rnpB* gene was expressed under control of the natural *E. coli rnpB* promoter from plasmid pSP64 as described (Hardt and Hartmann, 1996). For cloning of *B. subtilis rnpB* gene into the same plasmid, *B. subtilis rnpB* including its natural promoter and terminator was amplified from genomic *B. subtilis* DNA (strain W168) using primers 5'- GGC AGC AAG CTT TAT GAT TGA TCA C (including the native *Hind*III site upstream of *rnpB*) and 5'- CGC CCA AGC TTG TGT ATA CTT CTT CAT CGT ATC ACC CTG TC. The resulting PCR fragment was cloned in the *Hind*III site of pSP64; the orientation of the *rnpB* gene was such that its 3'-portion was adjacent to the *Xba*I site in the pSP64 multi-cloning site.

B. subtilis rnpB was excised from this pSP64 construct via *Hind*III and inserted into pHY300 (obtained from Takara Shuzo Co., Kyoto, Japan) cut with the same enzymes for complementation in *B. subtilis* SSB318. For complementation of *E. coli rnpB* in *B. subtilis* SSB318, an *Nhe*I/*Hind*III fragment from plasmid pSP64 carrying the *E. coli rnpB* gene (Hardt and Hartmann, 1996) under control of the native *E. coli rnpB* promoter was cloned into pHY300 cut with *Xba*I and *Hind*III. *E. coli rnpB* under control of the *B. subtilis rnpB* promoter and terminator for complementation in *B. subtilis* SSB318 was constructed as follows. For amplification of the *B. subtilis* promoter, the primer pair 5'- GGC AGC AAG CTT TAT GAT TGA TCA C and 5'- ATG AAT TAT TAT ATA ACA ACT GAT TAC was used; the *B. subtilis* terminator was amplified using the primer pair 5'- ACA TTT AAA ATG

ATG AAA ACA AGC and 5’- CGC CCA AGC TTG TGT ATA CTT CTT C; *E. coli rnpB* was amplified with primers 5’- GTA ATC AGT TGT TAT ATA ATA ATT CAT GAA GCT GAC CAG ACA GTC and 5’- GCT TGT TTT CAT CAT TTT AAA TGT AGG TGA AAC TGA AAC TGA CCG ATA AG, containing overlapping regions with the *B. subtilis rnpB* promoter and terminator, respectively. The *B. subtilis rnpB* promotor, the *E. coli* RNase P RNA-coding sequence and the *B. subtilis rnpB* terminator were combined by overlap extension PCR. This recombinant *E. coli rnpB* gene was cloned into the *Hind*III site of pHY300.

Construction of a strain containing *E. coli rnpB* with the native *B. subtilis* promoter and terminator integrated into the chromosome of *B. subtilis* SSB318

For construction of a strain containing *E. coli rnpB* with the native *B. subtilis* promoter and terminator integrated into the chromosome of *B. subtilis* SSB318, the *E. coli rnpB* fragment was cloned into the *Hind*III site of pDG364, a vector suitable for chromosomal integration into the *amy*E locus of *B. subtilis* (Cutting and Vander-Horn, 1990). *E. coli rnpB* was amplified with primers 5’- GTA ATC AGT TGT TAT ATA ATA ATT CAT GAA GCT GAC CAG ACA GTC and 5’- GCT TGT TTT CAT CAT TTT AAA TGT AGG TGA AAC TGA AAC TGA CCG ATA AG, using plasmid pSP64 harbouring *E. coli rnpB* (Hardt and Hartmann, 1996) as template, and combined with *B. subtilis* promoter and terminator fragments by PCR as described above.

Transformation of *E. coli* complementation strains

Recombinant pSP64 plasmids (10 ng) were introduced in DW2/pDW160 by electroporation, using a Biorad GenePulser (1.8 kV; 5 ms, 50 µF, 100 Ω). After the pulse, 1 ml SOC medium (per liter: 20 g peptone, 5 g yeast extract, 0.6 g NaCl, 0.17 g KCl, 20 mM glucose, 10 mM $MgCl_2$, 10 mM MgSO4, pH 7.5) was added and cells were shaken at 30°C for 1 h. Cell suspensions were plated directly in appropriate dilution on LB agar plates containing 100 µg/ml ampicillin and 30 µg/ml chloramphenicol. The two sets of plates were incubated in parallel at 30°C or 43°C, respectivlely, for 20 to 40 h. For elimination of pDW160, DW2/pDW160 cells harboring a second complementation plasmid cells were grown at 43°C and then tested for loss of pDW160-encoded kanamycin resistance (50 µg/ml).

Transformation of *B. subtilis* complementation strain SSB318

B. subtilis SSB318 was grown overnight at 37°C in HS medium (Spizizen, 1958) without glucose, but complemented with 0.8% arginie, 0.04% histidine, 0.1% yeast extract 0.0005%

L-tryptophan, 0.0005% L-phenylalanine and 0.02% casamino acids in the presence of 0.5 µg/ml erythromycin, 12.5 µg/ml lincomycin and 1 mM IPTG. Cultures were then diluted into 20 ml of LS medium (Spizizen minimal salts complemented with 0.1% yeast extract, 0.5 mM spermine, 2.5 mM $MgCl_2$, 0.01% casamino acids 0.0005% L-tryptophan and 0.0005% L-phenylalanine; Spizizen, 1958) to a starting OD_{600} of 0.05 - 0.1. Cells were then grown to an OD_{600} of 0.5 - 0.7 at 30°C under shaking. Approximately 1 µg DNA was added to 1 ml of this culture which was grown for another 1 to 2 h at 37°C. Cells were plated in parallel on LB agar plates with or without 1 mM IPTG and containing 0.5 µg/ml erythromycin, 12.5 µg/ml lincomycin and 30 µg/ml tetracycline (to select for the presence of pHY300). In cases of poor transformation efficiency, cells were first plated only in the presence of IPTG. For transformation of pDG364 derivatives, cells were plated on 0.5 µg/ml Erythromycin, 12.5 µg/ml lincomycin, 10 µg/ml chloramphenicol (encoded by pDG364) and 1 mM IPTG.

Determination of cell doubling time

E. coli DW2 cells harboring complementation plasmids were tested for the loss of kanamycin resistance (loss of pDW160). Kanamycin-sensitive and ampicillin- and chloramphenicol-resistant clones were grown overnight at 37°C and then diluted to a starting OD_{578} of 0.05 - 0.1 and grown at 37°C under aeration (180 rpm in a GFL Shaking Incubator 3033). In the case of complementation with *B. subtilis rnpB*, kanamycin-sensitive clones were verified by PCR to lack a chromosomal *E. coli rnpB* copy. *B. subtilis* cells were grown overnight at 37°C in the presence of the appropriate antibiotics and 1 mM IPTG. IPTG was then washed out by centrifugation and resuspension of the cell pellet in LB without IPTG, which was repeated; the final cell pellet was then resuspended in LB, adjusted to a starting OD_{578} of 0.05 - 0.1 in 50 mM LB and grown at 37°C without antibiotics at 180 rpm as above. After growth curve monitoring, samples were withdrawn from the cultures, diluted and plated in parallel on plates with and without antibiotics to exclude the loss of plasmids/resistance gene markers, both types of plates containing 1 mM IPTG. Cell doubling times were derived from early exponential phases and reproduced in at least 3 independent experiments.

Construction of ptRNA^{Gly} templates encoding variants with C to G exchanges at position 74 or 75

Mutations G74 and G75 were introduced by the site-directed *Dpn*I mutagenesis method according to the manual provided with the QuikChange XL Site-Directed Mutagenesis Kit (Stratagene); the primer pair for introduction of the G_{74} mutation was 5’-CCG TCT CCC

GCT **G**CA GTC ACC GGA TGT GC and 5’-GCA CAT CCG GTG ACT G**C**A GCG GGA GAC GG; for introduction of the G_{75} mutation, 5’-CCG TCT CCC GCT C**G**A GTC ACC GGA TGT GC and 5’-GCA CAT CCG GTG ACT **C**GA GCG GGA GAC GG were used.

References

Cutting, S.M., and Vander-Horn P.B. 1990. Genetic analysis, p. 27-74. *In* Molecular biological methods for *Bacillus*. eds Harwood, C.R. and Cutting S.M. , John Wiley & Sons Ltd., Chichester, United Kingdom.

Hardt, W.D. and Hartmann, R.K. 1996. Mutational analysis of the joining regions flanking helix P18 in E. coli RNase P RNA. *J. Mol. Biol.* **259:** 422–433.

Spizizen J. 1958. Trnasformation of biochemically deficient strains of *Bacillus subtilis* by deoxyribonucleate. *Proc. Natl. Acad. Sci. U S A* **44:** 1072-8.

Vagner, V., Dervyn, E. and Ehrlich, S.D. 1998. A vector for systematic gene inactivation in *Bacillus subtilis. Microbiology.* **144:** 3097–3104.

4.2 The precursor tRNA 3'-CCA interaction with *Escherichia coli* RNase P RNA is essential for catalysis by RNase P *in vivo*

Wegscheid B., Hartmann, R.K.

RNA, 2006

The precursor tRNA 3′-CCA interaction with *Escherichia coli* RNase P RNA is essential for catalysis by RNase P in vivo

BARBARA WEGSCHEID and ROLAND K. HARTMANN
Institut für Pharmazeutische Chemie, Philipps-Universität Marburg, D-35037 Marburg, Germany

ABSTRACT

The L15 region of *Escherichia coli* RNase P RNA forms two Watson–Crick base pairs with precursor tRNA 3′-CCA termini (G292-C_{75} and G293-C_{74}). Here, we analyzed the phenotypes associated with disruption of the G292-C_{75} or G293-C_{74} pair in vivo. Mutant RNase P RNA alleles (*rnpB*C292 and *rnpB*C293) caused severe growth defects in the *E. coli rnpB* mutant strain DW2 and abolished growth in the newly constructed mutant strain BW, in which chromosomal *rnpB* expression strictly depended on the presence of arabinose. An isosteric C293-G_{74} base pair, but not a C292-G_{75} pair, fully restored catalytic performance in vivo, as shown for processing of precursor 4.5S RNA. This demonstrates that the base identity of G292, but not G293, contributes to the catalytic process in vivo. Activity assays with mutant RNase P holoenzymes assembled in vivo or in vitro revealed that the C292/293 mutations cause a severe functional defect at low Mg^{2+} concentrations (2 mM), which we infer to be on the level of catalytically important Mg^{2+} recruitment. At 4.5 mM Mg^{2+}, activity of mutant relative to the wild-type holoenzyme, was decreased only about twofold, but 13- to 24-fold at 2 mM Mg^{2+}. Moreover, our findings make it unlikely that the C292/293 phenotypes include significant contributions from defects in protein binding, substrate affinity, or RNA degradation. However, native PAGE experiments revealed nonidentical RNA folding equilibria for the wild-type versus mutant RNase P RNAs, in a buffer- and preincubation-dependent manner. Thus, we cannot exclude that altered folding of the mutant RNAs may have also contributed to their in vivo defect.

Keywords: ***E. coli* ribonuclease P; CCA-RNase P RNA interaction; in vivo complementation studies; point mutations**

INTRODUCTION

Ribonuclease P (RNase P) is an essential ribonucleoprotein enzyme responsible for the 5′-end maturation of tRNAs (Altman and Kirsebom 1999; Schön 1999; Hartmann and Hartmann 2003; Evans et al. 2006). The bacterial RNase P holoenzyme consists of an RNA subunit of ∼380 nucleotides (nt) and a small basic protein (∼13 kDa), and in vitro, RNA subunits of bacterial RNase P enzymes are catalytically active in the absence of the protein subunit (Guerrier-Takada et al. 1983). Bacterial RNase P enzymes recognize the stacked acceptor stem-T arm module of precursor tRNA (ptRNA) substrates, including specific elements at the cleavage site, such as the residue at nucleotide –1 and the 3′-$_{73}$NCCA$_{76}$ end (Harris and Christian 2003). The two cytosines of tRNA 3′-CCA (C_{74} and C_{75}) termini were shown to form Watson–Crick (WC) base pairs with two conserved G residues (G292 and G293) in the loop L15 of *Escherichia coli* RNase P RNA (Fig. 1; Kirsebom and Svärd 1994). This interaction provides a substantial contribution to the free energy of ptRNA binding in vitro (Hardt et al. 1995; Oh et al. 1998; Busch et al. 2000), supports selection of the correct cleavage site (Kirsebom and Svärd 1994), and was suggested to play a role in the binding of catalytic Mg^{2+} (Oh et al. 1998; Busch et al. 2000). Another in vitro study provided evidence that base-pairing with 3′-CCA is also relevant to cleavage site selection in the holoenzyme reaction (Svärd et al. 1996).

We previously reported a kinetic and thermodynamic in vitro analysis of the G292-C_{75} and G293-C_{74} base-pairing

---

Reprint requests to: Roland K. Hartmann, Institut für Pharmazeutische Chemie, Philipps-Universität Marburg, Marbacher Weg 6, D-35037 Marburg, Germany; e-mail: roland.hartmann@staff.uni-marburg.de; fax: 6421-2825854.

Article published online ahead of print. Article and publication date are at http://www.rnajournal.org/cgi/doi/10.1261/rna.188306.

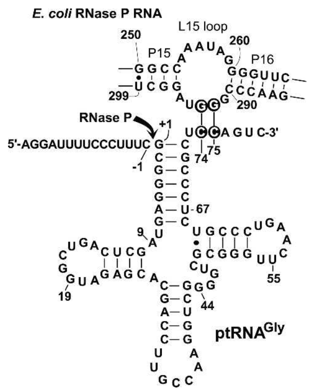

FIGURE 1. Interaction of *Thermus thermophilus* ptRNA^{Gly} with the L15 loop of *E. coli* RNase P RNA. Highlighted nucleotides mark the sites of mutation investigated in this study. The arrow indicates the canonical RNase P cleavage site (between nucleotides −1 and +1). Nucleotides 291–295 of *E. coli* RNase P RNA are also termed J16/15.

interaction in the reaction catalyzed by *E. coli* RNase P RNA (Busch et al. 2000). The results were based on the study of wild-type RNase P RNA along with two variants carrying a single G-to-C exchange (C292 or C293), either acting on wild-type ptRNA^{Gly} or derivatives with a compensatory mutation in the tRNA 3′-end (3′-$\mathbf{G}_{74}$CA or 3′-C$\mathbf{G}_{75}$A) (Fig. 1). Disruption of either of the two intermolecular base pairs largely reduced ground state binding to *E. coli* RNase P RNA. Disruption of the G293-C_{74} pair had a less detrimental effect on the single turnover kinetic parameters than did disruption of the G292-C_{75} pair (Busch et al. 2000). This was consistent with previous findings (Oh et al. 1998), suggesting that the reduction in the efficiency of cleavage of a mutant ptRNA-C$\mathbf{U}_{75}$A substrate resulted from impaired binding of Mg^{2+} important for catalysis. Restoration of base-pairing by compensatory base exchanges in the substrate (C293-G_{74} and C292-G_{75}) restored catalytic performance in vitro, almost fully for the C293-G_{74}, but clearly less for the C292-G_{75} combination (Busch et al. 2000).

Here, we investigated the role of the CCA interaction in vivo in *E. coli* to clarify how far previous in vitro findings, observed under unphysiologically high Mg^{2+} concentrations, are relevant to the cellular situation. This included the construction of a novel *E. coli rnpB* mutant strain (named BW), in which chromosomal *rnpB* expression is efficiently knocked down when glucose is substituted for arabinose in growth media. We demonstrate that the *rnpB*C292 and *rnpB*C293 mutant alleles are lethal in strain BW. In the case of the C293, but not the C292 mutant, a compensatory mutation in the substrate 3′ end fully restored processing capacity in vivo and in vitro. Processing assays with partially purified and in vitro assembled holoenzymes further revealed that the defect of the C292/293 enzymes is most evident at free Mg^{2+} concentrations assumed to be close to those in vivo. Since our results indicate that the phenotypes of the C292 and C293 mutations do not include substantial contributions from defects in protein binding, substrate affinity, or RNA degradation, we propose that the defect is primarily on the level of recruitment of catalytically important Mg^{2+}. Native PAGE experiments revealed nonidentical RNA folding equilibria for the wild-type versus mutant RNase P RNAs, in a buffer- and preincubation-dependent manner. Thus, a contribution from nonnative folding to the defect of the mutant RNAs in vivo cannot be ruled out at present.

RESULTS

In vivo complementation in *E. coli* DW2

To investigate the ptRNA 3′-CCA interaction with RNase P RNA under in vivo conditions, plasmids carrying the wild-type RNase P RNA gene (*rnpB*wt) or the C292 or C293 mutant alleles (*rnpB*C292, *rnpB*C293) were introduced into the temperature-sensitive *E. coli* RNase P mutant strain DW2/pDW160. In strain DW2/pDW160, the chromosomal gene encoding the RNase P RNA subunit (*rnpB*) is replaced with a chloramphenicol resistance cassette and a complementing *rnpB* gene is provided on a plasmid (pDW160) temperature sensitive for replication (Waugh and Pace, 1990). Suppression of the conditionally lethal phenotype at 43°C is achieved by expression of functional RNase P RNA from a second compatible plasmid.

As expected, *E. coli rnpB*wt provided on the multicopy plasmid pSP64 rescued growth of the mutant strain at the nonpermissive temperature of 43°C (Table 1). The *rnpB*C292 mutant allele caused only a partial rescue, and *rnpB*C293 showed very weak complementation. For bacteria transformed with *rnpB*C292 and *rnpB*C293 mutant alleles and grown at 43°C, the corresponding mutant RNAs were verified to be the dominant RNase P RNA species in the cell by primer extension analyses (data not shown; see Materials and Methods). These control experiments excluded reversion of mutant alleles to the wild-type sequence.

Construction of a novel *E. coli rnpB* knockdown strain

The impaired phenotype of the *rnpB*C293 allele relative to *rnpB*C292 in *E. coli* DW2 cells (Table 1) was the reverse of what we had expected based on our previous in vitro results (Busch et al. 2000). Moreover, the DW2 strain has the drawback that complementation analyses are performed under stress conditions at 43°C. The heat-shock response has a global effect on gene expression (Richmond et al. 1999; Li et al. 2003), and induced metabolic changes could alter the mutant phenotype. Also, even cells expressing the

TABLE 1. Complementation analyses of *E. coli* RNase P mutant strain DW2 by *rnpB* alleles

	DW2/pDW160	
RNase P RNA variant	30°C	43°C
pSP64 *E. coli rnpB*wt	+ + +	+ + +[a]
pSP64 *E. coli rnpB*C292	+ + +	+ +
pSP64 *E. coli rnpB*C293	+ + +	(+)
pSP64	+ + +	−

Growth of mutant strain DW2 transformed with different *rnpB* alleles (*E. coli rnpB*wt, *rnpB*C292, and *rnpB*C293) was analyzed on LB plates at the permissive (30°C) and nonpermissive (43°C) temperature. + + + > + + > (+) > −, decreasing order of complementation efficiency based on number and size of colonies.

[a] Growth phenotype of cells harboring pSP64 *E. coli rnpB*wt at 43°C was set as standard, although colonies at 43°C were smaller than at 30°C.

wild-type allele (pSP64 *E. coli rnpB*wt) (Table 1) grew slower at 43°C compared with 30°C. We thus constructed a novel *E. coli* mutant strain in which the chromosomal *rnpB* gene was put under control of the arabinose promoter and repressor system (Fig. 2A). In the absence of arabinose and presence of glucose, *rnpB* expression is switched off, and cell survival depends on a second functional *rnpB* gene provided on a plasmid. The *E. coli* mutant strain (termed BW) exactly displayed the anticipated phenotype (Fig. 2B). In the BW strain, only the *rnpB*wt allele, but not *rnpB*C292 and *rnpB*C293, restored growth in the absence of arabinose (Fig. 2C; Table 2A).

Defect in maturation exemplified for 4.5S RNA

We then analyzed if the *rnpB*C292 and *rnpB*C293 mutant alleles are associated with an RNase P processing defect in BW bacteria. For this purpose, BW cells expressing *rnpB*wt, *rnpB*C292, or *rnpB*C293 from plasmid pACYC177 were initially grown in medium containing arabinose, followed by transfer into medium without arabinose, further incubation for 3 h at 37°C, and preparation of total cellular RNA. We then analyzed processing of 4.5S RNA, a prominent non-tRNA substrate of *E. coli* RNase P (Bothwell et al. 1976; Peck-Miller and Altman 1991), by primer extension (Fig. 3). Exclusively mature 4.5S RNA was detected in RNA extracts from cells expressing plasmid-encoded *rnpB*wt (Fig. 3, lane 2), whereas cells harboring *rnpB*C292 and *rnpB*C293 accumulated a 4.5S RNA precursor extended by 3 nt at the 5′ end. Since the native 4.5S RNA primary transcript carries a 5′ leader of 24 nt (see Fig. 4), nucleolytic activities other than RNase P apparently trimmed the leader to 3 nt. Likewise, accumulation of immature RNA with an extra 2–5 nt at the 5′ end were observed for the bacteriophage P1/P7 regulatory C4 RNA, another non-tRNA substrate of *E. coli* RNase P, when processing by RNase P was defective (Hartmann et al. 1995). The ratio of 5′-extended to mature 4.5S RNA was reproducibly higher in the *rnpB*C292 than *rnpB*C293 background (Fig. 3, lanes 3,4), providing evidence that the processing defect of the C292 mutant RNA is more severe than that of the C293 variant, in line with the kinetic in vitro data (Busch et al. 2000).

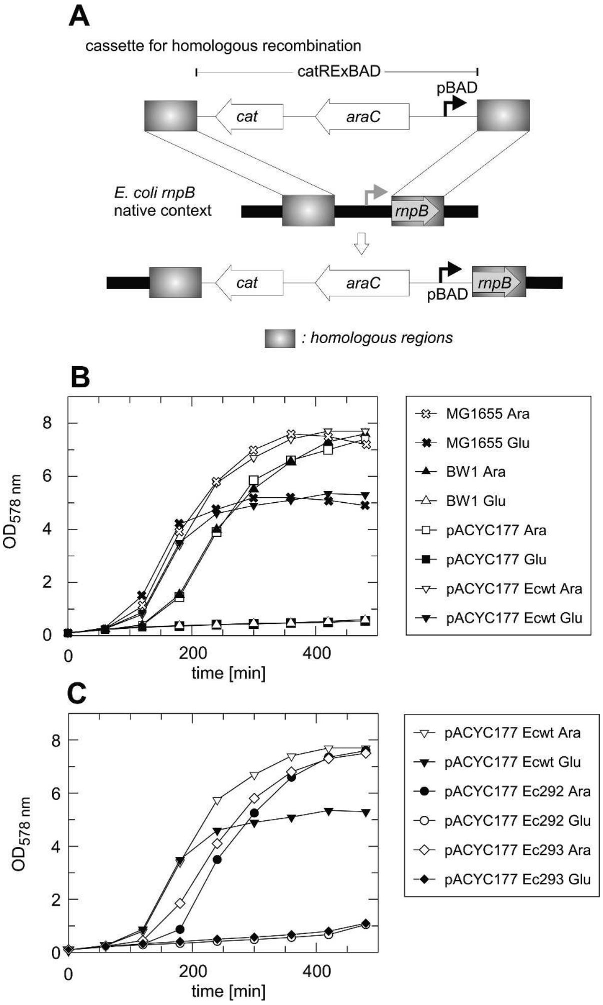

FIGURE 2. Construction and analysis of the *E. coli rnpB* mutant strain BW. (*A*) Schematic presentation of the strain construction strategy. The native *rnpB* promoter region was replaced with a cassette (catRExBAD, 2136 bp) carrying the chloramphenicol resistance gene (*cat*), a gene coding for an arabinose operon regulatory protein (*araC*), and the arabinose-inducible pBAD promoter. The cassette for homologous recombination (2669 bp) additionally contained flanking regions identical in sequence to *E. coli rnpB* and to a segment upstream of *rnpB*. (*B*) Cell growth rescue of strain BW in the presence of glucose (Glu) with a plasmid-encoded copy of *E. coli rnpB* (pACYC177 Ecwt). Note that growth curves in the presence of glucose versus arabinose differ in the same manner for strain BW and its progenitor MG1655. (*C*) Growth analyses of BW bacteria expressing plasmid-encoded *rnpB*wt, *rnpB*C292, or *rnpB*C293 alleles (pACYC177 Ecwt, Ec292, or Ec293) in the presence of arabinose (Ara) or glucose (Glu).

TABLE 2. Complementation analyses in *E. coli* RNase P mutant strain BW

(*A*) Complementation of *E. coli* RNase P mutant strain BW by *rnpB* alleles

RNase P RNA variant	10 mM arabinose	0.5% glucose
pACYC177 *E. coli rnpB*wt	+	+
pACYC177 *E. coli rnpB*C292	+	–
pACYC177 *E. coli rnpB*C293	+	–
pACYC177	+	–

(*B*) Complementation of *E. coli* RNase P mutant strain BW by *rnpB* alleles and simultaneous overexpression of *E. coli rnpA*

RNase P RNA variant	*rnpA*[a]	10 mM arabinose,1 mM IPTG	0.5% glucose,1 mM IPTG
pACYC177 *E. coli rnpB*wt	+ *E. coli rnpA*	+	+
pACYC177 *E. coli rnpB*C292	+ *E. coli rnpA*	+	–[b]
pACYC177 *E. coli rnpB*C293	+ *E. coli rnpA*	+	+[c]
pACYC177	+ *E. coli rnpA*	+	–

Growth of BW bacteria transformed with different *rnpB* alleles (*E. coli rnpB*wt, *rnpB*C292 and *rnpB*C293, part *A*) and simultaneously overexpressing *E. coli rnpA* (part *B*); growth was analyzed on LB plates in the presence of 10 mM arabinose or 0.5% (w/v) glucose; for bacteria expressing *rnpA*, 1 mM IPTG was added to the medium. + indicates growth with equal numbers of colonies on arabinose and glucose plates; –, no growth;

[a] Cloned in plasmid pBR322 under control of the inducible pTrc promoter.

[b] Retarded growth and less colonies on glucose plates (~10% of that of arabinose plates), likely revertants.

[c] Cells showed retarded growth.

Restoration of 4.5S RNA maturation in the *rnpB*C293 background by a compensatory substrate mutation

From our previous results obtained in the RNA-alone reaction (Busch et al. 2000), it seemed possible that an isosteric C293-G$_{74}$ pair in enzyme–substrate complexes may fully restore activity to that of wild-type complexes. To test if this also holds for the cellular context, we constructed a plasmid-borne 4.5S RNA gene, in which we switched the identity of four consecutive base pairs in the terminal stem region. Expression of the mutated 4.5S RNA was not detrimental to cell viability. The sequence alteration in 4.5S RNA permitted primer annealing exclusively to this 4.5S RNA variant, but not the chromosomally encoded wild-type 4.5S RNA. In addition, two variants with C-to-G exchanges (G$_{“74”}$ or G$_{“75”}$) in the dangling 3′-CCC terminus were constructed (Fig. 4A). Primer extension analysis, performed essentially as in Figure 3, indeed revealed full restoration of 4.5S RNA maturation efficacy for the C293 holoenzyme acting on the precursor 4.5S RNA with a 3′-G$_{“74”}$ CC terminus (Fig. 4, cf. lanes 1,6 and 2–5,7–9). In contrast, the combination of C292 P RNA and p4.5S RNA 3′-CG$_{“75”}$C (Fig. 4, lane 8), although restoring base-pairing, did not reestablish maturation capacity to wild-type levels.

Overexpression of *rnpA*

We speculated that overexpression of the *E. coli* RNase P protein might increase the steady-state level of the RNase P holoenzyme and thereby alleviate the processing defects

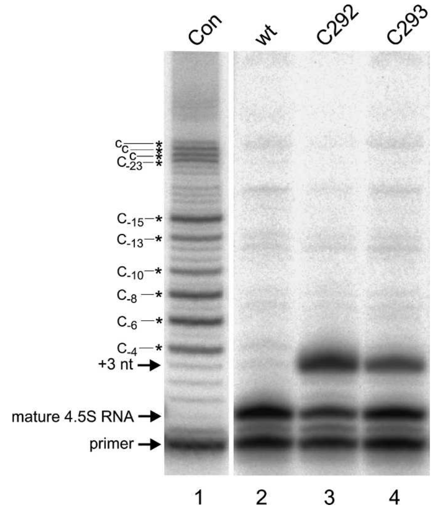

FIGURE 3. Primer extension analysis using a primer specific to *E. coli* 4.5S RNA and total RNA from strain BW expressing pACYC177-encoded *E. coli rnpB*wt (lane *2*), *rnpB*C292 (lane *3*), and *rnpB*C293 (lane *4*); Con (lane *1*) indicates products of reverse transcription in the presence of ddGTP and using in vitro transcribed precursor 4.5S RNA as the template; prominent bands resulted from premature termination of reverse transcription at template C residues (marked by asterisks); the precursor segment of the in vitro transcribed p4.5S RNA had the natural sequence up to residue –23, but was different beyond this position and carried additional nucleotides for cloning reasons (5′-ggg aga ccg gaa uuc ccC GUU GGU UCU CAA CGC UCU CAA U$_{-1}$, deviations from the wild-type sequence in small letters). Samples were analyzed by 20% PAGE in the presence of 8 M urea. For growth of BW cells harboring the different plasmids (lanes *2*–*4*) and preparation of total cellular RNA, see Materials and Methods.

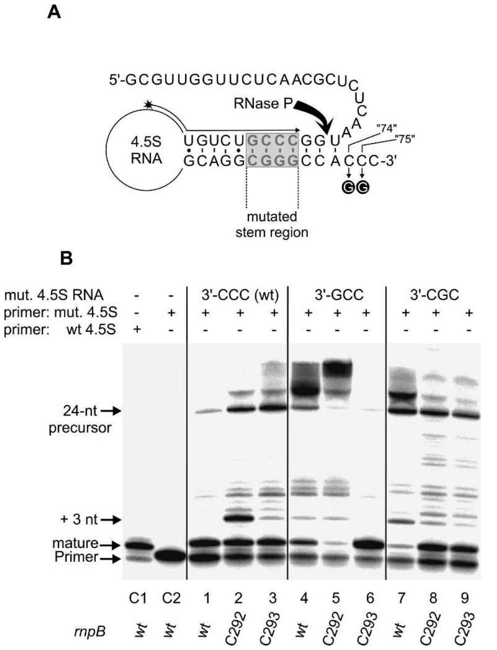
A
5'-GCGUUGGUUCUCAACGCUUCUCAA
RNase P
4.5S RNA
UGUCUGCCCGGU
GCAGGCGGGCCACCC-3'
"74"
"75"
G G
mutated stem region
B
mut. 4.5S RNA - - 3'-CCC (wt) 3'-GCC 3'-CGC
primer: mut. 4.5S - + + + + + + + + + +
primer: wt 4.5S + - - - - - - - - - -
24-nt precursor
+ 3 nt
mature
Primer
C1 C2 1 2 3 4 5 6 7 8 9
rnpB wt wt wt C292 C293 wt C292 C293 wt C292 C293

FIGURE 4. Primer extension experiments to analyze processing of pBR322-encoded mutant p4.5S RNA in strain BW expressing *E. coli rnpB*wt, *rnpB*C292, or *rnpB*C293. (*A*) Schematic of the mutant p4.5S RNA: The gray-shaded box indicates base-pair exchanges relative to wild-type 4.5S RNA, which were introduced to permit specific reverse transcription of mutant (*p*)4.5S RNA; two variants carried 3′-terminal C to G exchanges (highlighted) at positions equivalent to nucleotides 74 and 75 of tRNA 3′-CCA ends; the arrow aligned to the stem depicts the reverse transcription primer, with the terminal asterisk illustrating the 5′-^{32}P-endlabel. (*B*) Analysis of primer extension products by 20% PAGE in the presence of 8 M urea. (Lanes *C1,C2*) Primer extension using total RNA from BW cells grown in the presence of glucose and expressing pACYC177-encoded *E. coli rnpB*wt, either utilizing the primer for wild-type 4.5S RNA (*C1*) or mutant 4.5S RNA (*C2*); the *C2* control documents that the primer specific for mutant 4.5S RNA (panel *A*) did not prime on wild-type 4.5S RNA. (Lanes *1–9*) Primer extension using the primer specific for mutant 4.5S RNA; total RNA was from BW cells grown in the presence of glucose and expressing pACYC177-encoded *E. coli rnpB*wt (lanes *1,4,7*), *rnpB*C292 (lanes *2,5,8*), or *rnpB*C293 (lanes *3,6,9*); BW bacteria either expressed the pBR322-encoded mutant p4.5S RNA with the natural 3′-CCC (lanes *1–3*), a mutated 3′-GCC (lanes *4–6*), or a 3′-CGC (lanes *7–9*) terminus. The natural 4.5S RNA primary transcript has a 5′ leader of 24 nt (Bothwell et al. 1976; Hsu et al. 1984) as indicated on the *left*; longer transcripts in lanes *2–5* and *7–9* are attributable to transcriptional initiation from the β-lactamase promoter region still present in our pBR322 plasmid constructs.

caused by the *rnpB*C292 and *rnpB*C293 mutant alleles. Indeed, for BW cells expressing *rnpB*C293, concomitant overexpression of *rnpA* partially restored viability, although growth was retarded relative to cells harboring the *rnpB*wt allele (Table 2B). In contrast, the defect caused by the C292 mutation could not be cured by overexpressing *rnpA*. Overexpression of the *E. coli* RNase P protein (C5) was verified by Western blotting using an antiserum against the *E. coli* C5 protein (data not shown).

Processing of ptRNA by partially purified holoenzymes assembled in vivo

We partially purified in vivo assembled holoenzymes by anion exchange chromatography from DW2 cells grown at 43°C and either expressing *rnpB*wt, *rnpB*C292, or *rnpB*C293 from plasmid pSP64. Holoenzymes were analyzed by primer extension in the presence of ddGTP (see Materials and Methods) and confirmed to contain ≥95% of the respective mutant RNase P RNA (data not shown). We then tested these holoenzymes for processing of ptRNA^{Gly} (Fig. 1, termed ptRNAwt in the following) and the two variant substrates thereof, ptRNAG$_{74}$ and ptRNAG$_{75}$, with point mutations in 3′-CCA (3′- G$_{74}$CA and 3′- CG$_{75}$A) to compensate the C292/293 mutations in RNase P RNA. This enabled us to investigate rescue effects in terms of efficiency and cleavage site selection in the RNase P holoenzyme reaction. Processing assays contained 0.004 A$_{260}$ units of the partially purified holoenzyme fraction and trace amounts (<1 nM) of radiolabeled substrate. As illustrated in Figure 5, the wild-type holoenzyme substantially miscleaved the two mutant substrates (Fig. 5, panel A). As the wild-type holoenzyme, the C292 and C293 mutant holoenzymes cleaved ptRNAwt to >95% at the canonical site. However, the C292 mutation suppressed miscleavage of the ptRNAG$_{75}$ substrate (Fig. 5, panel B), as did the C293 mutant holoenzyme when acting on the ptRNAG$_{74}$ substrate (Fig. 5, panel C). These findings were expected based on restoration of the intermolecular base pairs and are in line with results from previous in vitro studies (Kirsebom and Svärd 1994; Svärd et al. 1996; Busch et al. 2000). However, the mutant holoenzymes cleaved ptRNAwt, the only substrate relevant to the in vivo situation, with good efficiency. The purification scheme was identical for DW2 cells expressing the *rnpB*wt, *rnpB*C292, or *rnpB*C293 alleles, and equal amounts of extract based on absorption at 260 nm were used in these processing assays. Although we are aware that exact holoenzyme concentrations may not have been identical for all three extracts, good processing efficiencies of the two mutant holoenzymes appeared not fully consistent with their severe in vivo defect. We thus decided to increase the stringency of our processing assay by lowering the Mg^{2+} concentration to 2 mM, assuming that this better mimics the free Mg^{2+} concentration (1–2 mM) in *E. coli* cells (Alatossava et al. 1985). For wild-type RNase P, the cleavage rate at 10 mM Mg^{2+} relative to 2 mM Mg^{2+} was 25-fold increased (k_{rel} = 25), but this difference increased to ≥650-fold for the C292 and C293 mutant enzymes. Thus, the defect of the mutant enzymes was exacerbated at low [Mg^{2+}]. However, the C293 mutant holoenzyme cleaved the ptRNAG$_{74}$ with the same efficiencies at 2 and 10 mM [Mg^{2+}] as the wild-type holoenzyme acting on ptRNAwt (Table 3), demonstrating that the natural G293-C$_{74}$ and the isosteric C293-G$_{74}$ pair are fully exchangeable. In contrast, the C292-G$_{75}$ pair only

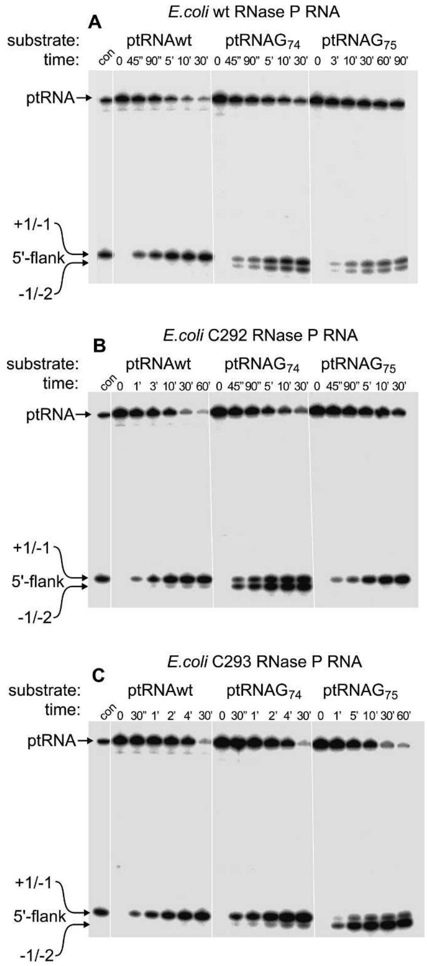

FIGURE 5. Processing assays using RNase P holoenzymes (0.004 A_{260} units) partially purified from strain DW2 grown at 43°C and complemented with *E. coli* (*A*) *rnpB*wt, (*B*) *rnpB*C292, and (*C*) *rnpB*C293; trace amounts (<1 nM) of 5′-endlabeled ptRNA^{Gly} (Fig. 1) and variants ptRNAG$_{74}$ and ptRNAG$_{75}$ with single point mutations were used as substrates in buffer A containing 10 mM Mg^{2+}; con indicates trace amounts (<1 nM) of 5′-endlabeled ptRNA^{Gly} incubated with 5 μM *E. coli* RNase P RNA for 5 sec at 37°C in 50 mM PIPES, 0.1 M Mg(OAc)$_2$, and 1 M NH$_4$OAc (pH 7.0 at 37°C). 5′-cleavage products are indicated on the *left* (canonical cleavage site at +1/−1, miscleavage at −1/−2).

showed a partial rescue (k_{rel} = 97) of the defect, emphasizing the importance of base identity at position 292. Full restoration of function in the presence of the C293-G$_{74}$ pair, but not the C292-G$_{75}$ pair, exactly corresponds with what we have seen for 4.5S RNA maturation in vivo (Fig. 4).

Processing of ptRNA by holoenzymes reconstituted in vitro

The findings of Table 3 suggested that conditions of 2 mM Mg^{2+} may better mimic the intracellular conditions than 10 mM. Since enzyme concentrations can be better defined and equalized for in vitro reconstituted enzymes relative to those purified from cells, we further tested in vitro assembled *E. coli* RNase P holoenzymes under conditions optimized for ribosome function (buffer KN; Materials and Methods) at two different Mg^{2+} concentrations, 2 and 4.5 mM, and applying multiple turnover kinetics. The wild-type holoenzyme cleaved ptRNAwt with identical rates at 2 and 4.5 mM Mg^{2+} (Table 4). The mutant enzymes showed cleavage rates reduced by a factor of ~2 at 4.5 mM Mg^{2+}, but this reduction amounted to 13- and 24-fold at 2 mM Mg^{2+}. The pronounced activity drop for the mutant holoenzymes when [Mg^{2+}] was only slightly lowered from 4.5 to 2 mM, which made it unlikely but did not exclude that a defect in substrate affinity or holoenzyme stability owing to the disruption of the CCA contact might be responsible for this effect. To address the latter possibilities, we tested processing activity under the same conditions but at a fivefold higher holoenzyme concentration (Table 4, lower part). If substrate binding or holoenzyme stability were substantially impaired in reactions catalyzed by the C292/3 mutant enzymes, one would have expected at least a partial activity rescue for the mutant enzymes at this higher enzyme concentration, which, however, was not observed (Table 4).

We then considered the possibility that the C292/3 mutant RNAs have an altered affinity for the protein subunit. This possibility was addressed by testing the activity of holoenzymes reconstituted at increasing excess amounts of RNase P protein over RNase P RNA. However, the dependence of cleavage rate on RNase P protein concentration showed a very similar saturation behavior for the wild-type and mutant RNase P RNAs, since in all cases activity leveled off above a protein:RNA ratio of 5:1 (Fig. 6). Likewise, the combination of RNase P RNA C293 and substrate ptRNAG$_{74}$ resulted in essentially the same activity profile as for wild-type RNase P RNA acting on ptRNAwt (Fig. 6).

Analysis of RNase P RNA folding equilibria

At low Mg^{2+} concentrations, such as 2 mM, RNase P RNA folding may be incomplete (Zarrinkar et al. 1996) and particularly sensitive to structural alterations. To test the possibility that differences in RNA folding might have contributed to the in vivo and in vitro phenotypes of the C292 and C293 mutant RNase P RNAs, we performed a native PAGE analysis using the buffer systems applied in our kinetic analyses. To our surprise, the folding equilibria of wild-type, C292, and C293 RNase P RNA displayed clear differences. Without a preincubation step (Fig. 7, lanes 1–3), two major bands appeared, which are interpreted as folding intermediates (I$_1$ and I$_2$). For the wild-type RNA, formation of the faster migrating intermediate was favored relative to the two mutant RNAs.

TABLE 3. Activity of mutant *E. coli* RNase P holoenzymes purified from strain DW2

RNase P RNA	substrate	[Mg^{2+}] (mM)	k_{obs} (min^{-1})	k_{rel}
Wild type	ptRNA wild type	2	$(15 \pm 0.03) \times 10^{-3}$	
		10	0.37 ± 0.03	25
Wild type	ptRNA G74	2	n.d.	
		10	0.21 ± 0.02	
Wild type	ptRNA G75	2	n.d.	
		10	0.047 ± 0.007	
C292	ptRNA wild type	2	$(17 \pm 3) \times 10^{-5}$	
		10	0.11 ± 0.02	647
C292	ptRNA G74	2	n.d.	
		10	0.31 ± 0.02	
C292	ptRNA G75	2	$(14.5 \pm 1.5) \times 10^{-4}$	
		10	0.14 ± 0.004	97
C293	ptRNA wild type	2	$(47 \pm 1) \times 10^{-5}$	
		10	0.38 ± 0.04	809
C293	ptRNA G74	2	$(17 \pm 1) \times 10^{-3}$	
		10	0.42 ± 0.04	25
C293	ptRNA G75	2	n.d.	
		10	0.13 ± 0.01	

Processing was assayed in buffer A: 50 mM Tris-HCl, 100 mM NH_4Cl, 6 mM DTT, 2 or 10 mM $Mg(OAc)_2$ (pH 7.5), 37°C ; assays contained 0.004 A_{260} units of partially purified holoenzymes and trace amounts (<1 nM) of 5′-endlabeled substrates. n.d. indicates no cleavage product detectable after 5 h of incubation; for further details, see Materials and Methods; k_{rel} is the ratio of k_{obs} values at 10 versus 2 mM Mg^{2+}; k_{obs} values are based on at least three independent experiments.

In buffers A10 and KN4.5 combined with electrophoresis at 10 mM Mg^{2+}, a preincubation step at 37°C (Fig. 7, lanes 4–9, A10 and KN4.5) led to formation of a more compacted species assumed to represent a native-like conformation (termed N_1), in accordance with a previous study (Buck et al. 2005). This conformer was in equilibrium with conformer I_2, and the protein subunit did not influence this folding equilibrium (Fig. 7, lanes 4–6 versus 7–9). Here, the pattern was essentially identical for the wild-type and C293 mutant RNA, whereas the C292 RNA was still in equilibrium with the I_1 conformer (Fig. 7, lanes 5,8). An additional temperature step at 55°C led to almost complete disappearance of the I_1 conformer, thus largely eliminating the difference between the C292 and wild-type/C293 RNAs (Fig. 7, lanes 10–12).

In buffer KN2 combined with electrophoresis at 2 mM Mg^{2+}, a band migrating slightly faster than the I_2 conformer appeared upon preincubation at 37°C or 55°C/37°C (Fig. 7, best visible in lane 1 versus lane 4, KN2), which we have termed N_2. This band migrated closer to conformer I_2 than did conformer N_1, but N_2 appeared on gels containing 2 mM Mg^{2+} and N_1 on those supplemented with 10 mM Mg^{2+}. Thus, it remains unclear if N_1 and N_2 represent identical or different conformers. Under KN2 conditions, all three RNAs mainly populated the N_2 fold, although gel migration of the C293 RNA was more smeary than that of wild-type and C292 RNA, and some I_1 conformer was still visible for the C292 RNA (Fig. 7, lanes 5,8). Upon additional preincubation at 55°C (Fig. 7, lanes 10–12), the differences between the wild-type and mutant RNAs were essentially eliminated.

In buffer A2 combined with electrophoresis at 2 mM Mg^{2+}, the N_2 conformer formed only partially with wild-type RNA (Fig. 7, lanes 7,10, A2), and apparently not at all with the mutant RNAs. This suggests that the KN2 buffer containing spermine and spermidine favors formation of a native fold relative to the A2 buffer. When the native PAGE analysis was conducted with 5′- instead of 3′-endlabeled RNase P RNA, results were identical to those shown in Figure 7 (data not shown).

Although the structural differences between the conformers termed I_1, I_2, N_1, and N_2 remain to be characterized, the data in Figure 7 illustrate that the folding equilibria of wild-type and C292/293 mutant RNase P RNAs may differ depending on the particular buffer and

TABLE 4. Cleavage rates for *E. coli* wild-type and mutant RNase P holoenzymes at low Mg^{2+} concentrations

RNase P RNA	Enzyme concentration	[Mg^{2+}]	k_{obs}	activity decrease
Wild type	10 nM P RNA/50 nM RnpA	4.5	11.2 ± 0.7	—
C292	10 nM P RNA/50 nM RnpA	4.5	4.8 ± 0.1	2.33
C293	10 nM P RNA/50 nM RnpA	4.5	6.0 ± 0.6	1.87
Wild type	10 nM P RNA/50 nM RnpA	2.0	12.0 ± 1.4	—
C292	10 nM P RNA/50 nM RnpA	2.0	0.5 ± 0.06	24.0
C293	10 nM P RNA/50 nM RnpA	2.0	0.9 ± 0.04	13.3
Wild type	50 nM P RNA/250 nM RnpA	2.0	21.9 ± 2.5	—
C292	50 nM P RNA/250 nM RnpA	2.0	0.6 ± 0.06	36.5
C293	50 nM P RNA/250 nM RnpA	2.0	0.6 ± 0.07	36.5

Processing was assayed in buffer KN: 20 mM Hepes (pH 7.4, 37°C), 2 or 4.5 mM $Mg(OAc)_2$, 150 mM NH_4OAc, 2 mM spermidine, 0.05 mM spermine, 4 mM β-mercaptoethanol, and RNase P RNA (P RNA) and *E. coli* RNase P protein (RnpA) concentrations as indicated; the ptRNAwt concentration was 100 nM; k_{obs} is given as nmol substrate converted per nmol of RNase P RNA per min; values are based on at least four independent experiments; activity decrease is defined as the ratio of k_{obs} obtained with wild-type versus mutant holoenzyme under the respective conditions.

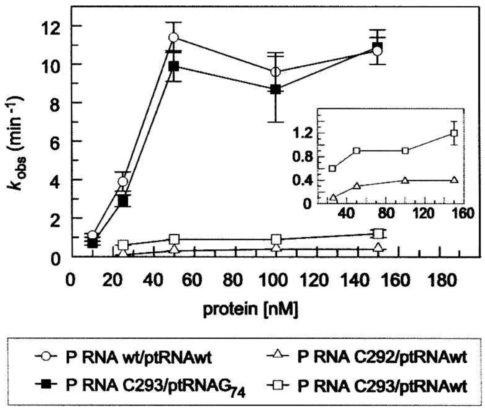

FIGURE 6. Activity of wild-type and mutant holoenzymes reconstituted at different RNase P protein/RNA ratios and acting on ptRNAwt; in addition, the activity profile for cleavage of ptRNAG$_{74}$ by the C293 mutant holoenzyme is shown. Assay conditions were 20 mM Hepes (pH 7.4, 37°C), 2 mM Mg(OAc)$_2$, 150 mM NH$_4$OAc, 2 mM spermidine, 0.05 mM spermine, and 4 mM β-mercaptoethanol. RNase P RNA concentration was kept constant at 10 nM, and substrate concentrations were 100 nM; k_{obs} is given as nmol substrate converted per nmol of RNase P RNA per min; values are based on at least four independent experiments. The *inset* is a magnification of the lowest activity curves. P RNA, *E. coli* RNase P RNA.

preincubation conditions. It thus remains a possibility that the folding properties of the two mutant RNase P RNAs contributed to their defect in vivo. Unlike a recent study (Buck et al. 2005), we did not observe major effects of the protein component on RNase P RNA folding equilibria. This may be related to the fact that stabilization of the RNA fold by the protein was analyzed at <1 mM Mg^{2+} (Buck et al. 2005).

DISCUSSION

We have assessed the role of the CCA interaction in vivo by complementation analyses in two RNase P mutant strains. In both strains (DW2 and BW), *rnpB*C292 and *rnpB*C293 alleles encoding P RNA variants with a disrupted CCA interaction impaired or abrogated cell vitality (Tables 1, 2). Particularly, the phenotypes in strain BW (Table 2) demonstrate that base-pairing of G292 and G293 with C$_{74}$ and C$_{75}$ of RNase P substrates is essential in vivo, and its disruption is not compensated by the presence of the RNase P protein subunit in holoenzyme complexes. The BW strain also reconciles in vivo phenotype with kinetic data obtained in vitro: RNase P RNA C292 was more defective than the C293 variant in RNA alone (Busch et al. 2000) as well as in holoenzyme reactions using ptRNAwt as the substrate (Table 4; Fig. 6). In agreement, concomitant *rnpA* overexpression slightly improved viability of BW cells expressing *rnpB*C293, but not *rnpB*C292 (Table 2B).

The molecular basis of increased viability owing to *rnpA* overexpression in BW bacteria expressing *rnpB*C293 is not fully clear yet. We think it likely that higher levels of RNase P protein lead to increased steady-state levels of holoenzyme, either by shifting the equilibrium between free RNase P subunits and holoenzyme toward holoenzyme or by a mechanism that couples RNase P RNA and protein expression, according to which increased RNase P protein levels would entail a corresponding increase in the level of the RNA subunit. The latter possibility has been discussed in the context of a study on RNase P RNA metabolism in *E. coli* (Kim et al. 2005). *E. coli rnpB* primary transcripts can undergo either 3′-end maturation or oligoadenylation resulting in degradation. A knockout of poly(A) polymerase (*pcnB*), which blocks the degradation pathway, thus increased the level of 3′-precursor RNase P RNA. However, this was not associated with a concomitant increase in the level of mature RNase P RNA, leading to the proposal that mature RNase P RNA may only stably accumulate when complexed with its protein subunit (Kim et al. 2005).

Previous in vitro studies, focusing on the *E. coli* RNA-alone reaction, have indicated that the CCA contact increases substrate affinity (Hardt et al. 1995; Oh et al. 1998;

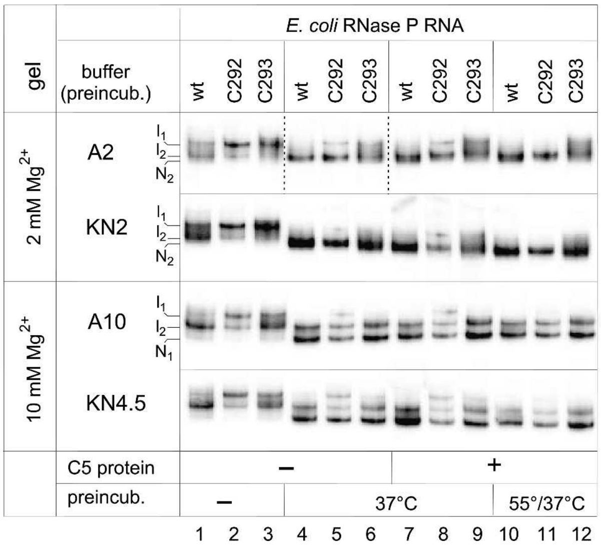

FIGURE 7. Analysis of folding equilibria for wild-type and C292/C293 mutant *E. coli* RNase P RNAs by native PAGE. RNAs (50 fmol, 3′ endlabeled) were preincubated either in buffer A containing 2 mM (*A2*) or 10 mM (*A10*) Mg^{2+}, or in buffer KN containing 2 mM (KN2) or 4.5 mM (KN4.5) Mg^{2+} in a volume of 4–5 µL (for buffer A and KN compositions, see Materials and Methods). (Lanes *1–3*) No preincubation (kept at 4°C); (lanes *4–6*) preincubation of RNase P RNAs for 70 min at 37°C; (lanes *7–9*) preincubation of RNase P RNAs for 55 min at 37°C, addition of 1 µL *E. coli* C5 protein (final concentration 50 nM) and further incubation for 15 min at 37°C; (lanes *10–12*) as in lanes *7–9*, but preincubation of RNase P RNAs for 5 min at 55°C and 50 min 37°C. Samples were run on 11.25% polyacrylamide gels in 1× THE buffer supplemented with 100 mM NH$_4$OAc and either 2 mM (A2, KN2) or 10 mM (A10, KN4.5) MgCl$_2$. The dashed lines confining lanes *4–6* in panel *A2* indicate that these lanes were taken from a different gel.

Busch et al. 2000) and supports selection of the correct cleavage site (Kirsebom and Svärd 1994) as well as catalysis (Oh et al. 1998; Busch et al. 2000; Brännvall et al. 2003). Based on the data presented here, we infer that disruption of the CCA interaction primarily causes a defect in the binding of catalytically important Mg^{2+} under in vivo conditions, based on the following argumentation: The activity of mutant holoenzymes, either assembled in vivo (Table 3) or in vitro (Table 4), was reduced only about two- to threefold relative to the wild-type holoenzyme at Mg^{2+} concentrations of 4.5–10 mM. However, a shift from 10 to 2 mM Mg^{2+} reduced the rate of ptRNAwt cleavage 25-fold for the wild-type holoenzyme, but 650- and 810-fold for the C292 and C293 mutant enzymes (Table 3). We are aware that these rate differences may include contributions from deviating folding properties of the mutant RNAs in buffer A containing 2 mM Mg^{2+} (Fig. 7, panel A2). Since folding equilibria of the wild-type and mutant RNase P RNAs were much more similar in the KN buffer system (Fig. 7), the results shown in Table 4 are thus likely to be most meaningful. Nevertheless, a similar trend was observed: The shift from 4.5 to 2.0 mM Mg^{2+} had a negligible effect on cleavage by the wild-type enzyme but reduced the cleavage rate 13- and 24-fold for the C293 and C292 mutant enzymes, respectively (Table 4). Such pronounced effects on cleavage rate in response to a shift from 4.5 to 2 mM Mg^{2+} are hard to explain by reasons other than a catalytic defect, although contributions from decreased substrate affinity or reduced affinity of the protein subunit cannot be excluded. The latter possibility might be suggested by the finding that the RNase P protein–RNA complex is stabilized by addition of substrate in the *Bacillus subtilis* system (Day-Storms et al. 2004). To test the possibility of decreased substrate affinity as the cause of low mutant enzyme activity at 2 mM Mg^{2+}, we increased the holoenzyme concentration by a factor of 5 (Table 4). However, this only increased the cleavage rate for the wild-type enzyme but not for the mutant holoenzymes, suggesting that decreased substrate affinity owing to disruption of the CCA contact is not a major cause for the defect of the mutant holoenzymes. Likewise, in the RNase P protein titration experiment (Fig. 6), activity essentially saturated at a protein/RNA ratio of 5:1 for the wild-type and mutant holoenzymes acting on ptRNAwt, thus providing no evidence for a major protein binding defect of the mutant RNase P RNAs. Finally, this is in line with the fact that we enriched the wild-type and mutant holoenzymes with comparable yields from cell extracts by anion exchange chromatography (Table 3).

Another potential defect of the C292 and C293 mutant RNAs in vivo could be aberrant folding leading to increased degradation. However, the mutant enzymes partially purified from strain DW2 had similar activities as the wild-type enzyme at 10 mM Mg^{2+} (Table 3). The same amounts of extract based on absorption at 260 nm were used in these processing assays, providing no evidence for altered RNase P levels in bacteria expressing *rnpB*C292 and *rnpB*C293. Likewise, wild-type-like maturation of plasmid-encoded 4.5S RNA by the C293 holoenzyme when base-pairing is restored by a compensatory mutation in the 3′ end of this substrate (Fig. 4) argues against substantial degradation of the mutant RNA.

On the basis of the data shown in Figure 7, it remains a possibility that differences in the folding equilibria of the wild-type versus mutant RNase P RNAs may have contributed to the mutant defects in vivo. The sensitivity of RNA folding toward point mutations in loop L15 might also provide a clue as to why the relative phenotypes of the C292 and C293 mutant RNAs deviated in strain DW2 grown at 43°C compared with strain BW grown at 37°C. In any case, the results of Figure 7 point to the sensitivity of RNase P RNA folding to structural changes as small as point mutations, particularly in low Mg^{2+} buffers. This seems surprising in view of the highly dynamic nature of the loop L15 region, as inferred from biochemical experiments (Ciesiolka et al. 1994; Brännvall et al. 2003) and evident in the crystal structure of *Thermotoga maritima* RNase P RNA (Torres-Larios et al. 2005). On the other hand, the dynamic nature of this region might increase its propensity to interfere with folding of other structural elements in the molecule. It will be interesting to see if mutations in other RNase P RNA elements may be able to exert similarly pronounced effects on folding at low Mg^{2+} concentrations.

The mutant holoenzymes cleaved the ptRNAwt substrate predominantly at the canonical site (Fig. 5), which also pertained to conditions of 2 mM Mg^{2+} (data not shown). Only the C292 enzyme showed some increase in miscleavage (<5%) (Fig. 5). A low extent of miscleavage is consistent with a previous study (Oh et al. 1998) analyzing processing of *B. subtilis* $\text{ptRNA}^{\text{Asp}}$ with CCA mutations by the *E. coli* wild-type holoenzyme. Oh et al. (1998) did not observe aberrant cleavage under any set of conditions. The $\text{ptRNA}^{\text{Asp}}$, as the $\text{ptRNA}^{\text{Gly}}$ used here, forms a canonical 7-bp acceptor stem and lacks any potential for extended acceptor stem base-pairing involving nucleotide −1/+73. Miscleavage in vivo may yet be increased for some ptRNAs, such as *E. coli* pSu1, which can form a C-1:G73 base pair (Svärd et al. 1996). In vitro processing of the latter substrate by reconstituted *E. coli* mutant holoenzymes gave substantial miscleavage (27% for the C293, 55% for the C292 variant) (Svärd et al. 1996). Thus, substantial aberrant cleavage of some cellular ptRNAs cannot be excluded and might contribute to the mutant phenotypes, particularly to that of *rnpB*292 in strain BW (Table 2).

Our results rationalize some previous in vitro data. For example, *E. coli* RNase P-catalyzed cleavage of ptRNA substrates with single nucleotide substitutions in CCA or a CCA deletion suggested that the protein subunit suppresses the binding defect for catalytic Mg^{2+} (Oh et al. 1998). However, these experiments were done at 100 mM

Mg^{2+}, conditions that mask the defect, as illustrated by the sharp activity differences we obtained at 2 versus 4.5 mM Mg^{2+} (Table 4).

The P15/L15/P16 region is a central Me^{2+} binding module in the active site of RNase P RNA (Kufel and Kirsebom, 1998; Altman and Kirsebom 1999; Brännvall et al. 2003). Binding of tRNA CCA ends suppresses, in vitro and in vivo, prominent Pb^{2+} hydrolysis at two locations in the L15 loop (sites III and V) and creates a new prominent Pb^{2+} hydrolysis site (IVb) nearby (Ciesiolka et al. 1994; Lindell et al. 2005). This indicates a structural rearrangement of the P15/L15/P16 region upon formation of the G292-C_{75} and G293-C_{74} intermolecular base pairs. The P15/L15/P16 module is also predicted to undergo a substantial conformational rearrangement upon substrate docking to the active site based on the recent crystal structure of *T. maritima* RNase P RNA (Torres-Larios et al. 2005). These observations combined with our findings presented here accentuate the need to include enzyme–substrate complexes in future structural analyses of RNase P in order to understand the catalytic mechanism of this ribozyme. Finally, our study suggests that activity tests of bacterial RNase P holoenzymes are better performed at Mg^{2+} concentrations <10 mM in order to be able to draw conclusions that are biologically relevant.

MATERIALS AND METHODS

Bacteria

E. coli strains DW2/pDW160 (Waugh and Pace 1990) and BW (this study) were used for complementation studies.

Complementation studies in strain DW2

For strain DW2/pDW160 (named DW2 in the following), complementing *rnpB* genes were under control of the native *E. coli rnpB* promoter and cloned in plasmid pSP64 as described (Hardt and Hartmann 1996). The pSP64 derivative carrying *E. coli rnpB* (pSP64 *E. coli rnpB*) served as template to introduce the point mutations C292 or C293 by the site-directed DpnI method according to the manual provided with the QuikChange XL Site-Directed mutagenesis Kit (Stratagene), using the primer pair 5′-GTA CTG AAC CCG CGT AGG CTG CTT GAGC and 5′-GCT CAA GCA GCC TAC GCG GGT TCA GTA C for the C292 mutation, and 5′-GTA CTG AAC CCG GCT AGG CTG CTT GAG C and 5′-GCT CAA GCA GCC TAG CCG GGT TCA GTA C for the C293 mutation (sites of mutation underlined). Recombinant *rnpB*-coding pSP64 derivatives (10 ng) were introduced into DW2 by electroporation, using a Biorad GenePulser (1.8 kV; 5 msec, 50 μF, 100 Ω). After the pulse, 1 mL SOC medium (per liter: 20 g peptone, 5 g yeast extract, 0.6 g NaCl, 0.17 g KCl, 20 mM glucose, 10 mM $MgCl_2$, 10 mM $MgSO_4$ at pH 7.5) was added, and cells were shaken for 1 h at 30°C. Appropriate dilutions of cell suspensions were plated on two LB agar plates, containing 100 μg/mL ampicillin and 30 μg/mL chloramphenicol. The two sets of plates were incubated in parallel at 30°C or 43°C, respectively, for 20–40 h.

Construction of *rnpB* mutant strain BW

Construction of strain BW followed the strategy described by Roux et al. (2005). The so-called catRExBAD cassette (Fig. 2A) was amplified from strain TG1 cat-AraC (Roux et al. 2005) using primers 135 (5′-CTT CAG CGT ATT GAC CAG CAT AGG TAC GTT GGA CGA AGC ATT CCG CGG GCT TGC ATA ATG TGC CTG TC; the underlined sequence is identical to the region upstream of the *E. coli rnpB* promoter) and 134 (5′-GTC TCC CCC GAA GAG GAC GAC GAC GAA GCG GCG ACT GTC TGG TCA GCT TCT ATG GAG AAA CAG TAG AGA GTT GC; the underlined sequence is complementary to *E. coli rnpB*, corresponding to nucleotides 1–50 of mature RNase P RNA). Initially, we could isolate a recombinant strain, which had the 5′ end of the described catRExBAD cassette successfully recombined within the 5′-*rnpB* promoter upstream region, but the 3′ boundary was altered. This strain was used to amplify a 326-bp fragment, containing the 5′ boundary, with primers 5′-*rnpB* ext (5′-CGA TTG GTG TCG CAA ACG TGG) and 3′-catRExBADveri (5′-CGC AAG GCG ACA AGG TGC TG). The *E. coli rnpB* gene was amplified from *E. coli* K12 with primers 3′-*rnpB* (5′-AGG TGA AAC TGA CCG ATA AGC C) and 5′-*rnpB* (5′-GAA GCT GAC CAG ACA GTC GC). This *rnpB* fragment and the 326-bp fragment with *E. coli rnpB* upstream sequence were combined with the catRExBAD cassette by overlapping PCR. The resulting PCR product was purified by agarose gel electrophoresis and transformed into *E. coli* MG1655 bacteria carrying pKD46 (temperature-sensitive helper plasmid expressing the λ *red* recombinase system) (Datsenko and Wanner 2000). For this purpose, MG1655/pKD46 cells were grown at 28°C to an OD_{578} of 0.15, followed by adjusting cultures to 10 mM arabinose to induce the λ *red* genes. Induced bacteria were then further grown to an OD_{578} of 0.6 and made electro-competent by 100-fold concentration and three washing steps with ice-cold 10% glycerol. Electroporation was performed with a Biorad Gene Pulser in 1-mm cuvettes (1.8 kV, 200 μF, 25 Ω) using 40 μL competent cells and 100–200 ng purified PCR fragment. Pulsed cells were added to 1 mL SOC medium supplemented with 10 mM arabinose, shaken for 1 h at 37°C and 900 rpm (Eppendorf Thermomixer comfort), and then plated and incubated at 37°C on LB agar plates containing 25 μg/mL chloramphenicol and 10 mM arabinose. Clones were analyzed by PCR for correct 5′ and 3′ boundaries of the integrated catRExBAD cassette and screened for ampicillin sensitivity to test for loss of the temperature-sensitive helper plasmid pKD46. The following primers were used to scrutinize correct insertion and sequence of the integrated cassette:

primer 195 (3′ AraC): 5′-GCA TGG AAG CGA TTA ACG AGT CGC

primer 194 (5′ AraC): 5′-GCG ACT CGT TAA TCG CTT CCA TGC

primer 193 (5′ *E. coli rnpB* promoter -58): 5′-CAC GTA ATA TCG CCG CGA CAC TGG

primer 158 (ext veri 3′ *rnpB*): 5′-GTG AAA CTG ACC GAT AAG CCG C

primer 157 (5′ ext veri *rnpB*): 5′-TGC AGG AGC TGC GGG TGG

primer 136 (RExBADveri 5′): 5′-CGG CGT CAC ACT TTG CTA TGC C

primer 138 (catBADveri3′): 5′-CGC AAG GCG ACA AGG TGC TG primer 49 (ecRevT3): 5′-CTC ACT GGC TCA AGC AGC CT

primer 186 (Ecm1 up +350): 5′-CAT TCG CGT CGC TTG TGA TGT C

primer 183 (Ecm1+350 3′): 5′-CGC CGG AAC GGT TTA TTA CGT AC

Integrity of the 5′ boundary was checked by primer combinations 157/138 and 138/186, and that of the 3′ boundary by the combinations 136/158 and 136/183; the absence of the native *rnpB* promoter region was verified with the primer pair 193/49, which produced a PCR fragment with genomic DNA from strain MG1655 (the original strain), but not with DNA from correct recombinants. Primer pairs 194/49 and 195/157 were used to amplify the inserted cassette in roughly two halves (upstream and downstream from *araC*) (see Fig. 2A) for verification by sequencing. Verified recombinant bacteria were named strain BW.

Construction of the low copy plasmid pACYC177 *E. coli rnpB*

To construct the derivatives of low copy plasmid pACYC177 encoding *E. coli rnpB*wt, *rnpB*C292, and *rnpB*C293, plasmids pSP64 *E. coli rnpB*wt, *rnpB*C292, or *rnpB*C293 were digested with NheI and HindIII and the fragments carrying the different *E. coli rnpB* alleles were inserted into pACYC177 cut with HindIII and NheI.

Complementation studies in strain BW

Derivatives of pACYC177 or pBR322 were introduced into strain BW by electroporation as described for DW2 bacteria. However, after the pulse, 1 mL SOC medium supplemented with 10 mM arabinose was added and cells were incubated for 1 h at 37°C; cells were twice pelleted by centrifugation and resuspended in 1 mL LB medium. After the second washing step, cells were plated in appropriate dilutions on LB agar plates containing 100 μg/mL ampicillin, 25 μg/mL chloramphenicol, and either 10 mM arabinose or 0.5% (w/v) glucose; 10 μg/mL tetracycline was added if BW bacteria additionally harbored pBR322 derivatives expressing *E. coli rnpA* or mutant 4.5S RNA; 1 mM IPTG was further added for induction of plasmid-encoded *rnpA*. For growth curve measurements, an overnight culture grown at 37°C in LB medium containing 10 mM arabinose and respective antibiotics (see above) was washed twice as described above, and then 50 mL volumes of LB were inoculated to an OD_{578} of 0.05–0.1, either supplemented with 10 mM arabinose or 0.5% glucose, followed by growth curve monitoring at 37°C and 180 rpm (Incubator GFL 3033).

Construction of pBR322 derivatives for expression of *E. coli rnpA*

To put *E. coli rnpA* under the control of the inducible pTrc-promoter (Amann et al. 1988), the *rnpA* gene was amplified with primers 5′-AGA CCA TGG TTA AGC TCG CAT TTC C (introducing an NcoI site, underlined, at the 5′ end of *rnpA*) and 5′-ATC TCT AGA GTC AGG ACC CGC GAG CCA (introducing an XbaI site, underlined, at the 3′ end of *rnpA*). The *E. coli rnpA* fragment was digested with NcoI and XbaI, and ligated into pTrc99a (Amann et al. 1988) also linearized with NcoI and XbaI, resulting in plasmid pTrc99a *E. coli rnpA*. This plasmid was unsuitable for our complementation studies, because it encodes an ampicillin resistance as plasmid pACYC177; also, the high copy number of pTrc99a *E. coli rnpA* would have potentially increased an imbalance between *rnpA* expression and that of *rnpB* genes encoded on the low copy plasmid pACYC177. Therefore, we amplified the *rnpA* gene including the pTrc promoter and the *rrnB*t1t2 terminator from pTrc99a *E. coli rnpA*, using the primers 5′-CAC ATG CAT GCA AAA AGG CCA TCC GTC AGG (introducing an Mph1103 I site, underlined) and 5′-ACA ATC GAT TCA ATT GCG CCG ACA TCA TAA CGG (introducing a MunI site, underlined) and ligated the fragment into pBR322 cut with PstI and EcoRI. Digestion of pBR322 with PstI and EcoRI (ends compatible with those of Mph11103 I and MunI, respectively) destroyed the ampicillin resistance, only leaving the tetracycline resistance.

Construction of pBR322 encoding mutated 4.5S RNAs

The chromosomal region of *E. coli* K12 harboring the bicistronic transcription unit of *ffs* (encoding 4.5S RNA) and *ybaA*, including the native promoter upstream of *ffs* as well as 100 bp downstream from *ybaA*, was amplified and cloned into pBR322. During PCR amplification, we already altered the terminal stem region by inversion of 4 bp within the stem structure (Fig. 4A) for specific reverse transcriptase priming in order to be able to distinguish native from plasmid-encoded 4.5S RNA. The promoter region and the 5′ end of *ffs* were amplified using primers 5′-ACA GAA TTC AGC ATA ATC TGG AAA AAC GCC C (introducing an EcoRI site, underlined) and 5′-CCA ACA GA**C GGG** CCA TTG AGA GCG TTG AGA ACC (5′-terminal 4.5S RNA stem mutations in bold); the 5′ portion of the *ffs* gene was amplified with the primer pair 5′-CTC AAT GGC CCG TCT GTT GGT TCT CCC GCA AC and 5′-TCT CTG CAG TAA CGC GTC ATC TGC CTT GGC (introducing MluI and PstI sites, underlined). These two fragments were combined by overlap extension PCR, cut with EcoRI and PstI, followed by ligation into pBR322 cut with the same enzymes. The 3′ half of *ffs* was amplified with primer pair 5′-CTC AAT GGC CCG TCT GTT GGT TCT CCC GCA AC and 5′-TGG **CCC G**CC TGC CAG CTA CAT CCC GG (3′-terminal stem mutations in bold). The chromosomal region spanning the 3′-terminal 19 bp of *ffs* and the *ybaA* cistron was amplified using forward primer 5′- GCT GGC AGG CGG GCC ACC CAT TTC TGC CTC CCA CCG TTT C and reverse primer 5′-CAC CTG CAG CAA GGC ATT ACC GAA AGA AG. To further introduce point mutations into the 3′-CCC end of 4.5S RNA, the same PCR reaction was performed except that 5′- GCT GGC AGG CGG GCC AGC CAT TTC TGC CTC CCA CCG TTT C (3′-GCC$_{“76”}$) or 5′- GCT GGC AGG CGG GCC ACG CAT TTC TGC CTC CCA CCG TTT C (3′-CGC$_{“76”}$) was used as the forward primer. The latter three amplification products were combined with the PCR fragment harboring the 3′ half of *ffs* (see above) by overlap extension PCR. The resulting product was then cut with PstI/MluI and ligated into the pBR322 derivative containing the promoter and 5′ half of *ffs* and cut with the same restriction enzymes.

In vitro transcription and 5′ and 3′ endlabeling

Runoff transcription with bacteriophage T7 RNA polymerase as well as 5′ and 3′ endlabling were performed essentially as described (Heide et al. 1999; Busch et al. 2000). The ptRNA^{Gly} substrate (Fig. 1) was transcribed from plasmid pSBpt3′HH (Busch et al. 2000). Mutations G74 and G75 were introduced by the site-directed DpnI mutagenesis method according to the manual provided with the QuikChange XL Site-Directed Mutagenesis Kit (Stratagene); the primer pair for introduction of the G_{74} mutation was 5′-CCG TCT CCC GCT GCA GTC ACC GGA TGT GC and 5′-GCA CAT CCG GTG ACT GCA GCG GGA GAC GG; for introduction of the G_{75} mutation, 5′-CCG TCT CCC GCT CGA GTC ACC GGA TGT GC and 5′-GCA CAT CCG GTG ACT CGA GCG GGA GAC GG were used (sites of mutation underlined). Precursor 4.5S RNA was transcribed from a PCR template under control of the T7 promoter; the PCR template was amplified from plasmid pT7-4.5S (constructed and kindly provided by Norman R. Pace, University of Colorado, Boulder, CO), a derivative of plasmid pT71 (Tabor and Richardson 1985) encoding *E. coli* 4.5S RNA with 23 nt of its natural 5′-flanking sequence and 17 additional 5′-flanking nucleotides; the 4.5S RNA precursor transcript carried an additional AUA at the 3′ end in comparison with natural mature 4.5S RNA (Peck-Miller and Altman 1991); PCR primers were 5′-CCA GAA TTC GAA ATT AAT ACG ACT CAC TAT A (T7 promoter underlined) and 5′-TAT GGG TGG GGG CCC TGC CAG CTA. *E. coli* RNase P RNA and C292/3 mutant variants were synthesized as described previously (Busch et al. 2000).

RNA isolation for primer extension analysis

DW2 bacteria harboring derivatives of plasmid pSP64 were grown at 30°C overnight in LB containing 100 μg/mL ampicillin and 30 μg/mL chloramphenicol. On the next morning, the same culture was incubated for 2 h at 43°C, followed by inoculation of fresh medium (100 or 250 mL) to a starting OD_{578} of 0.05–0.1, and further cultivation at 43°C until cell density reached an OD_{578} of ~0.6. BW cells harboring pACYC177 and pBR322 derivatives were grown overnight at 37°C in 3 mL LB medium supplemented with 100 μg/mL ampicillin, 25 μg/mL chloramphenicol, 10 mM arabinose, and 10 μg/mL tetracycline in the case of cells harboring pBR322 derivatives. Cells were then used to inoculate 50 mL of the same medium to a starting OD_{578} of 0.05–0.1, followed by incubation at 37°C. At an OD_{578} of ~0.5, cells were centrifuged for 5 min at 5000 rpm and washed once with 20 mL LB to remove residual arabinose. Cells were resuspended in 100 mL LB supplemented with antibiotics and 0.5% glucose and incubated for another 3 h at 37°C and 180 rpm. Total cellular RNA from strains DW2 and BW was isolated by the TRIzol method (Invitrogen) according to the protocol provided by the manufacturer. After concentration by ethanol precipitation, RNA was further digested with DNase I (Turbo DNase, Ambion) followed by phenol/chloroform (1:1) and chloroform extractions (Busch et al. 2000) and ethanol precipitation in the presence of 0.12 M NaOAc (pH 5.0). RNA was dissolved in double-distilled H_2O, and concentrations were measured in H_2O at 260 nm (1 A_{260} unit = 40 μg).

Primer extension assays

Primer extension assays were performed with total cellular RNA and primers specific to *E. coli* RNase P RNA (5′-CTC ACT GGC TCA AGC AGC CT), *E. coli* wild-type 4.5S RNA (5′-GGA GAA CCA ACA GAG CCC), or *E. coli* mutant 4.5S RNA (5′-GGA GAA CCA ACA GAC GGG). Primer annealing was conducted in 75 mM KCl and 68 mM Tris-HCl (pH 8.3) for ~60 min applying a linear temperature gradient from 90°C to 55°C. Reverse transcription was then performed at 55°C using ThermoScript reverse transcriptase (Invitrogen) according to the manufacturer's instructions. Nucleotide (dNTP) concentrations in primer extension assays were 0.5 mM each. For primer extension assays to verify expression of *E. coli rnpB*C292/293 mutant alleles, dGTP was replaced with ddGTP. For the size marker in Figure 3, lane 1, 0.5 mM dGTP and 0.5 mM ddGTP were used.

Partial purification of RNase P from *E. coli* cells

DW2 cells grown at 43°C as described (see RNA Isolation for Primer Extension Analysis) and resuspended in ~4 mL buffer A (60 mM NH_4Cl, 10 mM $Mg[OAc]_2$, 6 mM DTT, 50 mM Tris-HCl at pH 7.2–7.5) per 600 mg cell pellet were lysed by sonication (Branson Sonifier 250, output 20, duty cycle 30%–40%, 10 min on ice), followed by centrifugation for 45 min at 4°C and 10,000*g*. For the preparation of DEAE fractions, the supernatant was loaded onto a DEAE fast flow Sepharose column (Aekta basic, Pharmacia). Elution was performed by applying a continuous NH_4Cl gradient from 60–550 mM NH_4Cl. Active fractions eluted at ~300–400 mM NH_4Cl.

Preparation of recombinant RNase P protein

E. coli RNase P protein carrying an N-terminal His-tag (His-tagged peptide leader: MRGSHHHHHHGS, encoded in plasmid pQE-30 in *E. coli* JM109) was expressed essentially as described (Rivera-León et al. 1995). Cell cultures (LB broth containing 100 μg/mL ampicillin) were grown to an OD_{578} of 0.6, and IPTG was added to a final concentration 1 mM. Cells were harvested after 3 h (OD_{578} ~2.5) by centrifugation for 10 min at 5000 rpm at 4°C. The following steps were performed at 4°C or on ice, and all buffers contained 40 μg/mL of the protease inhibitor phenylmethylsulfonyl fluoride (PMSF). Cells were then resuspended in 10–15 mL sonication buffer SB (50 mM Tris-HCl at pH 8.0, 0.3 M NaCl, 0.1% triton X-100, 1 M NH_4Cl). After sonication (Branson Sonifier 250, output 20, duty cycle 50%, 15 min on ice), the sample was centrifuged for 30 min (4°C, 14,500*g*), and the supernatant was mixed with Ni-NTA agarose (400 μL for 2 L of cell culture), which had been prewashed twice with 10 mL SB buffer. The sample was incubated for 1–2 h at 4°C under gentle mixing or rotating. The Ni-NTA agarose slurry was washed three times (centrifugation–resuspension cycles; centrifugation at 4°C and 8500 rpm in a desktop centrifuge) with ice-cold washing buffer (30 mM imidazol, 50 mM Tris-HCl at pH 8.0, 8 M urea, 0.1% triton X-100). The RNase P protein started to precipitate during this procedure; therefore, the supernatant after each washing step was removed carefully to avoid release of protein aggregates from the matrix. The protein was then eluted with 500 μL elution buffer (50 mM Tris-HCl at pH 7.0, 10% glycerol, 7 M urea, 20 mM EDTA, 0.3 M imidazol) for 45 min at 4°C under gentle shaking. Eluates were dialyzed twice for 1 h and subsequently overnight against volumes of 500 mL dialysis buffer (50 mM Tris-HCl at pH 7.0, 0.1 M NaCl, 10% glycerol; dialysis bags: Roth, molecular weight cut off 12–14 kDa); during dialysis, a white precipitate forms. The content of the dialysis bags was transferred to a 2-mL Eppendorf tube and centrifuged for 20 min at 4°C and 12,000 rpm in a desktop centrifuge. The supernatant contained RNase P protein devoid of any RNase P RNA contamination, whereas the pellet included traces of RNase P

RNA and was therefore discarded. All purification steps were monitored by 17% SDS-PAGE to assess the purity and concentration of RNase P proteins.

Processing assays

For RNase P-catalyzed processing of *T. thermophilus* ptRNA^{Gly} (ptRNAwt), or G_{74} or G_{75} variants thereof, active DEAE fractions (0.25–1.0 μL; equal amounts [0.004 A_{260} units] based on A_{260} measurements) were incubated in buffer A (2 or 10 mM $Mg[OAc]_2$, 6 mM DTT, 50 mM Tris-HCl at pH 7.5) containing 100 mM NH_4Cl for 10 min at 37°C in a volume of 16 μL. Trace amounts (<1 nM) of the 5′-endlabeled ptRNA^{Gly} substrate were preincubated under the same conditions for 5 min at 55°C and 25 min at 37°C. Processing reactions were started by combining enzyme and substrate solutions (final volume, 20 μL) and assayed at 37°C. The $Mg(OAc)_2$ concentration was raised to 100 mM in control reactions with *E. coli* RNase P RNA alone. Buffer KN [20 mM Hepes-KOH at pH 7.4, 2 or 4.5 mM $Mg(OAc)_2$, 150 mM NH_4OAc, 2 mM spermidine, 0.05 mM spermine, and 4 mM β-mercaptoethanol] (Dinos et al. 2004), optimized for functional analyses of *E. coli* ribosomes, was used to closely mimic physiological conditions. In vitro reconstitution of RNase P holoenzymes was performed as follows: RNase P RNAs were incubated in buffer KN for 5 min at 55°C and 50 min at 37°C, after which RNase P protein was added, followed by another 5 min at 37°C before addition of substrate.

Folding analysis by native PAGE

We incubated 50 fmol of *E. coli* wild-type or C292/C293 mutant RNase P RNA, including trace amounts of 5′- or 3′-endlabeled material of the same RNA, in buffer A (100 mM NH_4Cl, 6 mM DTT, 50 mM Tris-HCl at pH 7.2–7.5, and 2 or 10 mM $Mg[OAc]_2$) or buffer KN (20 mM Hepes-KOH at pH 7.4, 150 mM NH_4OAc, 2 mM spermidine, 0.05 mM spermine, 4 mM β-mercaptoethanol, and 2 or 4.5 mM $Mg[OAc]_2$) in a volume of 5 μL or 4 μL if protein was added thereafter. Buffer conditions were the same as those used for the kinetic experiments. RNase P RNAs were either kept at 4°C (no preincubation) or preincubated for 55 min at 37°C, or 5 min at 55°C followed by 50 min at 37°C. We also tested a preincubation protocol starting with 2 min at 85°C, followed by 5 min at 55°C and 50 min at 37°C. The results were, however, identical to those obtained with 5 min at 55°C plus 50 min at 37°C. For samples including the protein subunit, 1 μL of *E. coli* C5 protein was added (final concentration, 50 nM) after the preincubation step. All samples, except for those kept at 4°C, were then incubated for another 15 min at 37°C and finally adjusted to room temperature. Immediately before gel loading, 1 volume of loading buffer (10% [v/v] glycerol, 2 mM $MgCl_2$, xylene cyanol, bromphenol blue) was added. The nondenaturing 11.25% (v/v) polyacrylamide gels (thickness <1 mm) contained 66 mM Hepes, 33 mM Tris (pH 7.4), and 0.1 mM EDTA (1× THE), supplemented with 100 mM NH_4OAc and 2 or 10 mM $MgCl_2$. Gels were run at 180–250 V until xylene cyanol had migrated 11.5 cm from the top. The gel temperature was controlled not to exceed 15°C. The RNA bands were visualized with a Bio-Imaging Analyzer (FLA 3000–2R, Fujifilm). Results were the same for 5′- and 3′-endlabeled RNase P RNAs. End homogeneity of RNase P RNAs was checked by denaturing PAGE. Results for RNase P RNAs preincubated in buffer KN containing 4.5 mM $MgCl_2$ were the same if gels were run in the presence of 4.5 or 10 mM $MgCl_2$ (data not shown).

ACKNOWLEDGMENTS

We thank Agustin Vioque (Universidad de Sevilla, Spain) for providing us with the antiserum specific for the *E. coli* RNase P protein, Michal Marszalkowski (Hartmann Laboratory) for preparation of recombinant *E. coli* RNase P protein, Jean-Marc Ghigo (Institut Pasteur, Paris, France) for putting strain TG1 cat-AraC at our disposal, Jörg Vogel (Max Planck Institute for Infection Biology, Berlin, Germany) for providing plasmid pKD46, and the reviewers for their insightful and encouraging comments. This work was supported by the Deutsche Forschungsgemeinschaft (HA 1672/7-4) and the Fonds der Chemischen Industrie.

Received June 12, 2006; accepted September 5, 2006.

REFERENCES

Alatossava, T., Jutte, H., Kuhn, A., and Kellenberger, E. 1985. Manipulation of intracellular magnesium content in polymyxin B nonapeptide-sensitized *Escherichia coli* by ionophore A23187. *J. Bacteriol.* **162:** 413–419.

Altman, S. and Kirsebom, L.A. 1999. *The RNA world* (eds. R.F. Gesteland et al.), pp. 351–380. Cold Spring Harbor Laboratory Press, Cold Spring Harbor, NY.

Amann, E., Ochs, B., and Abel, K.J. 1988. Tightly regulated tac promoter vectors useful for the expression of unfused and fused proteins in *Escherichia coli*. *Gene* **69:** 301–315.

Bothwell, A.L., Garber, R.L., and Altman, S. 1976. Nucleotide sequence and in vitro processing of a precursor molecule to *Escherichia coli* 4.5 S RNA. *J. Biol. Chem.* **251:** 7709–7716.

Brännvall, M., Pettersson, B.M.F., and Kirsebom, L.A. 2003. Importance of the +73/294 interaction in *Escherichia coli* RNase P RNA substrate complexes for cleavage and metal ion coordination. *J. Mol. Biol.* **325:** 697–709.

Buck, A.H., Dalby, A.B., Poole, A.W., Kazantsev, A.V., and Pace, N.R. 2005. Protein activation of a ribozyme: The role of bacterial RNase P protein. *EMBO J.* **24:** 3360–3368.

Busch, S., Kirsebom, L.A., Notbohm, H., and Hartmann, R.K. 2000. Differential role of the intermolecular base-pairs G292-C_{75} and G293-C_{74} in the reaction catalyzed by *Escherichia coli* RNase P RNA. *J. Mol. Biol.* **299:** 941–951.

Ciesiolka, J., Hardt, W.D., Schlegl, J., Erdmann, V.A., and Hartmann, R.K. 1994. Lead-ion induced cleavage of RNase P RNA. *Eur. J. Biochem.* **219:** 49–56.

Datsenko, K.A. and Wanner, B.L. 2000. One-step inactivation of chromosomal genes in *Escherichia coli* K-12 using PCR products. *Proc. Natl. Acad. Sci.* **97:** 6640–6645.

Day-Storms, J.J., Niranjanakumari, S., and Fierke, C.A. 2004. Ionic interactions between P RNA and P protein in *Bacillus subtilis* RNase P characterized using a magnetocapture-based assay. *RNA* **10:** 1595–1608.

Dinos, G., Wilson, D.N., Teraoka, Y., Szaflarski, W., Fucini, P., Kalpaxis, D., and Nierhaus, K.H. 2004. Dissecting the ribosomal inhibition mechanisms of edeine and pactamycin: The universally conserved residues G693 and C795 regulate P-site RNA binding. *Mol. Cell* **13:** 113–124.

Evans, D., Marquez, S.M., and Pace, N.R. 2006. RNase P: Interface of the RNA and protein worlds. *Trends Biochem. Sci.* **31:** 333–341.

Guerrier-Takada, C., Gardiner, K., Marsh, T., Pace, N., and Altman, S. 1983. The RNA moiety of ribonuclease P is the catalytic subunit of the enzyme. *Cell* **35:** 849–857.

Hardt, W.D. and Hartmann, R.K. 1996. Mutational analysis of the joining regions flanking helix P18 in *E. coli* RNase P RNA. *J. Mol. Biol.* **259:** 422–433.

Hardt, W.D., Schlegl, J., Erdmann, V.A., and Hartmann, R.K. 1995. Kinetics and thermodynamics of the RNase P RNA cleavage reaction: Analysis of tRNA 3′-end variants. *J. Mol. Biol.* **247:** 161–172.

Harris, M.E. and Christian, E.L. 2003. Recent insights into the structure and function of the ribonucleoprotein enzyme ribonuclease P. *Curr. Opin. Struct. Biol.* **13:** 325–333.

Hartmann, E. and Hartmann, R.K. 2003. The enigma of ribonuclease P evolution. *Trends Genet.* **19:** 561–569.

Hartmann, R.K., Heinrich, J., Schlegl, J., and Schuster, H. 1995. Precursor of C4 antisense RNA of bacteriophages P1 and P7 is a substrate for RNase P of *Escherichia coli*. *Proc. Natl. Acad. Sci.* **92:** 5822–5826.

Heide, C., Pfeiffer, T., Nolan, J.M., and Hartmann, R.K. 1999. Guanosine 2-NH_2 groups of *Escherichia coli* RNase P RNA involved in intramolecular tertiary contacts and direct interactions with tRNA. *RNA* **5:** 102–116.

Hsu, L.M., Zagorski, J., and Fournier, M.J. 1984. Cloning and sequence analysis of the *Escherichia coli* 4.5 S RNA gene. *J. Mol. Biol.* **178:** 509–531.

Kim, K.S., Sim, S., Ko, J.H., and Lee, Y. 2005. Processing of M1 RNA at the 3′ end protects its primary transcript from degradation. *J. Biol. Chem.* **280:** 34667–34674.

Kirsebom, L.A. and Svärd, S.G. 1994. Base pairing between *Escherichia coli* RNase P RNA and its substrate. *EMBO J.* **13:** 4870–4876.

Kufel, J. and Kirsebom, L.A. 1998. The P15-loop of *Escherichia coli* RNase P RNA is an autonomous divalent metal ion binding domain. *RNA* **4:** 777–788.

Li, Y., Cole, K., and Altman, S. 2003. The effect of a single, temperature-sensitive mutation on global gene expression in *Escherichia coli*. *RNA* **9:** 518–532.

Lindell, M., Brännvall, M., Wagner, E.G., and Kirsebom, L.A. 2005. Lead(II) cleavage analysis of RNase P RNA *in vivo*. *RNA* **11:** 1348–1354.

Oh, B.K., Frank, D.N., and Pace, N.R. 1998. Participation of the 3′-CCA of tRNA in the binding of catalytic Mg^{2+} ions by ribonuclease P. *Biochemistry* **37:** 7277–7283.

Peck-Miller, K.A. and Altman, S. 1991. Kinetics of the processing of the precursor to 4.5 S RNA, a naturally occurring substrate for RNase P from *Escherichia coli*. *J. Mol. Biol.* **221:** 1–5.

Richmond, C.S., Glasner, J.D., Mau, R., Jin, H., and Blattner, F.R. 1999. Genome-wide expression profiling in *Escherichia coli* K-12. *Nucleic Acids Res.* **27:** 3821–3835.

Rivera-León, R., Green, C.J., and Vold, B.S. 1995. High-level expression of soluble recombinant RNase P protein from *Escherichia coli*. *J. Bacteriol.* **177:** 2564–2566.

Roux, A., Beloin, C., and Ghigo, J.M. 2005. Combined inactivation and expression strategy to study gene function under physiological conditions: Application to identification of new *Escherichia coli* adhesins. *J. Bacteriol.* **187:** 1001–1013.

Schön, A. 1999. Ribonuclease P: The diversity of a ubiquitous RNA processing enzyme. *FEMS Microbiol. Rev.* **23:** 391–406.

Svärd, S.G., Kagardt, U., and Kirsebom, L.A. 1996. Phylogenetic comparative mutational analysis of the base-pairing between RNase P RNA and its substrate. *RNA* **2:** 463–472.

Tabor, S. and Richardson, C.C. 1985. A bacteriophage T7 RNA polymerase/promoter system for controlled exclusive expression of specific genes. *Proc. Natl. Acad. Sci.* **82:** 1074–1078.

Torres-Larios, A., Swinger, K.K., Krasilnikov, A.S., Pan, T., and Mondragon, A. 2005. Crystal structure of the RNA component of bacterial ribonuclease P. *Nature* **437:** 584–587.

Waugh, D.S. and Pace, N.R. 1990. Complementation of an RNase P RNA (*rnpB*) gene deletion in *Escherichia coli* by homologous genes from distantly related eubacteria. *J. Bacteriol.* **172:** 6316–6321.

Zarrinkar, P.P., Wang, J., and Williamson, J.R. 1996. Slow folding kinetics of RNase P RNA. *RNA* **2:** 564–573.

4.3 *In vivo* role of bacterial type B RNase P interaction with tRNA 3’-CCA

Wegscheid, B, Hartmann, R.K.

submitted, 2006

In vivo role of bacterial type B RNase P interaction with tRNA 3’-CCA

Barbara Wegscheid and Roland K. Hartmann[*]

Institut für Pharmazeutische Chemie, Philipps-Universität Marburg, Marbacher Weg 6, D-35037 Marburg, Germany

[*] Corresponding author: Roland K. Hartmann, Institut für Pharmazeutische Chemie, Philipps-Universität Marburg, Marbacher Weg 6, D-35037 Marburg, Germany,
Tel. +6421-2825827; Fax +6421-2825854; e-mail: roland.hartmann@staff.uni-marburg.de

Running head: tRNA 3’-CCA contact with type B RNase P *in vivo*

Character count: 53578

ABSTRACT (178 words)

It has been unclear if catalysis by bacterial type B RNase P involves a specific interaction with p(recursor)tRNA 3’-CCA termini. We show that point mutations at two guanosines in loop L15 result in growth inhibition, which correlates with an enzyme defect at low Mg^{2+}. For *Bacillus subtilis* RNase P, an isosteric C259-G_{74} bp fully and a C258-G_{75} bp slightly rescued catalytic proficiency, demonstrating Watson-Crick base-pairing to tRNA 3’-CCA and emphasizing the importance of G258 identity. We infer the defect of the mutant enzymes to be primarily on the level of recruitment of catalytically relevant Mg^{2+}, with a possible contribution from altered RNA folding. Cell viability of bacteria expressing mutant RNase P RNAs could be (partially) restored by RNase P protein overexpression due to increasing cellular RNase P levels. Finally, we demonstrate that *B. subtilis* RNase P is able to cleave CCA-less ptRNAs *in vivo.* We conclude that the *in vivo* phenotype upon disruption of the CCA interaction is either due to a global deceleration in ptRNA maturation kinetics or severe blockage of 5’-maturation for a subset of ptRNAs.

Keywords: bacterial type B RNase P; CCA interaction; *in vivo* complementation studies;

Introduction

Ribonuclease P (RNase P), an essential ribonucleoprotein enzyme, catalyzes the 5'-end maturation of tRNAs in all Kingdoms of life (Hartmann & Hartmann, 2003; Evans *et al*, 2006). The bacterial RNase P holoenzyme consists of an RNA subunit (P RNA) of approx. 400 nt and a small basic protein (P protein) of approx. 13 kDa. *In vitro*, RNA subunits of bacterial RNase P enzymes are catalytically active in the absence of the protein subunit (Guerrrier-Takada *et al*, 1983), but the protein is essential *in vivo* (Schedl *et al*, 1974; Gößringer *et al*, 2006). Two major architectural subtypes of bacterial RNase P RNA are known, namely type A (for ancestral, prototype *Escherichia coli*) and type B (represented by *Bacillus subtilis*; Hall & Brown 2001), each containing several secondary structural elements not present in the other. A major difference between type A and B structures is the L15 loop of the catalytic domain, which is an internal one in type A but apical in type B (Fig. 1 A-C). For *E. coli* P RNA, the gold standard of type A structures, it has been shown that two conserved G residues (G293 and G292) in the loop L15 form Watson-Crick base pairs with the two cytosines of tRNA 3'-CCA (C_{74} and C_{75}) termini (Kirsebom & Svärd, 1994). Several *in vitro* studies, focussing on the *E. coli* RNA-alone reaction, have indicated that the CCA contact increases substrate affinity (Hardt *et al*, 1995; Oh *et al*, 1998; Busch *et al*, 2000), supports selection of the correct cleavage site (Kirsebom & Svärd, 1994; Svärd *et al*, 1996) as well as catalysis (Oh *et al*, 1998; Busch *et al*, 2000; Brännvall *et al*, 2003). Recently, disruption of this interaction was demonstrated to have lethal consequences for *E. coli* cells (Wegscheid & Hartmann, 2006). Analysis of processing of 4.5S RNA, a non-tRNA substrate of RNase P in *E. coli*, revealed that restoration of base-pairing by an isosteric C293-G_{74} base pair, but not a C292-G_{75} pair, fully restored catalytic performance *in vivo. In vitro* activity assays of wild-type (wt) and C292/C293 mutant RNase P holoenzymes at magnesium concentrations as low as 2 mM Mg^{2+} suggested a defect in the recruitment of catalytically active Mg^{2+} ions as the major cause for the lethal phentotype of the mutant P RNAs (Wegscheid & Hartmann, 2006)

Type B RNAs, represented by the one from *B. subtilis*, also encode a conserved GG dinucleotide in their L15 loop (Fig. 1 A and B, G258/G259 in *B. subtilis* and G238/G239 in *S. aureus* P RNA). Comparative photo-crosslinking analyses of *E. coli* and *B. subtilis* P RNAs using tRNAs with photoreactive groups at the 3'-end of tRNA have indicated that the tRNA 3'-CCA terminus is positioned close to the L15 loop region in enzyme-substrate complexes of both P RNA types (Oh & Pace, 1994). G258 and G259 of *B. subtilis* P RNA were also shown to be protected from kethoxal modification upon complexation with mature tRNA or precursor tRNA (ptRNA), and this protection was reduced with ptRNA lacking 3’-CCA (LaGrandeur *et al*, 1994). Potential base pairing to 3’-CCA was addressed by a mutational analysis using another type B RNA from *Mycoplasma hyopneumoniae* and testing for cleavage site selection (Svärd *et al*, 1996). With *E. coli* P RNA, C292/C293 mutations substantially increased miscleavage of the wt substrate, while compensatory mutations in the substrate 3’-CCA restored cleavage at the canonical site. However, with *M. hyopneumoniae* P RNA, corresponding mutations in L15 (C272/C273) had little effect on the proportion of miscleaved wt substrate. Also, a compensatory G_{74} mutation in the substrate did not significantly increase the fraction of substrate cleaved at the canonical site by the C273 mutant ribozyme; the proportion of canonical cleavage, relative to the wt substrate, was even decreased when the C272 mutant ribozyme acted on the substrate providing the compensatory mutation (3’-CG_{75}A; Svärd *et al*, 1996).

These findings did not provide clear evidence as to whether the two G residues in L15 of type B RNAs indeed form specific interactions with tRNA 3’-CCA. The physiological role of a CCA contact was also questionable based on the observation that *B. subtilis* P RNA, in contrast to its *E. coli* counterpart, is rather insensitive to 3’-CCA mutations in terms of cleavage site selection (Wegscheid *et al*, 2006). Furthermore, the P protein of *B. subtilis* RNase P increases the affinity for the ptRNA more than 10^4-fold (Kurz *et al*, 1998; Buck *et al*, 2005), making a substantial contribution of the CCA interaction to substrate affinity rather unlikely. This notion is supported by the finding that *E. coli* and *B. subtilis* RNase P holoenzymes remained unaffected by the absence of CCA in terms of their K_m values in multiple turnover reactions (Oh & Pace, 1994).

In *B. subtilis*, one-third of tRNAs (27 out of 86) do not have the CCA motif encoded by their genes. RNase Z removes the 3’-trailers of such CCA-less tRNA primary transcripts by endonucleolytic cleavage 3’ of the discriminator nucleotide as a prerequisite for CCA addition by tRNA nucleotidyl-transferase (CCase); RNase Z is blocked by the presence of 3’-CCA and thus acts specifically on tRNA transcripts lacking the 3’-CCA motif (Pellegrini *et al*, 2003). However, *B. subtilis* RNase Z activity inversely correlates with the length of tRNA 5’ extensions, which led to the proposal that processing by RNase P precedes that of RNase Z in the case of tRNA transcripts with larger 5’ extensions (> 30 nt; Pellegrini *et al*, 2003). This would suggest that 3’-CCA in the substrate is dispensable for processing by *B. subtilis* RNase P *in vivo*.

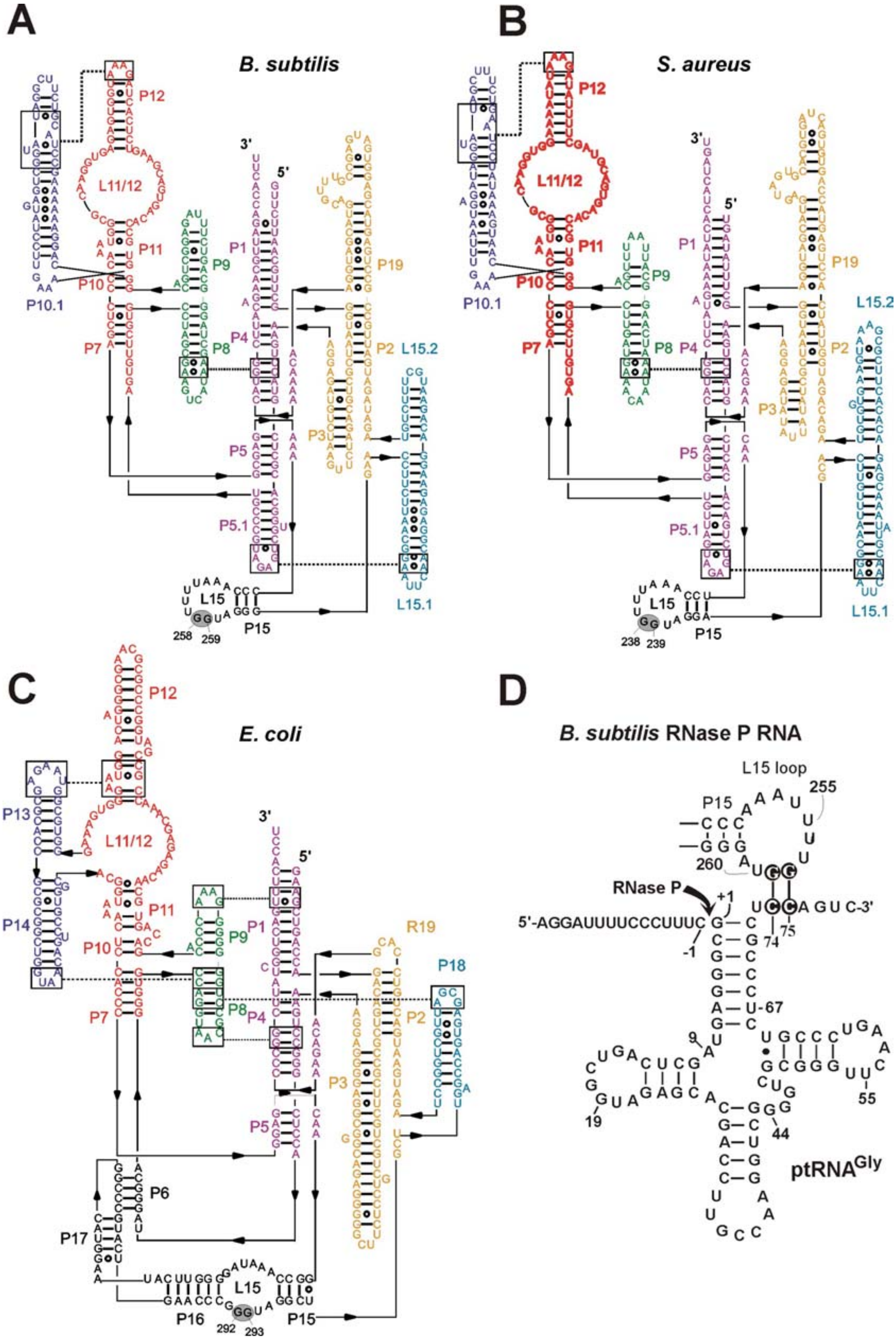
A
B. subtilis
P12
L11/12
P11
P10
P10.1
P9
P8
P7
P1
P4
P5
P5.1
P19
P2
P3
L15.2
L15.1
L15
P15
3'
5'
258
259
B
S. aureus
P12
L11/12
P11
P10
P10.1
P9
P8
P7
P1
P4
P5
P5.1
P19
P2
P3
L15.2
L15.1
L15
P15
3'
5'
238
239
C
E. coli
P12
L11/12
P13
P14
P11
P10
P9
P8
P7
P1
P4
P5
P6
P17
P16
L15
P15
R19
P18
P2
P3
3'
5'
292
293
D
B. subtilis RNase P RNA
L15 loop
P15
255
260
RNase P
+1
5'-AGGAUUUUCCCUUUC
-1
74
75
GUC C-3'
U-67
9
19
44
55
ptRNA^Gly

Fig. 1. Secondary structure illustrations of (**A**) *Bacillus subtilis* (type B), (**B**) *Staphylococcus aureus* (type B) and (**C**) *Escherichia coli* (type A) RNase P RNA according to Tsai *et al* (2003). The two G residues in L15, known (*E. coli*) or suspected (*B. subtilis, S. aureus*) to be involved in the interaction with tRNA 3'-CCA, are highlighted by grey ovals. (**D**) Proposed interaction of a canonical bacterial ptRNA (*Thermus thermophilus* ptRNA^{Gly}) with the L15 loop of *B. subtilis* RNase P RNA. Highlighted nucleotides mark the sites of mutation investigated in this study. The arrow indicates the canonical RNase P cleavage site (between nucleotide –1 and +1).

In vitro evidence for the CCA interaction with type B RNase P RNAs has been at best suggestive, and nothing is known on the role of the CCA interaction *in vivo* in type B bacteria. Here we have addressed this question *in vitro* as well as *in vivo* by mutational analysis. We demonstrate that *B. subtilis rnpB*C258 and *rnpB*C259 mutant alleles carrying a G to C258 or G to C259 mutation in the L15 loop are lethal in *B. subtilis rnpB* mutant strain SSB318. We also included a second type B RNA from *Staphylococcus aureus* in our complementation study. Corresponding *S. aureus rnpB*C238 and *rnpB*C239 mutant alleles also decreased cell viability of *B. subtili*s SSB318 cells, although not being lethal. Even so the growth defects could be rescued by parallel overexpression of the *B. subtilis* P protein, we found no evidence for defects of the mutant P RNAs in P protein or substrate binding. Processing assays with *in vitro* assembled holoenzymes then revealed a defect of the C258/C259 mutant enzymes at free Mg^{2+} concentrations assumed to be close to those *in vivo*. We infer that the defect is primarily on the level of recruitment of catalytically important Mg^{2+}. An isosteric C259-G_{74} base pair fully, but a C258-G_{75} pair only slightly, restored catalytic performance *in vitro*, demonstrating that the identity of G258, but not G259, is crucial for enzyme function. This is surprisingly similar to what has been found for *E. coli* RNase P (Wegscheid & Hartmann, 2006). Native PAGE experiments further unveiled some differences in RNA folding equilibria between the wt and mutant P RNAs at low [Mg^{2+}], which remained unaffected by the presence of the P protein. This raises the possibility that a contribution from non-native folding might have exacerbated the defect of the C258/C259 mutant RNAs *in vivo*. We finally addressed the question if RNase P can act on CCA-less ptRNAs in *B. subtilis* by 5'-RACE experiments in *B. subtilis* strain SSB320, an RNase Z-deficient strain that accumulates ptRNA transcripts with CCA-less 3'-extensions. We could demonstrate 5'-end maturation of such ptRNAs by RNase P *in vivo*, documenting that the presence of 3'-CCA is not an absolute requirement for catalysis by *B. subtilis* RNase P *in vivo*. We propose that the lethal phenotype of the *B. subtilis rnpB*C258 and *rnpB*C259 mutant alleles results from a global deterioration of tRNA 5'-end maturation.

Results

Complementation studies in *B. subtilis*

The *B. subtilis rnpB* mutant strain SSB318 was employed to investigate the *in vivo* role of the tRNA 3'-CCA interaction with type B RNase P RNA. In strain SSB318, the chromosomal *rnpB* gene is under the control of an IPTG-inducible P_{spac} promoter (Wegscheid *et al*, 2006). In the absence of IPTG, cell growth depends on the presence of a functional *rnpB* gene provided on a plasmid (pHY300 derivatives in our study). Complementation was assayed for *B. subtilis* wt RNase P RNA (*rnpB*wt), and the C258 or C259 mutant alleles (*rnpB*C258, *rnpB*C259). *B. subtilis rnpB*wt rescued cell growth in the absence of IPTG, as expected, no matter if expressed from the native *B. subtilis rnpB* promoter (Wegscheid *et al*, 2006) or the xylose-inducible P_{xyl} promoter (Table I). Even basal expression of P_{xyl} under repressed conditions (medium supplemented with glucose instead of xylose) sufficed for cell growth. In contrast, with complementation plasmids encoding *B. subtilis rnpB*C258 and *rnpB*C259 under control of the native *B. subtilis rnpB* promoter we could not get a single transformant in strain SSB318. For the *rnpB*C259 allele, some transformants were obtained after substituting the native for the P_{xyl} promoter; for some clones, we could indeed confirm the mutant *rnpB*C259 genotype by sequencing, whereas others turned out to be revertants to *rnpB*wt. However, cells expressing *rnpB*C259 had a lethal phenotype in the absence of IPTG, which may explain our severe cloning problems. We could not isolate a single colony expressing C258 P RNA.

Simultaneous overexpression of *B. subtilis rnpA*

We recently reported increased viability of *E. coli* cells expressing the *E. coli rnpB*C293 mutant gene when simultaneously overexpressing the homologous P protein (Wegscheid & Hartmann, 2006). We thus transformed *B. subtilis* SSB318 cells with plasmids encoding the *B. subtilis rnpA* gene and either *rnpB*wt, *rnpB*C258 or *rnpB*C259, with both *rnpA* and *rnpB* alleles under control of the xylose promoter. In the presence of xylose, conditions which fully induced *rnpA* expression, cell viability in the absence of IPTG could indeed be substantially improved for cells expressing *rnpB*C258 or *rnpB*C259. For *rnpB*C259 basal expression of the P_{xyl} promoter (in the absence of xylose) supported (retarded) growth of SSB318 cells in the absence of IPTG. In contrast, for *rnpB*C258 full induction of the xylose promoter was required, with growth somewhat retarded relative to *rnpB*wt and *rnpB*C259 (Table I). In conclusion, P protein overexpression restored growth of bacteria expressing the *rnpB* mutant alleles, but fitness did not fully reach that of bacteria expressing the *rnpB*wt allele. To demonstrate that *rnpA*-related rescue effects were due to higher expression levels of the *B. subtilis* P protein and not unspecific effects caused by the presence of additional copies of the *rnpA* gene, we also tested complementation with an *rnpA* gene with two stop codons in its 5’-portion (*rnpA*-stop) and thus directing expression of a truncated inactive protein (Gößringer *et al*, 2006). However, *rnpA*-stop expression was unable to restore growth of SSB318 bacteria expressing *rnpB*C258 or *rnpB*C259 (Table I). Our findings document a lethal phenotype associated with point mutations at G258 and G259 in L15 of *B. subtilis* P RNA. However, concomitant overexpression of the P protein (also verified by Western blot analysis, data not shown) largely rescued cell viability. Furthermore, the phenotype was more severe for the C258 than C259 mutant RNA.

Table I. Homologous complementation of *B. subtilis* RNase P mutant strain SSB318 by *B. subtilis rnpB* wild-type and mutant alleles.

rnpB variants in pHY300	+ IPTG	- IPTG	aldose
B. subtilis P$_{\mathit{Bs\ rnpB}}$ *rnpB*wt	+ + +	+ + +	none
B. subtilis P$_{\mathit{Bs\ rnpB}}$ *rnpB*C258	1)		none
B. subtilis P$_{\mathit{Bs\ rnpB}}$ *rnpB*C259	1)		none
B. subtilis P$_{\mathrm{xyl}}$ *rnpB*wt	+ + +	+ + + 2)	xylose or glucose
B. subtilis P$_{\mathrm{xyl}}$ *rnpB*C258	1)		
B. subtilis P$_{\mathrm{xyl}}$ *rnpB*C259	+ + +	-	xylose
B. subtilis P$_{\mathrm{xyl}}$ *rnpB*wt + P$_{\mathrm{xyl}}$ *rnp*A	+ + +	+ + +	xylose
B. subtilis P$_{\mathrm{xyl}}$ *rnpB*C258 + P$_{\mathrm{xyl}}$ *rnp*A	+ + +	+ + (+)3)	xylose
B. subtilis P$_{\mathrm{xyl}}$ *rnpB*C259 + P$_{\mathrm{xyl}}$ *rnp*A	+ + +	+ + +4)	xylose
B. subtilis P$_{\mathrm{xyl}}$ *rnpB*wt + P$_{\mathrm{xyl}}$ *rnp*A-stop	+ + +	+ + +	xylose
B. subtilis P$_{\mathrm{xyl}}$ *rnpB*C258 + P$_{\mathrm{xyl}}$ *rnp*A-stop	+ + +5)	-	xylose
B. subtilis P$_{\mathrm{xyl}}$ *rnpB*C259 + P$_{\mathrm{xyl}}$ *rnp*A-stop	+ + +	-	xylose
pHY300	+ + +	-	xylose
pHY300 + P$_{\mathrm{xyl}}$ *rnpA*	+ + +	-	xylose
pHY300 + P$_{\mathrm{xyl}}$ *rnpA*-stop	+ + +	-	xylose

Growth of mutant strain SSB318 transformed with wild-type *B. subtilis rnpB* (*rnpB*wt) and mutant (*rnpB*C258, *rnpB*C259) alleles on plasmid pHY300; promoter types: P$_{\mathit{Bs\ rnpB}}$, native *B. subtilis rnpB* promoter; P$_{\mathrm{xyl}}$, inducible xylose promoter; *B. subtilis rnpA* was ovrexpressed in parallel from the same plasmid as indicated; *rnpA*-stop designates the *B. subtilis rnpA* gene with two stop codons in the 5'-coding region. Cell growth was analyzed on LB plates (with appropriate antibiotics) in the presence (1 mM) or absence of IPTG; an aldose (xylose or glucose) at 2% (w/v) was added where indicated.

+ + +: growth with equal numbers of colonies on +/- IPTG plates

-: no growth;

1) unable to construct

2) basal expression of xylose promoter (in the presence of 2% glucose) is sufficient for cell growth in the absence of IPTG

3) basal expression of xylose promoter (in the presence of 2% glucose) is not sufficient for cell growth in the absence of IPTG

4) basal expression of xylose promoter (in the presence of 2% glucose) is sufficient for cell growth in the absence of IPTG, but retarded cell growth

5) here we succeeded to isolate a single colony with a stable *rnpB*C258 genotype; however, the majority of SSB318 cells transformed with *rnpB*C258 were still unstable and tended to form revertants to the wild-type, most likely by recombination with the chromosomal *rnpB*wt gene.

Complementation with *S. aureus* P RNA

The heterologous type B RNA from *S. aureus* was included in our complementation analysis to be able to generalize the findings on the CCA interaction of type B RNase P RNAs. Residues G238 and G239 in *S. aureus* P RNA correspond to G258 and G259 of *B. subtilis* P RNA (Fig. 1 A, B). Whereas *S. aureus rnpB*wt was fully functional in *B. subtilis*, the mutant alleles *rnpB*C238/C239 resulted in a significant growth defect, though not being lethal (Table II). This was also confirmed by monitoring growth curves in liquid culture (Fig. 2). Here, the phenotypes of *rnpB*C238 and *rnpB*C239 were very similar, thus deviating from the observation that the *B. subtilis rnpB*C258 allele was more deleterious than *rnpB*C259 (see above). The growth defect caused by the *S. aureus rnpB*C238/239 mutant alleles could be completely rescued by overexpression of *B. subtilis rnpA* (Table II).

Table II. Heterologous complementation of *B. subtilis* RNase P mutant strain SSB318 by *S. aureus* (type B) and *E. coli* (type A) *rnp*B alleles

rnpB variants in pHY300	+ IPTG	- IPTG	aldose
S. aureus P$_{Bs\ rnpB}$ *rnpB*wt	+ + +	+ + +	none
S. aureus P$_{Bs\ rnpB}$ *rnpB*C238	+ + +	+	none
S. aureus P$_{Bs\ rnpB}$ *rnpB*C239	+ + +	+	none
S. aureus P$_{Bs\ rnpB}$ *rnpB*wt + P$_{xyl}$ *rnp*A	+ + +	+ + +	xylose
S. aureus P$_{Bs\ rnpB}$ *rnpB*C238 + P$_{xyl}$ *rnp*A	+ + +	+ + +	xylose
S. aureus P$_{Bs\ rnpB}$ *rnpB*C239 + P$_{xyl}$ *rnp*A	+ + +	+ + +	xylose
E. coli P$_{Ec\ rnpB}$ *rnpB*wt	+ + +	+ + +	none
E. coli P$_{Ec\ rnpB}$ *rnpB*C292	+	-	none
E. coli P$_{Ec\ rnpB}$ *rnpB*C293	+	-	none
E. coli P$_{Ec\ rnpB}$ *rnpB*wt + P$_{xyl}$ *rnp*A	n. d.		
E. coli P$_{Ec\ rnpB}$ *rnpB*C292 + P$_{xyl}$ *rnp*A	+	-	xylose
E. coli P$_{Ec\ rnpB}$ *rnpB*C293 + P$_{xyl}$ *rnp*A	+	-	xylose

Growth of mutant strain SSB318 transformed with wild-type *S. aureus or E. coli rnpB* (*rnpB*wt) and respective mutant alleles on plasmid pHY300; promoter types: P$_{Bs\ rnpB}$, native *B. subtilis rnpB* promoter; P$_{Ec\ rnpB}$, native *E. coli rnpB* promoter; P$_{xyl}$, inducible xylose promoter; *B. subtilis rnpA* was overexpressed in parallel from the same plasmid as indicated. Cell growth was analyzed on LB plates in the presence (1 mM) or absence of IPTG; the aldose xylose was added to 2% (w/v) for pHY300 derivatives encoding *B. subtilis rnpA*.

+ + +: growth with equal numbers of colonies on +/- IPTG plates;
+: retarded cell growth;
-: no growth;
n. d.: not determined

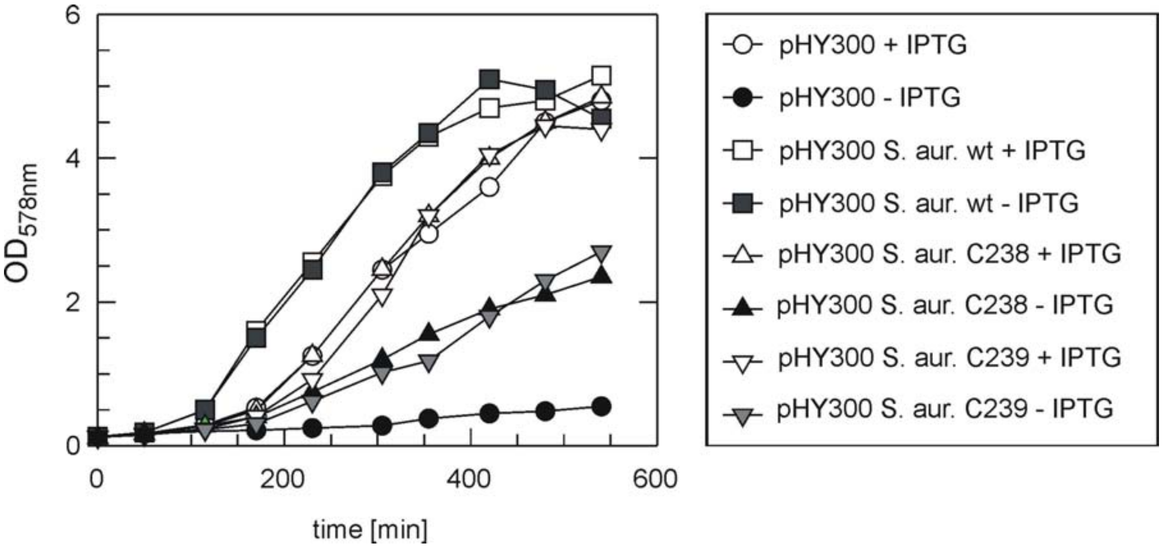

Fig. 2. Growth curves of SSB318 cells complemented with pHY300 derivatives, carrying *S. aureus rnpB*wt (squares) or *rnpB*C238 (triangles with apex at the top) or *rnpB*C239 (triangles with apex at the bottom) mutant alleles in the presence (+) or absence (-) of IPTG.

Complementation with *E. coli* P RNA

We have recently shown that *E. coli* P RNA (type A) can functionally replace *B. subtilis* P RNA (type B) *in vivo*, no matter if *E. coli rnpB*wt was expressed from its own native or from the *B. subtilis rnpB* promoter, and even a single copy of *E. coli rnpB*wt integrated into the *amyE* site of the *B. subtilis* chromosome was sufficient for cell viability (Wegscheid *et al*, 2006). Since the *S. aureus rnpB*C238/C239 mutant alleles displayed a somewhat relaxed phenotype relative to *B. subtilis rnpB*C258/C259, we also tested function of the corresponding *E. coli* mutant alleles (*rnpB*C292/C293) in the *B. subtilis* background of strain SSB318. The *E. coli* mutant alleles were unable to restore growth under non-permissive conditions (without IPTG, Table II). Even when co-expressed with *B. subtilis rnpB* (in the presence of IPTG), the *E. coli rnpB*C292/C293 mutant alleles impaired cell growth; overexpression of *B. subtilis rnpA* did not rescue this growth defect (Table II).

Overexpression of *rnpA* – effect on P RNA levels

The complementation results shown in Tables I and II revealed a rescue of the *B. subtilis rnpB*C258/C259 and *S. aureus rnpB*C238/C239 mutant phenotypes when the *B. subtilis* P protein was overexpressed. One explanation may be that higher levels of P protein increase the steady-state level of RNase P holoenzyme, thereby alleviating the processing defects caused by the mutant alleles. To test this possibility, we used SSB318 bacteria expressing the *S. aureus rnpB* mutant alleles, because here the rescue by *rnpA* overexpression was complete, reducing the risk that spontaneous mutant bacteria might have dominated the liquid cultures. PCR reactions were limited to 12 cycles, because under these conditions product yields were essentially linearly dependent on RNA template amounts (Fig. 3, lanes 25 to 30). The mRNA for ribosomal protein S18 served as the control to be able to assess experimental fluctuations. Overexpression of *rnpA* caused, on average, a 3 to 5-fold increase in the yields for the P RNA-specific product, independent of whether bacteria expressed the *rnpB*wt or one of the mutant alleles (Fig. 3, lanes 1 to 12). No increase in the S18-specific RT-PCR product was observed upon overexpression of *rnpA* (lanes 13 to 24). The results demonstrate that overexpression of the P protein results in an increase in the steady-state levels of P RNA, and thus RNase P holoenzyme, which explains the observed rescue effects (Tables I and II). The data of Fig. 3 further document indistinguishable cellular levels of wt and mutant P RNAs.

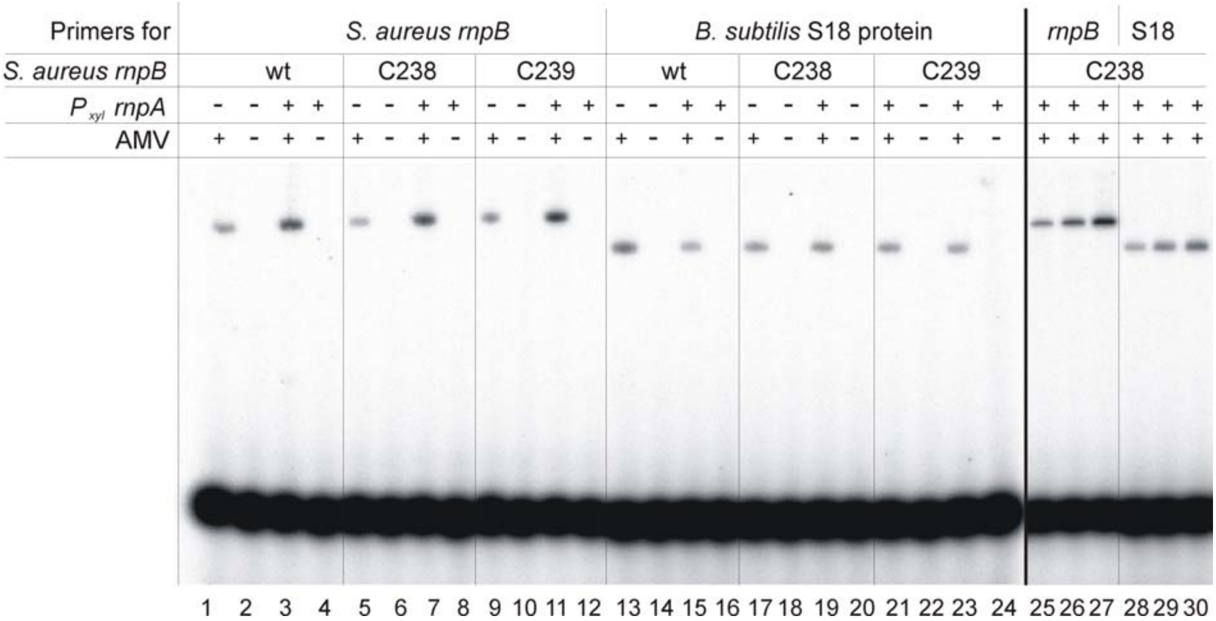

Fig. 3. Radioactive reverse transcription PCR (RT-PCR) analysis of strain SSB318 complemented with *S. aureus rnpB*wt or *rnpB*C238/C239. PCR products were analyzed on a 10% polyacrylamide/8 M urea gel. Lanes 1–30: total RNA from SSB318 complemented with *S. aureus rnpB*wt (lanes 1-4 and 13-16), *rnpB*C238 (lanes 5-8, 17-20 and 25-30) or *rnpB*C239 (lanes 9-12 and 21-24) grown at 37°C in the absence of IPTG and in the presence of 2% xylose (w/v); amounts of total RNA were 200 ng in lanes 1 –24, 26 and 29, 100 ng in lanes 25 and 28, and 400 ng in lanes 27 and 30. P_{xyl} *rnpA*: + or – indicates the presence (+) or absence (–) of an xylose-inducible, plasmid-encoded *B. subtilis rnpA* gene. Lanes 1-12 and 25-27: primers specific for *S. aureus rnpB (rnpB)*; lanes 13-24 and 28-30: primers specific for the mRNA encoding *B. subtilis* ribosomal protein S18 (S18). AMV: + or – indicates the presence (+) or absence (-) of reverse transcriptase. For details on RT-PCR, see Material and methods. Lanes 25-30 document that the amount of RT-PCR product was sensitive to RNA template concentration.

In vitro processing of ptRNA by *B. subtilis* RNase P holoenzymes

To shed light on the nature of the *in vivo* defect of the C258/C259 mutant P RNAs, we analyzed the kinetics of *B. subtilis* RNase P holoenzymes assembled *in vitro*. The rescue effect observed when the *B. subtilis* P protein was overexpressed (Table I) pointed, among several possibilities, to a protein affinity defect of the mutant P RNAs. We thus tested the activity of *B. subtilis* wt and mutant holoenzymes as a function of P protein concentration. We applied a buffer system which has been used for *B. subtilis* holoenzyme kinetics, containing 10 mM $MgCl_2$, 50 mM Mes pH 6.0 and 100 mM KCl (referred to as buffer F10; adapted from Day-Storms *et al*, 2004). Surprisingly, activities were indistinguishable for the wt and mutant holoenzymes at all P protein concentrations (Fig. 4). We then decreased the Mg^{2+} concentration to 2 mM (buffer F2), assuming that this more closely mimics the intracellular free Mg^{2+}-concentration (1 to 2 mM; Alatossava *et al*, 1985). Now the two mutant holoenzymes were more than 100-fold less active than wt RNase P (Table III) when acting on $ptRNA^{Gly}$ with a canonical 3'-CCA terminus (termed ptRNAwt in the following). However, combining the C259 enzyme with the mutant substrate ptRNAG74 restoring base pairing to the C259 P RNA resulted in cleavage efficiencies as good as for the wt enzyme acting on ptRNAwt, whereas the wt and C258 enzymes cleaved ptRNAG74 at a more than 100-fold decreased rate. Likewise, the C258 mutant enzyme performed best with ptRNAG75 as the substrate, but the improvement in catalytic performance was only two- to sixfold (Table III). This indicated that nt 258 and 259 indeed form Watson-Crick base pairs with C75 and C74 of tRNA 3'-CCA. However, only the isosteric C259-G74 pair, but not the C258-G75 pair, in the E-S complex fully restored activity to that of wt complexes, illustrating the importance of G258 identity. A rescue of activity in the presence of the ptRNAG74 substrate was also observed for chimeric holoenzymes composed of the *B. subtilis* P protein and the *S. aureus* C239 mutant P RNA partially purified from SSB318 bacteria (data not shown).

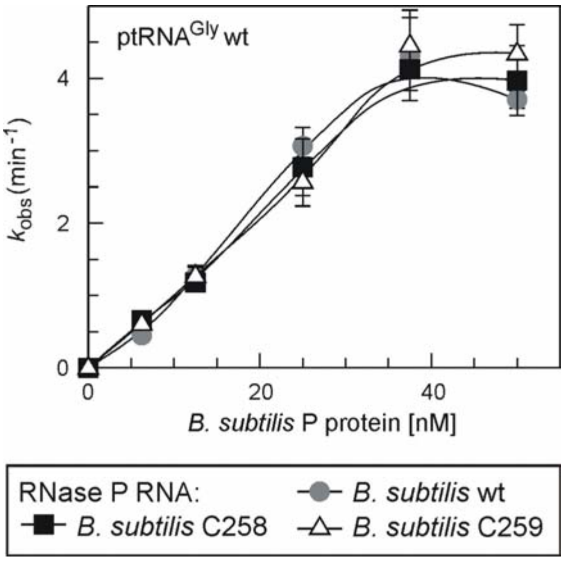

Fig. 4. Activity of *in vitro* reconstituted *B. subtilis* RNase P wt and mutant holoenzymes as a function of protein concentration; k_{obs} is given as nmol substrate converted per nmol of RNase P RNA per min; assay conditions: 50 mM Mes pH 6.1, 100 mM KCl and 10 mM $MgCl_2$; P RNA concentration was 20 nM, protein concentration as indicated and ptRNAwt concentration was 200 nM, including trace amounts (< 1 nM) of 5'-endlabeled substrate.

Table III. Cleavage activity of *B. subtilis* wt and mutant RNase P holoenzymes acting on ptRNA^{Gly} wt and G74 or G75 mutant substrates at 2 mM Mg^{2+} and two protein concentrations

RNase P RNA	ptRNA^{Gly}	*B. subtilis* P protein [nM]	k_{obs}
B. subtilis wt	wt	37.5	0.18 ± 0.03
B. subtilis wt	wt	62.5	0.20 ± 0.04
B. subtilis C258	wt	37.5	$(4.0 \pm 2.0) \times 10^{-4}$
B. subtilis C258	wt	62.5	$(1.3 \pm 0.5) \times 10^{-3}$
B. subtilis C259	wt	37.5	$(5.0 \pm 1.0) \times 10^{-4}$
B. subtilis C259	wt	62.5	$(1.6 \pm 0.9) \times 10^{-3}$
B. subtilis wt	G74	37.5	$(7.0 \pm 1.0) \times 10^{-4}$
B. subtilis wt	G74	62.5	$(1.3 \pm 0.3) \times 10^{-3}$
B. subtilis C258	G74	37.5	$(2.0 \pm 1.0) \times 10^{-4}$
B. subtilis C258	G74	62.5	$(3.0 \pm 2.0) \times 10^{-4}$
B. subtilis C259	G74	37.5	0.15 ± 0.006
B. subtilis C259	G74	62.5	0.30 ± 0.04
B. subtilis wt	G75	37.5	$(3.0 \pm 1.0) \times 10^{-4}$
B. subtilis wt	G75	62.5	$(4.0 \pm 3.0) \times 10^{-4}$
B. subtilis C258	G75	37.5	$(6.0 \pm 4.0) \times 10^{-4}$
B. subtilis C258	G75	62.5	$(1.8 \pm 0.2) \times 10^{-3}$
B. subtilis C259	G75	37.5	$(1.0 \pm 1.0) \times 10^{-4}$
B. subtilis C259	G75	62.5	$(5.0 \pm 0.1) \times 10^{-4}$

Assay conditions: 50 mM Mes pH 6.1, 100 mM KCl, 2 mM $MgCl_2$; RNase P RNA concentration was 20 nM, protein concentration as indicated and substrate concentration was 200 nM. 5’-endlabelled substrate was added in trace amounts. (< 1 nM).
k_{obs} is given in nmol substrate converted per nmol of RNase P RNA per min; values are based on at least three independent experiments.

In vitro processing of ptRNA by *B. subtilis* holoenzymes in a buffer assumed to closely mimic intracellular conditions

We recently showed (Wegscheid & Hartmann, 2006) for *E. coli* P RNA that folding of the catalytic RNA may be incomplete in low Mg^{2+} buffers, such as buffer F2 (Table III). However, a buffer originally optimized for ribosome function (buffer KN, see Material and methods) and containing spermine and spermidine appears to favour formation of a native fold (Wegscheid & Hartmann, 2006). We therefore tested activity of the wt and mutant *B. subtilis* holoenzymes in buffer KN at two different Mg^{2+} concentrations (2 and 4.5 mM, KN2 and KN4.5). At 4.5 mM Mg^{2+}, the mutant enzymes cleaved ptRNAwt at almost identical (C259) or two-fold reduced (C258) rates. However, at 2 mM Mg^{2+}, the rate dropped two-fold for the wt enzyme, but about six-fold for the mutant enzymes (Table IV). Thus, the minor shift from 4.5 to 2 mM Mg^{2+} exacerbated the defect of the mutant enzymes. To analyze if the defect was on the level of substrate affinity or holoenzyme stability, we tested processing activity under the same conditions but at a fivefold higher holoenzyme concentration (Table IV). If substrate binding or holoenzyme stability were the major defect in reactions catalyzed by the C258/C259 mutant enzymes at 2 mM Mg^{2+}, one would have expected that the ratio of cleavage rates for the mutant enzyme versus wt enzymes (k_{rel}, Table IV) improves at the higher enzyme concentration. However, k_{rel} values rather showed a tendency to further decrease (0.12 and 0.13 versus 0.17 and 0.30, Table IV).

We also analyzed cleavage of ptRNAG74 by the C259 mutant enzyme in buffer KN2 (Table IV). This fully restored the cleavage rate to that of the wt enzyme, in line with the results of Table III.

Table IV. Cleavage rates for *B. subtilis* holoenzymes and *E. coli* hybrid holoenzymes reconstituted *in vitro* at low Mg^{2+} concentrations.

RNase P RNA	$ptRNA^{Gly}$	enzyme concentration	$[Mg^{2+}]$	k_{obs}	k_{rel}
B. subtilis wt	wt	10 nM P RNA/37 nM RnpA	4.5	9.7 ± 0.08	1.0
B. subtilis C258	wt	10 nM P RNA/37 nM RnpA	4.5	4.4 ± 0.08	0.45
B. subtilis C259	wt	10 nM P RNA/37 nM RnpA	4.5	8.4 ± 0.12	0.87
B. subtilis wt	wt	10 nM P RNA/37 nM RnpA	2.0	4.6 ± 0.09	1.0
B. subtilis C258	wt	10 nM P RNA/37 nM RnpA	2.0	0.8 ± 0.01	0.17
B. subtilis C259	wt	10 nM P RNA/37 nM RnpA	2.0	1.4 ± 0.03	0.30
B. subtilis C259	G74	10 nM P RNA/37 nM RnpA	2.0	6.5 ± 0.08	
B. subtilis wt	wt	50 nM P RNA/185 nM RnpA	2.0	47.7 ± 0.68	1.0
B. subtilis C258	wt	50 nM P RNA/185 nM RnpA	2.0	5.9 ± 0.07	0.12
B. subtilis C259	wt	50 nM P RNA/185 nM RnpA	2.0	6.2 ± 0.05	0.13
E. coli wt	wt	10 nM P RNA/37 nM RnpA	4.5	6.3 ± 0.02	1.0
E. coli C292	wt	10 nM P RNA/37 nM RnpA	4.5	2.3 ± 0.05	0.37
E. coli C293	wt	10 nM P RNA/37 nM RnpA	4.5	7.3 ± 0.08	1.16
E. coli wt	wt	10 nM P RNA/37 nM RnpA	2.0	7.3 ± 0.12	1.0
E. coli C292	wt	10 nM P RNA/37 nM RnpA	2.0	0.5 ± 0.01	0.07
E. coli C293	wt	10 nM P RNA/37 nM RnpA	2.0	1.9 ± 0.02	0.26
E. coli wt	wt	50 nM P RNA/185 nM RnpA	2.0	26.8 ± 0.41	1.0
E. coli C292	wt	50 nM P RNA/185 nM RnpA	2.0	1.5 ± 0.03	0.06
E. coli C293	wt	50 nM P RNA/185 nM RnpA	2.0	3.5 ± 0.02	0.13

Assay conditions: 20 mM Hepes pH 7.4 (37°C), 2 mM $Mg(OAc)_2$, 150 mM NH_4OAc, 2 mM spermidine, 0.05 mM spermine, 4 mM ß-mercaptoethanol, and RNase P RNA (P RNA) and *B. subtilis* RNase P protein (RnpA) concentrations as indicated; the substrate concentration was 100 nM; 5'-endlabeled substrate was added in trace amounts (< 1 nM); k_{obs} is given in nmol substrate converted per nmol of RNase P RNA per min; k_{rel} is defined as the ratio of k_{obs} obtained with wt versus mutant holoenzymes under the respective conditions; values are based on at least four independent experiments.

Activity assays performed with chimeric holoenzymes consisting of *E. coli* P RNA (wt and the corresponding C292/C293 mutant variants) and the *B. subtilis* P protein (Table IV, lower part) resulted in essentially the same findings as with the *B. subtilis* holoenzymes.

Analysis of *B. subtilis* P RNA folding equilibria

Incomplete (Zarrinkar *et al*, 1996) or aberrant folding might have contributed to the *in vivo* and *in vitro* phenotypes of the C258/C259 mutant P RNAs. To address this possibility, we performed a native PAGE analysis using the same buffer systems as for the kinetic experiments. When 5'-endlabeled wt, C258 or C259 P RNAs were directly loaded (after gel purification and ethanol precipitation) onto the native gel without a preincubation step, two major bands appeared under all four tested conditions, which we termed I_1 and I_2 (Fig. 5, lanes 1 to 3). We are aware that I_1 and I_2 observed in the presence of 2 mM Mg^{2+} during electrophoresis may not necessarily identical to those seen at 10 mM Mg^{2+}. Upon RNA preincubation at 37°C or 55°/37°C, a faster migrating conformer appeared, which we assign to the native fold (termed "N"), in line with a previous study (Buck *et al*, 2005). Remarkably, in buffer F2 (2 mM Mg^{2+}) the N conformer was much less populated in the case of the two mutant relative to the wt P RNA (Fig. 5, lanes 4 to 12). This difference was largely reduced in buffer KN2. When preincubation was performed in buffers F10 and KN4.5 (10 and 4.5 mM Mg^{2+}, respectively) and native PAGE at 10 mM Mg^{2+}, differences between wt and mutant P RNAs were further mitigated (lanes 4 to 9) and essentially abolished after preincubation at 55°/37°C (lanes 10 to 12). No substantial changes were seen when the P protein was added to the preincubation mix (lanes 4 to 6 versus 7 to 9). In summary, our native PAGE analysis indicates that (i) the KN2 buffer containing spermine and spermidine favours formation of the native fold relative to the F2 buffer and (ii) folding differences can be considered insignificant in buffer KN4.5 combined with our standard preincubation (5 min at 55°C, 50 min at 37°C). The data in Fig. 5 illustrate that the folding equilibria of wt and C258/C259 mutant RNase P RNAs are sensitive to the buffer conditions. As we do not know the exact ionic milieu *in vivo*, we cannot rule out a contribution from impaired folding of the mutant P RNAs to their growth defect *in vivo*.

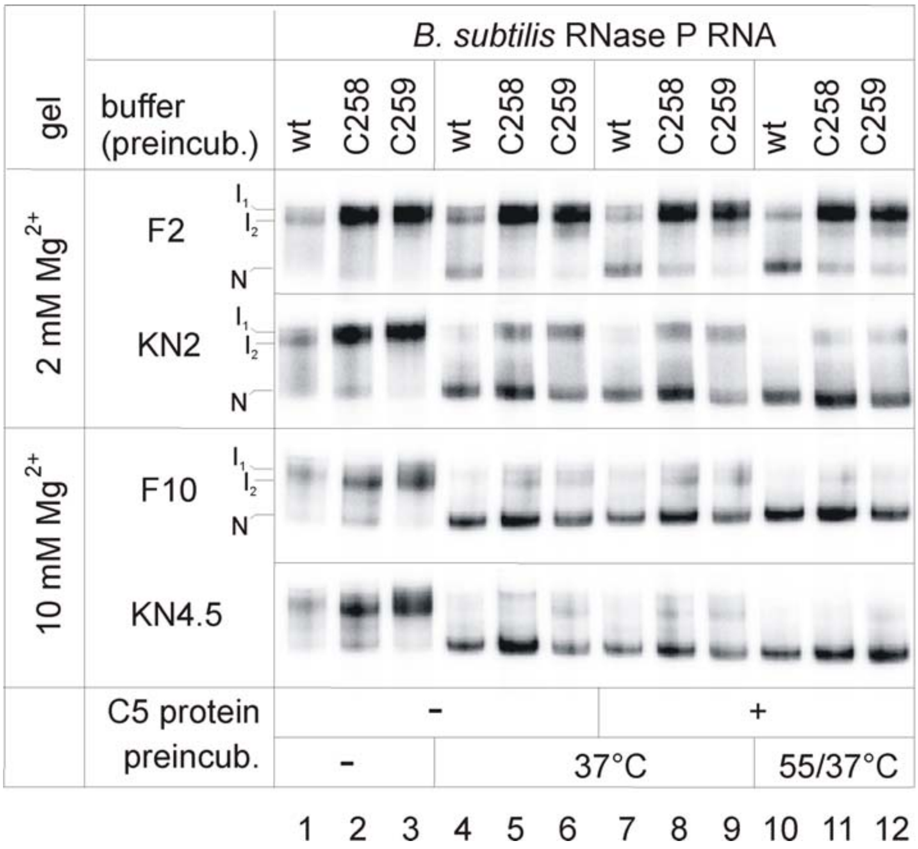
B. subtilis RNase P RNA
gel
buffer (preincub.)
wt
C258
C259
wt
C258
C259
wt
C258
C259
wt
C258
C259
2 mM Mg2+
F2
I1
I2
N
KN2
I1
I2
N
10 mM Mg2+
F10
I1
I2
N
KN4.5
C5 protein
preincub.
-
+
-
37°C
55/37°C
1
2
3
4
5
6
7
8
9
10
11
12

Fig. 5. Analysis of folding equilibria for wt and C258/C259 mutant *B. subtilis* P RNAs by native PAGE. RNAs (50 fmol, 5'-endlabeled) were preincubated either in buffer F containing 2 mM (F2) or 10 mM (F10) Mg^{2+}, or in buffer KN containing 2 mM (KN2) or 4.5 mM (KN4.5) Mg^{2+} in a volume of 4 to 5 µl (for buffer F and KN compositions, see Materials and methods). Lanes 1 to 3: no preincubation (kept at 4°C); lanes 4 to 6: preincubation of P RNAs for 70 min at 37°C; lanes 7 to 9: preincubation of P RNAs for 55 min at 37°C, addition of 1 µl *B. subtilis* C5 protein (final concentration 37 nM) and further incubation for 15 min at 37°C; lanes 10 to 12: as in lanes 7 to 9, but preincubation of P RNAs for 5 min at 55°C and 50 min 37°C. Samples were run on 11.25% polyacrylamide gels in 1 x THE buffer supplemented with 100 mM NH_4OAc and either 2 mM (F2, KN2) or 10 mM (F10, KN4.5) $MgCl_2$.

Processing of CCA-less ptRNAs

Since in *B. subtilis* only one-third of the tRNA genes encode 3'-CCA, the question arose whether tRNA transcripts not encoding 3'-CCA have to undergo 3'-end processing and CCA addition before 5'-end maturation by RNase P can occur. To address this question, we constructed $ptRNA^{Gly}$ 3'-variants, either encoding 3'-U_{73}**CCA**AUA, 3'-U_{73}**UAA**AUA or lacking CCA (3'-U_{73} = ΔCCA); UAA instead of CCA downstream of the discriminator base is found in the native *B. subtilis trnI-Thr* precursor (Pellegrini *et al*, 2003). Processing of these substrates by wt RNase P was tested in buffer KN, either at 4.5 or 2 mM Mg^{2+}, and for 2 mM Mg^{2+} also at a fivefold higher P RNA and P protein concentration (Table V). The obtained pattern of relative cleavage rates roughly mirror-imaged what we had seen with the

C258/C259 mutant enzymes in Table IV: (i) the cleavage rate was reduced for the UAA and ΔCCA variant, and the ratio of rates for the canonical versus mutant substrates worsened when the Mg^{2+} concentration was reduced from 4.5 to 2 mM; (ii) a fivefold increase in P RNA and protein concentration did not improve performance of the mutant substrates relative to the canonical ptRNA (Table V), suggesting that substrate affinity is not the major cause of the defect.

Table V. Cleavage rates for the *B. subtilis* wild-type RNase P holoenzyme acting on substrates with 3'-end variations at low magnesium concentrations

$ptRNA^{Gly}$	enzyme concentration	$[Mg^{2+}]$	k_{obs}	k_{rel}
U73	10 nM P RNA/37 nM RnpA	4.5	4.3 ± 0.08	0.36
U73UAAAUA	10 nM P RNA/37 nM RnpA	4.5	3.3 ± 0.05	0.28
U73CCAAUA	10 nM P RNA/37 nM RnpA	4.5	11.8 ± 0.15	1.0
U73	10 nM P RNA/37 nM RnpA	2.0	1.5 ± 0.01	0.21
U73UAAAUA	10 nM P RNA/37 nM RnpA	2.0	1.4 ± 0.01	0.2
U73CCAAUA	10 nM P RNA/37 nM RnpA	2.0	7.0 ± 0.04	1.0
U73	50 nM P RNA/185 nM RnpA	2.0	9.5 ± 0.08	0.19
U73UAAAUA	50 nM P RNA/185 nM RnpA	2.0	6.8 ± 0.03	0.13
U73CCAAUA	50 nM P RNA/185 nM RnpA	2.0	49.9 ± 0.43	1.0

For assay conditions, see legend to Table IV; k_{rel} is defined as the ratio of k_{obs} obtained with the wild-type (U73CCAAUA) versus mutant holoenzymes under the respective conditions; values are based on at least four independent experiments.

5'-RACE experiment of trnSL-Ala1 and trnSL-Val2

That processing of the CCA-less substrates was impaired but not abolished *in vitro* posed the question whether this residual activity would suffice for RNase P cleavage of CCA-less tRNA transcripts *in vivo*. This was addressed by 5'-RACE experiments. For this purpose, we used strain SSB320, in which the chromosomal *rnz* gene (encoding RNase Z) is put under control of the IPTG-inducible P_{spac} promoter. In *B. subtilis*, RNase Z is involved in the 3'-maturation of tRNAs lacking an encoded CCA motif. We chose two native tRNAs (*trnSL-Ala1* and *trnSL-Val2*), which were shown to accumulate as 3'-precursors in strain SSB320 when *rnz* expression is decreased (Pellegrini *et al*, 2003). Both tRNAs are transcribed from monocistronic genes with 5'-precursor segments of 8 nt (*trnSL-Ala1*) and 38 nt (*trnSL-Val2*), and both are 3'-extended by their transcription terminator stem-loop (Pellegrini *et al*, 2003; Fig. 6 A). To ensure that only tRNAs with unprocessed 3'-ends were reverse transcribed during 5'-RACE, we designed a primer for reverse transcription whose 5'-proximal and central portion targeted the 3'-precursor sequences (Fig. 6 A). A control experiment performed with RNA from SSB320 cells grown in the presence of IPTG (normal RNase Z expression) did not produce RT-PCR products (Fig. 6 B, lane 3) demonstrating that our primer was specific for the 3'-extended tRNA. Using total RNA isolated from SSB320 cells grown in the absence of IPTG we obtained a prominent 5'-RACE product, roughly corresponding to the size of 5'-matured 3'-precursor tRNA (ca. 110 nt). An additional TAP treatment (to permit RT-PCR of primary transcripts with 5'-triphosphates) did not give rise to an additional RT-PCR product. In the case of inefficient 5'-end processing we would have expected a product extended by 8 nt for tRNA^{Ala1}. To ensure that RT-PCR products corresponded to 5'-matured transcripts, we cloned the main band of Fig. 6 B (lanes 1 and 2) into the pCR2.1-TOPO vector (Invitrogen) and sequenced 5 clones (the same was done for *trnSL-Val2*; data not shown). Sequencing analysis confirmed mature 5'-ends for both tRNAs. This was surprising as we would have anticipated, based on our kinetic *in vitro* results (Table V), to detect at least some 3'-extended tRNA with immature 5'-ends. These results clearly demonstrated that RNase P processing can proceed *in vivo* in the absence of the CCA interaction.

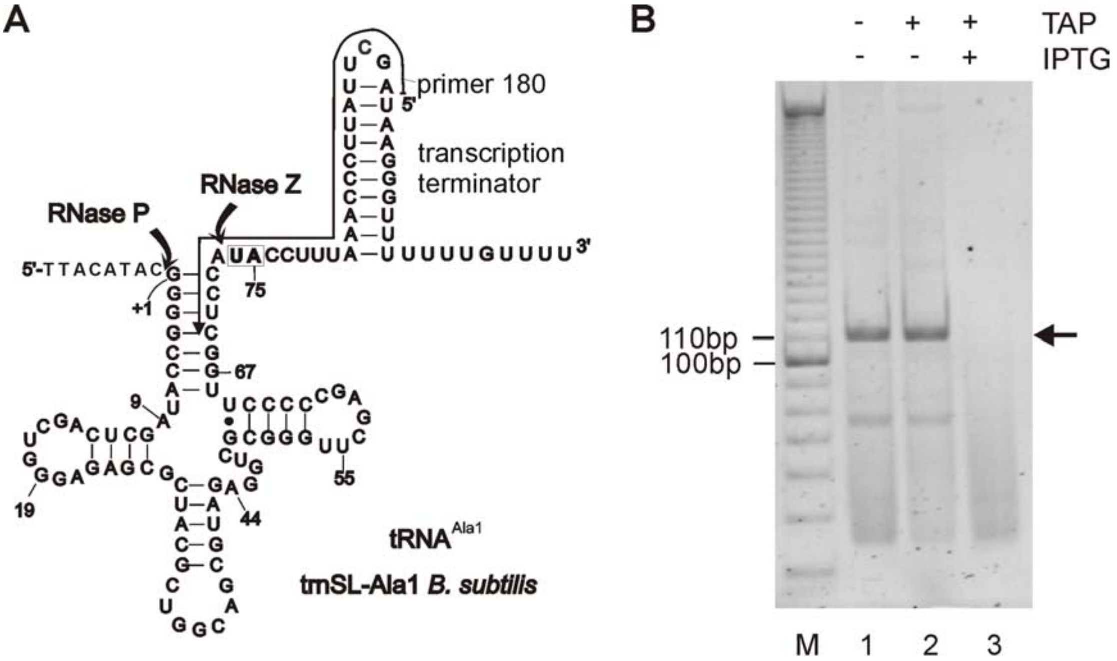

Fig. 6. 5'-RACE analysis of *B. subtilis* trnSL-Ala1 3'-precursors. (**A**) Secondary structure of tRNA^{Ala1} primary transcripts with RNase P and Z cleavage sites indicated; the arrow aligning the transcription terminator and tRNA acceptor stem indicates the position of the primer ("180") used for the 5'-RACE experiment; the boxed nucleotides (U74, A75) are replaced with the two C residues after RNase Z cleavage and CCA addition. (**B**) Analysis of 5'-RACE RT-PCR products on a native 10% PAA gel; M, 10 bp ladder as size marker; the arrow on the right indicates the main amplification product, its size was expected for a processing intermediate with a mature 5'-end but carrying the entire 3'-extension as in the primary tRNA transcripts; this type of product was only detected in total RNA isolated from SSB320 cells grown in the absence of IPTG (lanes 1 and 2), but not in the presence of IPTG (lane 3); before reverse transcription, total RNA preparations were treated (+ TAP) or not treated (- TAP) with Tobacco Acid Pyrophosphatase (TAP).

Discussion

We have investigated the tRNA 3'-CCA interaction with type B RNase P under *in vivo* conditions, using *B. subtilis* mutant strain SSB318 which has the chromosomal *rnpB* gene under control of the IPTG-inducible P_{spac} promoter (Wegscheid *et al*, 2006). For this purpose, complementation efficiencies of *B. subtilis rnpB*wt relative to *rnpB*C258/C259 mutant alleles were analyzed in strain SSB318 under non-permissive conditions (- IPTG). The latter two *rnpB* alleles encode P RNAs with point mutations of the nucleotides thought to be involved in the CCA interaction. We also tested the functionality of *S. aureus rnpB*wt and its mutant *rnpB*C238/C239 alleles (as representatives of an heterologous type B P RNA) and that of the corresponding *E. coli rnpB*C292/C293 alleles representing type A RNase P RNA architecture. All *rnpB*wt alleles (*B. subtilis, S. aureus, E. coli*) were functional in SSB318 bacteria (Tables I and II). However, the mutant P RNA alleles resulted either in a severe growth defect (*S. aureus rnpB*C238/C239) or were even lethal (*B. subtilis rnpB*C258/C259 and *E. coli rnpB*C292/C293; Tables I and II). Until now, it was assumed that the CCA interaction is not critical in reactions catalyzed by type B RNase P holoenzymes (Oh & Pace, 1994). We could confirm this assumption when activity was tested at 10 mM Mg^{2+} (Fig. 4), which has been the "gold standard" magnesium concentration for the testing of bacterial holoenzymes. However, here we demonstrate, for the first time, that the CCA interaction is (i) essential for vitality of *B. subtilis* cells (Tables I and II), (ii) critical *in vitro* at low Mg^{2+} concentrations, such as 2 mM, assumed to better mimic the cellular milieu than 10 mM Mg^{2+}, and (iii) that tRNA 3'-CCA ends form Watson-Crick base pairs with two guanosines in the L15 loop of type B RNase P RNAs. As found for *E. coli* (Wegscheid & Hartmann, 2006), an isosteric C259-G_{74} base pair, but not a C258-G_{75} pair, fully restored catalytic performance of type B RNase P to that of the wt holoenzyme acting on ptRNA with a canonical 3'-CCA end (Tables III and IV). This indicates that the nucleotide identity of the 5'-proximal G residue (G258 in *B. subtilis* and G239 in *S. aureus*) is critical for catalytic performance, as observed for G292 of *E. coli* P RNA (Wegscheid & Hartmann, 2006).

Overexpression of the *B. subtilis* P protein partially or fully (for *S. aureus rnpB* alleles) restored cell viability of bacteria expressing the mutant *rnpB* alleles (Tables I and II). This phenomenon was also observed for the *E. coli* C293 mutant RNA in its natural host (Wegscheid & Hartmann, 2006), but was not scrutinized there. Here we could attribute the rescue to a severalfold increase in P RNA steady-state levels owing to P protein overexpression (Fig. 3). In a study on P RNA metabolism in *E. coli* (Kim *et al*, 2005) it was found that *rnpB* primary transcripts can undergo either 3'-end maturation or oligoadenylation resulting in degradation. A knockout of poly(A) polymerase (*pcnB*) blocked the degradation pathway and consequently increased the level of 3’-precursor P RNA. Since these higher levels of 3’-precursor P RNA did not entail an increase in the level of mature P RNA, the authors proposed that mature RNase P RNA may only stably accumulate when complexed with its protein subunit (Kim *et al*, 2005). Our results in Fig. 3 are consistent with this model, suggesting similar mechanisms to regulate cellular RNase P levels in *E. coli* and *B. subtilis* despite fundamentally different P RNA maturation pathways in the two organisms. Whereas the mature 5’- and 3’-ends of *B. subtilis* P RNA appear to be generated by autolytic processing of precursor P RNA (Loria & Pan, 2000), *E. coli* P RNA primary transcripts are mainly intitiated at the mature 5’-end, and 3’-precursor sequences are removed by RNase E followed by exonucleolytic removal of 1 or 2 additional nucleotides (Lundberg & Altman, 1995; Kim et al, 2005).

The defect of the *B. subtilis* C258/C259 mutant RNAs was exacerbated when the Mg^{2+} concentration was lowered from 4.5 to 2 mM (Table IV). This correlated with some reduction in the fraction of correctly folded P RNA molecules relative to the wt P RNA (Fig. 5). The latter result was surprising as the L15 loop is thought to be quite unstructured in free P RNA based on its low resolution in the X-ray structure of *B. stearothermophilus* P RNA (Kazantsev *et al*, 2005). Although the effect of the two point mutations in L15 on P RNA folding is not understood, this underscores the high sensitivity of P RNA folding to minimal structural changes at low Mg^{2+} concentrations.

In *E. coli*, the P15/L15/P16 region has been identified as a central Me^{2+} binding module in the active site of P RNA (Kufel & Kirsebom, 1998; Brännvall *et al*, 2003). There are sites of prominent Pb^{2+} hydrolysis at two locations in the internal L15 loop (sites III and V). Binding of tRNA 3’-CCA suppresses, *in vitro* and *in vivo*, Pb^{2+} hydrolysis at sites III and V and creates a new prominent Pb^{2+} hydrolysis site (IVb) nearby (Ciesiolka *et al*, 1994; Lindell *et al*, 2005). This indicates a structural rearrangement of the P15/L15/P16 region upon formation of the G292-C_{75} and G293-C_{74} intermolecular base pairs. For *B. subtilis* P RNA, four out of nine prominent Pb^{2+} hydrolysis sites could also be assigned to its apical L15 loop (Zito *et al*, 1993). This combined with the phenotypic similarities of C258/C259 (C292/C293 in *E. coli*) mutations in the *E. coli* and *B. subtilis* systems supports the notion that the L15 loop is a central Me^{2+} binding module in the active site of type B RNAs as well. We thus attribute the deterioration in catalytic performance of the C258/C259 mutant RNAs upon a decrease of $[Mg^{2+}]$ from 4.5 to 2 mM primarily to a defect in binding of catalytically relevant Mg^{2+} to the L15 loop in E-S complexes. As in the *E. coli* system (Wegscheid & Hartmann, 2006), the identity of G258 plays a key role in this process, as an isosteric C258-G_{75} base pair only marginally rescued the defect (Table III). One could argue here that the low activity of mutant holoenzymes at 2 mM Mg^{2+} may have its major cause in the folding defect (Fig. 5). However, the results of Table V argue against this view. When we deleted or mutated 3’-CCA in the substrate and assayed processing by wt RNase P, results were essentially a mirror image of what we had seen with the mutant enzymes acting on ptRNAwt (cf. Table IV and V): catalytic performance of the mutant substrates relative to ptRNAwt deteriorated upon a reduction of [Mg^{2+}] from 4.5 to 2 mM, and the relative catalytic performance of the mutant substrates did not improve at a fivefold P RNA and protein concentration.

Despite the striking similarities in the CCA interaction of type A and B RNase P RNAs, some details are different. For *E. coli* RNase P, a fivefold increase in P RNA and protein concentrations did not increase the cleavage rate for the C293 and C292 mutant enzymes at 2 mM Mg^{2+} (Wegscheid & Hartmann, 2006). In contrast, the *B. subtilis* C258 and C259 mutant enzymes cleaved ptRNAwt at a 4 to 7-fold higher rate when P RNA and protein concentrations were increased fivefold (Table IV). Activity of the chimeric holoenzymes consisting of *E. coli* P RNA and *B. subtilis* P protein also improved 2 to 3-fold at the higher RNase P subunit levels. This may point to a specific effect exerted by the *B. subtilis* P protein, which could be related to the finding that binding of P protein and substrate to P RNA are cooperative in the *B. subtilis* system (Day-Storms *et al*, 2004).

Also, the *in vivo* phenotype of the C258 (*B. subtilis*) and C238 (*S. aureus*) type B mutant P RNAs could be partially (*B. subtilis*; Table I) or fully (*S. aureus*; Table II) rescued by overexpression of *B. subtilis rnpA*. However, in the *E. coli* system essentially no rescue was observed for the corresponding *E. coli* C292 mutant P RNA upon overexpression of *E. coli rnpA* (Wegscheid & Hartmann, 2006). In this context, the better complementation efficiency of mutant *S. aureus* versus *B. subtilis rnpB* alleles was surprising. The *S. aureus rnpB*C238/C239 alleles even enabled some cell growth at normal P protein levels (Table II). This might be related to the general problem associated with studies of homologous genes especially in *B. subtilis* which is known to possess an efficient recombination machinery. The presence of homologous *rnpB* genes carrying point mutations may interfere with genetic repair systems, especially if the mutant genes cause stress to the cells. This may also explain our severe problems to transform SSB318 bacteria with the homologous *B. subtilis rnpB*C258/C259 alleles. Finally, the severeness of phenotypes for *B. subtilis rnpB*C258 and *E. coli rnpB*C292 exceeded that of *B. subtilis rnpB*C259 and *E. coli rnpB*C293, respectively (Tables I and II; Wegscheid & Hartmann, 2006). In contrast, the *in vivo* phenotypes of *S.*

*aureus rnpB*C238 and *rnpB*C239 were indistinguishable (Table II; Fig. 2), which we do not understand at present.

In vitro at 10 mM Mg^{2+} (buffer F10) and increasing P protein concentrations, the reconstituted *B. subtilis* C258 and C259 mutant holoenzymes had activities indistinguishable form the wt enzyme (Fig. 4). Likewise, in buffer KN supplemented with 4.5 mM Mg^{2+}, activity reductions for the mutant holoenzymes were marginal. Only at 2 mM Mg^{2+}, a substantial loss of activity was seen for the mutant enzymes, which correlated with the severe *in vivo* defects. Since the reduction from 4.5 to 2.0 mM Mg^{2+} causes only a very minor decrease in ionic strength and based on equal activities and P protein titration profiles (Fig. 4) of wt and mutant enzymes in buffer F10, we think it unlikely that the major defect of the mutant P RNAs is related to impaired P protein and/or substrate affinity. We rather infer that the L15 loop mutations lower the affinity for catalytically relevant Mg^{2+} ions that either directly contribute to the catalytic process or help to fold the L15-CCA interaction module as part of the active site in E-S complexes.

Our 5'-RACE experiments performed in the RNase Z mutant strain revealed that RNase P cleaves CCA-less ptRNAs *in vivo* (Fig. 6). Since RNase Z, which acts on CCA-less tRNA 3'-precursors, has largely impaired activity on ptRNAs with long 5'-leaders, RNase P cleavage was proposed to precede RNase Z cleavage on CCA-less ptRNAs carrying expanded 5'- in addition to 3'-extensions (Pellegrini *et al*, 2003). Our results verify this hypothesis. The finding that *B. subtilis* RNase P is able to process CCA-less ptRNAs then raises the question why the C258/C259 mutations caused a lethal phenotype in the presence of normal amounts of P protein (Table I). Most likely, the general deceleration in ptRNA maturation kinetics adds up to a collective collapse caused by the incapability of the tRNA biosynthesis machinery to meet the demands of the protein synthesis apparatus. This collapse is mitigated when the steady-state amounts of the RNase P holoenzyme increase severalfold as a result of P protein overproduction. It can also not be ruled out that disruption of the CCA interaction may block 5'-maturation of a subset of ptRNAs more severely than that of the bulk of ptRNAs.

Materials and Methods

Bacteria

B. subtilis strain SSB318 (Wegscheid *et al*, 2006) was used for complementation studies and SSB320 (Pellegrini *et al*, 2003) for 5'-RACE experiments.

Complementation studies in strain SSB318

Recombinant *rnpB*-coding pHY300 derivatives were introduced into SSB318 using the LS/HS-medium protocol as described (Wegscheid *et al*, 2006). Residual IPTG was removed by centrifugation (1 min, 6000 rpm, Eppendorf Minispin) and resuspension of the cells in LB medium. Cells were plated in parallel on LB agar plates with or without 1 mM IPTG and containing 0.5 µg/ml erythromycin, 12.5 µg/ml lincomycin and 30 µg/ml tetracycline (to select for the presence of pHY300). In cases of poor transformation efficiency, cells were first plated exclusively in the presence of IPTG. For plasmids encoding *rnpB* or *rnpA* genes under control of the P_{xyl} promoter, the medium was additionally supplemented with 2% (w/v) glucose or 2% (w/v) xylose. For the construction of complementation plasmids, see Supplementary data.

Growth curve monitoring

B. subtilis SSB318 cells were grown overnight at 37°C in the presence of the appropriate antibiotics and 1 mM IPTG. IPTG was then washed out by repeated centrifugation and resuspension of the cell pellet in LB without IPTG; the final cell pellet was resuspended in LB, adjusted to a starting OD_{578} of 0.05 - 0.1 in 50 mM LB supplemented with the respective antibiotics and grown at 37°C at 180 rpm under aeration (180 rpm in a GFL Shaking Incubator 3033).

In vitro transcription and 5'-endlabeling

T7 runoff transcription and 5'-endlabeling was performed as described (Busch *et al*, 2000). For transcription of ptRNA^{Gly} (and G74 and G75 variants thereof) as well as *E. coli* P RNAs, see Wegscheid & Hartmann (2006). For transcription of *B. subtilis* wt and mutant P RNAs, as well as other mutant substrates (see Table V), see Supplementary data.

Preparation of recombinant RNase P protein

B. subtilis RNase P protein carrying an N-terminal His-tag (His-tagged peptide leader: MRGSHHHHHHGS, encoded in plasmid pQE-30 in *E. coli* JM109) was prepared as described (Wegscheid & Hartmann, 2006).

Processing assays

RNase P holoenzyme kinetics were performed in buffer F (2 or 10 mM $MgCl_2$, 50 mM Mes pH 6.1, 100 mM KCl) or buffer KN (20 mM Hepes-KOH, pH 7.4, 2 or 4.5 mM $Mg(OAc)_2$, 150 mM NH_4OAc, 2 mM spermidine, 0.05 mM spermine and 4 mM β-mercaptoethanol; Dinos *et al*, 2004). *In vitro* reconstitution of RNase P holoenzymes was performed as follows: RNase P RNAs were incubated in the respective buffer for 5 min at 55°C and 50 min at 37°C, after which RNase P protein was added, followed by another 5 min at 37°C before addition of substrate. Processing reactions were started by combining enzyme and substrate solutions (final volume 10 µl) and assayed at 37°C.

Folding analysis by native PAGE

Folding analyses were conducted exactly as described (Wegscheid & Hartmann, 2006).

5'-RACE

SSB320 cells were grown in parallel either in the presence or absence of IPTG to an OD_{578} of 0.6. Total RNA was isolated using the TRIzol (Invitrogen) method. In order to include primary transcripts, one half of total RNA was treated with Tobacco Acid Pyrophosphatase (TAP, Epicentre). Afterwards, the adapter oligonucleotide A1 (5'- GTC AGC AAT CCC TAA GGA G; the three 3'-terminal residues were RNA, the remainder DNA) was ligated to the 5'-monophosphates of RNA molecules. Specific primers were designed to map 3'-unprocessed transcripts of trnSL-Ala1 (primer 180, 5'- TCG AAT AAG GGT TTA AAG GTA TGG AG) and trnSL-Val2 (primer 178, 5'- CTG CGC AAG GGT TTA AGC TAT GAT T). These primers were used in cDNA synthesis and in combination with primer 5'- GTC AGC AAT CCC TAA GGA G (matches the sequence introduced by the adapter oligonucleotide) in the following PCR reaction. PCR products were identified by native 8% PAGE, gel-purified and cloned into pCR2.1-TOPO for sequencing. Five clones were sequenced for each tRNA.

Overexpression of *rnpA* – effect on P RNA levels

To determine *rnpB* expression levels in strain SSB318 complemented with *S. aureus rnpB*wt or *rnpB*C239/C239 as a function of *B. subtilis rnpA* overexpression, cells were grown overnight at 37°C in 3 ml LB medium supplemented with 1 mM IPTG, 12.5 µg/ml lincomycin, 0.5 µg/ml erythromycin and 30 µg/ml tetracycline. IPTG was then washed out by by repeated centrifugation/resuspension of the cell pellet in LB without IPTG; the final cell pellet was then resuspended in LB, and adjusted to a starting OD_{578} of 0.05 to 0.1 in 50 ml LB; antibiotics (see above) and 2% xylose (w/v) were added and cells were grown at 37°C under aeration to an OD_{578} of 0.5 to 0.6. Aliquots of the cell suspensions were then diluted and plated in parallel on four plates (+ xylose, + IPTG / + xylose, - IPTG / + glucose, + IPTG / + glucose, - IPTG) supplemented with antibiotics to verify the original growth phenotype (retarded growth with mutant *rnpB* alleles in the absence of P_{xyl} *rnp*A, Table II). Total RNA from the cultures was prepared using the RNeasy Mini/Midi Kit from Qiagen according to the protocol provided by the manufacturer, followed by DNase I treatment (Turbo DNase, Ambion). RT-PCR was performed with the Access RT-PCR System (Promega). PCR was stopped after 12 cycles within the exponential phase of amplification. Primers specific for *S. aureus rnpB* were 5'- ATT TGG ATT GCT CAC TCG AGG G (5'-endlabeled in Fig. 3) and 5'- GGG TAA TCG CTA TAT TAT ATA GAG G; primers specific for *B. subtilis* ribosomal protein S18 were 5'-ACG TGC GCG TTT GAT CGC TGC A (5'-endlabeled in Fig. 3) and 5'- GCA GAG GCG GTC GTG CGA AA. RT-PCR reactions contained the normal amounts of unlabeled primers, and, in addition, trace amounts of the respective 5'-endlabeled primer.

Acknowledgments

We like to thank Ciaran Condon for providing *B. subtilis* strain SSB320, B. M. Fredrik Pettersson and Leif A. Kirsebom for providing genomic DNA of *S. aureus*, and Michal Marszalkowski for preparation of recombinant *B. subtilis* RNase P protein. This work was supported by the Deutsche Forschungsgemeinschaft (HA 1672/7-4) and the Fonds der Chemischen Industrie.

References

Alatossava T, Jutte H, Kuhn A, Kellenberger E (1985) Manipulation of intracellular magnesium content in polymyxin B nonapeptide-sensitized *Escherichia coli* by ionophore A23187. *J Bacteriol* **162**: 413-419

Brännvall M, Pettersson BMF, Kirsebom LA (2003) Importance of the +73/294 interaction in *Escherichia coli* RNase P RNA substrate complexes for cleavage and metal ion coordination. *J Mol Biol* **325**: 697-709

Buck AH, Dalby AB, Poole AW, Kazantsev AV, Pace NR (2005) Protein activation of a ribozyme: the role of bacterial RNase P protein. *EMBO J* **24**: 3360-3368

Busch S, Kirsebom LA, Notbohm H, Hartmann RK (2000). Differential role of the intermolecular base-pairs G292-C(75) and G293-C(74) in the reaction catalyzed by *Escherichia coli* RNase P RNA. *J Mol Biol* **299**: 941-951

Ciesiolka J, Hardt WD, Schlegl J, Erdmann VA, Hartmann RK (1994) Lead-ion induced cleavage of RNase P RNA. *Eur J Biochem* **219**: 49-56

Day-Storms JJ, Niranjanakumari S, Fierke CA (2004) Ionic interactions between PRNA and P protein in *Bacillus subtilis* RNase P characterized using a magnetocapture-based assay. *RNA* **10**: 1595–1608

Dinos G, Wilson DN, Teraoka Y, Szaflarski W, Fucini P, Kalpaxis D, Nierhaus KH (2004) Dissecting the ribosomal inhibition mechanisms of edeine and pactamycin: the universally conserved residues G693 and C795 regulate P-site RNA binding. *Mol Cell* **13**: 113-24

Evans D, Marquez SM, Pace NR (2006) RNase P: interface of the RNA and protein worlds. *Trends Biochem Sci* **31**: 333-341

Gößringer M, Kretschmar-Kazemir Far R, Hartmann RK (2006) Analysis of RNase P Protein (*rnpA*) Expression in *Bacillus subtilis* Utilizing Strains with Suppressible *rnpA* Expression. *J Bacteriol* **188:** 6816-6823

Guerrier-Takada C, Gardiner K, Marsh T, Pace N, Altman S (1983) The RNA moiety of ribonuclease P is the catalytic subunit of the enzyme. *Cell* **35**: 849-857

Hall TA, Brown JW (2001) The ribonuclease P family. *Methods Enzymol* **341**: 56–77

Hardt WD, Schlegl J, Erdmann VA, Hartmann RK (1995). Kinetics and thermodynamics of the RNase P RNA cleavage reaction: Analysis of tRNA 3´-end variants. *J Mol Biol* **247**: 161-172

Hartmann E, Hartmann RK (2003) The enigma of ribonuclease P evolution. *Trends Genet* **19**: 561-569

Kazantsev AV, Krivenko AA, Harrington DJ, Holbrook SR, Adams PD, Pace NR (2005) Crystal structure of a bacterial ribonuclease P RNA. *Proc Natl Acad Sci USA* **102**: 13392–13397

Kim KS, Sim S, Ko JH, Lee Y (2005) Processing of M1 RNA at the 3' end protects its primary transcript from degradation. *J Biol Chem* **280**: 34667-34674

Kirsebom LA, Svärd SG (1994) Base pairing between *Escherichia coli* RNase P RNA and its substrate. *EMBO J* **13**: 4870-4876

Kufel J, Kirsebom LA (1998) The P15-loop of *Escherichia coli* RNase P RNA is an autonomous divalent metal ion binding domain. *RNA* **4**:777-788

Kurz JC, Niranjanakumari S, Fierke CA (1998) Protein component of *Bacillus subtilis* RNase P specifically enhances the affinity for precursor-tRNAAsp. *Biochemistry* **37**:2393-400

LaGrandeur TE, Huttenhofer A, Noller HF, Pace NR (1994) Phylogenetic comparative chemical footprint analysis of the interaction between ribonuclease P RNA and tRNA. *EMBO J* **13**: 3945-52

Lindell M, Brännvall M, Wagner EG, Kirsebom LA (2005) Lead(II) cleavage analysis of RNase P RNA *in vivo*. *RNA* **11**: 1348-1354

Loria A, Pan T (2000) The 3' substrate determinants for the catalytic efficiency of the Bacillus subtilis RNase P holoenzyme suggest autolytic processing of the RNase P RNA *in vivo*. *RNA* **6**:1413-22

Lundberg U, Altman S (1995) Processing of the precursor to the catalytic RNA subunit of RNase P from *Escherichia coli*. *RNA* **1**:327-34

Oh BK, Pace NR (1994) Interaction of the 3'end of tRNA with ribonuclease P RNA. *Nucleic Acids Res* **22**: 4087-4094

Oh BK, Frank DN, Pace NR (1998) Participation of the 3'-CCA of tRNA in the binding of catalytic Mg^{2+} ions by ribonuclease P. *Biochemistry* **37**: 7277-7283

Pellegrini O, Nezzar J, Marchfelder A, Putzer H, Condon C (2003) Endonucleolytic processing of CCA-less tRNA precursors by RNase Z in *Bacillus subtilis*. *EMBO J* **22**: 4534–4543

Schedl P, Primakoff P, Roberts J (1974) Processing of *E. coli* tRNA precursors. *Brookhaven Symp Biol* **26**: 53–76

Svärd SG, Kagardt U, Kirsebom LA (1996) Phylogenetic comparative mutational analysis of the base-pairing between Rnase P RNA and its substrate. *RNA* **2**: 463-472

Tsai HY, Masquida B, Biswas R, Westhof E, Gopalan V (2003) Molecular modeling of the three-dimensional structure of the bacterial RNase P holoenzyme. *J Mol Biol* **325**: 661-675

Wegscheid B, Condon C, Hartmann RK (2006) Type A and B RNase P RNAs are interchangeable *in vivo* despite substantial biophysical differences. *EMBO Rep* **7**: 411-417

Wegscheid B, Hartmann RK (2006) The precursor tRNA 3'-CCA interaction with *Escherichia coli* RNase P RNA is essential for catalysis by RNase P *in vivo. RNA* **12**: 2135-2148

Zarrinkar PP, Wang J, Williamson JR (1996) Slow folding kinetics of RNase P RNA. *RNA* **2**: 564-573

Zito K, Hüttenhofer A, Pace NR (1993) Lead-catalyzed cleavage of ribonuclease P RNA as a probe for integrity of tertiary structure. *Nucleic Acids Res* **21**:5916-20

Supplementary data

to the manuscript

In vivo role of bacterial type B RNase P interaction with tRNA 3’-CCA

Wegscheid, B., Hartmann, R.K.

Construction of *B. subtilis rnpB* complementation plasmids

For complementation, the *B. subtilis rnpB* wild-type gene (*rnpB*wt) under control of its native *rnpB* promoter and terminator was cloned into pHY300 as described (Wegscheid *et al*, 2006). *B. subtilis* complementation plasmids under control of the xylose repressor (*xylR*) and promoter (P_{xyl}) were constructed in two steps: first, the fragment encoding *xylR* and P_{xyl} was amplified from plasmid pX2 (Mogk *et al*, 1997) using phosphorylated primers "100", 5'-CGC GGA TCC AGG TTT GCT AAC CTT TGC G (introducing a *Bam* HI site, underlined), and "105", 5'-GGG ACA CAT GTT ATC TCA TCA TAT ACA AAA TAA ATG TTT (introducing a *Psc* I and a half *Sma* I site, underlined); the PCR product was cloned into pHY300 cut with *Sma* I and *Bam* HI, resulting in plasmid pHY300 xylRP. *B. subtilis rnpB*wt was amplified from genomic DNA of strain W168 with primer "102", 5'-GAT GAG ATA ACA TGT TCT TAA CGT TCG GGT (introducing a region overlapping with the xylose promoter, underlined, at the 5'-end of *B. subtilis rnpB*), and primer "103", 5'-CGT CCC GGG CTT CAT CGT ATC ACC CTG TC (introducing a *Sma* I site 3'-adjacent to *rnpB*, underlined); the PCR product was cloned into the unique *Psc* I and *Sma* I sites of pHY300 xylRP. This plasmid is referred to as pHY300 *B. subtilis* P_{xyl} *rnpB*wt (Table I). Mutations C258 and C259 were introduced by the site-directed *Dpn* I method according to the manual provided with the QuikChange XL Site-Directed mutagenesis Kit (Stratagene), using the primer pair 5'-TCC GTT AAG AAG GTT CCC CTA C**G**A AAA TTT GGG TTT CTC GCT CGA G and 5'- CTC GAG CGA GAA ACC CAA ATT TT**C** GTA GGG GAA CCT TCT TAA CGG A for the C258 mutation, and 5'-TCC GTT AAG AAG GTT CCC CTA **G**CA AAA TTT GGG TTT CTC GCT CGA G and 5'-CTC GAG CGA GAA ACC CAA ATT TTG **C**TA GGG GAA CCT TCT TAA CGG A for the C259 mutation (introduced point mutations underlined).

For parallel overexpression of the *B. subtilis* RNase P protein, *B. subtilis rnpA* was amplified including the xylose promoter from strain *sb* (Gößringer *et al*, 2006), using primers "115", 5'-CAG GAT CCG ATT TAG TAC ATA GCG AAT CTT ACC, and "116", 5'-CAG GAT CCA ACC AGA AAG GAA GCG C (both introducing a *Bam* HI site, underlined); the PCR product was cloned into the *Bam* HI site of pHY300 *B. subtilis* P_{xyl} *rnpB*(wt, 258 or 259). Constructs with the insert "P_{xyl} *rnpA*-stop" carried point mutations close to the 5'-end of the xylose-inducible *rnpA* gene, resulting in two stop codons; for this purpose, the xylose promoter region was amplified from genomic DNA of strain *sb* (Gößringer *et al*, 2006) with primer "114", 5'- TTT CGC TTC TTC AAA TGA CTC AT, and primer "115" (see above). The *rnpA* gene with the two stop codons was amplified from plasmid p3dstop (Gößringer *et* *al*, 2006) with primer “116” (see above) and primer “113”, 5’- ATG AGT CAT TTG AAG AAG CGA AA. Those two fragments were combined by overlap extension PCR using primers “115” and “116”, and the product was cloned into the *Bam* HI site of pHY300 *B. subtilis* P_{xyl} *rnpB*(wt, 258 or 259).

Construction of *S. aureus rnpB* complementation plasmids

The *S. aureus rnpB* gene was cloned under control of the natural *B. subtilis rnpB* promoter and terminator. For amplification of the *B. subtilis* promoter, we used primer “19”, 5’-GGC AGC AAG CTT TAT GAT TGA TCA C (including the naturally occurring *Hind* III site upstream of the *B. subtilis rnpB* promoter, underlined), and primer “44”, 5’-ATG AAT TAT TAT ATA ACA ACT GAT TAC (covering the 3’-part of the *B. subtilis rnpB* promoter). The *B. subtilis* terminator was amplified using primer “45”, 5’-ACA TTT AAA ATG ATG AAA ACA AGC, and primer “21”, 5’-CGC CCA AGC TTG TGT ATA CTT CTT C (introducing a *Hind* III site, underlined, at the 3’-end of the *B. subtilis rnpB* terminator). *S. aureus rnpB* was amplified from genomic DNA of *Staphylococcus aureus* subsp. *aureus* Rosenbach (ATCC 12600) with primer “42”, 5’-GTA ATC AGT TGT TAT ATA ATA ATT CAT TGA TAT TTT GGG TAA TCG C, and primer “47”, 5’-GCT TGT TTT CAT CAT TTT AAA TGT ACT AGT AGT GAT ATT TCT ATA AGC C (containing overlapping regions with *B. subtilis rnpB* promoter and terminator, respectively). Fragments encoding the *B. subtilis rnpB* promotor, *S. aureus rnpB* and the *B. subtilis rnpB* terminator were combined by overlap extension PCR. The resulting PCR product was cloned into the *Hind* III site of pHY300, yielding plasmid pHY300 *S. aureus* $P_{Bs\ rnpB}$ *rnpB*wt. Point mutations at position G238 and G239 within the *S. aureus rnpB* gene were introduced by the site-directed *Dpn* I method as described above. For introduction of the C238 mutation, the following primers were used: 5’-CGA GTG AGC AAT CCA AAT TT**C** GTA GGA GCA CTT GTT TAA CGG and 5’-CCG TTA AAC AAG TGC TCC TAC **G**AA ATT TGG ATT GCT CAC TCG; for the C239 mutation: 5’-CGA GTG AGC AAT CCA AAT TT**G** CTA GGA GCA CTT GTT TAA CGG and 5’-CCG TTA AAC AAG TGC TCC TAG **C**AA ATT TGG ATT GCT CAC TCG (introduced point mutations are underlined). For the construction of pHY300 *S. aureus* $P_{Bs\ rnpB}$ *rnpB*(wt, 238 or 239) + P_{xyl} *rnp*A, the *B. subtilis rnpA* under control of the xylose promoter was amplified from strain *sb* (Gößringer et al, 2006) using phosphorylated primers “108”, 5’-CCC GAT TTA GTA CAT AGC GAA TCT TAC C, and “107”, 5’-GGG CAA CCA GAA AGG AAG CGC; the PCR product was cloned into the *Sma* I site of pHY300 *S. aureus* $P_{Bs\ rnpB}$ *rnpB*(wt, 238 or 239).

Construction of *E. coli rnpB* complementation plasmids

Complementation plasmids encoding *E. coli rnpB*wt, *rnpB*C292 and *rnpB*C293 under control of its native promoter ($P_{Ec\ rnpB}$) were cloned as described previously (Wegscheid *et al*, 2006). *B. subtilis rnpA* under control of the xylose promoter was amplified from plasmid pHY300 *S. aureus* $P_{Bs\ rnpB}$ *rnpB*wt + P_{xyl} *rnp*A using primers 115 and 116 (see above, both introducing *Bam* HI sites); PCR products were digested with *Bam* HI and cloned into the *Bgl* II site of pHY300 *E. coli* $P_{Ec\ rnpB}$ *rnpB*(wt, 292 or 293).

Construction of pHY300 + P_{xyl} *rnpA*

B. subtilis rnpA under the control of the xylose-inducible promoter was amplified from plasmid pHY300 *B. subtilis* P_{xyl} *rnpB* + P_{xyl} *rnpA* with phosphorylated primers 107 and 108 (see above). The fragment was then cloned into the *Sma* I site of pHY300. The same was done for the xylose-inducible *rnpA* gene with two stop codons close to the 5'-end of *rnpA* (P_{xyl} *rnpA*-stop).

Construction of templates for T7 transcription

C258 and C259 mutations were introduced into *B. subtilis rnpB* by site-directed *Dpn* I mutagenesis (see above) using pDW66 (Smith *et al*, 1992) as the template; pDW66 derivatives were linearized with *Dra* I for T7 runoff transcription; *E. coli* P RNAs were transcribed from plasmid pJA2' linearized with *Fok* I (Vioque *et al,* 1988); ptRNA^{Gly}U$_{73}$, ptRNA^{Gly}U$_{73}$UAAAUA and ptRNA^{Gly}U$_{73}$CCAAUA were transcribed from PCR templates amplified with primer "167" (5'-ATT AAT ACG ACT CAC TAT AGG) as forward primer, and primer "169" (5'-AGC GGG AGA CGG GAC TTG), or primer "170" (5'- TAT TTA AGC GGG AGA CGG GAC TTG), or primer "171" (5'-TAT TGG AGC GGG AGA CGG GAC) as reverse primer, respectively; plasmid pSBpt3'HH (Busch *et al*, 1999) was used as the PCR template.

References

Busch S, Kirsebom LA, Notbohm H, Hartmann RK (2000). Differential role of the intermolecular base-pairs G292-C(75) and G293-C(74) in the reaction catalyzed by *Escherichia coli* RNase P RNA. *J Mol Biol* **299**: 941-951

Gößringer M, Kretschmar-Kazemir Far R, Hartmann RK (2006) Analysis of RNase P Protein (*rnpA*) Expression in *Bacillus subtilis* Utilizing Strains with Suppressible *rnpA* Expression. *J Bacteriol* **188:** 6816-6823

Mogk A, Homuth G, Scholz C, Kim L, Schmid FX, Schumann W (1997) The GroE chaperonin machine is a major modulator of the CIRCE heat shock regulon of *Bacillus subtilis*. *EMBO J* **16**: 4579–4590

Smith D, Burgin AB, Haas ES, Pace NR (1992) Influence of Metal Ions on the Ribonuclease P Reaction. *J Biol Chem* **267**: 2429-2436

Vioque A, Arnez J, Altman S (1988) Protein-RNA interactions in the RNase P holoenzyme from *Escherichia coli*. *J Mol Biol* **202**: 835-848

Wegscheid B, Condon C, Hartmann RK (2006) Type A and B RNase P RNAs are interchangeable *in vivo* despite substantial biophysical differences. *EMBO Rep* **7**: 411-417

Wegscheid B, Hartmann RK (2006) The precursor tRNA 3'-CCA interaction with *Escherichia coli* RNase P RNA is essential for catalysis by RNase P *in vivo. RNA* **12**: 2135-2148

5 Summary

The Ribonuclease P (RNase P) is a ribonucleoprotein enzyme, which catalyses the 5'-maturation of precursor tRNAs. Bacterial RNase P consists of one RNA subunit (P RNA; encoded by *rnpB*; ~400 nt), and a protein subunit (P protein, encoded by *rnpA*; ~120 aa). *In vitro* under elevated salt concentrations the RNA subunit is catalytically active. However, under physiological conditions the protein subunit is essential for activity.

Type A and B RNase P RNAs are interchangeable *in vivo* despite substantial biophysical differences

It could be demonstrated that structural type A and type B bacterial RNase P RNAs can fully replace each other *in vivo* despite the many reported differences in their biogenesis, biochemical/biophysical properties and enzyme function *in vitro*. Even a single copy of *E. coli rnpB*wt integrated into the *amyE* site of the *B. subtilis* chromosome was sufficient for cell viability. The findings suggest that many of the reported idiosyncrasies of type A and B enzymes either do not reflect the *in vivo* situation or are not critical for RNase P function *in vivo*, at least under standard growth conditions.

The precursor tRNA 3'-CCA interaction with *Escherichia coli* RNase P RNA is essential for catalysis by RNase P *in vivo*

The L15 region of *Escherichia coli* RNase P RNA forms two Watson-Crick base pairs with precursor tRNA 3'-CCA termini (G292-C_{75} and G293-C_{74}). Here, the phenotyes associated with disruption of the G292-C_{75} or G293-C_{74} pair *in vivo* was analyzed. Mutant RNase P RNA alleles (*rnpB*C292 and *rnpB*C293) caused severe growth defects in the *E. coli rnpB* mutant strain DW2 and abolished growth in the newly constructed mutant strain BW in which chromosomal *rnpB* expression strictly depended on the presence of arabinose. An isosteric C293-G_{74} base pair, but not a C292-G_{75} pair, fully restored catalytic performance *in vivo,* as shown for processing of precursor 4.5S RNA. This demonstrates that the base identity of G292, but not G293, contributes to the catalytic process *in vivo*. Activity assays with mutant RNase P holoenzymes assembled *in vivo* or *in vitro* revealed that the C292/293 mutations cause a severe functional defect at low Mg^{2+} concentrations (2 mM), which can be infered to be on the level of catalytically important Mg^{2+} recruitment. At 4.5 mM Mg^{2+}, activity of mutant relative to the wild-type holoenzyme, was decreased only about 2-fold, but 13-24-fold at 2 mM Mg^{2+}. Moreover, the findings make it unlikely that the C292/293 phenotypes include

significant contributions from defects in protein binding, substrate affinity or RNA degradation. However, native PAGE experiments revealed non-identical RNA folding equilibria for the wild-type versus mutant RNase P RNAs, in a buffer- and preincubation-dependent manner. Thus, it cannot be excluded that altered folding of the mutant RNAs may have also contributed to their *in vivo* defect.

In vivo **role of bacterial type B RNase P interaction with tRNA 3'-CCA**

It has been unclear if catalysis by bacterial type B RNase P involves a specific interaction with p(recursor)tRNA 3'-CCA termini. We show that point mutations at two guanosines in loop L15 result in growth inhibition, which correlates with an enzyme defect at low Mg^{2+}. For *Bacillus subtilis* RNase P, an isosteric C259-G_{74} bp fully and a C258-G_{75} bp slightly rescued catalytic proficiency, demonstrating Watson-Crick base-pairing to tRNA 3'-CCA and emphasizing the importance of G258 identity. We infer the defect of the mutant enzymes to be primarily on the level of recruitment of catalytically relevant Mg^{2+}, with a possible contribution from altered RNA folding. Cell viability of bacteria expressing mutant RNase P RNAs could be (partially) restored by RNase P protein overexpression, resulting in increased cellular RNase P levels. Finally, we demonstrate that *B. subtilis* RNase P is able to cleave CCA-less ptRNAs *in vivo.* We conclude that the *in vivo* phenotype upon disruption of the CCA interaction is either due to a global deceleration in ptRNA maturation kinetics or severe blockage of 5'-maturation for a subset of ptRNAs.

6 Zusammenfassung

Die Ribonuclease P (RNase P) ist ein Ribonucleoproteinenzym, das die Reifung der Vorläufer tRNAs (ptRNAs) katalysiert. Die bakterielle RNase P besteht aus einer RNA- (P RNA, kodiert durch *rnpB*; ~ 400 nt) und einer Protein-Untereinheit (P Protein; kodiert durch *rnpA*; ~ 120 aa). *In vitro* unter erhöhten Salzkonzentrationen ist die RNA-Untereinheit katalytisch aktiv. Unter physiologischen Bedingungen ist jedoch die Protein-Untereinheit essentiell für die katalytische Aktivität.

Typ A und Typ B RNase P RNAs sind *in vivo* austauschbar trotz erheblicher biophysikalischer Unterschiede

Es konnte gezeigt werden, dass die bakteriellen RNase P RNAs vom strukturellen Typ A und Typ B sich gegenseitig vollständig *in vivo* ersetzen können, trotz der vielen dokumentierten Unterschiede in der Biogenese, in den biochemischen und biophysikalischen Eigenschaften und in der Enzymfunktion *in vitro*. Selbst eine einzelne Kopie des *E. coli rnpB*wt-Gens, integriert in den *AmyE*-Locus des *B. subtilis* Chromosoms, war ausreichend für die Lebensfähigkeit der Zellen. Die Ergebnisse deuten an, dass viele der berichteten Eigenheiten der RNase P Enzyme vom Typ A und B entweder nicht die *in vivo*-Situation widerspiegeln oder für die Funktion *in vivo* nicht kritisch sind, zumindest unter Standardwachstumsbedingungen.

Die Interaktion des 3'-CCA Endes von Vorläufer tRNAs mit *Escherichia coli* RNase P RNA ist essentiell *in vivo*

Die L15-Region der *Escherichia coli* RNase P RNA bildet zwei Watson-Crick Basenpaare mit dem 3'-CCA Ende von Vorläufer tRNAs (G292-C_{75} und G293-C_{74}). Im Rahmen dieser Arbeit wurde der *in vivo*-Phenotyp untersucht, der mit einer Zerstörung des G292-C_{75} oder G293-C_{74} Basenpaares assoziiert ist. Die mutanten RNase P RNA-Allele (*rnpB*C292 and *rnpB*C293) verursachten einen schweren Wachstumsdefekt in dem *E. coli rnpB*-Mutantenstamm DW2 und vernichteten das Wachstum vollständig in dem neu konstruierten *E. coli* Mutantenstamm BW, in dem die Expression des chromosomalen *rnpB*-Gens strikt von der Anwesenheit von Arabinose abhängt. Am Beispiel der Prozessierung von Vorläufer-4.5S RNA konnte gezeigt werden, dass ein isosterisches C293-G_{74} Basenpaar, jedoch nicht ein C292-G_{75} Paar, die katalytische Funktion *in vivo* vollständig wiederherstellt. Dies demonstriert, dass die Identität der Base G292, jedoch nicht von G293, zum katalytischen Prozess *in vivo* beiträgt. Aktivitätsassays mit *in vivo* und *in vitro* assemblierten Holoenzymen zeigten, dass die C292/C293-Mutationen einen schweren funktionellen Defekt bei niedrigen

Mg^{2+}-Konzentrationen (2 mM) verursachen, welcher auf Ebene der Rekrutierung von katalytisch aktivem Magnesium anzusiedeln ist. Bei 4.5 mM Mg^{2+} war die Aktivität der mutanten relativ zum Wildtyp-Holoenzym nur ca. 2-fach erniedrigt, jedoch 13-24-fach bei 2 mM Mg^{2+}. Darüber hinaus deuten unsere Ergebnisse darauf hin, dass es unwahrscheinlich ist, dass Defekte in der Proteinbinding, Substrataffinität oder RNA-Stabilität signifikant zum C292/C293-Phenotyp beitragen. In nativen PAGE-Experimenten wurden jedoch nicht-identische Faltungsgleichgewichte für Wildtyp vs. mutanten RNase P RNAs aufgedeckt, welche sowohl puffer- als auch präinkubationsabhängig waren. Deshalb kann nicht ausgeschlossen werden, dass eine veränderte Faltung der mutanten RNAs zum *in vivo* Defekt partiell beiträgt.

Die Rolle der Interaktion zwischen Typ B RNase P und dem tRNA 3'-CCA Ende *in vivo*

Bisher war es unklar, ob RNase P vom (strukturellen) Typ B eine spezifische Interaktion mit dem 3'-CCA Ende von Vorläufer tRNAs (ptRNAs) eingeht und ob diese Wechselwirkung gegebenenfalls für den katalytischen Prozess eine Rolle spielt. Es konnte gezeigt werden, dass Punktmutationen der zwei Guanosine im L15-Loop, für welche eine Interaktion mit dem 3'-CCA Ende vermutet wird, das Zellwachstum hemmen (*S. aureus rnpB*) oder unterdrücken (*B. subtilis* oder *E. coli rnpB*). Dies korreliert mit einem Enzymdefekt bei niedrigen Mg^{2+}-Konzentrationen. Für *B. subtilis* RNase P stellte ein isosterisches C259-G_{74} Basenpaar die katalytische Prozessivität vollständig wieder her, während ein C258-G_{75} Basenpaar nur einen schwachen Kurierungseffekt bewirkte. Dies weist auf eine Waston-Crick Basenpaarung der zwei Guanosine mit dem 3'-CCA Ende von tRNAs hin und unterstreicht zugleich die Wichtigkeit der Basenidentität an der Postition G258. Kinetische Untersuchungen lassen die Folgerung zu, dass der Defekt der mutanten Enzyme hauptsächlich auf Ebene der Rekrutierung von katalytisch aktivem Mg^{2+} anzusiedeln ist. Es kann jedoch nicht ausgeschlossen werden, dass Unterschiede in der RNA-Faltung einen Beitrag zum *in vivo* Defekt der Mutanten leisten. Die Lebensfähigkeit der Bakterien, welche mutierte RNase P RNA exprimierten, konnte (teilweise) durch parallele Überexpression des *B. subtilis* RNase P Proteins wiederhergestellt werden; dieser Effekt konnte auf erhöhte intrazelluläre RNase P-Mengen zurückgeführt werden. Des weiteren konnte gezeigt werden, das *B. subtilis* RNase P 3'-Vorläufer tRNAs ohne 3'-CCA Ende *in vivo* prozessieren kann. Wir folgern daraus, dass der *in vivo*-Phenotyp, der mit einer Unterbrechung der CCA-Interaktion assoziiert ist, entweder durch eine globale kinetische Verlangsamung der 5'-Reifung von tRNAs oder durch eine kritische Blockierung der 5'-Maturierung einer Subgruppe von tRNAs verursacht wird.

7 Outlook

Within this study the *E. coli rnpB* mutant strain BW was constructed and the *B. subtilis rnpB* mutant strain SSB318 was established for *in vivo* complementation analyses. By introducing and utilizing such “clean” type A and B RNase P mutant strains, we have paved the way for sophisticated future studies that enable the parallel analysis of RNase P function *in vivo* and *in vitro*. Combined with previous RNase P mutant strains, the two strains of this work have the advantage that the chromosomal *rnpB* genes can be completely silenced, and that stresses such as heat shock are avoided during complementation analyses.

The mutant strains permit systematic investigations of structurally different P RNAs in order to define the architectural constraints for type A and B RNase P function in the cellular milieu. Such investigations can be further extended by including archaeal P RNAs. Also, some cyanobacterial RNase P RNAs lack the two conserved G residues involved in the CCA interaction, raising the question how cyanobacterial RNase P enzymes accomplish efficient catalysis *in vivo*. The function of cyanobacterial P RNAs could be tested in the *E. coli* BW and *B. subtilis* SSB318 RNase P mutant strains. Concomitant expression of cyanobacterial P proteins will answer the question if features of the cyanobacterial P proteins may compensate for the absence of the CCA interaction.

The *rnpB* mutant strains provide a useful tool for *in vivo* folding studies of RNase P. For example, *in vitro* experiments have revealed that S- and C-domain of bacterial P RNA fold independently of each other. However, nothing is known on the physiological relevance of this finding. With the *rnpB* mutant strains, assembly and function of independently expressed S- and C-domains can be examined *in vivo*.

The *rnpB* mutant strains could also be exploited to isolate *in vivo* assembled holoenzymes e.g. for structural analyses. For this purpose, one could express a P RNA carrying one or two affinity tags for enzyme purification (e.g. a small hairpin binding to a phage coat protein combined with a tobramycin aptamer). As the native *rnpB* can be tighly down-regulated in strain BW and SSB318, titration effects resulting from competition of native P RNA and tagged P RNA for binding to the native P protein can be avoided. Possible interference of purification tags with holoenzyme functionality can be eliminated by initial complementation analyses. Double-tagged P RNAs expressed in the *rnpB* mutant strains also provide a means to isolate cellular components associated with RNase P. Previous studies have suggested interactions between bacterial RNase P with ribosomes as well as other RNases (RNase E, RNase III). Archaeal RNase P has a more complex architecture (1 RNA, 4 protein subunits) than the bacterial enzyme, cellular levels of the enzyme are low, and *in vitro* reconstitution of active archaeal RNase P is still an unsolved problem. Tagged archaeal P RNAs may be overexpressed in strains BW and SSB318 together with the archaeal P proteins, and the archaeal holoenzyme assembled in the bacterial host may be isolated in large quantities for structural and biochemical studies.

The mutant strains are also a helpful tool to identify new substrates of RNase P. In microarray analyses potential candidates might be identified which accumulate upon repression of *rnpB*. Such candidate substrates could be characterized within the framework of combined *in vitro* investigations (kinetics and RNA folding studies at low Mg^{2+}) and *in vivo* analyses (complementation, determination of RNase P steady-state levels) established in this Ph.D. work.

8 Appendix

8.1 Chemicals

Acrylamide M-Bis (50 % stock solution 24:1)	Gerbu
Agar Agar	Serva
Agarose	Roth
Ampicillin	Gerbu
Ammonium acetate	Fluka
Ammoniumperoxodisulfate	Roth
BlueSlick	Serva
Boric acid	Roth
Bromophenol blue (BPB)	Merck
Chloramphenicol	Sigma
Chloroform	Merck
Crystal violet	Fluka
Deoxynucleosidtriphosphates (dNTPs)	Boehringer
Disodiumhydrogenphosphate	Merck
Dithiothreitol (DTT)	Gerbu
Erythromycin	Merck
Ethanol p.a. 99.8 %	Roth
Ethidiumbromide	Roth
Glycerol	Gerbu
Glycogen	Roche
Urea	Gerbu
Yeast extract	Gerbu
Isopropanol	Roth
Lincomycin	Sigma
β-Mercaptoethanol	Serva
Potassiumdihydrogenphosphate	Fluka
Sodiumacetate	Merck
Nucleosidtriphosphates (NTPs)	Roche
Peptone	Roth
Phenol	Roth
Bovine serum albumin (BSA)	Sigma
Skim milk powder (blotting grade)	Roth
N,N,N‘,N‘-Tetraethylmethylenediamin (TEMED)	Serva
Tetracyclin	Sigma
Tris-(hydroxymethyl)aminomethane	Gerbu
Trizol®	Invitrogen
Xylenecyanol blue (XCB)	Serva

All other chemicals (not listed above) were purchased from Sigma, Gerbu or Life Technologies and had a purity grade “pro analysis”.

8.2 Radioisotopes

[γ-^{32}P] ATP	Hartmann Analytic ICN Radiochemicals
[5’-^{32}P] pCp	Hartmann Analytic ICN Radiochemicals

8.3 Size markers

1 kb DNA ladder	New England Biolabs
10 bp DNA ladder	Invitrogen
2 Log DNA ladder	New England Biolabs
PageRuler™ Prestained Protein Ladder	MBI Fermentas
PageRuler™ Prestained Protein Ladder Plus	MBI Fermentas

8.4 Enzymes

Alkaline Phosphatase	MBI Fermentas
DNase I	Promega, Ambion
Klenow Fragment	MBI Fermentas
Nuclease P1	Biomol
Pfu-Polymerase	Promega and our lab
Pyrophosphatase	Roche
Restriction endonucleases	MBI Fermentas and New England Biolabs
Taq polymerase	MBI Fermentas and our lab
Thermoscript	Invitrogen
T4 DNA ligase	Gibco BRL and MBI Fermentas
T4 Polynucleotide kinase	New England Biolabs
T4 RNA-ligase	MBI Fermentas
T7 RNA polymerase	MBI Fermentas;
T7 RNA polymerase (Y639F)	our lab
Turbo DNase	Ambion

8.5 Equipment

Agarose gel chamber	Biorad, Mini Sub Cell
Autoclave	Systec V95
Blotting device	Schleicher & Schuell, SammyDry
Electroporator	Biorad, Gene Pulser Xcell, PC- and CE- module
FPLC	Amersham, ÄktaBasic
Gel documentation system	Cybertech, CS1 with Mitsubishi Video Copy Processor; Biostep, GelSystem MINI
Gel dryer	Biorad, Model 483 SLAB Dryer
Hand-monitor	Berthold, LB 1210 B
Heating blocks	Techne, Dri-Block DB-3D; Biometra, TB1
Incubator	Memmert BE400
Imager cassettes	Fuji Film, Bas cassette 4043, Rego, 35,6x43,2cm
Magnetic stirrers	Heidolph, MR 2002
Power supply	Pharmacia, EPS 3500; Bio Rad, Power Supply160/1.6 (Power Pac 3000); Apelex, PS 9009T
PAA-gel chamber	Custom-made, University of Lübeck
PCR cycler	Biometra, TGradient Thermocycler
pH-Meter	WTW, pH Level 1
Phosphoimager	Raytest, Bio-Imaging Analyser BAS 1000 (Fujifilm); FLA 3000, (Fujifilm)
Pipettes	Gilson-Pipetman, P20, P200, P1000 Abimed 0.1-2µl
Protein Gel chamber	Mini Protean 3 cell, Biorad

Quartz cuvette	Hellma 104-QS, 105.202, 115B-QS, 105
Mixer	IKA, Vibrax-VXR; Eppendorf, Thermomixer 5436, Thermomixer comfort
Shaking incubator	GFL 3033
Spectrophotometer	Hewlett Packard, Photometer 8453; Varian, Cary 50 Conc; Thermo Spectronic, Biomate 3
Software	PCBas/Aida Image Analyser v.3.45, Corel Graphics Suite; GraFit 3.0; Microsoft Office; Pymol, Delano, W.L. 2002 Vector NTI®, Invitrogen
Speedvac	Heto vacuum centrifuge
Scintillation counters	Perkin Elmer, Wallac WINSPECTRAL a/b 1414 Liquid Scintillation Counter; Packard, Tricarb 2000CA
Centrifuges	Heraeus, Biofuge pico, biofuge fresco; Sigma, Typ 112; Eppendorf, centrifuge 5810R, minispin plus Stratagene, PicoFuge

8.6 Antibodies

Primary antibodies

Anti-*B. subtilis* RnpA-Antiserum from rabbits (P.ab syra 6)	C. A. Fierke, University of Michigan, U.S.A.
Anti-*E. coli* RnpA-Antiserum from rabbits	A. Vioque, University of Sevilla, Spain (Pascual and Vioque, 1996)

Secondary antibodies

Anti-Rabbit IgG made in goat (affinity purified), conjugated with alakaline phosphatase	Roche Diagnostics

8.7 Synthetic DNA Oligonucleotides

DNA oligonucleotides were obtained from Invitrogen or Metabion. The sequence of DNA oligonucleotides is given in the 5' to 3' direction. Nt in **bold** letters indicate introduced mutations. Underlined sequences indicate either restriction enzyme recognition sites, overlapping regions or the T7 promoter sequence.

Primer Nº	Name	Used for	5’→ 3’ sequence
1	*E. coli* M1 G292C sense	*E. coli* C292 mutagenesis	GTA CTG AAC CCG **C**GT AGG CTG CTT GAG C
2	*E. coli* M1 G293C sense	*E. coli* C293 mutagenesis	GTA CTG AAC CCG G**C**T AGG CTG CTT GAG C

3	*E. coli* M1 G293C antisense	*E. coli* C293 mutagenesis	GCT CAA GCA GCC TA**G** CCG GGT TCA GTA C
4	*E. coli* M1 G292C antisense	*E. coli* C292 mutagenesis	GCT CAA GCA GCC TAC **G**CG GGT TCA GTAC
12	*rnpB* (–96) pSP64 seq	*B. subtilis rnpB EP;* sequencing	CAT ATT GTC GTT AGA ACG CG
15	*S. aur*. M1 G238C sense	*S. aureus* C238 mutagenesis	CGA GTG AGC AAT CCA AAT TT**C** GTA GGA GCA CTT GTT TAA CGG
16	*S. aur*. M1 G238C antisense	*S. aureus* C238 mutagenesis	CCG TTA AAC AAG TGC TCC TAC **G**AA ATT TGG ATT GCT CAC TCG
17	*S. aur*. M1 G239C sense	*S. aureus* C239 mutagenesis	GAG TGA GCA ATC CAA ATT T**G**C TAG GAG CAC TTG TTT AAC GG
18	*S. aur*. M1 G239C antisense	*S. aureus* C239 mutagenesis	CCG TTA AAC AAG TGC TCC TAG **C**AA ATT TGG ATT GCT CAC TC
19	5' *B. sub*. *rnpB* – *Hind*III	*B. subtilis rnpB* promoter	GGC AGC AAG CTT TAT GAT TGA TCA C
21	3' *B. sub*. *rnpB Hind*III	*B. subtilis rnpB* terminator	CGC CCA AGC TTG TGT ATA CTT CTT C
34	pACYC177 Seq	sequencing	CTA TTA ATT TCC CCT CGT C
41	5' *E. coli* M1+*B. sub*. promoter	*E. coli rnpB* BPT	GTA ATC AGT TGT TAT ATA ATA ATT CAT GAA GCT GAC CAG ACA GTC
42	5' *S. aur*. M1 + *B. sub*. terminator	*S. aureus rnpB* BPT	GTA ATC AGT TGT TAT ATA ATA ATT CAT TGA TAT TTT GGG TAA TCG C
44	3' *B. sub*. promoter	*B. subtilis rnpB* promoter	ATG AAT TAT TAT ATA ACA ACT GAT TAC
45	5' *B. sub*. terminator	*B. subtilis rnpB* terminator	ACA TTT AAA ATG ATG AAA ACA AGC
46	3' *E. coli* M1+*B. sub*. terminator	*E. coli rnpB* BPT	GCT TGT TTT CAT CAT TTT AAA TGT AGG TGA AAC TGA CCG ATA AG
47	3' *S. aur* M1 +*B. sub* terminator	*S. aureus rnpB* BPT	GCT TGT TTT CAT CAT TTT AAA TGT ACT AGT AGT GAT ATT TCT ATA AGC C
49	*E. c*. RevT 3	Primer extension *E. coli rnpB*, RT-PCR	CTC ACT GGC TCA AGC AGC CT

52	pHY300 Seq (PLS)	sequencing	CTA AAT CGT TAA GGG ATC AAC
53	*S. a.* RevT 3	Primer extension *S. aureus rnpB*	GAA TTC CGT TAA ACA AGT GCT CCT
66	pHY300 Seq rev MCS	sequencing	CCT GTC GGG TTT CGC C
82’	3’ *B. sub* M1 C258	*B. subtilis* C258 mutagenesis	TCC GTT AAG AAG GTT CCC CTA C**G**A AAA TTT GGG TTT CTC GCT CGA G
83’	3’ *B. sub* M1 C259	*B. subtilis* C259 mutagenesis	TCC GTT AAG AAG GTT CCC CTA **G**CA AAA TTT GGG TTT CTC GCT CGA G
84	3’ ptgly G74	ptgly G74 mutagenesis	GCA CAT CCG GTG ACT G**C**A GCG GGA GAC GG
85	3’ ptgly G75	ptgly G75 mutagenesis	GCA CAT CCG GTG ACT **C**GA GCG GGA GAC GG
86’	5’ *B. sub* M1 C258	*B. subtilis* C258 mutagenesis	CTC GAG CGA GAA ACC CAA ATT TT**C** GTA GGG GAA CCT TCT TAA CGG A
87’	5’ *B. sub* M1 C259	*B. subtilis* C259 mutagenesis	CTC GAG CGA GAA ACC CAA ATT TTG **C**TA GGG GAA CCT TCT TAA CGG A
88	5’ ptgly G74	ptgly G74 mutagenesis	CCG TCT CCC GCT **G**CA GTC ACC GGA TGT GC
89	5’ ptgly G75	ptgly G75 mutagenesis	CCG TCT CCC GCT C**G**A GTC ACC GGA TGT GC
92	*B. sub*. P4_5’	Primer extension *B. subtilis/S. aureus rnpB*	GAG CAT GGA CTT TCC TCT
93	*B. sub* RevT 1	Primer extension *B. subtilis rnpB,* RT-PCR	TTC CGT TAA GAA GGT TCC CCT
96	4.5S RevT 1	Primer extension 4.5S RNA	GGA GAA CCA ACA GAG CCC
100	5’ xylR *Bam*HI	xyl *B.subtilis rnpB*	CGC GGA TCC AGG TTT GCT AAC CTT TGC G
102	5’ *B. sub* M1 mit xyl	xyl *B.subtilis rnpB*	GAT GAG ATA ACA TGT TCT TAA CGT TCG GGT
103	3’ *B. sub* M1 *Sma*I	xyl *B.subtilis rnpB*	CGT CCC GGG CTT CAT CGT ATC ACC CTG TC
105	3’ xylR *Psc*I(*Xce*I)/*Sma*I	xyl *B.subtilis rnpB*	GGG ACA CAT GTT ATC TCA TCA TAT ACA AAA TAA ATG TTT

107	3’ xyl *rnpA*	xyl *B. subtilis rnpA/rnpA*-stop	GGG CAA CCA GAA AGG AAG CGC
108	5’ xyl *rnpA*	xyl *B. subtilis rnpA/rnpA*-stop	CCC GAT TTA GTA CAT AGC GAA TCT TAC C
113	5’ *rnpA* direct	xyl *B. subtilis rnpA*-stop	ATG AGT CAT TTG AAG AAG CGA AA
114	5’ antisense *rnpA* direct	xyl *B. subtilis rnpA*-stop	TTT CGC TTC TTC AAA TGA CTC AT
115	5’ xyl *rnp*A *Bam*HI	xyl *B. subtilis rnpA*	CAG GAT CCG ATT TAG TAC ATA GCG AAT CTT ACC
116	3’ xyl *rnpA Bam*HI	xyl *B. subtilis rnpA*	CAG GAT CCA ACC AGA AAG GAA GCG C
134	3’ *rnpB* +1start RExBAD	BW	GTC TCC CCC GAA GAG GAC GAC GAC GAA GCG GCG ACT GTC TGG TCA GCT TCT ATG GAG AAA CAG TAG AGA GTT GC
135	5’ *rnpB* upstr RExBAD	BW	CTT CAG CGT ATT GAC CAG CAT AGG TAC GTT GGA CGA AGC ATT CCG CGG GCT TGC ATA ATG TGC CTG TC
136	5’RExBADveri	BW	CGG CGT CAC ACT TTG CTA TGC C
137	5’-*rnpB* ext	BW	CGA TTG GTG TCG CAA ACG TGG
138	3’ catRExBAD veri	BW	CGC AAG GCG ACA AGG TGC TG
149	5’*B. sub* M1	RT-PCR	CTT AAC GTT CGG GTA ATC GC
150	5’ *E. coli* M1	RT-PCR; BW	GAA GCT GAC CAG ACA GTC GC
156	3’ *E. c.* prom + *B. sub.* M1	*B. subtilis rnpB* EP	CAG CGA TTA CCC GAA CGT TAA GAA CGG CGC GCA GTA TAG AGG G
157	5’ ext veri *rnpB*	*B. subtilis rnpB* EP; BW	TGC AGG AGC TGC GGG TGG
158	3’ext veri *rnpB*	BW	GTG AAA CTG ACC GAT AAG CCG C
163	3’ *E. coli rnpB*	BW	AGG TGA AAC TGA CCG ATA AGC C

167	T7	ptRNA 3'-variants	ATT AAT ACG ACT CAC TAT AGG
169	U73 ptgly 3'	ptRNA 3'-variants	AGC GGG AGA CGG GAC TTG
170	U73UAAAUA ptgly3'	ptRNA 3'-variants	TAT TTA AGC GGG AGA CGG GAC TTG
171	U73CCAAUA ptgly 3'	ptRNA 3'-variants	TAT TGG AGC GGG AGA CGG GAC
177	trnSL-Val2 RT1	5'-RACE	GCG CAA GGG TTT AAG CTA TGA TTC CG
178	trnSL-Val2 RT2	5'-RACE	CTG CGC AAG GGT TTA AGC TAT GAT T
179	trnSL-Ala1 RT1	5'-RACE	CGA ATA AGG GTT TAA AGG TAT GGA GCC A
180	trnSL-Ala1 RT2	5'-RACE	TCG AAT AAG GGT TTA AAG GTA TGG AG
183	3' *E. c.* M1 +350	BW	CGC CGG AAC GGT TTA TTA CGT AC
186	*E. c.* M1 up +350	BW	CAT TCG CGT CGC TTG TGA TGT C
193	5' *E. coli rnpB* promoter -58	BW	CAC GTA ATA TCG CCG CGA CAC TGG
194	5' AraC	BW	GCG ACT CGT TAA TCG CTT CCA TGC
195	3' AraC	BW	GCA TGG AAG CGA TTA ACG AGT CGC
196	5' *E. c. rnpA Nco*I	pTrc *E. coli rnpA*	AGA CCA TGG TTA AGC TCG CAT TTC C
197	3' *E. c. rnpA Xba*I	pTrc *E. coli rnpA*	ATC TCT AGA GTC AGG ACC CGC GAG CCA
203	t1t2 *Nsi*I	pTrc *E. coli rnpA*	CAC ATG CAT GCA AAA AGG CCA TCC GTC AGG
206	pTrc *Mfe*I/*Cla*I	pTrc *E. coli rnpA*	ACA ATC GAT TCA ATT GCG CCG ACA TCA TAA CGG
207	5' 4.5S prom + *Eco*RI	mutated 4.5S RNA	ACA GAA TTC AGC ATA ATC TGG AAA AAC GCC C
208	3' 4.5S prec + mod stem	mutated 4.5S RNA	CCA ACA GA**C GGG** CCA TTG AGA GCG TTG AGA ACC

209	5’ 4.5S + mod stem	mutated 4.5S RNA	CTC AAT GGC CCG TCT GTT GGT TCT CCC GCA AC
210	3’ 4.5S + mod stem	mutated 4.5S RNA	TGG **CCC G**CC TGC CAG CTA CAT CCC GG
211	5’wt CCC	mutated 4.5S RNA	GCT GGC AGG CGG GCC ACC CAT TTC TGC CTC CCA CCG TTT C
212	5’ G74 GCC	mutated 4.5S RNA	GCT GGC AGG CGG GCC A**G**C CAT TTC TGC CTC CCA CCG TTT C
213	5’ G75 CGC	mutated 4.5S RNA	GCT GGC AGG CGG GCC AC**G** CAT TTC TGC CTC CCA CCG TTT C
214	3’ *ybaA PstI*	mutated 4.5S RNA	CAC CTG CAG CAA GGC ATT ACC GAA AGA AG
215	4.5S RT mod	Primer extension mod. 4.5S RNA	GGA GAA CCA ACA GAC GGG
216	3’ *Mlu*I + *Pst*I 4.5S RNA	mutated 4.5S RNA	TCT CTG CAG TAA CGC GTC ATC TGC CTT GGC
223	*E. c*. prom + *Nhe*I	*B. subtilis rnpB* EP	GCA TGC TAG CGA TTG GTG TCG CAA ACG TGG C
224	3’ *S. aur. rnpB* -GG	RT-PCR *S. aureus rnpB*	ATT TGG ATT GCT CAC TCG AGG G
225	5’ *S. aur. rnpB*	RT-PCR *S. aureus rnpB*	GGG TAA TCG CTA TAT TAT ATA GAG G
X1	5’- p4.5S RNA + T7	4.5S RNA marker	CCA GAA TTC GAA ATT AAT ACG ACT CAC TAT A
X2	3’- p4.5S RNA	4.5S RNA marker	TAT GGG TGG GGG CCC TGC CAG CTA
X3	Primer (Adapter):	5’-RACE experiments	GTC AGC AAT CCC TAA GGA G
HP499	*B. sub rnpB Hind*III	SSB318 construction	ACC AAA GCT TGT TCT TAA CGT TCG GGT AAT CGC TG
HP500	*B. sub rnpB Bam*HI	SSB318 construction	TCC AGG ATC CGT TTA CCG CGT TCC ACT CTC ACC ATT TC
M1	*rpsR*-R	RT-PCR *B. subtilis* S18	ACG TGC GCG TTT GAT CGC TGC A
M2	*rpsR*-F	RT-PCR *B. subtilis* S18	GCA GAG GCG GTC GTG CGA AA

8.8 DNA/RNA-Oligonucleotides

Underlined nt are ribonucleotides, all others are deoxyribonucleotides.

Primer Nº	Name	Used for	5'→ 3' sequence
A1	Adapter	5'-RACE experiments, adapter ligation	GTC AGC AAT CCC TAA GGA G

8.9 Bacterial strains

Strain	Relevant Genotype	Reference
E. coli BW	pBAD::*rnpB*, Cam^{r}	Wegscheid and Hartmann, 2006
E. coli DH5α	*supE*44 delta*lacU*169 (phi80 *lacZ* deltaM15) *hsdR*17 *recA*1 *endA*1 *gyrA*96 *thi*-1 *relA*1	Sambrook *et al.*, 1989
E. coli K12 MG1655	F- lambda- *ilvG*- *rfb*-50 *rph*-1	Guyer *et al.*, 1981
E. coli DW2/pDW160	Δ*rnpB*, pDW160 ts rnpB Kan^{R}	Waugh and Pace, 1990
E. coli TG1*cat-araC*	TG1, *cat* gene inserted downstream of the *araC* gene, Cam^{r}	Roux *et al.*, 2005
E. coli XL-2 Blue	*recA1 endA1 gyrA96 thi-1 hsdR17 supE44 relA1 lac* [F´ *proAB lacI*q*Z.M15* Tn*10* (Tet^{r}) Amy Cam^{r}]	Stratagene
B. subtilis W168	wildtype	Bacillus genetic stock center
B. subtilis SB	P$_{xyl}$ *B. subtilis rnpA*	Gößringer *et al.*, 2006
B. subtilis SSB318	P$_{spac}$::*rnpB* mls^{r} (ery)	Wegscheid *et al.*, 2006
B. subtilis SSB320	P$_{spac}$::*rnz* mls^{r} (ery)	Pellegrini *et al.*, 2003
B. subtilis SSB321	P$_{spac}$::*rnz* mls^{r} (ery) pMAP65 lacI^{++} Kan^{r}	C. Condon, Paris

8.10 Plasmid vectors

Vector	Relevant Genotype	Reference
pMAP65	pUB110 $lacI^{++}$ Kan^r	Petit *et al.*, 1998
pSP64	ori pMB1 Amp^r	Promega
pDG364	Amp^r Cam^r	Cutting *et al.* 1990
pACYC177	p15A Amp^r Kan^r	Chang *et al.*, 1978
pBR322	pMB1 rop Amp^r Tet^r	Bolviar *et al.* 1977
pHY300 PLK	Tet^r Amp^r pAMα1 p15A	Ishiwa et Shibahara-Sone, 1986
pTrc99A	pMB1 $lacI^q$ Amp^r pTrc	Amann *et al.* 1988
pKD46	pBAD γ β exo repA101ts Amp^r	Datsenko et Wanner, 2000
p3dstop	P_{spac} *B. subtilis rnpA*-stop	Gößringer, 2004; Gößringer *et al.*, 2006

8.11 Plasmid vectors for T7 transcriptions

Vector	Genotype	Reference	Linearised with
pDW66	*B. subtilis* P RNA	Smith *et al.*, 1992	*Dra* I
pSBpt3'HH	$ptRNA^{Gly}$ from *Thermus thermophilus* with 14mer flank	Busch *et al.*, 2000	*Bam* HI
pJA2'	*E. coli* P RNA, (wt or C292/C23 variants)	Vioque *et al.,* 1988	*Fok* I

For plasmid vectors constructed within this study see chapters 3.7.2 and 3.7.4.

Those plasmids were used as template, to introduce point mutations by site-directed *Dpn* I mutagenesis (chapter 3.3.9).

8.12 PCR Mutagenesis performed within this study

Point mutations were introduced by site-directed *Dpn* I mutagenesis (chapter 3.3.9).

Gene/target	Introduced mutation	Primers	plasmid
E. coli rnpB	C292	1, 3	1)
E. coli rnpB	C293	2, 4	1)
S. aureus rnpB	C238	15, 16	2)
S. aureus rnpB	C239	17, 18	2)
B. subtilis rnpB	C258	86', 82'	3)
B. subtilis rnpB	C259	87', 83'	3)
$ptRNA^{Gly}$ *T. thermophilus*	G74	84, 88	pSBpt3'HH
$ptRNA^{Gly}$ *T. thermophilus*	G75	85, 89	pSBpt3'HH

1) all plasmids encoding *E. coli rnpB* (see chapter 3.7.2 and 3.7.4)

2) all plasmids encoding *S. aureus rnpB* (see chapter 3.7.2 and 3.7.4)

3) all plasmids encoding *B. subtilis rnpB* (see chapter 3.7.2 and 3.7.4) and plasmid pDW66

8.13 Abbreviations and Units

A_{260}	absorption at 260 nm
A	Adenosine
aa	amino acid(s)
Amp	Ampicillin
AP	Alkaline Phosphatase
APS	Ammonium peroxodisulfat
BCIP	5-Brom-4-Chlor-3-Indolylphosphat
Bp	base pair(s)
BPB	Bromophenol blue
BPT	native *B. subtilis rnpB* promoter and terminator
BSA	Bovine serum albumine
C	cytosine
C5	protein subunit of *E. coli* RNase P
cam	Chloramphenicol
c_{End}	end concentration
c_{Stock}	stock concentration
cpm	counts per minute
Da	dalton
DNA	deoxyribonucleic acid
DNase	deoxyribonuclease
dNTP	deoxynucleoside triphosphates
DTT	dithiothreitol
E	extinction
ε	molar extinction coefficient
EDTA	Ethylenediamine tetraacedic acid
EP	native *E. coli rnpB* promoter
Fig.	Figure
g	gram
G	guanosine
h	hour(s)
HEPES	N-2-Hydroxyethylpiperazin-N’-2-ethane sulfonic acid
IPTG	Isopropyl-β-D-thiogalactopyranosid
kan	Kanamycin
kb	kilo bases
l	liter

LB	Luria-Bertani
M	molar [mol/l]
mA	milliampere
MBq	Megabecquerel
min	Minute
MW	Molecular weight
NBT	p-Nitroblue-tetrazolium chloride
nt(s)	Nucleotide(s)
NTP	Ribonucleosidtriphosphate
OD_{578}	optical density at 578 nm
p.a.	pro analysis
PAA	Polyacrylamide
PAGE	Polyacrylamid gel elektrophoresis
$P_{B.s.\ rnpB}$	native *B. subtilis rnpB* promoter
PCR	Polymerase chain reaction
$P_{E.c.\ rnpB}$	native *E. coli rnpB* promoter
pmol	Picomol
P Protein	Protein subunit of RNase P
P RNA	RNA subunit of RNase P
RACE	rapid amplification of cDNA ends
RNA	ribonucleic acid
RNase	ribonuclease
rpm	rounds per minute
RT	reverse transcriptase
SDS	natriumdodecylsulfat
s	second
T	thymine
TBE	Tris-Borat-EDTA Buffer
Tet	tetracycline
T_m	melting temperature
Tris	Tris-hydroxymethylaminomethan
(p)tRNA	(precursor) transfer RNA
U	Unit(s) (unit for enzyme activity)
U	Uridine
wt	wild-type
XCB	Xylene cyanol blue

8.14 Index of Buffers and Solutions

5 x Anode buffer (Schägger) 63
Arg/His-Mix 27
Blocking Buffer (Western blot) 66
Buffer A (FPLC) 60
Buffer F 2/10 60
Buffer KN 2/4.5 60
Buffers used for preparative plasmid preparation 42
5 x Cathode buffer (Schägger) 63
denaturing sample buffer 32
denaturing sample buffer/EDTA 70
5 x DNA sample buffer 31
Elution buffer 1 39
Elution buffer 2 39
3 x Gel buffer (Schägger) 63
5 x Gel running buffer (Laemmli) 64
Gel staining solution (Coomassie) 65
Growth Medium (electrocompetent cells *B. subtilis)* 26
HS Medium 26
LB (Luria Bertani) Medium 23
LS Medium 27
2 x native loading buffer 34
Outgrowth Medium (electrocompetent cells *B. subtilis)* 30
PAA gel solution (nativ, THE) 35
PAA gel solution (TBE) 33
PUV Buffer 62
5 x RT Annealing Buffer 55
10 x S-Base 27
4 x SDS-PAGE sample buffer (Schägger) 63
4 x Separation gel buffer (Laemmli) 64
SOC Medium 29
SpC Medium 28
SpII Medium 28
8 x Stacking gel buffer (Laemmli) 64
Substrate Buffer (Western blot) 66
T-Base 28
5 x TBE buffer 31
5 x TBS Buffer 66
TFB1-Solution 25

TFB3-Solution 25
10 x THE buffer 34
Transfer buffer (Western blot) 65
Washing Buffer (Western blot) 66
Washing solution (electrocompetent cells *B. subtilis)* 26

8.15 Sequence of the *E. coli rnpB* context in strain BW

cagtgggctggagctggtacctgcggaaaaacgcgatccactcgtgaccacttcacgcggcacaggcgagttaatcctgcaggcgctggagagc
ggtgcgacaaacattattatcggcattggcggcagcgctacaaatgatggcggcgcaggcatggtacaggcgctgggggcgaaattatgcgacg
ccaacggcaatgaaattggttttggcggcggtagtcttaatactctgaatgatattgatatttccggcctcgatccgcgcttaaaagattgcgtcattcgc
gtcgcttgtgatgtcaccaatccgctggtgggcgataacggcgcatcgcgcatctttggcccacaaaagggagccagtgaagcgatgattgttgag
ctggacaataacctctctcactatgccgaggtcattaaaaaagcgctgcatgttgatgtgaaagatgtccccggtgcaggagctgcgggtggtatgg
gcgcggcgctaatggcgtttcttggtgcggaactgaaaagtggtattgaaatcgtcactacggcgctgaatctggaggaacatattcacgattgtacg
ctggtgatcaccggtgaagggcgtattgacagccagagtattcacgggaaggtaccgattggtgtcgcaaacgtggcgaagaagtaccataaacc
ggtgattggcattgcgggtagcctgaccgatgatgttggcgttgtacatcagcatggcattgatgcggtcttcagcgtattgaccagcataggtacgtt
ggacgaagcattccgcgggcttgcataatgtgcctgtcaaatggacgaagcagggattcttacgccccgccctgccactcatcgcagtactgttgta
attcattaagcattctgccgacatggaagccatcacaaacggcatgatgaacctgaatcgccagcggcatcagcaccttgtcgccttgcgtataatatt
tgcccatggtgaaaacgggggcgaagaagttgtccatattggccacgtttaaatcaaaactggtgaaactcacccagggattggctgagacgaaaa
acatattctcaataaaccctttagggaaataggccaggttttcaccgtaacacgccacatcttgcgaatatatgtgtagaaactgccggaaatcgtcgtg
gtattcactccagagcgatgaaaacgtttcagtttgctcatggaaaacggtgtaacaagggtgaacactatcccatatcaccagctcaccgtctttcatt
gccatacggaattccggatgagcattcatcaggcgggcaagaatgtgaataaaggccggataaaacttgtgcttatttttctttacggtctttaaaaagg
ccgtaatatccagctgaacggtctggttataggtacattgagcaactgactgaaatgcctcaaaatgttctttacgatgccattgggatatatcaacggt
ggtatatccagtgatttttttctccatttagcttccttagctcctgaaaatctcgataactcaaaaaatacgcccggtagtgatcttatttcattatggtgaaa
gttggaacctcttacgtgccgatcaacgtctcattttcgccaaaagttggcccagggcttcccggtatcaacagggacaccaggatttatttattctgcg
aagtgatcttccgtcacagccctatgctactccgtcaagccgtcaattgtctgattcgttaccaattatgacaacttgacggctacatcattcactttttcttc
acaaccggcacgaaactcgctcgggctggccccggtgcattttttaaatactcgcgagaaatagagttgatcgtcaaaaccaacattgcgaccgacg
gtggcgataggcatccgggtagtgctcaaaagcagcttcgcctgactaatgcgttggtcctcgcgccagcttaagacgctaatccctaactgctggc
ggaaaagatgtgacagacgcgacggcgacaagcaaacatgctgtgcgacgctggcgatatcaaaattgctgtctgccaggtgatcgctgatgtact
gacaagcctcgcgtacccgattatccatcggtggatggagcgactcgttaatcgcttccatgcgccgcagtaacaattgctcaagcagatttatcgcc
agcagctccgaatagcgcccttccccttgcccggcgttaatgatttgcccaaacaggtcgctgaaatgcggctggtgcgcttcatccgggcgaaag
aaacccgtattggcaaatattgacggccagttaagccattcatgccagtaggcgcgcggacgaaagtaaacccactggtgataccattcgcgagcc
tccggatgacgaccgtagtgatgaatctctcctggcgggaacagcaaaatatcacccggtcggcagacaaattctcgtccctgatttttcaccacccc
ctgaccgcgaatggtgagattgagaatataacctttcattcccagcggtcggtcgataaaaaaatcgagataaccgttggcctcaatcggcgttaaac
ccgccaccagatgggcgttaaacgagtatcccggcagcaggggatcattttgcgcttcagccatacttttcatactcccaccattcagagaagaaacc
aattgtccatattgcatcagacattgccgtcactgcgtcttttactggctcttctcgctaacccaaccggtaaccccgcttattaaaagcattctgtaacaa
agcgggaccaaagccatgacaaaaacgcgtaacaaaagtgtctataatcacggcagaaaagtccacattgattatttgcacggcgtcacactttgct
atgccatagcatttttatccataagattagcggatcctacctgacgctttttatcgcaactctctactgtttctccatagaagctgaccagacagtcgccgc
ttcgtcgtcgtcctcttcgggggagacgggcggagggggaggaaagtccgggctccatagggcagggtgccaggtaacgcctgggggggaaac
ccacgaccagtgcaacagagagcaaaccgccgatggcccgcgcaagcgggatcaggtaagggtgaaagggtgcggtaagagcgcaccgcgc
ggctggtaacagtccgtggcacggtaaactccacccggagcaaggccaaatagggggttcataaggtacggcccgtactgaacccgggtaggctg
cttgagccagtgagcgattgctggcctagatgaatgactgtccacgacagaacccggcttatcggtcagtttcacctgatttacgtaaaaacccgcttc
ggcgggtttttgcttttggaggggcagaaagatgaatgactgtccacgacgctatacccaaaagaaagcggcttatcggtcagtttcacctggtttac
gtaaaaacccgcttcggcgggtttttgcttttggaggggcagaaagatgaatgactgtccacgacactatacccaaaagaaagcggcttatcggtca
gtttcacctgttttacgtaaaaacccgcttcggcgggtttttacttttggaggggcagaaagatgaatgactgtccacgacactatacccaaaagaaag
cggcttatcggtcagttttacctgatgtacgtaataaaccgttccggcgggtttcagattgttgagtgcgctttattcatgccggatgcggcgtgaacgc
cttatcctgcctacaaaagcacgcaaattcaatatattgcagagatggcgtaggcctgataagcgtagcgcatcaggcatttttgcggttgccatcagtt
tcaaacccgcgtcagtgagtttttgcttttggtgcacagggtaagatgaataaatatctacggtattaataatagactttgtaagaa

chloramphenicol resistance cassette
E. coli rnpB gene
transcription start of pBAD
araC

8.16 References

Amann, E., Ochs, B. and Abel, K.J. 1988. Tightly regulated tac promoter vectors useful for the expression of unfused and fused proteins in *Escherichia coli*. *Gene* **69(2):** 301-15.

Bolivar, F., Rodriguez, R.L., Greene, P.J., Betlach, M.C., Heyneker. H,L. and Boyer, H.W. 1977. Construction and characterization of new cloning vehicles. II. A multipurpose cloning system. *Gene* **2:** 95-113.

Chang, A.C.Y. and Cohen, S.N. 1978. Construction and characterization of amplifiable multicopy DNA cloning vehicles derived from the P15A cryptic miniplasmid. *J. Bacteriol.*, **134:** 1141-1156.

Cutting, S.M., and Vander-Horn P.B. 1990. Genetic analysis, p. 27-74. *In* Molecular biological methods for *Bacillus*. eds Harwood, C.R. and Cutting S.M. , John Wiley & Sons Ltd., Chichester, United Kingdom.

Datsenko, K.A. and Wanner, B.L. 2000. One-step inactivation of chromosomal genes in Escherichia coli K-12 using PCR products. *Proc. Natl. Acad. Sci.* **97:** 6640–6645.

DeLano, W.L. The PyMOL Molecular Graphics System (2002) on World Wide Web http://www.pymol.org

Gößringer, M. 2004. *In vivo*-Analysen zur Funktion bakterieller RNase P-Proteine in *Bacillus subtilis.* URL http://archiv.ub.uni-marburg.de/diss/z2004/0529/ Stand 07.2006

Gößringer, M., Kretschmar-Kazemir Far, R., and Hartmann, R.K. 2006. Analysis of RNase P protein (*rnpA*) expression in *Bacillus subtilis* utilizing strains with suppressible *rnpA* expression. *J. Bacteriol.* **188(19):** 6816-23.

Guyer, M.S., Reed, R.R., Steitz, J.A. and Low, K.B. 1981. Identification of a sexfactor-affinity site in *E. coli* as gamma delta. *Cold Spring Harbor. Symp. Quant. Biol.* **45:** 135–140

Ishiwa, H. and Shibahara-Sone, H. 1986. New shuttle vectors for *Escherichia coli* and *Bacillus subtilis*. IV. The nucleotide sequence of pHY300PLK and some properties in relation to transformation; *Jpn. J. Genet.* **61:** 515-528.

Pascual, A. and Vioque, A. 1996. Cloning, purification and characterization of the protein subunit of ribonuclease P from the cyanobacterium *Synechocystis* sp. PCC 6803. *Eur J Biochem*. **241(1):** 17-24.

Pellegrini, O., Nezzar, J., Marchfelder, A., Putzer, H. and Condon, C. 2003. Endonucleolytic processing of CCA-less tRNA precursors by RNase Z in *Bacillus subtilis*. *EMBO J.* **22**: 4534–4543.

Roux, A., Beloin, C. and Ghigo, J.M. 2005. Combined inactivation and expression strategy to study gene function under physiological conditions: Application to identification of new *Escherichia coli* adhesins. *J. Bacteriol.* **187:** 1001–1013.

Sambrook, J., Fritsch, E.F. and Maniatis, T.E. 1989. Molecular cloning. A laboratory manual. Cold spring Harbor Laboratory, Cold Spring Harbor, N.Y.

Smith, D., Burgin, A.B., Haas, E.S. and Pace, N.R. 1992. Influence of Metal Ions on the Ribonuclease P Reaction. *J. Biol. Chem.* **267:** 2429-2436.

Vioque, A., Arnez, J. and Altman, S. 1988. Protein-RNA interactions in the RNase P holoenzyme from *Escherichia coli*. *J. Mol. Biol.* **202:** 835-848.

Waugh, D.S. and Pace, N.R. 1990. Complementation of an RNase P RNA (*rnpB*) gene deletion in *Escherichia coli* by homologous genes from distantly related eubacteria. *J. Bacteriol.* **172(11):** 6316-22.

Wegscheid, B. and Hartmann, R.K. 2006. The precursor tRNA 3'-CCA interaction with *Escherichia coli* RNase P RNA is essential for catalysis by RNase P *in vivo*. *RNA* doi: 10.1261/rna.188306.

Wegscheid, B., Condon, C. and Hartmann, R.K. 2006. Type A and B RNase P RNAs are interchangeable *in vivo* despite substantial biophysical differences. *EMBO Rep.* **7**: 411-417.

Acknowledgements

I would like to thank…

… Prof. Dr. Roland K. Hartmann for the excellent scientific supervision of my work, for always showing interest in the progress of the project and supporting with his insightful discussions and helpful advices.

… PD Dr. Klaus Reuter for being the second referee of my work.

… Prof. Dr. Maike Petersen and Prof. Dr. Udo Bakowsky for participation in the examination commission.

… Dr. Ciarán Condon for putting strain SSB318 and SSB320 at our disposal and for critical support of our first manuscript.

… Dr. Dagmar K. Willkomm for introducing me into the basics of molecular biology at the beginning of my work and writing protocol during the exam.

… Dr. Markus Gößringer and Dr. Simona Cuzic-Feltens for helpful discussions on cloning strategies, bacterial genetics, kinetics etc, for proofreading of my dissertation and finally but not least for always providing a "therapy chair".

… Michal Marszalkowski for preparation of *E. coli* and *B. subtilis* recombinant RNase P proteins.

… Dominick Helmecke for always being available as an additional hand if necessary.

… Sybille Siedler for introducing me into the basics of kinetic experiments in Lübeck.

… Andreas Ratje for pharmaceutical discussions and enlivening the lab routine.

… Dr. Heike Wünnenberg for fruitful office-discussions.

… all members of the Hartmann group for always being open for discussion, cooperativeness and helpfulness in problem-solving strategies and especially for the friendly atmosphere in- and outside the lab.

… my family for their love and support during my entire PhD.

… Christof for always encouraging and supporting me during this time.

Publications arising from this work

Articles

B. Wegscheid, C. Condon and R.K. Hartmann (2006)
Type A and B RNase P RNAs are interchangeable *in vivo* despite substantial biophysical differences. EMBO Reports **7(4):** 411-7

B. Wegscheid and R.K. Hartmann (2006)
The precursor tRNA 3'-CCA interaction with *Escherichia coli* RNase P RNA is essential for catalysis by RNase P *in vivo*. RNA **12**: 2135-2148

B. Wegscheid and R.K. Hartmann (submitted)
In vivo role of bacterial type B RNase P interaction with tRNA 3'-CCA.

Posters

B. Wegscheid and R.K. Hartmann (2004)
In vivo role of bacterial RNase P interaction with tRNA 3'-CCA.
3. Tagung der GBM-Studiengruppe "RNA-Biochemie", Blaubeuren
Posterprize: Nucleic Acids Research Award

B. Wegscheid and R.K. Hartmann (2006)
In vivo role of *E. coli* RNase P interaction with tRNA 3'-CCA.
EUCHEM Conference on RNA Chemistry meets Biology, Lund, Schweden
Posterprize supported by NAR

Oral presentations

B. Wegscheid and R.K. Hartmann (2004)
In vivo role of the bacterial RNase P interaction with tRNA 3'-CCA.
NorFa Network on Molecular biology of RNA; Meeting in Bergen, Norwegen

B. Wegscheid, D.K. Willkomm and R.K. Hartmann (2003)
In vivo role of the bacterial RNase P interaction with tRNA 3'-CCA.
NorFa Network on Molecular biology of RNA; Meeting in Amsterdam, Niederlande

Lebenslauf

Barbara Wegscheid

Geburtsdatum	24.08.1977
Geburtsort	Werneck
Familienstand	ledig
Nationalität	deutsch

09/1984-08/1988	Grundschule Werneck
09/1988-06/1997	Celtis Gymnasium, Schweinfurt
06/1997	Abitur
10/1997-10/2001	Studium der Pharmazie an der Philipps-Universität Marburg
08/1999	1. Abschnitt der Pharmazeutischen Prüfung
09/2001	2. Abschnitt der Pharmazeutischen Prüfung
11/2001-04/2002	Praktikum im Rahmen des Praktischen Jahres für Pharmazeuten am Cambridge Crystallographic Data Centre, Cambridge, UK Diplomarbeit unter Anleitung von Herrn Dr. A. Bergner und Herrn Prof. Dr. G. Klebe, Philipps-Universität Marburg Thema: „Crystal packing effects in protein-ligand binding sites – A systematic analysis using docking methods” Verteidung im Februar 2004
05-10/2002	Praktikum im Rahmen des Praktischen Jahres für Pharmazeuten in der Gorch-Fock Apotheke, Wilhelmshaven
11/2002	3. Abschnitt der Pharmazeutischen Prüfung
11/2002	Approbation als Apothekerin
seit 21.01.2003	Doktorarbeit in der Arbeitsgruppe von Herrn Prof. Dr. R. K. Hartmann am Institut für Biochemie an der Universität Lübeck
05/2003	Umzug der Arbeitsgruppe an die Philipps-Universität Marburg, Institut für Pharmazeutische Chemie

Selbstständigkeitserklärung

Ich versichere, dass ich meine Dissertation

„*In vitro* and *in vivo* investigations on the interaction of bacterial RNase P with tRNA 3'-CCA"

selbstständig, ohne unerlaubte Hilfe angefertigt und mich dabei keiner anderen als der von mir ausdrücklich bezeichneten Quellen und Hilfen bedient habe.

Die Dissertation wurde in der jetzigen oder einer ähnlichen Form noch an keiner anderen Hochschule eingereicht und hat noch keinen sonstigen Prüfungszwecken gedient.

(Ort/Datum) (Unterschrift mit Vor- und Zuname)